

JOURNAL OF FACADE DESIGN & ENGINEERING

VOLUME 10 / NUMBER 1 / 2022

DESIGN

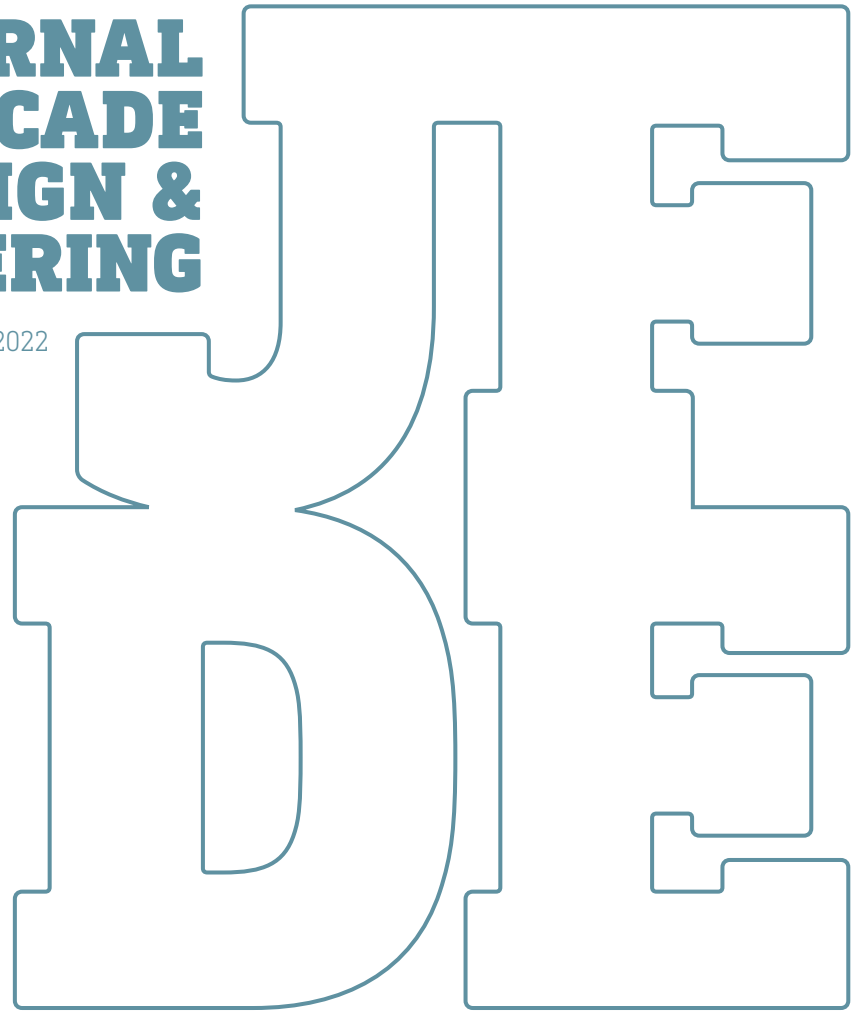
EDITORS IN CHIEF

ULRICH KNAACK & THALEIA KONSTANTINO

SUPPORTED BY THE EUROPEAN FACADE NETWORK

**JOURNAL
OF FACADE
DESIGN &
ENGINEERING**

VOLUME 10 / NUMBER 1 / 2022



EDITORS IN CHIEF

ULRICH KNAACK AND THALEIA KONSTANTINO

SUPPORTED BY THE EUROPEAN FACADE NETWORK

JFDE Journal of Facade Design and Engineering

JFDE presents new research results and new proven practice of the field of facade design and engineering. The goal is to improve building technologies, as well as process management and architectural design. JFDE is a valuable resource for professionals and academics involved in the design and engineering of building envelopes, including the following disciplines:

- Architecture
- Building Engineering
- Structural design
- Climate design
- Building Services Engineering
- Building Physics
- Design Management
- Facility Management

JFDE is directed at the scientific community, but it will also feature papers that focus on the dissemination of science into practice and industrial innovations. In this way, readers explore the interaction between scientific developments, technical considerations and management issues.

Publisher

TU Delft / Faculty of Architecture and the Built Environment
Julianalaan 134, 2628 BL Delft, The Netherlands

Contact

Alessandra Luna Navarro
editors@jfde.eu
<https://jfde.eu/>

Policies

Peer Review Process – The papers published in JFDE are double-blind peer reviewed.

Open Access – JFDE provides immediate Open Access (OA) to its content on the principle that making research freely available to the public supports a greater global exchange of knowledge.

Licensed under a Creative Commons Attribution 4.0 International License (CC BY 4.0).

Indexation – JFDE is indexed in the Directory of Open Access Journals (DOAJ), Google Scholar, Inspec IET and Scopus.

Publication Ethics – Editors, authors and publisher adopt the guidelines, codes of conduct and best practices developed by the Committee on Publication Ethics (COPE).

Copyright Notice – Author(s) hold their copyright without restrictions.

Design & layout

Design – Sirene Ontwerpers, Amsterdam

Layout – Stichting OpenAccess, Rotterdam

Open access

Website, indexing, DOIs – Stichting OpenAccess, Rotterdam

ISSN 2213-302X (Print)
ISSN 2213-3038 (Online)
ISBN 978-90-832713-3-0

Editorial board

Editors in Chief

Ulrich Knaack
Thaleia Konstantinou
Delft University of Technology, The Netherlands

Editors

Alessandra Luna Navarro
Tatiana Armijos Moya
Delft University of Technology, The Netherlands

Editorial Board

Tillmann Klein, *Delft University of Technology, Architecture and the Built Environment, Netherlands* // Alejandro Prieto Hoces, *Universidad Diego Portales, Escuela de Arquitectura, Chile* // Daniel Aelenei, *Universidade Nova de Lisboa, Lisbon, Portugal* // Enrico de Angelis, *Polytechnico Milano, Milan, Italy* // Julen Astudillo, *TECNALIA Research & Innovation, San Sebastian, Spain* // Carlo Battisti, *IDM Südtirol - Alto Adige, Italy* // Anne Beim, *Royal Danish Academy of Fine Arts, Copenhagen, Denmark, Denmark* // Jan Belis, *Ghent University, Belgium* // Jan Cremers, *Hochschule für Technik Stuttgart (HFT), Germany* // Andy van den Dobbelaere, *Delft University of Technology, Delft, the Netherlands* // Paul Donnelly, *Washington University, St. Louis, USA* // Chris Geurts, *TNO, Delft, Netherlands* // Mikkel K. Kragh, *University of Southern Denmark, Odense, Denmark* // Klaus Kreher, *Lucerne University of Applied Sciences and Art, Lucerne, Switzerland* // Bert Lieverse, *Association of the Dutch Façade Industry, Nieuwegein, The Netherlands* // Steve Lo, *University of Bath, Bath, United Kingdom* // Andreas Luible, *Lucerne University of Applied Sciences and Art, Lucerne, Switzerland* // Enrico Sergio Mazzucchelli, *Politecnico di Milano ABC Department, Italy* // David Metcalfe, *Centre for Window and Cladding Technology, United Kingdom* // Mauro Overend, *University of Cambridge, Cambridge, United Kingdom* // Uta Pottgiesser, *Delft University of Technology, Architecture and the Built Environment, Netherlands* // Josemi Rico-Martinez, *University of the Basque Country, Donostia- San Sebastian, Spain* // Paolo Rigone, *UNICMI, Milan, Italy* // Holger Strauss, *Innobuild GmbH, Berlin, Germany* // Jens Schneider, *University of Darmstadt, Darmstadt, Germany* // Holger Techen, *University of Applied Sciences Frankfurt, Frankfurt, Germany* // Nil Turkeri, *Istanbul Technical University, Istanbul, Turkey* // Claudio Vásquez Zaldívar, *Pontificia Universidad Católica de Chile, Santiago, Chile* // Aslihan Ünlü Tavil, *Istanbul Technical University, Istanbul, Turkey* // Stephen Wittkopf, *Lucerne University of Applied Sciences and Art, Lucerne, Switzerland*

Submissions

All manuscripts and any supplementary material should be submitted to the Editorial Office (editors@jfde.eu), through the Open Journal System (OJS) at the following link: <https://jfde.eu/>

Author Guidelines

Detailed guidelines concerning the preparation and submission of manuscripts can be found at the following link:
<https://jfde.eu/index.php/jfde/about/submissions>

Contents

- v **Editorial**
Ulrich Knaack, Thaleia Konstantinou
- 001 **Selection of Exterior Wall System and MCDM Derived Decision**
Anđelka Štilić, Igor Štilić
- 029 **Towards a Human Centred Approach for Adaptive Façades**
Mine Koyaz, Alejandro Prieto, Aslıhan Ünlü, Ulrich Knaack
- 055 **Exploring the Impact of Geometry and Fibre Arrangements on Daylight Control in Bistable Kinetic Shades**
Elena Vazquez, Jose Duarte
- 075 **Circular, biomimicry-based, and energy-efficient façade development for renovating terraced dwellings in the Netherlands**
Ana Luíza Binow Bitar, Ivar Bergmans, Michiel Ritzen
- 105 **Process Automation to Improve the Building Engineering Design Analysis of Non-Repetitive Façade Geometries**
Jacopo Montali, Thomas Henriksen
- 119 **Empirical validation of co-simulation models for adaptive building envelopes**
Esther Borkowski, Alessandra Luna-Navarro, Michalis Michael, Mauro Overend, Dimitrios Rovas, Rokia Raslan
- 155 **The acoustic and daylighting effects of external façade sun shading systems**
Simone Secchi, Patrizio Fausti, Gianfranco Cellai, Martina Parente, Andrea Santoni, Nicolò Zuccherini Martello

Editorial

Ulrich Knaack ¹, Thaleia Konstantinou ¹

¹ Delft University of Technology

We are proud to publish a new issue of the Journal of Façade Design and Engineering. This first issue of volume 10 covers a broad range of themes such as adaptivity, automation, circularity, refurbishment, daylight, acoustics, and user interaction are addressed by peer-reviewed articles.

We would also like to take this opportunity to share some changes in the JFDE editorial team and publishing process. Prof. Tillmann Klein is changing his role from editor-in-chief to editorial board member. Tillmann Klein has been a front-runner in open-access publishing since JFDE was launched in 2013. Together with Ulrich Knaack he was responding to a call from the Netherlands Organisation for Scientific Research (NWO) to develop new Journal models. The editorial team is most grateful for its outstanding contribution to making JFDE a reference point in the façade design and engineering field. The role is taken over by Dr. Thaleia Konstantinou, who has been promoting the Journal as managerial editor in the past years.

As we go forward, we strive to ensure scientific quality as well as relevance for society and industry. JFDE has revised the editorial process giving a larger responsibility to the editorial board to control the scientific rigour of our published articles. We have also introduced procedures to regularly extend the editorial board.

It makes us very proud to have reached the 10th year of publishing with JFDE, respected and valued by our authors and readers. Thanks for this! And, of course: to be continued!

Ulrich Knaack and Thaleia Konstantinou - Editors in Chief

DOI

<http://doi.org/10.47982/jfde.2022.1.00>

Selection of Exterior Wall System and MCDM Derived Decision

Andelka Štilić ¹, Igor Štilić ²

* Corresponding author

1 Academy of Applied Studies Belgrade, Serbia, andjelka.stilic@gmail.com

2 Founder of architecture and design bureau Igor Štilić, Belgrade, Serbia

Abstract

In the field of construction practice, decisions regarding material selection frequently come down to a choice based on tradition, i.e. recommendations based on the experience of the engineers hired by an employer as designers, contractors, or energy efficiency engineers.

In the presented research, in addition to the Employer, technical individuals were involved in the decision-making process. The harmonisation of Employer opinions and those of experts were obtained through NGT technique and Delphi based method, due to the fact that different criteria for a decision could represent a field of interest of an individual participant in the process. The result was determining the criteria, their strictness, and their weighted effect.

As multi-criteria decision analysis has evolved into a powerful tool that assists decision-makers in generating "a cut above" choice in resolving specific cases and overcoming certain problems in the architectural and construction industry, the use of the MCDM method EDAS+ in the research ensured an exterior wall system ranking that was not influenced by experience or marketing.

Without intending to favour any manufacturer of building materials, the research presents eight exterior wall systems belonging to different categories of core materials, all with individual features, similarities, and differences.

When compared to otherwise arbitrary estimates or recommendations based on experience and the most commonly used building materials, the application of multi-criteria decision analysis in the case of exterior wall system selection for a particular 1938 Belgrade building generated more relevant selection results.

Keywords

exterior wall system, building materials, EDAS+, multi-criteria decision making

DOI

<http://doi.org/10.47982/jfde.2022.1.01>

1 INTRODUCTION

The construction industry has developed significantly as it has taken into account conflicting, immeasurable, and experientially determined decision-making criteria. Environmental and social aspects are becoming more important and their proper synergy with economic aspects is the cornerstone for success in any construction business or procedure.

When facing a wide range of options in resolving specific cases and overcoming certain problems in the architectural – construction industry, multi-criteria decision making and analysis have become powerful tools that help decision-makers to generate “a cut above” choice. These tools are much more than simply a collection of theories, methodologies, and procedures; they are a distinct approach in dealing with decision problems (Greco et al., 2016). The evolution in the use of multi-criteria decision analysis techniques clearly shows an increased level of confidence in their assistance in the decision-making process (Jato-Espino et al., 2014). Multi-criteria decision-making methods are not only comprehensive, but also well-known instruments that are used for resolving decision-making dilemmas in architecture, construction, urban planning, and energy efficiency projects. As shown in territorial delimitation presented in articles by Ogrodnik (2019) and Bruen (2021), Asia, North America, and Europe (notably Poland and Lithuania, followed by Italy, Spain, Czech Republic, and France) are the leading study hubs on the topic of multi-criteria decision-making in architecture and civil engineering. In the aforementioned articles, researched authors used wide range of different methods, i.e.: AHP, ANP, CBA, COPRAS, CRITIC, (...), TODIM, TOPSIS and VIKOR. According to Ogrodnik's (2019) survey of the literature, MCDM approaches enable the deconstruction of different decision problems, increase the transparency of decision processes, allow the comparison of various decision alternatives, and reveal their strengths and shortcomings. (De Toro & Iodice, 2016; Šiožinyte & Antuchevičienė, 2013).

At the moment, there are no clear guidelines on how to choose the optimal exterior wall system or structural wall, which meets all the required criteria set by various intertwining disciplines. The question of how to make a more relevant selection of an exterior wall system arises when decisions about material selection frequently come down to a choice based on tradition, and recommendations based on the experience of the engineers hired by an employer as designers, contractors, or energy efficiency engineers. Construction and energy efficiency standards in different countries establish minimum requirements (Pérez-Lombard et al., 2009), but the design process should not be reduced to choosing the best alternative solely in terms of standards and initial design requirements. When Terms of Reference cannot be accomplished all at once it is necessary for the designer to define project objectives first and then limitations (Moghtadernejad et al., 2018).

The aim of the research study is the selection of a contact façade alternative (exterior wall system) in the specific case presented in this paper – the extension of a three-storey over ground downtown Belgrade (Serbia) building dating from 1938 by adding two more floors (Figure 1).

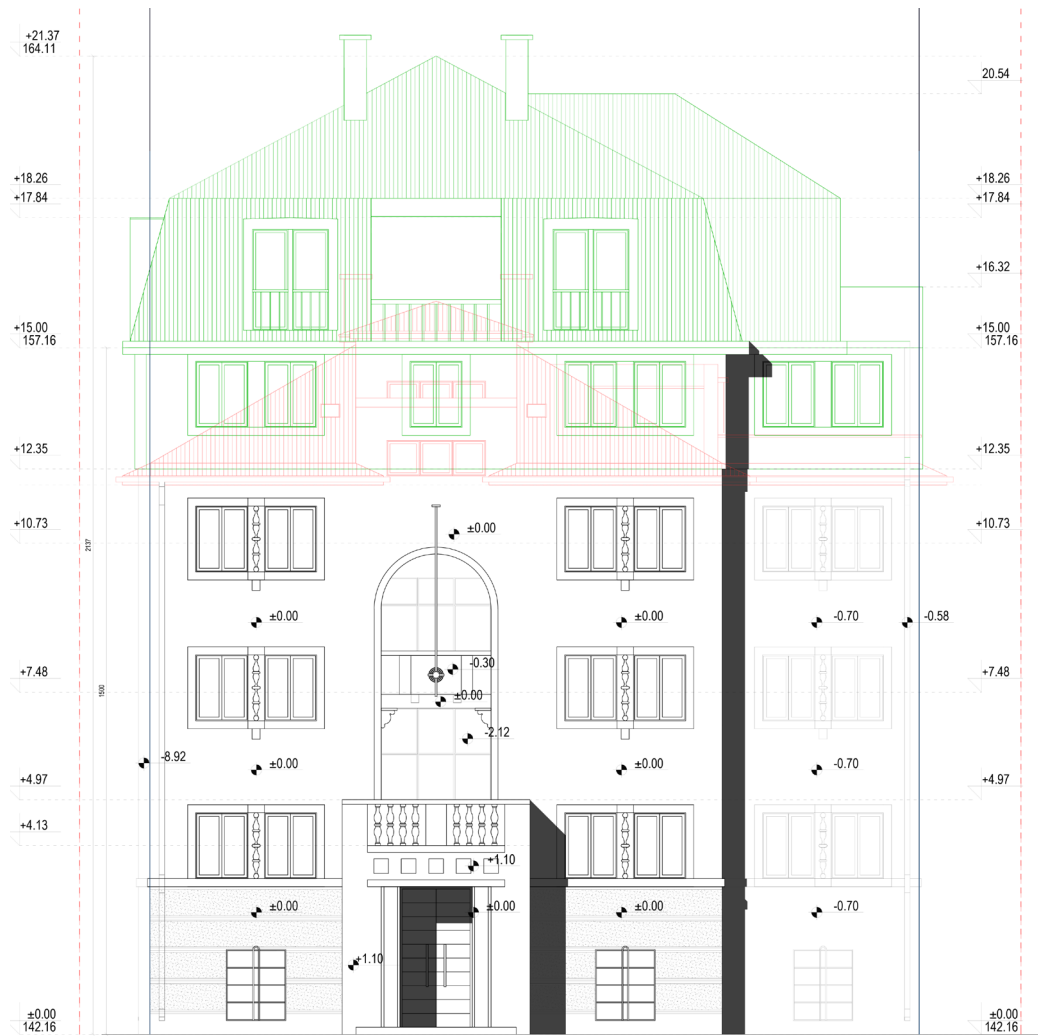


FIG. 1 Existing building and planned extension overlapped, Author's drawing based on Archive design, on-site measurements and planned extension

Since certain criteria could be in seemingly direct contradiction, for example the cost of construction compared to that of energy-efficiency, the success of such choices will not be reflected in maximising each of the criteria (Moghtadernejad et al., 2020). For these reasons, finding a balance between the criteria will be a requirement that must be met for the selection to be adequate. In the specific case presented in this paper, design teams must consider a wide range of options during the early phases of a project, both materials (exterior wall systems) and the process of their selection, in order to select those that best address the project constraints and objectives (Donato et al., 2017). Therefore, it is necessary to conduct a series of reviews and actions in order to find the optimal solution. Otherwise – in the building permit project and construction phase, the design would be modified through unnecessary, time-consuming and costly changes (Moghtadernejad et al., 2019).

The objective of the research is to provide a systematic decision-making process for selecting an exterior wall system that may be utilized in both particular project and future extension projects of the same multi-family building typology.

2 METHODOLOGY

The paper aims to provide a selection of exterior wall systems that can be used in the project, for the extension building permit and detailed design of the specific multi-family building typology.

The methodology was developed in the context of the selection of the exterior wall system, as a part of the thermal envelope of a multi-family residential building at a geographically determined location, through the application of the multi-criteria decision-making method (MCDM).

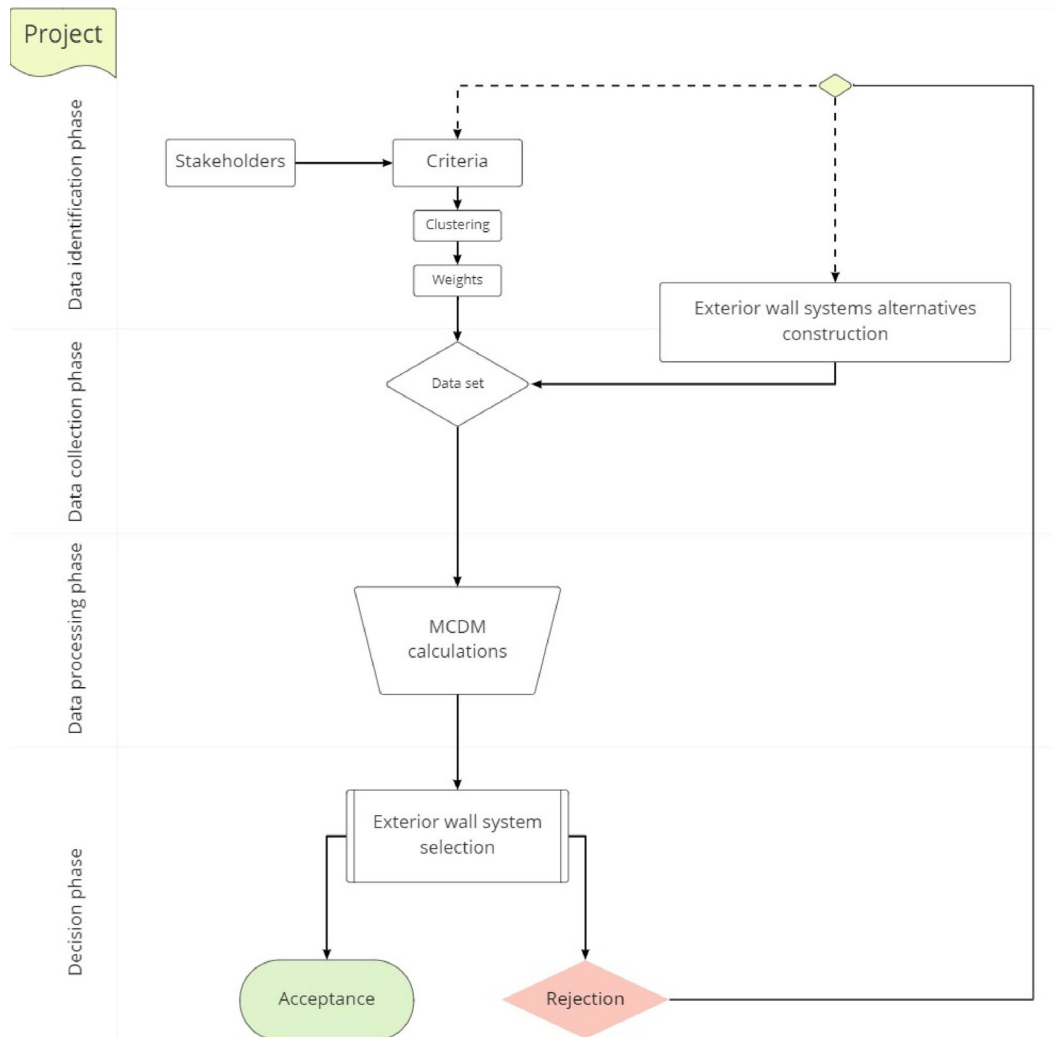


FIG. 2 Research methodology

The research methodology recognized four phases of the research. The phases consisted of Data Identification, Data Collection, Data Processing, and Decision Phase, which dealt with tasks of stakeholder identification; criteria, clustering and weights; exterior wall system alternatives construction; MCDM calculations; and selection of exterior wall system as the objective. The methodology is presented in Figure 2, and phases are explained through the individual tasks in subsections 2.1 – 2.5.

2.1 STAKEHOLDERS

In terms of the paper's research, identification of the stakeholders – decision makers was established as the earliest stage of the research, as a collaborative approach to design and delivery that is supported by key stakeholders – employers, architects, engineers and contractors is a characteristic of idealistic building information modelling (McAdam, 2010).

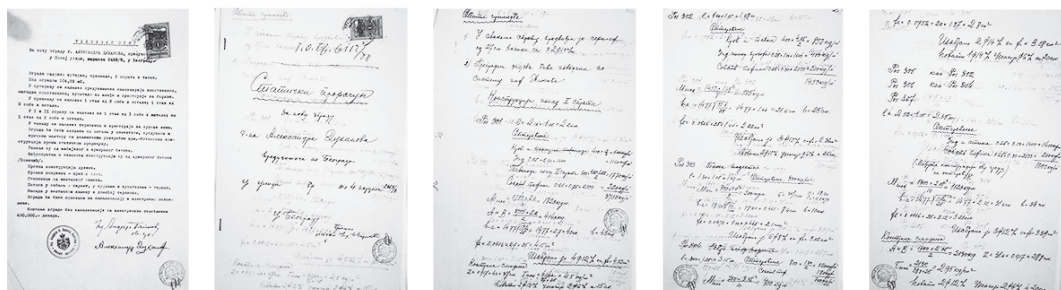
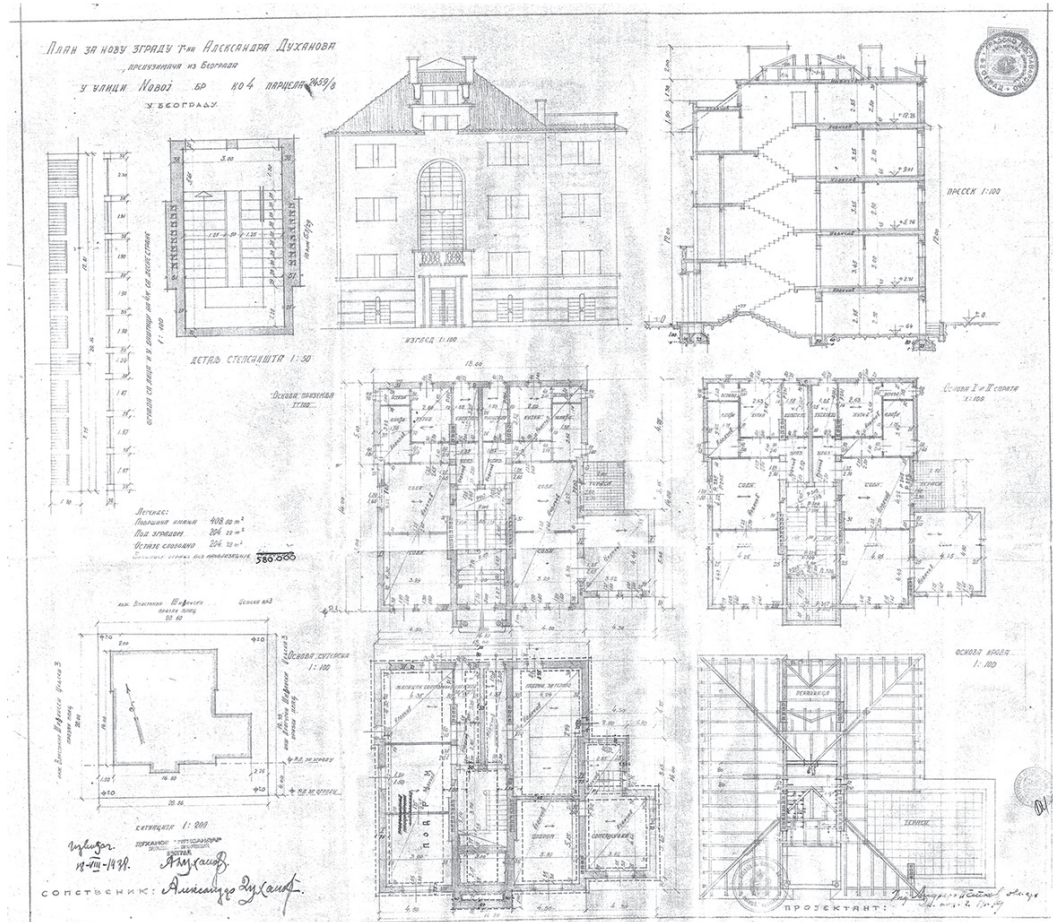


FIG. 3 Archive design and part of static calculations obtained from Historical Archive of Belgrade, Author's presentation

The group of stakeholders included three independent experts: an architect and two civil engineers – building physics and construction expert, who were appointed to the project of additions and

extensions of the case building, as well as the Employer¹. The contractor (who was also the vendor) was excluded from participating as a stakeholder in this particular case considering his appointment would be made at the stage when exterior wall system has already been selected.

The initial requirements of the Employer were determined in discussions, as well as through the experts' assessment of static impacts and loads by analysing static calculation obtained from the archive design (Figure 3). The initial requirements were prioritising construction deadlines, lightness of the structure (due to a layman's position of the Employer on avoiding the existing structure load), minimizing exploitation costs, and first and foremost: minimizing construction costs.

According to the Employer's request, the Terms of Reference, inter alia, stipulated the desired net usable area of the added section. Therefore, the spatial arrangement had led to the conclusion that it is possible to provide the desired area within the overall horizontal dimensions of the building, only if the façade wall has a maximum layer thickness of 36cm (Figure 4).

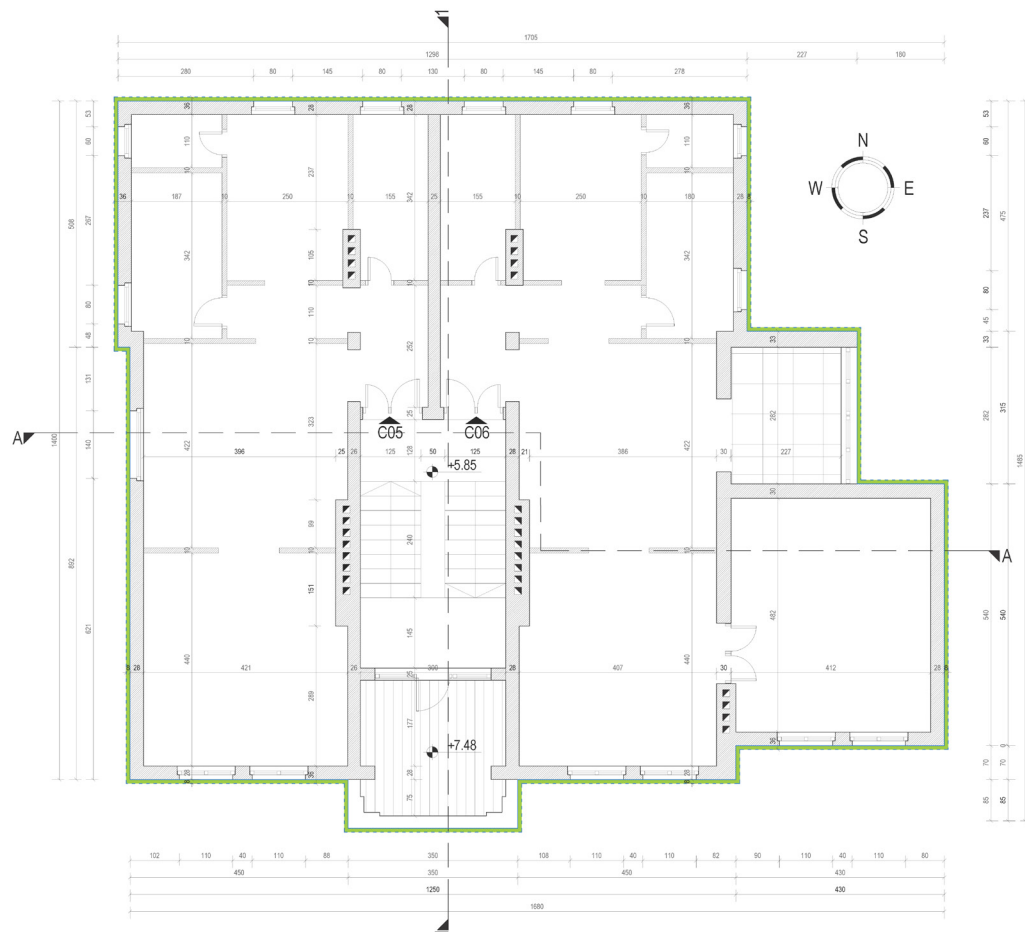


FIG. 4 Typical floor plan of the case study building, Author's drawing based on Archive design and on-site measurements

1

Representative of the group of investors – owners of the apartments in the existing building.

Accordingly, after appointed experts provided a brief explanation of other important factors, the Employer was required to specify the order of priority of stated subjective criteria, while technical criteria were applied based on experts' review of the matter from several different perspectives. Nevertheless, there were also legal and technical frameworks which stipulated possibilities and limitations.

2.2 CRITERIA

As questions expressed as criteria involve decisions in a dynamic environment in which the outcome of a decision is influenced to some extent by the decisions of others, and decisions are frequently dictated by the context in which judgements are made (Weber & Johnson, 2009), the stakeholders were expected to explore and generate "ideas" on their own (Van de Ven & Delbecq, 1971; Harvey & Holmes, 2012; Hugé & Mukherjee, 2018) and to identify criteria using the Nominal Group Technique². Criteria clustering into income and expenditure was conducted and the Delphi based weight determining technique (Hecht, 1977) was used as a tool for determining criteria weights (Figure 5).

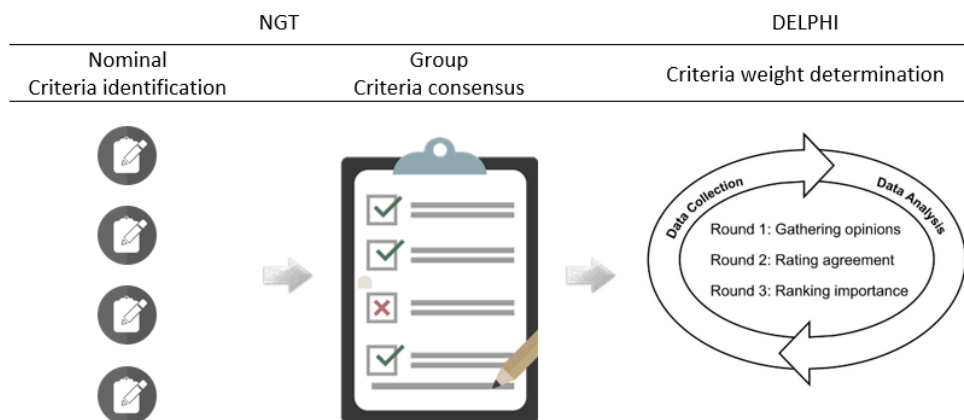


FIG. 5 Criteria identification, clustering and weights phase

In terms of the research presented in this paper, the Employer prepared verbal terms of reference, with the intention of achieving maximum returns with minimum investments. After reviewing the archives (Figure 3), design and static impacts were analysed, the benefits and negative impacts of the location were considered, technical-technological problems, urban conditions (which are not the subject matter in this case) were observed, and the subject matter was reviewed.

By applying NGT, stakeholders proposed two (2) expenditure criteria and eight (8) income criteria, which were in compliance with the commonly-used criteria involved in the decision-making problems in the field (Wen et al., 2021). Detailed descriptions of each criterion will be described hereinafter.

2

The nominal group technique (NGT) is a structured group-based consensus-building approach. The NGT terminology is derived from the fact that participants are nominally in a group, but are working individually, as NGT is based on a combination of individual and collective reflection. In this case, NGT will be used to identify and clarify problems, as well as to produce appropriate research questions in order to develop solutions and prioritize actions (Hugé & Mukherjee, 2018)

2.2.1 EXPENDITURE CRITERIA

Criterion K1 – Weight – negative impact on the foundation load, was established as the case study of this paper, relating to the extension of and addition to a specified existing building built in 1938. The starting point of discussion was the stability of the facility itself. Considering the facility's and the used materials' life span (Akanbi et al., 2018), as well as the available static calculation (Figure 3) and the currently valid local standards for calculating the load on the existing structure and ground, as well as seismic, wind, and atmospheric phenomena (Bylaw on building constructions, 2020), it was concluded that, in order to avoid additional settling of the structure and its potential collapse, the total mass of the extended part of the building must have as little vertical influence on the existing structure, foundations, and soil as possible (Fajfar, 2017). The presented values of the alternatives will be calculated as actual weight values of the exterior wall system. The values of the alternatives will represent the weight of the exterior wall system, expressed in kg/m^2 . (International Organization for Standardization [ISO], 2007b)

Criterion K2 – Total price, i.e. cost of construction – was one of the determining factors (Bari et al., 2012). Pricing is a complex process that requires exact input data obtained through understanding the technologies used to accomplish particular job activities, construction conditions, facility location, and construction standards (Stojanović et al., 2004). Norms applicable in the Serbian region, levelled with average prices on the local market, were used to calculate the labour required to execute and complete the entire, bilaterally processed system. When establishing the price, the purchase price of materials on the local market will be considered, and the values will represent the cost of building a square metre of the exterior wall system. All layers of the system, plastered on the interior side using flexible mortar, whose exterior side is finished with acrylic façade plaster, will be calculated and expressed in EUR/m^2 of the exterior wall system. The total price of system will include the fire protection of core materials that could not obtain a flammability certificate (i.e. wood and steel).

2.2.2 INCOME CRITERIA

Criterion K3 – Reduction in costs of exploitation – will represent the numerical indicator of the exterior wall system maintenance, which will be derived from the aggregate scoring results for the selection of different materials, systems and designs, performance variability, etc. (Chev & De Silva, 2004; Chev et al., 2006). A sustainable façade is defined by the ease of maintenance in terms of design and management, therefore, it is weather resistant and requires minimal life cycle costs, including cleaning, repair and replacement (Yeoh, 1990; Honstede, 1990; Chev et al., 2006). The quantitative indicator will represent aggregated scores of a discrete scale ranging from low (1) to high (5) that will be used to reflect the degree of individual longevity, possibility of intervention on the inner side of the wall, further new or additional installations, possibility of surface cracks, possibility of window replacement or servicing, loss of performance in case of moisture, and behaviour under fire.

Criterion K4³ – Ease of processing, as an additional acceleration of execution of specialist's trades – has an impact on all subsequent interventions executed on buildings, such as adaptations, change of the intended purpose, laying additional installations. Therefore, it could be referred to as transformability. In addition to convenience and an accelerated installation-laying procedure and finishing of structural elements, workability after installation is exceptionally important (Hendry, 2001). When installing heating, water supply, sewage, and electrical infrastructure, in the case of materials that are not easily workable, if the materials in their structure are not compact, are brittle or excessively hard, the energy efficiency characteristics of the material itself will be affected. The values of the alternatives will present a 1 to 5 scoring scale and will refer to the exterior wall system itself.

Criterion K5 – Local availability of materials – will be presented after careful consideration of the availability of materials in warehouses, the time required to deliver the required quantity of materials, transportation costs (primarily depending on whether material is available on the local / regional / EU market). The transportation of material was taken into consideration as local availability of materials is particularly important, as the ecological and economic advantages could derive from local availability of materials (Rückert et al., 2014). In the case of the addition and extension to an existing building (Figures 1, 3, and 4), which invariably results in unforeseen and additional work, the unavailability of materials due to i.e. country lockdown (Covid-19 era) and border procedures (for transporting imported building materials) would significantly compromise the entire process. A 1 to 5 scoring scale will be established to assess availability.

Criterion K6 – Thermal conductivity coefficient : For many years now, awareness of energy saving, reducing emissions of harmful gases into the atmosphere, using alternative energy sources, all in order to preserve the planet, general health, and the commitment to leave a better living environment for future generations, has been high (Clarke, 2003). Criterion K6 -Thermal conductivity coefficient will be presented through values of the alternatives which refer to the thermal conductivity of the exterior wall system per $1m^2$ of wall surface, expressed in W/m^2K units. The criterion will be determined through the heat transfer coefficient of the applied structural system of the façade wall by applying the calculation methodology stipulated by locally applicable legislation: Serbian Law on planning and construction (2021) and Bylaw on energy efficiency of buildings (2011), based on ISO (2007a), revised version ISO (2017):

$$U = \frac{1}{R_{si} + \sum_n \frac{d_n}{\lambda_n} + R_{se}}$$

Where R_{si} – is heat transfer resistance at entrance, R_{se} – is heat transfer resistance at exit, d_n is n layer thickness expressed in m (meters) and λ_n – is thermal conductivity coefficient of the n layer. As the role of layers in selected systems is to prevent outdoor heat release in winter conditions, as well as to reduce the amount of heat that penetrates inside during summer, thermal mass, i.e. the mass of materials used as a part of the façade wall, plays an important part in this process.

Criterion K7 – Weight – positive impact on the thermal stability of the building will be presented through the values of the alternatives: actual wall weight expressed in kg/m^2 of the system (ISO, 2007b), and the values will be identical to those given for criterion 1. However, the impact will be as income criterion, as energy savings potential of heavy walls is high (Bellamy & Mackenzie, 2001). The greater the mass of the wall, the more thermally inert the building is.

Criterion K8 – Labour force availability – The need to find skilled labour force (Bari et al., 2012) or provide training for the existing human resources arises in the case of all non-standard procedures. However, even if the training may be simple, it could be lengthy. A 1 to 5 scoring scale will be applied to criterion K8, based on the harmonisation of norms (Mijatović, 2008), building material manufacturer recommendations, and the assessment of experienced human resources available to local companies.

Criterion K9 – Construction speed – was agreed on as an important criterion (Bari et al., 2012) in this case. Criterion will be evaluated by applying the 1 to 5 scoring scale, through the method of execution. Diversification is performed according to the variety of required work – masonry, carpentry, façade, joinery work, ease of handling and workability of elements in terms of construction, transportation, etc. - all based on the harmonisation of norms (Mijatović, 2008) and the recommendations of manufacturers for non-standard building elements.

Criterion K10 – Regulations – certification by domestic institutions- is related to the design phase, where designated institutions (The Ministry of the Interior of the Republic of Serbia) should approve the use of construction materials and where the problem of nostrification of foreign certificates and standards and the need for local standardisation is quite frequent. In addition, the strictness of institutions (The Ministry of the Interior of the Republic of Serbia) regarding fire protection standards for highly flammable materials (Law on fire protection, 2018) slows down the process of issuing building approvals. Therefore, this is considered to be an aggravating factor for walls whose core material is made of wood or steel.

As ten (10) criteria were selected for making a decision regarding the selection of the exterior wall system, they are presented in Table 1.

TABLE 1 Selected criteria

CRITERIA CODE	CRITERIA EXPLANATION	INFLUENCE
K1	Weight - negative impact on the foundation load	Expenditure criterion (↓)
K2	Construction cost	Expenditure criterion (↓)
K3	Reduction in costs of exploitation	Income criterion (↑)
K4	Ease of processing, as an additional acceleration in the execution of specialist's trades	Income criterion (↑)
K5	Local availability of materials	Income criterion (↑)
K6	Thermal conductivity coefficient	Income criterion (↑)
K7	Weight - positive impact on the thermal stability of the building	Income criterion (↑)
K8	Labour force availability	Income criterion (↑)
K9	Construction speed	Income criterion (↑)
K10	Regulations - certification by domestic institutions	Income criterion (↑)

2.2.3 CRITERIA WEIGHT

As elaborated in the description of criteria, there were a certain number of both mutually inclusive and exclusive factors. Therefore, it was decided to weigh criteria based on which materials, i.e. exterior wall system, would be selected. With a small but finite number of stakeholders involved in the reconstruction project, therefore—in the particular case of the extension of a downtown Belgrade building—the Delphi based weight determining technique (Hecht, 1977) as a tool for determining criterions weights, was used to reconcile the individual opinions of the experts and stakeholders, in a group decision.

Both NGT and the modified Delphi technique foresaw the existence of a moderator who communicated with group members independently. After compiling a questionnaire and having individual communications with the team of experts, the focus was placed on those subject matters where disagreement existed among the group members in terms of argumentation or quantitative assessment. More specifically, experts and other stakeholders with the status of decision-makers were asked to express their preferences regarding each criterion individually by giving a percentage score; an example is presented in Figure 6.

Subject: Selection of the exterior wall system, case of [REDACTED]
Round: 1

After achieved consensus on criteria identification and their clustering, at this time you are expected to assign each criterion weight, expressed in percentage on a linear scale next to the criterion. Please note that the sum of the percentages you assign cannot exceed total of 100%.

Thank you for your collaboration.

Criteria explanation	Influence	Weight
Weight - negative impact on the foundation load	↓	0 10 20 30 40 50 60 70 80 90 100 [Handwritten mark at 20]
Construction cost	↓	0 10 20 30 40 50 60 70 80 90 100 [Handwritten mark at 20]
Reduction in costs of exploitation	↑	0 10 20 30 40 50 60 70 80 90 100 [Handwritten mark at 10]

FIG. 6 Criteria percentage scoring

The process of answer approximation, decreasing standard deviation, increasing the correlation level – reducing the variation level process, as part of Delphi method (Linstone & Turoff, 2002), was completed after the 3rd round, after which the following weights to the criteria were allocated, as presented in Table 2.

TABLE 2 NGT technique and Delphi method results

CRITERIA CODE	CRITERIA EXPLANATION	WEIGHT	INFLUENCE
K1	Weight - negative impact on the foundation load	0.08	↓
K2	Construction cost	0.22	↓
K3	Reduction in costs of exploitation	0.06	↑
K4	Ease of processing, as an additional acceleration in the execution of specialist's trades	0.08	↑
K5	Local availability of materials	0.10	↑
K6	Thermal conductivity coefficient	0.12	↑
K7	Weight - positive impact on the thermal stability of the building	0.16	↑
K8	Labour force availability	0.06	↑
K9	Construction speed	0.06	↑
K10	Regulations - certification by domestic institutions	0.06	↑

2.3 EXTERIOR WALL SYSTEM ALTERNATIVES

Exterior wall systems are constructed with different physical structures, thermal capacities, and specific gravities, with different installation methods used to achieve the best possible performance of the components of each system, and described in detail.

Within a given total thickness of maximum 36 cm, as presented in Figure 4, exterior wall systems will be formed with core materials belonging to different groups, different physical structures, thermal capacities, and specific gravities, and with different installation methods.

2.4 MCDM CALCULATION

Different MCDM methods, which are employed in the architectural and construction industries, offer generating outputs that can be shown in the form of results and ranking of alternatives. The objective of introducing a MCDM method was to generate a hierarchy (rank) from the set of alternatives.

As a decision-making method, the EDAS method (Keshavarz Ghorabae et al., 2015) is set for the ranking of exterior wall systems, as one of the methods of multi-criteria decision analysis whose result distribution consistency is confirmed by its high level of Spearman correlation coefficient (Mathew & Sahu, 2018) and which, during segment calculation of positive and negative distance from the mean, and sum weighting, provides insight into the structure of input data and the flows of their transformation up to ranking, inclusive, which may possibly result in the correction of criteria. As some criteria could have a narrow and some could have a broad range of attribute values by criteria, the extension of EDAS method – EDAS+ method (Štilić et al., 2019) is proposed, as the latter eliminates favouring criteria with broader ranges of attribute values. On the other hand, the normalisation implied by EDAS+ makes it somewhat difficult to monitor the fluctuation values of the positive and negative distances from the mean, however, monitoring is still possible.

The method's calculation steps (Štilić et al., 2019; Štilić, 2020) are given hereinafter:

Step 1. Recognizing key criteria, weighting factors for criteria and alternatives in solving the problem of multi-criteria decision making.

Step 2. Forming a decision-making matrix:

$$X = [X_{ij}]_{n \times m} = \begin{bmatrix} x_{11} & x_{12} & x_{13} & \dots & x_{1m} \\ x_{21} & x_{22} & x_{23} & \dots & x_{2m} \\ x_{31} & x_{32} & x_{33} & \dots & x_{3m} \\ \dots & \dots & \dots & \dots & \dots \\ x_{n1} & x_{n2} & x_{n3} & \dots & x_{nm} \end{bmatrix}.$$

Step 3. Normalizing the decision-making matrix by applying the "Correct mapping":

$$R = [R_{ij}]_{n \times m} = \begin{bmatrix} r_{11} & r_{12} & r_{13} & \dots & r_{1m} \\ r_{21} & r_{22} & r_{23} & \dots & r_{2m} \\ r_{31} & r_{32} & r_{33} & \dots & r_{3m} \\ \dots & \dots & \dots & \dots & \dots \\ r_{n1} & r_{n2} & r_{n3} & \dots & r_{nm} \end{bmatrix},$$

where $r_{ij} = \frac{x_{ij} - x_j^-}{x_j^+ - x_j^-}$, with $i = 1, 2, \dots, m$; $j = 1, 2, \dots, n$.

Step 4. Determining the average solution for each criterion separately:

$$AV = [AV_j]_{1 \times m} = \left[\frac{\sum_{i=1}^n x_{i1}}{n} \quad \frac{\sum_{i=1}^n x_{i2}}{n} \quad \dots \quad \frac{\sum_{i=1}^n x_{im}}{n} \right] = [x_1^*, x_2^*, \dots, x_m^*].$$

Step 5. Calculating the positive and negative distance from the mean by taking into account the type of criterion function – income or expenditure:

$$[PDA_{ij}]_{n \times m} : d_{ij}^+ = \begin{cases} \frac{\max(0, (x_{ij} - x_j^*))}{x_j^*} ; j \in \Omega_{max} \\ \frac{\max(0, (x_j^* - x_{ij}))}{x_j^*} ; j \in \Omega_{min} \end{cases},$$

$$[NDA_{ij}]_{n \times m} : d_{ij}^- = \begin{cases} \frac{\max(0, (x_j^* - x_{ij}))}{x_j^*} ; j \in \Omega_{max} \\ \frac{\max(0, (x_{ij} - x_j^*))}{x_j^*} ; j \in \Omega_{min} \end{cases},$$

where Ω_{max} represents a group of “income” criteria, and Ω_{min} the group of “expenditure” criteria.

Step 6. Calculating the weighted sum matrices:

$$[SP_i]_{nx1} = [PDA_{ij}]_{nxm} * [W]_{mx1} \quad \text{and} \quad [SN_i]_{nx1} = [NDA_{ij}]_{nxm} * [W]_{mx1} .$$

Step 7. Normalizing the values of $[SP]$ and $[SN]$ for the alternatives:

$$[NSP_i]_{nx1} = \frac{[SP_i]_{nx1}}{(\max [SP_i]_{nx1})} = \frac{1}{(\max [SP_i]_{nx1})} * [SP_i]_{nx1} \quad \text{and}$$

$$[NSN_i]_{nx1} = 1 - \frac{[SN_i]_{nx1}}{(\max [SP_i]_{nx1})} = 1 - \frac{1}{(\max [SP_i]_{nx1})} * [SN_i]_{nx1} .$$

Step 8. Calculating the appraisal score (AS) for the alternatives:

$$AS_i = \frac{1}{2} (NSP_i + NSN_i) , \text{ where: } 0 \leq AS_i \leq 1 .$$

Step 9. Ranking the alternatives in order of decreasing of appraisal score (AS) worth. The best option among alternatives is the one with highest AS (Keshavarz Ghorabae et al., 2017).

2.5 SELECTION BASED ON RESULTS

Comprehension of the ranking results and implementation of the MCDM-derived selection of exterior wall system, as a part of the thermal envelope in the extension building permit and detailed design project, is set as a final phase of the research.

Acceptance of a hierarchy of exterior wall system alternatives should follow, however if the optimal alternative is not adopted in other cases of building extensions, the research phases could be iterated again.

3 EXTERIOR WALL SYSTEM ALTERNATIVES

In order to avoid a naive discussion about generally known materials that could and should be used as core materials for the addition and extension of a multi-floor residential building and to base the selection on an experiential assessment, the employer was presented with exterior wall systems with different physical structures, thermal capacities, specific gravities, and with different installation methods.

In order to form the exterior wall system, core materials belonging to different groups were selected: groups of polystyrene concrete, ceramic/structural clay products, aerated concrete, as well as wooden and steel structures. Fillings, and internal and external linings were arranged so that all systems could have the most similar thermal properties and be mutually competitive. The aim was to achieve the best possible performance of the previously mentioned components of each system, within the given total maximum thickness of 36 cm, which was presented in Figure 4. As an outcome, only contact façades were evaluated.

A more detailed description of selected exterior wall systems is provided hereinafter, and all eight (8) exterior wall systems will be presented through their data in Table 11.

As decided by the authors of this research, the identity of manufacturers of specific materials shall remain confidential, in order to avoid different interpretations of the quality of certain products. The paper's research focuses on a particular case study and therefore does not offer a general classification of materials at this stage.

3.1 THE EXTERIOR WALL SYSTEM S1 (system belonging to the polystyrene concrete group)

The exterior wall system designated as "S1", presented in Figure 7, is a wall made of polystyrene concrete blocks as core material, with intermittent vertical concrete cores in block cavities. The exterior wall system S1 could be observed through its vertical cross section: interior plaster -1cm, insulated foam block with periodic concrete cores - 30cm, thermal insulation (XPS) - 5cm, and façade acrylic plaster as the outer layer - 0.5cm.

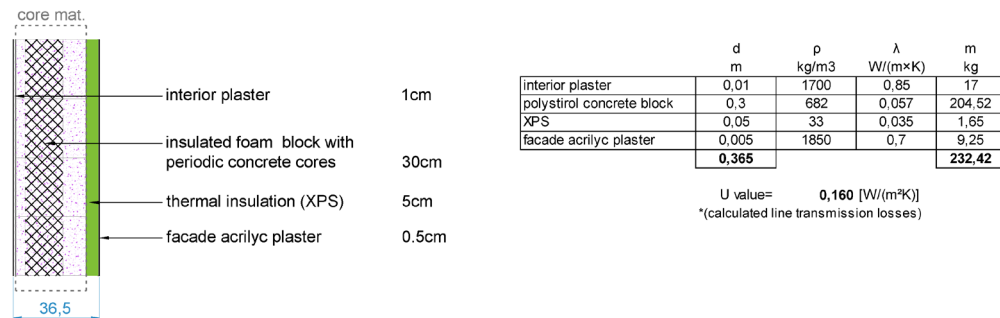


FIG. 7 Exterior wall system S1

This type of wall is characterised by highly rated system solutions in terms of construction, but may have limited availability on the local market depending on the manufacturer and the availability of skilled labour (Table 3). Extremely good thermal characteristics (Ismail et al., 2021), but also high price (Figure 7), are some of the distinctive characteristics of this system.

TABLE 3 Exterior wall system S1: Numerical values by criteria

S1	K1	K2	K3	K4	K5	K6	K7	K8	K9	K10
	232.42	101	33	5	2	0.160	232.42	2	4	2

3.2 THE EXTERIOR WALL SYSTEM S2 (system belonging to the polystyrene concrete group)

The exterior wall system designated as "S2", presented in Figure 8, is an exterior wall system whose core material is made of concrete-core polystyrene or extruded polystyrene blocks filled with concrete, as a very good and precise system solution in terms of construction. The exterior wall system S2 could be observed through its vertical cross section: interior plaster -1cm, insulated foam block with constant concrete cores – 30cm, thermal insulation (XPS) – 5cm, and façade acrylic plaster as the outer layer – 0.5cm.

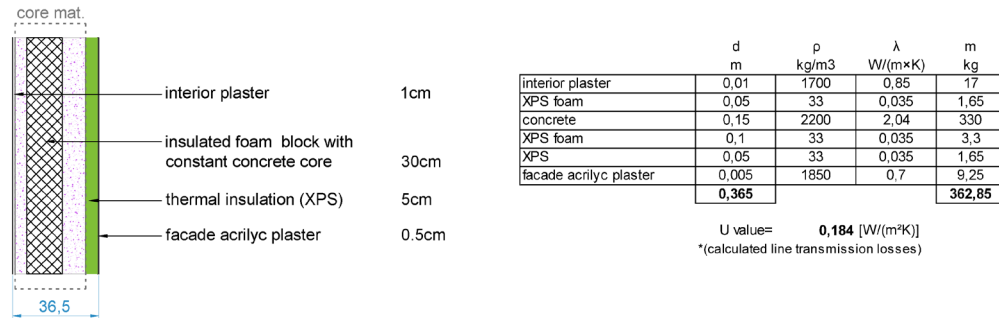


FIG. 8 Exterior wall system S2

This type of wall is characterised by its poor availability on the local market and a significant lack of skilled labour (Table 4). It does not have a wide range of applications, due to smaller design ranges available, however its thermal performances are high (Figure 8). (Ismail et al., 2021)

TABLE 4 Exterior wall system S2: Numerical values by criteria

S2	K1	K2	K3	K4	K5	K6	K7	K8	K9	K10
	362.85	109	32	5	1	0.184	362.85	1	4	1

3.3 THE EXTERIOR WALL SYSTEM S3 (system belonging to the ceramic / structural clay products group)

The exterior wall system designated as "S3", presented in Figure 9, is the system whose core material is made of clay. The exterior wall system S3 could be observed through its vertical cross section: interior plaster -1cm, thermally improved ceramic block – 25cm, thermal insulation (XPS) – 10cm and façade acrylic plaster as the outer layer – 0.5cm.

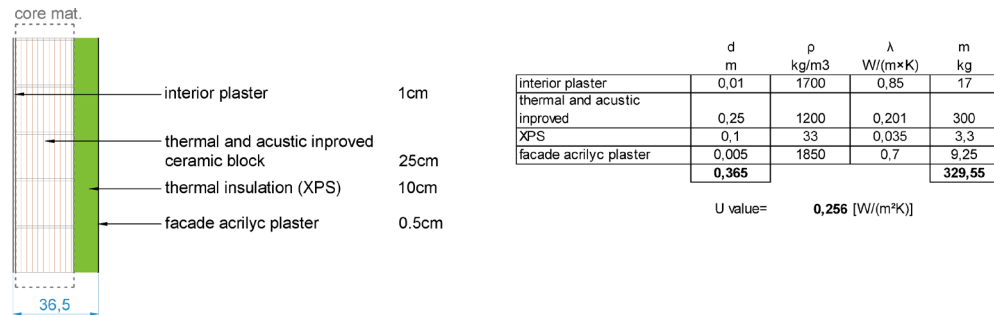


FIG. 9 Exterior wall system S3

It has improved thermal properties (Fioretti & Principi, 2014) due to the geometry of the horizontal cross section of the block, lambda value presented in Figure 8, but due to their dimensions the blocks tend to be heavy, and thus, difficult to handle, and processed later. They do offer good availability on local market, there is qualified labour, but like all walls in this group, they do not have sufficiently good thermal characteristics (Caruana et al., 2017), and during the design phase and the actual execution of work, thermal bridges and linear transmission losses are common (Ismail et al., 2021).

TABLE 5 Exterior wall system S3: Numerical values by criteria

S3	K1	K2	K3	K4	K5	K6	K7	K8	K9	K10
	329,55	71	22	1	5	0,256	329,55	4	2	5

3.4 THE EXTERIOR WALL SYSTEM S4 (system belonging to the group of ceramic / structural clay products)

The exterior wall system designated as "S4" is a standard hollow ceramic block (ISO, 2007b) presented in Figure 10. The exterior wall system S4 could be observed through its vertical cross section: interior plaster -1cm, standard hollow ceramic block – 25cm, thermal insulation (XPS) – 10cm and façade acrylic plaster as the outer layer – 0.5cm.

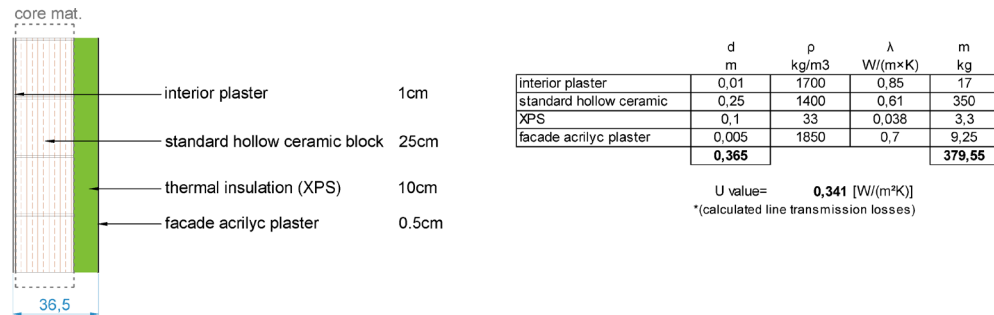


FIG. 10 Exterior wall system S4

System S4, with poor thermal properties (Al-Tamimi et al., 2020), is relatively easy to acquire in the Serbian market, local labour force is available, and the cost of construction is very affordable. (Mijatović, 2008) Though as is true of the previous system, there is a risk of thermal bridges, and consequent condensation, moisture, and mould, which results in major problems in terms of its utility.

TABLE 6 Exterior wall system S4: Numerical values by criteria

S4	K1	K2	K3	K4	K5	K6	K7	K8	K9	K10
	379.55	64	21	1	5	0.341	379.55	5	2	5

3.5 THE EXTERIOR WALL SYSTEM S5 (system belonging to the ceramic / structural clay products group)

The exterior wall system designated as "S5" is presented in Figure 11. Standard brick is the most traditional material (Fioretti & Principi, 2014), which is the basis of the system S5. The exterior wall system S5 could be observed through its vertical cross section: interior plaster -1cm, standard brick (25x12.5x6.25cm) – 25cm, thermal insulation (XPS) – 10cm and façade acrylic plaster as the outer layer – 0.5cm.

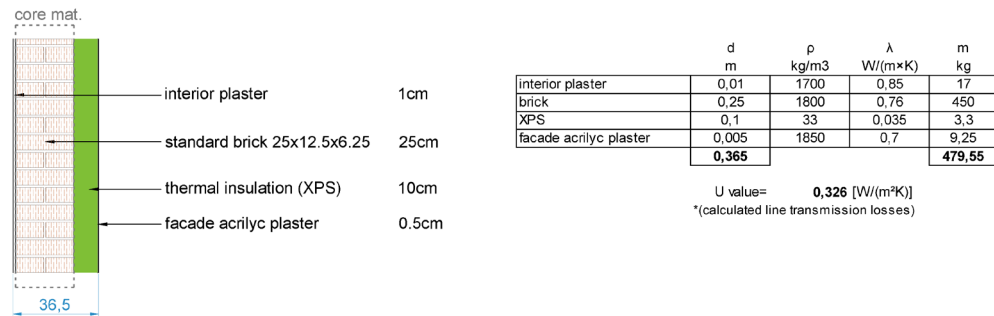


FIG. 11 Exterior wall system S5

This is the system that requires the longest construction time (Mijatović, 2008), and consequently it incurs the highest labour costs (Mijatović, 2008). Construction errors are difficult to correct, despite the fact that elements are easy to process, but subsequent interventions are quite difficult. The great weight of this system ensures the greatest inertia of the building, i.e. temperature stability (Kumar et al., 2017), but it also poses the greatest risk of collapse of the existing structure in the case of poorly installed material. The material is readily available.

TABLE 7 Exterior wall system S5: Numerical values by criteria

S5	K1	K2	K3	K4	K5	K6	K7	K8	K9	K10
	479.55	85	21	2	5	0.326	479.55	5	1	5

3.6 THE EXTERIOR WALL SYSTEM S6 (system belonging to the aerated concrete group)

The exterior wall system designated as "S6", presented in Figure 12, belongs to the aerated concrete group. The exterior wall system S6 could be observed through its vertical cross section: interior plaster -1cm, aerated concrete block – 25cm, thermal insulation (XPS) – 10cm and façade acrylic plaster as the outer layer – 0.5cm.

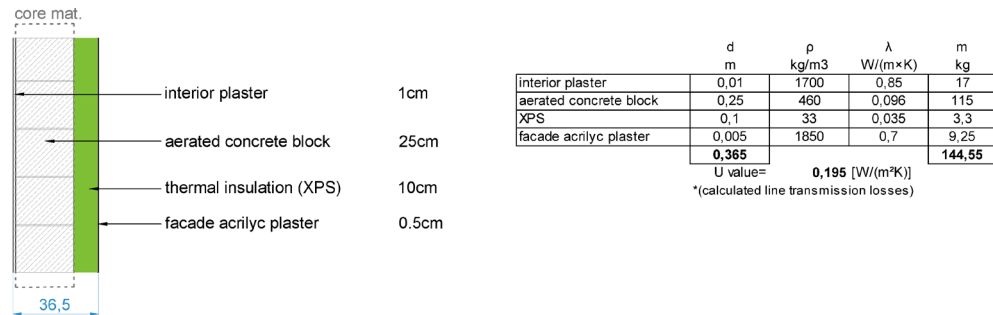


FIG. 12 Exterior wall system S6

With a slightly higher price on the local market than the clay blocks, system S6 is considered to be a desirable exterior wall system due to its plasticity, workability, and relatively good availability on the local market. It has good thermal properties (Ulykbanov et al., 2019), due to its weight aerated concrete block being easy to handle and process, and a labour force is available. The system S6, as observed from practice, is commonly chosen as a (core) building material in Serbia.

TABLE 8 Exterior wall system S6: Numerical values by criteria

S6	K1	K2	K3	K4	K5	K6	K7	K8	K9	K10
	144.55	86	23	4	4	0.195	144.55	4	3	5

3.7 THE EXTERIOR WALL SYSTEM S7 (system belonging to the standard wooden structures' group)

The exterior wall system designated as "S7" is presented in Figure 13. The exterior wall system S7 could be observed through its vertical cross section: double plaster board – 2.5cm, thermal insulation (rockwool) – 8cm, wood board – 2.5cm, thermal insulation (rockwool) between wooden grill construction – 10cm, wood board – 2.5cm, thermal insulation (XPS) – 10cm and façade acrylic plaster as the outer layer – 0.5cm. Construction of this system was decided based on good practice and the traditional assembly of wooden structures. (Gojković, 1989)

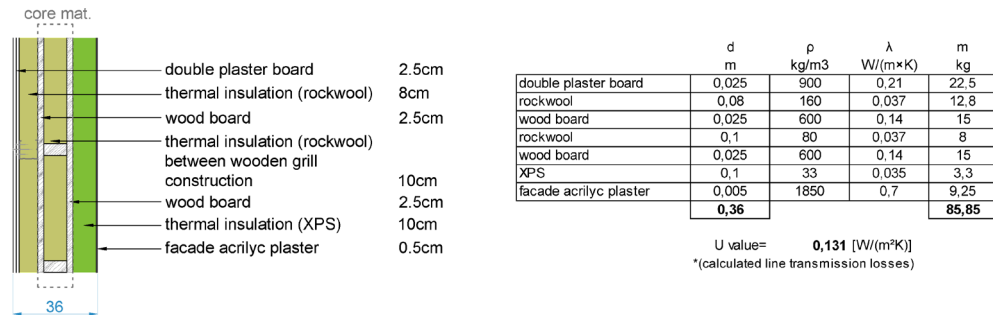


FIG. 13 Exterior wall system S7

The wooden structure of this façade wall has significant advantages, but also limitations. Wood is easily accessible on the local market and it is extremely easy to process. However, a major part of the system consists of thermal insulation materials in the form of filling. Taking into consideration the need to install moisture barriers, multilayer linings, thermal insulation panels, as well as the price thereof, the speed of construction cannot justify the cost (Mijatović, 2008) of such a system. The material is easily accessible, transportable, extremely workable, and easy to handle (Gojković, 1989), but the weight of the wall obtained in this way is low. Therefore, thermal stability represents an unfavourable factor in this system, with summer overheating and winter heat release being poor features of such a wooden wall.

TABLE 9 Exterior wall system S7: Numerical values by criteria

S7	K1	K2	K3	K4	K5	K6	K7	K8	K9	K10
	85.85	92.3	23	3	4	0.131	85.85	3	5	4

3.8 THE EXTERIOR WALL SYSTEM S8 (system belonging to the adapted steel structures' group)

The exterior wall system designated as "S8" is presented in Figure 14. The exterior wall system S8 could be observed through its vertical cross section: double plaster board – 2.5cm, thermal insulation (rockwool) – 8cm, polyurethane sandwich panel – 2.5cm, hollow steel box and steel beam – 8cm, thermal insulation (rockwool) – 8cm, polyurethane sandwich panel – 2.5cm, thermal insulation (XPS) – 8cm and façade acrylic plaster as the outer layer – 0.5cm.



FIG. 14 Exterior wall system S8

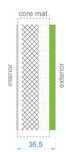
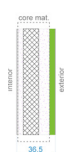

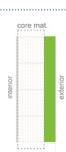


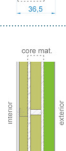
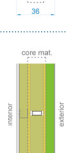
Steel structures are frequently utilized to save space because of their density, which results in compact dimensions as a structural element, ensuring space reductions. Steel structures need a highly qualified workforce for the building process, which has a negative impact on price criteria. The dry process during installation certainly allows a faster completion of the building procedure, and accordingly, like the previous exterior wall system (S7), it differs from the other in terms of the interior layer.

TABLE 10 Exterior wall system S8: Numerical values by criteria

S8	K1	K2	K3	K4	K5	K6	K7	K8	K9	K10
	71.89	97	21	2	3	0.135	71.89	3	4	4

For better comparison, exterior wall systems are presented in Table 11. The table is populated with numerical presentation of systems by determined criteria.

TABLE 11 Presenting values of the alternatives by selected criteria

EXTERIOR WALL SYSTEM	K1	K2	K3	K4	K5	K6	K7	K8	K9	K10
	↓ w ₁ 0,08	↓ w ₂ 0,22	↑ w ₃ 0,06	↑ w ₄ 0,08	↑ w ₅ 0,10	↑ w ₆ 0,12	↑ w ₇ 0,06	↑ w ₈ 0,06	↑ w ₉ 0,06	↑ w ₁₀ 0,06
S1 	232.42	101	33	5	2	0.160	232.42	2	4	2
S2 	362.85	109	32	5	1	0.184	362.85	1	4	1
S3 	329.55	71	22	1	5	0.256	329.55	4	2	5
S4 	379.55	64	21	1	5	0.341	379.55	5	2	5
S5 	479.55	85	21	2	5	0.326	479.55	5	1	5
S6 	144.55	86	23	4	4	0.195	144.55	4	3	5
S7 	85.85	92.3	23	3	4	0.131	85.85	3	5	4
S8 	71.89	97	21	2	3	0.135	71.89	3	4	4

4 RESULTS AND DISCUSSION

With wide range attribute values observed in Table 11, the extension of EDAS method – EDAS+ method (Štilić et al., 2019) was applied as the method eliminates favouring criteria with broader ranges of attribute values. The application of the method began with the presentation of key criteria and direction of the criterion function, weighting factors for the criteria and alternatives for making choices (Table 11). Under Step 2, formation of a decision-making matrix based on calculated values of different exterior wall systems followed:

$$X = [X_{ij}]_{n \times m} = \begin{bmatrix} X_{11} X_{12} X_{13} \dots X_{1m} \\ X_{21} X_{22} X_{23} \dots X_{2m} \\ X_{31} X_{32} X_{33} \dots X_{3m} \\ \dots \dots \dots \dots \dots \\ X_{n1} X_{n2} X_{n3} \dots X_{nm} \end{bmatrix} =$$

$$\begin{bmatrix} 232.42 & 101 & 33 & 5 & 2 & 0.160 & 232.42 & 2 & 4 & 2 \\ 362.85 & 109 & 32 & 5 & 1 & 0.184 & 362.85 & 1 & 4 & 1 \\ 329.55 & 71 & 22 & 1 & 5 & 0.256 & 329.55 & 4 & 2 & 5 \\ 379.55 & 64 & 21 & 1 & 5 & 0.341 & 379.55 & 5 & 2 & 5 \\ 479.55 & 85 & 21 & 2 & 5 & 0.326 & 479.55 & 5 & 1 & 5 \\ 144.55 & 86 & 23 & 4 & 4 & 0.195 & 144.55 & 4 & 3 & 5 \\ 85.85 & 92.3 & 23 & 3 & 4 & 0.131 & 85.85 & 3 & 5 & 4 \\ 71.89 & 97 & 21 & 2 & 3 & 0.135 & 71.89 & 3 & 4 & 4 \end{bmatrix}$$

As the Step 3 process continued with normalisation performed by applying a fair mapping method, it resulted in:

$$R = [R_{ij}]_{n \times m} = \begin{bmatrix} r_{11} r_{12} r_{13} \dots r_{1m} \\ r_{21} r_{22} r_{23} \dots r_{2m} \\ r_{31} r_{32} r_{33} \dots r_{3m} \\ \dots \dots \dots \dots \dots \\ r_{n1} r_{n2} r_{n3} \dots r_{nm} \end{bmatrix} =$$

$$\begin{bmatrix} 0.394 & 0.822 & 1.000 & 1.000 & 0.250 & 0.138 & 0.394 & 0.250 & 0.750 & 0.250 \\ 0.714 & 1.000 & 0.917 & 1.000 & 0.000 & 0.252 & 0.714 & 0.000 & 0.750 & 0.000 \\ 0.632 & 0.156 & 0.083 & 0.000 & 1.000 & 0.595 & 0.632 & 0.750 & 0.250 & 1.000 \\ 0.755 & 0.000 & 0.000 & 0.000 & 1.000 & 1.000 & 0.755 & 1.000 & 0.250 & 1.000 \\ 1.000 & 0.467 & 0.000 & 0.250 & 1.000 & 0.929 & 1.000 & 1.000 & 0.000 & 1.000 \\ 0.178 & 0.489 & 0.167 & 0.750 & 0.750 & 0.305 & 0.178 & 0.750 & 0.500 & 1.000 \\ 0.034 & 0.629 & 0.167 & 0.500 & 0.750 & 0.000 & 0.034 & 0.500 & 1.000 & 0.750 \\ 0.000 & 0.733 & 0.000 & 0.250 & 0.500 & 0.019 & 0.000 & 0.500 & 0.750 & 0.750 \end{bmatrix}$$

Step 4 of the calculation followed:

$$AV = [AV_j]_{1 \times m} = \left[\frac{\sum_{i=1}^n x_{i1}}{n} \quad \frac{\sum_{i=1}^n x_{i2}}{n} \quad \dots \quad \frac{\sum_{i=1}^n x_{im}}{n} \right] = [x_1^*, x_2^*, \dots, x_m^*] =$$

$$[0.463 \quad 0.292 \quad 0.469 \quad 0.656 \quad 0.405 \quad 0.463 \quad 0.537 \quad 0.594 \quad 0.531 \quad 0.719].$$

Steps 5-9, with positive and negative distance from the mean calculations, weighted sum matrices, normalised weighted sums; determined the alternative ranking. Results of the calculation are presented in Table 12.

TABLE 12 Ranking result obtained by applying EDAS+ method

EXTERIOR WALL SYSTEM	SP _i	SN _i	NSP _i	NSN _i	AS _i	RANK
S1	0.352	0.277	0.805	0.389	0.597	1
S2	0.376	0.453	0.858	0.000	0.429	7
S3	0.306	0.240	0.700	0.470	0.585	3
S4	0.438	0.399	1.000	0.120	0.560	5
S5	0.331	0.405	0.757	0.105	0.431	6
S6	0.200	0.128	0.457	0.718	0.588	2
S7	0.269	0.221	0.615	0.512	0.564	4
S8	0.222	0.371	0.507	0.181	0.344	8

As presented in Table 12, calculated AS_i values vary from 0.597 to 0.344, based on which the ranking was obtained. The exterior wall system with the highest AS_i is the best ranked exterior wall system and the results could be observed in the following manner: $S1 < S6 < S3 < S7 < S4 < S5 < S2 < S8$, where the smallest number in the ranking represents the best ranked exterior wall system.

Among eight constructed and presented alternatives of the exterior wall systems, the exterior wall system "S1", a wall made of polystyrene concrete blocks as the core material, with intermittent vertical concrete cores in block cavities, achieved the highest rank by selected and weighted criteria, where the highs of construction possibilities and good thermal characteristics, easy workability and maintainability, counterbalanced the lows of limited availability on the local market, a lack of skilled labour and a high price, among other criteria.

Taking into account the three most highly valued criteria, we could observe that the exterior wall system "S1" (Figure 7) has the most unfavourable values reflected in the price, which is often the key determinant for investors. On the other hand, "S1" values in the other two criteria, thermal mass and thermal conductivity, stay ahead in the competition. By examining the ranking results, the rank of the exterior wall system "S1" could raise the question of production representation, and future prospects of specific core materials on the Serbian market.

In case of selection of the exterior wall system as a part of the thermal envelope for the extension of a multi-family 1938 residential building in Belgrade – Serbia, the Employer accepted the MCDM derived selection, and system "S1" will be used in the project for the extension building permit and detailed design.

5 CONCLUSION

Architecture, urban planning, and energy-efficient construction often recognize the need to take into account a wide range of preferences and opinions, both from experts and residents/users of the facilities (Ogrodnik, 2019). In the architectural – construction industry, selection of the optimal materials and exterior wall systems is a complex task (Tian et al., 2018).

Following the methodology of the research, involving experts as stakeholders through NGT and Delphi based method and applying MCDM method (EDAS+) in the process of selection of the *exterior wall system* as a part of the thermal envelope for the extension of a multi-family 1938 residential building in Belgrade – Serbia, resulted in determining measurable and comparable values of the systems and ranking that was presented.

The question of how to make the most appropriate selection of an exterior wall system, when decisions about material selection frequently come down to a choice based on tradition or recommendations based on the experience of the appointed engineers, was answered through the selection of the optimal and adequate exterior wall system whose rank was not reflected in maximising each of the criteria (Moghtadernejad et al., 2020) but through a balance between the various criteria in the set.

The study's research resulted in an exterior wall selection hierarchy that benefited both the employer and the appointed engineers. The numerical indicator ranked the most commonly used (locally) exterior wall system second, after the S1 system; this comprised a wall made of polystyrene concrete blocks with intermittent vertical concrete cores in block cavities, which is not commonly used in practice in Serbia. The Employer's standpoint shifted from recommendations to concise data on which he could make an educated decision as a result of a systematic decision-making process.

The freestanding, multi-family subject building is typical of the Belgrade municipality where it is located. Bearing in mind the typology of the building and urban constraints in GRP by The Institute of Urbanism Belgrade (2016) for the building area of the local self-government unit – the City of Belgrade, study results are applicable to other cases of building extensions. From this perspective, benefits for the (appointed) engineers could be in support of the exterior wall systems' proposal in future projects.

Even though limitations of the rank could represent its singularity, the case of the extension of the particular 1938 Belgrade building and a "real-life" situation of involved stakeholders' subjective opinions, as well as experts' opinions, through the selection of criteria, assigned weights, and proposed exterior wall systems, provided a replicable systematic decision-making process for selecting an exterior wall system that may be utilized in future extension projects of the same multi-family building typology.

References

- Akanbi, L. A., Oyedele, L. O., Akinade, O. O., Ajayi, A. O., Davila Delgado, M., Bilal, M., & Bello, S. A. (2018). Salvaging building materials in a circular economy: A BIM-based whole-life performance estimator. *Resources, Conservation and Recycling*, 129, 175–186.
- Al-Tamimi, A. S., Baghabra Al-Amoudi, O. S., Al-Osta, M. A., Ali, M. R., & Ahmad, A. (2020). Effect of insulation materials and cavity layout on heat transfer of concrete masonry hollow blocks. *Construction and Building Materials*, 254, 119300.
- Bari, N. A. A., Yusuff, R., Ismail, N., Jaapar, A., & Ahmad, R. (2012). Factors Influencing the Construction Cost of Industrialised Building System (IBS) Projects. *Procedia – Social and Behavioral Sciences*, 35, 689–696.
- Bellamy, L.A., Mackenzie, D.W. (2001) Thermal performance of buildings with heavy walls. *BRANZ Building Research Association of New Zealand study report 108*, 1–45. ISSN: 0113-3675
- Bruen, M. (2021). Uptake and Dissemination of Multi-Criteria Decision Support Methods in Civil Engineering—Lessons from the Literature. *Applied Sciences*, 11(7), 2940. MDPI AG.
- Bylaw on building constructions (2020). Official Gazette of the Republic of Serbia, No.122/2020. Retrieved from <http://www.pravno-informacioni-sistem.rs/SlGlasnikPortal/eli/rep/sgrs/ministarstva/pravilnik/2020/122/1>
- Bylaw on energy efficiency of buildings (2011). Official Gazette of the Republic of Serbia, No.61/2011. Retrieved from <https://www.mgsi.gov.rs/lat/dokumenti/pravilnik-o-energetskoj-efikasnosti-zgrada>
- Caruana, C., Yousif, C., Bacher, P., Buhagiar, S., & Grima, C. (2017). Determination of thermal characteristics of standard and improved hollow concrete blocks using different measurement techniques. *Journal of Building Engineering*, 13, 336–346.
- Chew, M. Y. L., Silva, N., Tan, P. P., & Das, S. (2006). Grading of risk parameters for façade maintainability. *International Journal on Architectural Science*, 7(3), 77–87.
- Chew, M., & Tan, P. (2004). Assessing the Maintainability of Building Façades in the Tropics.
- Chew, M., de Silva, N., & Tan, S. (2004). A neural network approach to assessing building façade maintainability in the tropics. *Construction Management and Economics*, 22(6), 581–594.
- Chew, M.Y.L., De Silva, N. (2004). Factorial method for performance assessment of building façades. *Journal of Construction Engineering and Management*, Vol. 130, No. 4, pp. 525–533.
- Clarke, D. R. (2003). Materials selection guidelines for low thermal conductivity thermal barrier coatings. *Surface and Coatings Technology*, 163–164, 67–74.
- De Toro, P., & Iodice, S. (2017). Evaluation in Urban Planning: a multi-criteria approach for the choice of alternative Operational Plans in Cava De' Tirreni. *Aestimum*, (69), 93–112.
- Donato, M., Zemella, G., Rapone, G., Hussain, J., & Black, C. (2017). An innovative app for a parametric, holistic and multidisciplinary approach to early design stages. *Journal of Façade Design and Engineering*, 5(2), 113–127
- Fajfar, P. (2017). Analysis in seismic provisions for buildings: past, present and future. *Bulletin of Earthquake Engineering*, 16(7), 2567–2608.
- Fioretti, R., & Principi, P. (2014). Thermal performance of hollow clay brick with low emissivity treatment in surface enclosures. *Coatings*, 4(4), 715–731.
- Gojković, M. (1989). *Drvene konstrukcije – fakultetski udžbenik* [Wooden constructions – Faculty textbook]. *Gradevinski fakultet*, Beograd. ISBN: 8623410289 9788623410284
- Greco, S., Ehr Gott, M., & Figueira, J. R. (2016). *Multiple Criteria Decision Analysis*. Springer Publishing.
- Harvey, N., & Holmes, C. A. (2012). Nominal group technique: an effective method for obtaining group consensus. *International Journal of Nursing Practice*, 18(2), 188–194.
- Hecht, A. R. (1977). A Modified Delphi Technique for Obtaining Consensus on Institutional Research Priorities. Research Brief.
- Hendry, E. A. (2001). Masonry walls: materials and construction. *Construction and Building Materials*, 15(8), 323–330.
- Honstede, W.V. (1990). Research into the quality of housing stocks in the Netherlands, *Building Maintenance and Modernization Worldwide*, Vol. 2 (Edited by L.K. Quah), pp. 659–668, Singapore, Longman.
- Hugé, J., & Mukherjee, N. (2018). The nominal group technique in ecology & conservation: Application and challenges. *Methods in Ecology and Evolution*, 9(1), 33–41.
- International Organization for Standardization. (2007a). Building components and building elements — Thermal resistance and thermal transmittance — Calculation methods (ISO 6946:2007). Retrieved from <https://www.iso.org/standard/40968.html>
- International Organization for Standardization. (2007b). Building materials and products — Hygrothermal properties — Tabulated design values and procedures for determining declared and design thermal values (ISO 10456:2007). Retrieved from <https://www.iso.org/standard/40966.html>
- International Organization for Standardization. (2017). Building components and building elements — Thermal resistance and thermal transmittance — Calculation methods (ISO 6946:2017). Retrieved from <https://www.iso.org/standard/65708.html>
- Ismail, M., Chen, Y., Cruz-Noguez, C., & Hagel, M. (2021). Thermal resistance of masonry walls: a literature review on influence factors, evaluation, and improvement. *Journal of Building Physics*.
- Jato-Espino, D., Castillo-Lopez, E., Rodriguez-Hernandez, J., & Canteras-Jordana, J. C. (2014). A review of application of multi-criteria decision making methods in construction. *Automation in Construction*, 45, 151–162.
- Keshavarz Ghorabae, M., Zavadskas, E. K., Olfat, L., & Turskis, Z. (2015). Multi-criteria inventory classification using a new method of evaluation based on distance from average solution (EDAS). *Informatica*, 26(3), 435–451.
- Keshavarz Ghorabae, M., Amiri, M., Zavadskas, E. K., Turskis, Z., & Antucheviciene, J. (2017). Stochastic EDAS method for multi-criteria decision-making with normally distributed data. *Journal of Intelligent & Fuzzy Systems*, 33(3), 1627–1638. <https://doi.org/10.3233/jifs-17184>
- Kumar, S., Tewari, P., Mathur, S., & Mathur, J. (2017). Development of mathematical correlations for indoor temperature from field observations of the performance of high thermal mass buildings in India. *Building and Environment*, 122, 324–342.

- Law on fire protection (2018). Official Gazette of the Republic of Serbia, No.87/2018. Retrieved from <http://www.pravno-informacioni-sistem.rs/SlGlasnikPortal/eli/rep/sgrs/skupstina/zakon/2009/111/2/reg/20181121>
- Law on Planning and Construction (2021). Official Gazette of the Republic of Serbia, No.9/2020. Retrieved from <https://www.mgsi.gov.rs/lat/dokumenti/zakon-o-planiranju-i-izgradnji>
- Linstone, H. A., & Turoff, M. (2002). *The Delphi Method*. Van Haren Publishing.
- Marković, Z. (2007) Jedan pristup normalizaciji matrice podataka u višekriterijumskoj analizi. [One of the approaches to the normalization of the data matrix in multi-criteria analysis]. XXV Simpozijum o novim tehnologijama u poštanskom i telekomunikacionom saobraćaju [XXV Symposium on New Technologies in Postal and Telecommunication Traffic]. *PosTel 2007*, 71–80.
- Mathew, M., & Sahu, S. (2018). Comparison of new multi-criteria decision making methods for material handling equipment selection. *Management Science Letters*, 139–150.
- McAdam, B. (2010). Building information modelling: the UK legal context. *International Journal of Law in the Built Environment*, 2(3), 246–259.
- Mijatović, R. (Ed.). (2008). *NORMATIVI I STANDARDI RADA U GRAĐEVINARSTVU, VISOKOGRADNJA, GRAĐEVINSKI RADOVI, KNJIGA 1 I 2* [Normatives and Standards in Construction, Building Construction and Construction Works, Book 1 and 2]. *Građevinska knjiga*. ISBN: 978-86-395-0543-1
- Moghtadernejad, S., Chouinard, L. E., & Mirza, M. S. (2018). Multi-criteria decision-making methods for preliminary design of sustainable façades. *Journal of Building Engineering*, 19, 181–190.
- Moghtadernejad, S., Chouinard, L. E., & Mirza, M. S. (2020). Design strategies using multi-criteria decision-making tools to enhance the performance of building façades. *Journal of Building Engineering*, 30, 101274.
- Moghtadernejad, S., Mirza, M. S., & Chouinard, L. E. (2019). Façade Design Stages: Issues and Considerations. *Journal of Architectural Engineering*, 25(1)
- Mukherjee, N., Dicks, L. V., Shackelford, G. E., Vira, B., & Sutherland, W. J. (2016). Comparing groups versus individuals in decision making: a systematic review protocol. *Environmental Evidence*, 5(1), 1–9.
- Ogrodnik, K. (2019). Multi-Criteria Analysis of Design Solutions in Architecture and Engineering: Review of Applications and a Case Study. *Buildings*, 9(12), 244.
- Pérez-Lombard, L., Ortiz, J., González, R., & Maestre, I. R. (2009). A review of benchmarking, rating and labelling concepts within the framework of building energy certification schemes. *Energy and Buildings*, 41(3), 272–278.
- Puška, A. (2013). Normalizacija podataka i njen uticaj na rangiranje investicionih projekata [Normalization data and impact of in ranking investment projects]. *Poslovni Konsultant*, 5(22), 30–41.
- Rückert, K., Shahriari, E., & Markaz-i Tahqīqât-i Sâkhtimân va Maskan (Iran). (2014). Guideline for Sustainable, Energy Efficient Architecture & Construction. *Deutscher Universitätsverlag*. ISBN: 6001131147.
- Šiožinytė, E., & Antuchevičienė, J. (2013). Solving the problems of daylighting and tradition continuity in a reconstructed vernacular building. *Journal of Civil Engineering and Management*, 19(6), 873–882.
- Štilić, A. (2020). Novel EDAS++ method: Interval type criteria and extension to EDAS. *Turisticko Poslovanje*, 25–26, 39–52. <https://doi.org/10.5937/turpos0-29612>
- Štilić, A., Nicić, M., Zimonjić, B., & Njeguš, A. (2019). Application of multi-criteria method EDAS in tourism industry candidates' ranking and the introduction of corrective step. *Turisticko Poslovanje*, 23, 61–75. <https://doi.org/10.5937/turpos0-21644>
- Stojanović, Z., Kurtović-Folić, N., & Jakovljević, Z. (2004). Predmer i predračun radova [Bill of Quantities and Estimate of Works]. *Studio 14*. ISBN: 86-905335-0-8
- The Institute of Urbanism Belgrade. (2016). General Regulation Plan (GRP) for the building area of the local self-government unit – the City of Belgrade (units I-XIX). *Official Gazette of the City of Belgrade*, No.20. Retrieved from https://www.beoland.com/wp-content/uploads/planovi/pgr-beograda/PGR_Tekst_SL_20-2016.pdf
- Tian, G., Zhang, H., Feng, Y., Wang, D., Peng, Y., & Jia, H. (2018). Green decoration materials selection under interior environment characteristics: A grey-correlation based hybrid MCDM method. *Renewable and Sustainable Energy Reviews*, 81, 682–692.
- Ulykbanov, A., Sharafutdinov, E., Chung, C. W., Zhang, D., & Shon, C. S. (2019). Performance-based model to predict thermal conductivity of non-autoclaved aerated concrete through linearization approach. *Construction and Building Materials*, 196, 555–563.
- Van de Ven, A., Delbecq, A. L., & Nominal Versus Interacting Group Processes for Committee. (1971). Decision-Making Effectiveness. *Academy of Management Journal*, 14(2), 203–212.
- Weber, E. U., & Johnson, E. J. (2009). Mindful judgment and decision making. *Annual review of psychology*, 60, 53–85.
- Wen, Z., Liao, H., Zavadskas, E. K., & Antuchevičienė, J. (2021). Applications of fuzzy multiple criteria decision making methods in civil engineering: a state-of-the-art survey. *Journal of Civil Engineering and Management*, 27(6), 358–371.
- Yeoh, B. (1990). Singapore – Singapore. Compiled by Stella R. Quah and Jon S.T. Quah. World Bibliographical Series Vol. 95. Oxford, Santa Barbara, Denver: Clio Press, 1988. Pp. 258. Map, Indexes. *Journal of Southeast Asian Studies*, 21(2), 504–506.

Towards a Human Centred Approach for Adaptive Façades

An Overview of User Experiences in Work Environments

Mine Koyaz^{1-2*}, Alejandro Prieto³⁻⁵, Aslıhan Ünlü⁴, Ulrich Knaack³

* Corresponding author

1 Istanbul Technical University, Construction Sciences Doctoral Program. Turkey, koyaz@itu.edu.tr

2 Istanbul Bilgi University, Faculty of Architecture, Department of Architecture. Turkey

3 Delft University of Technology, Faculty of Architecture and the Built Environment, Department of Architectural Engineering + Technology, Architectural Façades & Products Research Group. The Netherlands

4 Özyeğin University, Faculty of Architecture and Design. Istanbul, Turkey

5 Universidad Diego Portales, School of Architecture; Faculty of Architecture, Art and Design. Santiago, Chile

Abstract

Adaptive façades are multifunctional systems that are able to change their functions, features, or behaviour over time in response to changing boundary conditions or performance requirements. As one of the significant developments in the façade industry over the last decade, the adaptive façade offers an intelligent solution that can decrease energy consumption and potentially increase users' comfort in a building. From an engineering perspective, these advanced technologies aim to improve the overall performance of the building while generating a better indoor environment for the users, but unfortunately, investigations show that this goal is not always achieved. This is why, to bridge this performance gap, we embark on a change of perspective in façade design, from a technology-centred to a human-centred one. This research emphasizes that, with their changeability aspects, adaptive façade technologies offer unique potential, although the design of such façades requires a deeper understanding of users. With this as its focus, this paper aims to identify the factors affecting the user experience in a working environment, considering the interactions of the user with building services and façade systems from a holistic point of view, in which façade-user relationships are to be distinguished, towards the larger aim of developing a human-centred approach for adaptive façade design.

Keywords

human centred design, user experience, adaptive behaviour, adaptive façade, façade design, changeability, interaction

DOI

<http://doi.org/10.47982/jfde.2022.1.02>

1 INTRODUCTION

The complex multifunctional aspects of façade design hold an inherent duality between optimizing the energy performance of a building and providing comfort for its users (Klein, 2013). Although these two sides are inseparable and highly intertwined, as a result of their conflicting nature one could be easily overlooked in favour of the other, which unfortunately would result in poor design on both sides.

Worldwide, there have been several research projects that have searched for new ways and developed new technologies to design more energy efficient buildings for a more sustainable future (Aelenei et al., 2018). The belief that “technology will save us” has been a clear trend in building engineering, but there has been a general disregard for the people who will use it. Even with the use of high technology solutions, in practice we may end up with the following scenarios: a building may be highly energy efficient but its users could be dissatisfied or because of users’ interference the building may not achieve the predicted levels of energy performance and we may end up with dissatisfied users anyway (Lazarova-Molnar & Mohamed, 2017).

Since the façade is the *mediator* between the exterior and interior environments, it could be said that its design is the key to shaping the whole performance of the building (Knaack et al., 2014). However, implementing high technology solutions to reduce energy consumption should not turn the façade into a *barrier* between the indoor and outdoor, which would create hermetically sealed spaces in which every physical aspect is regulated through HVAC systems (Addington, 2009). Instead, the façade needs to be carefully designed and integrated with the service systems, where smart technologies would be used as the tools to provide desired indoor environmental conditions in harmony with the users and to find an optimal energy efficient balance. In order to achieve that goal, a human-centred approach in façade design, rather than a technology centred focus, needs to be embraced.

The current applications of high performance buildings with smart building automation systems stress even further the need for such human-centred approach (Capeluto & Ochoa, 2017). These so-called intelligent systems are creating new pathways for user interactions, where user expectations and user experiences are changing along with it (Kaasinen et al., 2013). *Wigginton and Harris* used the analogy of the human body’s neural system to explain their user-centred perspective on the topic, in which the *somatic* system that is responsible for the voluntary actions of the muscles that create movement is likened to the actions of the users in the building. Conversely, the *autonomic* system refers to the building’s intrinsic responsive envelope (Wigginton & Harris, 2002). This approach highlights the co-existent nature of users’ adaptive behaviours and the automated dynamic responses of the building systems.

A paradigm shift from occupants being *passive* subjects in a building to being *active* participants has begun by acknowledging the effects of occupant behaviour on the energy performance of the building (Yan & Hong, 2018). Although significant efforts are being made to better understand and simulate the adaptive behaviours of the users, the influencing factors behind these interactions and how these affect the user experience in the first place, are still quite theoretical (Heydarian et al., 2020). There needs to be further interdisciplinary studies investigating multi-domain exposure situations on users’ satisfaction and behaviour, humans’ perception of the built environment, and user-oriented design of the control interfaces, in order to achieve an occupant-centric building design approach (O’Brien et al., 2020).

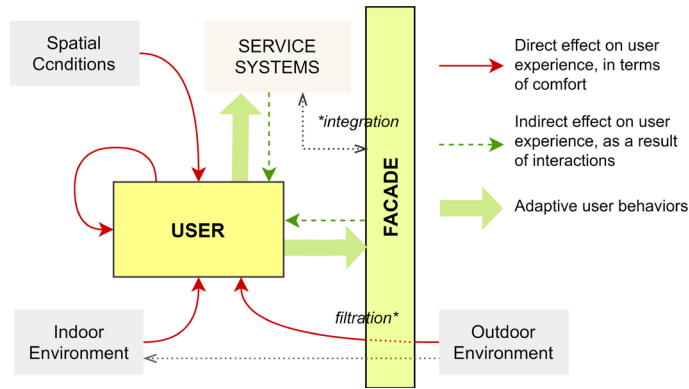


FIG. 1 Façade – User – Building relationships

There are many factors affecting and shaping users' experience in a building (Figure 1). The feeling of comfort (or discomfort) brought about by the effects of the factors related to the indoor and/or outdoor environment, spatial conditions, as well as the individual parameters related to the user itself are the main elements that could be listed. It is not just the comfort-related satisfaction, but also the overall user sensation and perception that results in interactions with the building façade and/or service systems, that are important parts of the user experience in the indoor environment (Law et al., 2009). Considering the amount of time we spend inside, especially in work environments, several studies highlight the importance of users' comfort and wellbeing on their health and productivity (Bluyssen, 2019; Fisk, 2000; Humphreys, 2005).

Even though the façade is highly significant in shaping the indoor environment, there seems to be a lack of understanding about its effects on the overall user experience (Alavi et al., 2017). Even in low technology buildings, the façade is a system that users commonly engage with, by opening the windows, closing the window blinds, or simply by looking outside. It does not seem far-fetched to state that these interactions have a crucial effect on users' experience, while they also create a gap between the predicted and achieved performance of the building (Masoso & Grobler, 2010). Such adaptive behaviours of users are one of the key factors that influences a building's design, performance optimization, and energy simulation (Yan & Hong, 2018). In the case of adaptive façades, with their smart and dynamic automation systems, it could be said that interactions between the façade and the user become even more significant. From an engineering perspective, being able to change façade properties would enhance their performance –by providing dynamic responses to ever-changing external stimuli–, but this dynamic character may also enhance the effect of the façade on the user experience, hence, it may also potentially deepen the aforementioned performance gap.

There is a limited number of studies focusing on adaptive façades, investigating the comfort and well-being of the users as they relate to their interactions. In a recent study, *Luna-Navarro* presents a classification scheme for different pathways in occupant façade interaction, which offers a deeper understanding of the conflicts and relationships between the user and intelligent control strategies in adaptive façades (Luna-Navarro et al., 2020). Another study on occupant-centric control strategies for adaptive façades discusses the implementations of adaptive comfort models and personalized control strategies to improve user satisfaction (Tabadkani et al., 2021). In addition, there are a few other research studies on post-occupancy evaluations and real-time occupant feedback in buildings with adaptive façades, demonstrating the influences of different physical factors on the feeling of comfort in users (Alavi et al., 2017; Attia et al., 2018; Bakker et al., 2014; Lassen et al., 2021; Luna-Navarro et al., 2021).

Acknowledging the contributions of such research towards reaching a human-centred adaptive façade, the influence of human factors on user behaviours and the indirect effects of interactions on the user experience still requires further investigation. Therefore, this paper (1) investigates how different factors affect the user experience in a working environment, (2) presents an overview of adaptive user behaviours with a human-centred approach, (3) distinguishes the façade - user relationship within the larger context, and (4) identifies the missing links towards reaching the full potential of adaptive façades.

A holistic perspective is embraced in this study and the presented overview is built over the user experience concept, which covers all human senses, emotions, behaviours, and interactions with the façade and/or environment. With this focus, this paper aims to bring the scattered information in the literature from different fields of expertise like engineering, architecture and social sciences together, ensuring that not just the effects of the environmental factors but also the human factors on user experience are investigated. As a broader aim, the information provided in this paper offers a starting point towards developing a human-centred approach for adaptive façades.

2 SCOPE AND METHOD OF RESEARCH

Research presented in this paper starts with an initial exploration of literature, which draws the context for further investigation. Exploratory research is conducted using Science Direct, Google Scholar, ITU and TU Delft Libraries, with the keywords: *human-centred design, adaptive façade, user experience*. Because of the lack of literature specifically focused on the façade and user relationship, the scope of the overview later widens to involve: *human-centred design in various fields, façade technologies and applications (traditional or advanced), façade properties and performances in general (physical and energy related), user comfort, satisfaction, well-being, and related studies to improve indoor environment quality*. After reading the titles, abstracts, keywords, and highlights of the papers collected in the initial exploration, the context of the detailed investigation is formulated. Figure 2 below portrays the research boundaries around respective keywords and concepts, presents an outline of this paper, and draws the relationship of its sections.

The users or the occupants are the main *subjects* of this overview. The *scope* of the study evolves around the user experience concept, which embraces a holistic approach to cover the users' comfort, satisfaction, and well-being, as well as users' emotions, behaviours, and interactions. The relationship between these concepts and their relevance to user experience are examined through studies of human-centred design, from different fields (social sciences, industrial design, environmental psychology, etc.). Although the main *focus* is on the adaptive façades and distinguishing its dynamic relationship with the users, since there is a scarcity of literature with this specific focus, studies related to user experience in indoor environments are investigated in general. Workplaces are chosen as the main *domain* of the research. In order to define a whole list of influencing factors, several *agents* of the indoor environment and adaptive façades are searched within the context of user experience. Thus, various studies evaluating users' comfort during the occupancy stage, theoretical studies investigating different parameters affecting user's satisfaction, studies regarding users' adaptive behaviours and the motivations behind that, users' effects on the energy performance of the building, studies investigating occupant-centric design and automation of the adaptive façade, and other relevant studies within its broader reach, formed part of the review process.

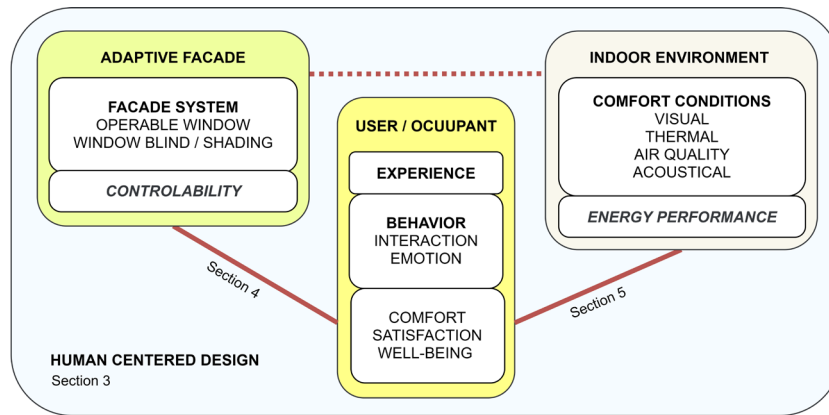


FIG. 2 Scope and boundaries of the research

As for the structure of the paper, Section 3 presents background information on different approaches of *human-centred design* to establish the point of view of this research, and to describe the relationship between adaptive behaviour and user experience. Section 4 introduces the potentials of adaptive façades, presents a brief overview of their relationship with the users, identifying the missing links, demonstrating the perspective of the authors and relevance of the research. Section 5 is the main body of the paper, where the findings of the review process are presented in a systematic way and different factors affecting user experience in working environments are identified, through a mechanism of change. Lastly, Section 6 presents an overall discussion and highlights relevant issues that require further investigation for a human-centred approach for adaptive façades.

3 HUMAN-CENTRED DESIGN

Human-centred (or centric) design is a concept which, over the years, has found application in various different fields, mainly in industrial design and software engineering (Hoffman et al., 2002). Different approaches to the concept in architecture and related behavioural theories that highlight a deeper understanding of the user experience are overviewed in this section.

3.1 HUMAN-CENTRED DESIGN APPROACHES

Norman describes human centred design as *the process which ensures that the designs match the needs and capabilities of the people for whom they are intended* (Norman, 1988). In other words, it is a philosophy that starts with understanding humans, to support the design of a useful, usable, pleasurable, and meaningful product/system (IDEO.org, 2015; Norman, 2013).

Designing *for* the users has been a part of design thinking since early ages. The evolution of the concept has started with the consideration of the physical *ergonomics* of the users while engaging with the product/system (Verbeek & Slob, 2006). Later, this concept evolved into *usability*, which covers the effectiveness, efficiency, and satisfaction in a specified context of use (ISO 9241-210, 2010). Then, the consideration of *emotions*, *behaviours*, and users' *experiences* became part of the approach, often referred to as *interaction design* in the literature (T. Zhang & Dong, 2008). Recent approaches aim to cover not just the present experiences but also the *needs and aspirations* of the future (van

der Bijl-Brouwer & Dorst, 2017). Designing *with* the users on the other hand, by means of involving them in the design process (participatory design and generative techniques) or asking for feedback regarding the design (human-computer interaction), could be traced back to the 1970s – 1980s (Damodaran, 1996; Maguire, 2001; Visser et al., 2005; Zoltowski et al., 2012).

Sanders maps the different human-centred approaches in design practice and defines the designer's mindset as two categories; *expert* or *participatory* (Sanders, 2008). Expert mindset refers to the case where users are seen as *subjects* and the design aims to achieve the best possible usability for them. Participatory mindset, on the other hand, refers to the case when users are seen as *partners* and are actively involved in the design process from the beginning (Abrams et al., 2004). Involvement of the users in the design phase is a way of ensuring that the design would match their needs, but unfortunately, there are operational barriers (Chammas et al., 2015). Consequently, in the case of building design, engagement of the users mostly occurs only at the occupancy phase, in the form of post-occupancy evaluations with real-time occupant sensing and/or feedback technologies (Wagner et al., 2018).

A collective perspective of the different approaches is offered by ISO 9241-210, where the human-centred design is defined as *an approach to systems design and development that aims to make interactive systems more usable by focusing on the use of the system and applying human factors/ergonomics and usability knowledge and techniques* (ISO 9241-210, 2010). Feedback and communication between the stakeholders (users and designers) are highlighted as the key to this approach. By acknowledging ISO's definition of human-centred design and embracing an *expert* mindset, we are taking the user as the subject of this research. Hence, we start by investigating how users interact with and experience their surroundings, thereby aiming to translate and transfer the information learned from users to the designers.

3.2 ADAPTIVE BEHAVIOUR AND USER EXPERIENCE RELATIONSHIP

The term experience is used to define the encounter of an event or occurrence and the *takeaways* from it. It could be a piece of knowledge, a skill or an impression, a feeling. In other words, experience defines *how people remember their interactions* (Norman, 2013). From a human centred point of view, any system that interacts in some way with its users should be designed with consideration given to users' needs and capabilities. Therefore, in order to achieve the *best* user experience, it is crucial to understand the factors that shape the nature of such interactions and how these may differ from one individual to another.

According to the *stages of action* model (Norman, 2013), an action (or behaviour) like opening a window is a *goal-driven* activity that could be triggered by various different physiological, psychological, or sociological factors. The activity starts by making the decision to take action, which is defined as the *planning* stage, followed by *specifying* the action and *performing* it by engaging with the window. The effects of the action will begin to show themselves, like creating changes in the air quality and temperature of the room. Then the user will *perceive* the new condition, *interpret* the reason behind it, *compare* it with the previous situation and make a decision to either close the window or keep it open. In this instance a *data/event-driven* activity occurs, which has surfaced as a result of the user's emotions in the initial condition (Naqvi et al., 2006). In other words, the perception of the environment triggered the interaction with the surroundings, while at the same time the interaction created a change in the perception.

Even though *Norman's* model defines a certain loop between perception and behaviour, it does not explain what exactly drives the behaviour itself. There are several other cognitive behaviour theories used in explaining occupant interactions with different building systems. From these theories, five commonly acknowledged models could be listed as: Theory of Reasoned Action - TRA, Theory of Planned Behaviour - TPB, Theory of Interpersonal Behaviour -TIB, Norm Activation Model – NAM and Value, Belief, Norm Theory – VBNT (Ajzen, 1991; Heydarian et al., 2020; Triandis, 1977), in which *affect*, *attitude*, *social norms*, *perceived control*, and *habits* are referred to as the main elements that create the *intention* of taking an action. *Affect* refers to what the organism feels, and defines the value, in other words, the quality of the experience. Interpretation of such feelings could be referred to as emotions that shape preferences for the future or moods for the present situation (Ortony et al., 2005). Along with the affect, different *personal or social norms* and individual *beliefs* are also related to the *intention* of a behaviour (Pee et al., 2008). The *perceived control* and individual's *attitude* towards taking an action are other elements that generate behavioural motivations (Heydarian et al., 2020). In addition to these conscious behaviours, *habit* refers to a sequence of behaviour that has become an automatic response to specific cues in the environment (Verplanken & Aarts, 1999), which can be defined as an unconscious behaviour or an intentional one.

All in all, a behaviour could surface because of a poor affect, with the intention to make it better and as a result, it will create an interaction to change the values of the experience. This phenomenon could also be explained with the concept of adaptive behaviour which is often referred to in the literature as follows: *if a change occurs such as to produce discomfort, people react in ways that tend to restore their comfort* (Nicol & Humphreys, 2002). Such comfort-driven behaviours are an important part of the user experience and simultaneously affect the overall energy performance of the building by creating unforeseen energy consumptions (Jia et al., 2017; Stern, 1992)

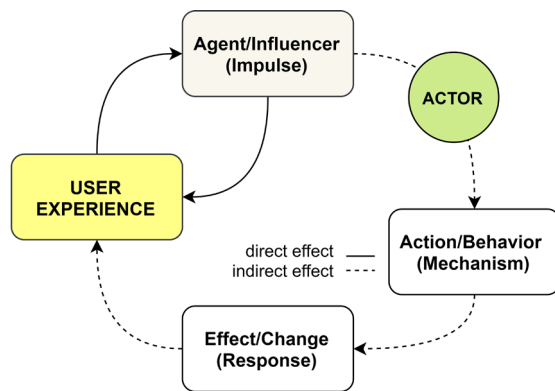


FIG. 3 The dynamic cycle of the user experience: the mechanism of change

Within the context of the built environment, users' behaviours, in terms of interactions with the building's service systems or façades, are significant elements of the user experience, which either (1) shape or (2) reflect upon the experience itself (Alavi et al., 2017). These behaviours may differ for each individual, due to their different physiological, psychological, or sociological conditions/backgrounds (Khalid, 2006). Therefore, understanding the mechanism of change is considered to be an important step towards defining how different factors affect the user experience in work environments.

4 POTENTIALS OF ADAPTIVE FAÇADES

The previous section introduced the dynamic cycle of user experience over a mechanism of change (Figure 3). In the case of adaptive behaviours, users are the actors that trigger the mechanism of change. Influencers that affect the users' behaviours may be related to human or environmental factors, which will be overviewed in the following section in relation to the user experience. Triggered by those factors in a case of discomfort, to achieve a more desired comfort condition, users can either choose to alter themselves, like changing their clothing level or the occupancy conditions, or they can alter their environmental conditions by interacting with the building's façade and/or service systems (O'Brien & Gunay, 2014) (Figure 4). Adaptive façades with their smart automation systems have a similar mechanism of change, by creating an artificial response to certain impulses, which results in a change in the indoor environmental conditions.

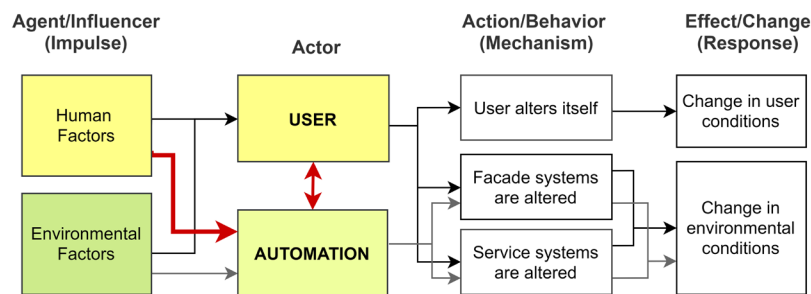


FIG. 4 Relationship of factors indirectly affecting user experience

If we take a holistic approach to façade design, it could be said that today's challenge is to find an energy efficient façade solution that would also create a positive user experience. To deal with that complexity, and with their changeability aspect, adaptive façades offer a unique opportunity. This research explores the hypothesis that there is a missing link (shown in red lines on Figure 4) between the human factor and the adaptive façade. The operation of the adaptive façade by means of automation should regard the human factors as agents, along with the environmental factors. Moreover, automation systems should be designed to co-exist with and learn from the users' adaptive behaviours, and to consider the indirect effects on the user experience. If these gaps could be bridged, only then would adaptive façades reach their full potential.

Adaptive technologies have the potential to significantly reduce the energy use of the buildings (Perino & Serra, 2015) along with having a profound influence on user satisfaction (Attia, 2017). The performance of the adaptive façade – in terms of comfort and energy – is highly dependent on its dynamic operation strategies (Favoino et al., 2018). The automation system is another actor like the user, which is used to manipulate the change in indoor environmental conditions, thus directly and/or indirectly altering the user experience. Therefore, design consideration of an adaptive façade system should consider the implementation of occupant-centric automation and integration with the operation of other building services systems, along with the functional requirements of the façade.

Each adaptive façade technology (such as movable solar shading, switchable glazing, phase change materials, dynamic insulation, multifunctional façades ...etc.) requires a unique consideration since they offer different ways of interaction with the user and may have different effects on users satisfaction and well-being (Attia et al., 2019). In terms of a human-centred design approach to

adaptive technologies, existing studies and performance modelling approaches are limited to considering environmental factors as the main agent of change, thus missing the relationship with the human factors and user experience.

Along this path, one of the key issues that needs to be investigated is the balance between automation and user control. Adaptive façades controlled by an intelligent automation system could be designed to predict a possible result of discomfort and act on behalf of the users to alter the indoor environmental conditions (Böke et al., 2020). However, there are also studies indicating that users are more satisfied, happier, and more productive when they are given at least a certain degree of control (Samani, 2015). This opens up the discussion on how much control should be left to the users considering the building's energy performance. Educating the users and improving the response feedback mechanism would be the highlighted ways to deal with a possible performance gap between the predicted and actual energy consumption of the building (Al-Obaidi et al., 2017).

Another issue is the diversity of each user's needs and preferences. There have been several studies aiming to model the reasoning behind users' behaviours and simulate them in order to demonstrate the actual energy performance (Yan et al., 2015). However, it is quite impossible to predict how each user would react to a certain situation. From another perspective, despite the variety of each human factor and its endless combinations, by observing user's behaviour under certain conditions, it could be possible to identify some user types (Ortiz, 2019), which requires a deeper understanding of the human factor and an interdisciplinary study that incorporates architecture, engineering, and social science. From an expert point of view, by identifying what are the key factors that affect the experience and how they show diversity, the level and type of adaptation that is needed for certain user types could be defined. Thus, this would be used as a starting point towards a human-centred adaptive façade design approach.

From this perspective, which aims towards a human centred design approach, we are looking from the users' point of view to understand what experiences that they expect from their façades. Identifying the complex and dynamic mechanisms of the user experience in an indoor environment (workspaces in the context of this paper) would be the first step. To that end, this research investigates how each factor affects the mechanism of change and portrays a better understanding of the triggers that make users take action. From there, it would be possible to (1) identify certain patterns in users' adaptive behaviours that could be mimicked with the adaptive façades, (2) determine the effects of human factors and define certain expectancies of different user groups, (3) distinguish certain aspects of the façades that need to be variable in order to satisfy individual adaptive comfort needs.

5 USER EXPERIENCE IN WORK ENVIRONMENTS

User experience is defined as *a person's perceptions and responses that result from the use or anticipated use of a product, system, or service* (ISO 9241-210, 2010; Law et al., 2009). It is a concept that not only covers the past and present experiences but also those *anticipated* for the future. In the context of this paper, experience is used as a holistic term to cover all human senses and refers to any kind of emotion, perception, sensation over interaction, and any feeling of comfort, satisfaction, or well-being.

Although the façade is one of the main systems that shapes the indoor environment, there has been only a limited number of studies exploring how it affects users' experiences. The ways in which users engage with their façade and experience it could be defined in two ways: *active or passive*. (1) Passive experience refers to the perception, for instance, of feeling the sunlight coming through the glazing or looking outside the window. (2) Active experience refers to interaction, for instance, opening the window because of feeling warm, closing the window blind to prevent glare. In other words, passive experience indicates a path for the direct effect of an influencer, while active experience draws an indirect path where certain behaviour is triggered.

Based on the review of the existing literature, the effects of different factors on the user experience, in a working environment, are identified. Figure 5 shows the relationship of the parameters from the findings of the review, which are systematically organized in a way to demonstrate the dynamics between the influencing factor, the mechanism that is triggered by it, the response that results in a change of the initial state, and how this whole cycle affects related user experiences (Figure 3).

Referring to the aforementioned mechanism of change, we classify the influencing factors under two main groups: *human* and *environment*. According to occupant behaviour studies, it could be said that it is not only physical factors of the environment, but also the individual factors for each user, that influence the experience in an indoor environment (Frontczak & Wargocki, 2011). As the elements that could be easily manipulated by the building design, the general tendency in the related research projects is to focus on the environmental factors. There are only a few studies that investigate the diversity of individual factors and their relationship with users' adaptive behaviours (Hong et al., 2017). Taking the human as the centre of focus, first of all, *personal descriptors and needs* that are different for each individual and which affect the experience are outlined. Environmental factors, on the other hand, are related to the surroundings of the user. On a building scale, these would be divided into three subcategories: *external, internal, and spatial* factors.

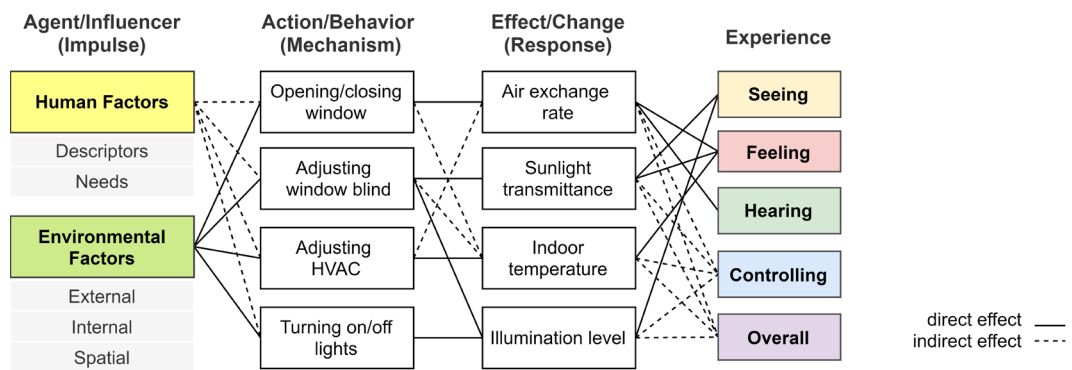


FIG. 5 Relationship between the parameters within the mechanism of change

The main adaptive behaviours that users would take to alter their indoor environment, based on the common mentions within the existing literature as potential causes of unpredicted energy consumptions, could be listed as (1) *opening/closing windows*, (2) *adjusting window blinds (shading elements)*, (3) *adjusting HVAC systems (heating, cooling, ventilation units)*, (4) *turning on/off lighting* (Boerstra, 2016; Delzendeh et al., 2017; Nicol & Humphreys, 2002). In addition to these, in cases of discomfort, users may also choose to (5) *adjust their clothing* or upon arriving/departing the space (6) *change their presence* without engaging with their surroundings (Haldi & Robinson, 2008; Zhang et al., 2018). The main focus of this paper is on the experiences of the users that resulted

from their comfort-driven interactions with their façade and integrated service systems, thus the first four behaviours that require engagement with the windows, shading, HVAC, or lighting systems are investigated, in the context of a working environment. Each of these actions creates a reaction and alters at least one of the properties of the façade and/or the indoor environment. These could be respectively defined as the changes at (1) *air exchange rate*, level of (2) *sunlight transmittance*, value of (3) *indoor temperature*, (4) *illumination level* (Frontczak & Wargocki, 2011; Wagner et al., 2018). The changed conditions that resulted from the adaptive behaviours indirectly affect the user experience, and thereby become an influencer once again.

As mentioned before, within the context of this research, the *user experience* concept is issued from a holistic point of view that covers all human senses, emotions, behaviours and interactions with the façade and/or environment. It not only refers to a state of comfort or discomfort, but it is about the overall sense of satisfaction that occurs before, during, and after use (ISO 9241-210, 2010; Law et al., 2009). Therefore, from a human-centred point of view, this paper takes the human senses to its centre and classifies user experiences as *seeing, feeling, hearing, and controlling*. The aim is to broaden the commonly used visual, thermal, air quality, and acoustical comfort titles, and to investigate the indirect effects of comfort-driven adaptive behaviours on the user experience. With that perspective, *seeing* refers to any experience related to sight, issues regarding visual comfort and aesthetics are covered under this title. *Feeling* is used to cover the experiences related to the haptic and olfactory senses of the human. The factors that are mentioned in relation to the experience of feeling show a similar mechanism of change and are related to the thermal comfort and indoor air quality collectively, and therefore could not be separated. *Hearing* refers to the audial experiences and is related to acoustical comfort. *Controlling* is added since the main focus of this study is adaptive façades and it refers to the anticipation of control during user interaction and its psychological effect on user experience. In addition to these, the *overall* experience title is also used, referring to the factors that may not have a direct effect on a specific sense, but still found to be in relation to a general positive sensation of the human being.

Based on the above-mentioned classification, collected and interpreted information from the literature on how each human or environmental factor triggers each comfort-driven adaptive behaviour, which in turn creates a change in the environment that affects user experience, (Figure 5), are systematically presented in this section over the defined mechanism of change.

5.1 HUMAN FACTORS

Each person by nature has their own unique traits. These are not just physiological factors, but also psychological, social, cultural, economic, or other contextual factors that show diversity among each individual. These different characteristics alter a person's needs, habits, aspirations and influence his/her experience (Khalid, 2006). These human factors are grouped as *personal descriptors* and *needs*. A holistic approach to how each human factor triggers an adaptive behaviour and alters the experience in a working environment is found to be lacking in the literature. Therefore, an attempt to gather the existing but scattered information from the literature is made and presented in detail in this section. Table 1 below presents the relationship of each factor with each adaptive behaviour and user experience

TABLE 1 The human factors that affect user experience in a mechanism of change

IMPULSE (Influencer / Agent)		MECHANISM (Action / Behaviour)				RESPONSE (Effect / Change)				RELATED EXPERIENCE				
HUMAN FACTORS		Opening / Closing window	Adjusting window blind	Adjusting HVAC	Turning on/off lights	Air exchange rate	Sunlight transmittance	Indoor temperature	Illumination level	Seeing	Feeling	Hearing	Controlling	Overall
Personal Descriptors	Age	+	-	+	-	+	-	+	-	+	+	-	+	0
	Gender	+	-	0	-	+	-	+	-	+	+	-	0	+
	Country of Origin	-	-	0	0	-	-	0	0	0	+	+	0	+
	EducationLevel	0	-	0	0	0	-	0	0	0	+	-	+	+
	Type of Job	+	+	+	+	+	+	+	+	+	+	0	+	+
	Socio-personal traits	+	+	+	0	+	+	+	+	+	+	0	+	0
Personal Needs	Security	+	0	-	-	0	0	0	0	0	0	-	+	+
	Privacy	-	+	-	-	-	0	-	0	+	0	+	0	0
	Hygiene	0	-	-	-	0	-	0	-	0	0	-	-	+
	View	-	+	-	0	-	+	-	+	+	0	-	0	+

(+) Direct mention in the literature, (o) Interpreted from the literature, (-) Not mentioned in the literature

5.1.1 Personal Descriptors

The factors mentioned in this category refer to the characteristic features of an individual, which may be quantifiable tangible conditions or identifiable intangible aspects of the users.

Age

Age is mentioned as one of the physiological factors that have an impact on the users' comfort requirements and mainly on the thermal comfort perceived by the occupants (Al horr et al., 2016; D'Oca et al., 2016; Fanger, 1970). *Frontczak & Wargocki*, in their research, portray how individual characteristics influence satisfaction with indoor environmental quality, and age is associated with subjective air quality, visual satisfaction, and adverse perception (Frontczak & Wargocki, 2011). In another study that identifies the influencing factors on occupants' energy related behaviours, age is listed as one of the social and personal parameters (Delzende et al., 2017). In terms of adaptive behaviours, window opening behaviour (Fabi et al. 2012; Zhang et al. 2018), heating thermostat adjustment (Deme Belafi et al., 2018), and in general the need for personal control (Boerstra, 2016) are affected by the age factor.

Gender

Another frequently mentioned physiological factor that influences thermal satisfaction and the overall comfort perception of the users is gender (Al horr et al., 2016; Boerstra, 2016; D'Oca et al.,

2016; Day & Gunderson, 2015). It is an acknowledged fact in the field that in general, due to different body compositions, thermal preference and satisfactory set temperature for a female and a male differ from each other (Delzende et al., 2017; Fanger, 1970; Huizenga et al., 2006). In the case of discomfort, altering clothing (Holopainen et al., 2014) could be the initial act followed by heating thermostat adjustment (Deme Belafi et al., 2018), opening or closing the windows (Fabi et al., 2012; Zhang et al., 2018) or interfering with the HVAC system to alter the intensity of airflow (Fountain et al., 1996). Along with thermal sensation, *Frontczak & Wargocki* also mention gender as influencing the satisfaction with air quality and the visual satisfaction along with general preference on indoor environmental conditions (Frontczak & Wargocki, 2011).

Country of Origin

Country of origin is listed as another human factor that has both physical and socio-economic aspects. First of all, due to racial features and/or accustomed climatic conditions, users may have different means of thermal comfort (Al horr et al., 2016). In addition, the expectation of thermal conditions would also vary from country to country due to cultural differences and defined local standards, which would result in different experiences in terms of feeling (Day & Gunderson, 2015). As a result of various customs and habits, individuals' acoustical dissatisfaction and any overall adverse perceptions would also show diversity (Frontczak & Wargocki, 2011). Lastly, in terms of adaptive behaviour, cultural norms are mentioned as an influence on the use of electrical systems (O'Brien & Gunay, 2014).

Education Level

The level of education is mentioned in relation to the user's knowledge and awareness. As a socio-personal factor, education affects users' attitudes, motivations, and behaviours in their working environment (Delzende et al., 2017). Although it is not possible to define a direct correlation, users with different levels of education have a different perception of thermal comfort, air quality, and overall satisfaction (Frontczak & Wargocki, 2011). *Day & Gunderson* states that to minimize energy consumption, especially in high-performance buildings, training and education have a crucial effect (Day & Gunderson, 2015). Informing users on how to control the façade and service systems, and in which way their actions would affect the energy performance of the , greatly influence adaptive behaviours such as opening/closing windows, adjusting HVAC units, and turning on/off lighting (Yan & Hong, 2018).

Type of Job

Type of job is one of the most comprehensive factors that covers dress codes and activity levels, working hours, time pressure and stress levels, relationship with colleagues, relationship with employees/employers, and overall contentment with the job. According to *Frontczak & Wargocki* different factors related to different professions, defining a variety of needs and influencing the perception of thermal comfort, visual comfort, and air quality, as well as overall satisfaction (Frontczak & Wargocki, 2011). Job satisfaction in general is shown to have a significant effect on work performance, productivity, and psychological well-being (Samani, 2015). Depending on the job description, the required level of activity would define a metabolic rate and clearly have an influence on the thermal comfort parameters (Delzende et al., 2017; Haldi & Robinson, 2008; Holopainen

et al., 2014; Nicol & Humphreys, 2002). Another influencing factor in terms of thermal satisfaction is clothing (Al horr et al., 2016; Day & Gunderson, 2015). The level of clothing could be defined by a dress code for certain professions or it could be a parameter that is for users to alter and adapt (Fanger, 1970; Huizenga et al., 2006). In any case, clothing could be mentioned as one of the factors that influences users to take adaptive actions in order to control the indoor temperature (Fountain et al., 1996). In addition to these, working routine and arrival and departure patterns are found to be important motivational factors for adaptive behaviours (D'Oca et al., 2016). Opening the windows on arrival to the office and closing them upon departure is a common habit (O'Brien & Gunay, 2014). Adjusting the window blinds, turning on/off heating and lighting are other actions that are consistent with the working schedule (Deme Belafi et al., 2018; Wagner et al., 2018). Moreover, these could be listed as some of the main occupant behaviours that create the gap in the predicted and actual energy performance of the buildings (Masoso & Grobler, 2010).

Socio-Personal Traits

The main intangible factors that show diversity among the users and influence behaviours in various different ways are grouped under the title socio-personal traits. There are several behavioural models that try to portray the intentions and motivations of users' adaptive behaviours based on their personal and social properties (Deme Belafi et al., 2018). Personal factors could be listed as individual traits, beliefs, and attitudes which are the reflections of one's character (Fabi et al., 2012). A study investigating the influence of personality traits on occupant behaviour shows how the *Big Five Personality Traits* influence the behaviours associated with window opening, adjusting blinds, fans, or clothing, in addition to how thermal sensation and preference are affected (Schweiker et al., 2016; Wagner et al., 2018). Briefly, it states that people with high *neuroticism* traits tend to stick to the actions that they know and are able to control more, like clothing adjustments or operating windows. On the other hand, the *extraversion* trait could define a person who may very likely act quickly against any discomfort. Similarly, people with a high degree of openness to experience would be more open to changes, and hence feel less need to engage in adaptive behaviour. In other words, depending on their level of willingness to take action, a person could be defined as more active or passive (D'Oca et al., 2016). Apart from the personal profiles, social parameters could also be highly influential as a behavioural motivation (Zhang et al., 2018). Social constraints, norms, and pressure in a shared office are some of the most effective factors in terms of energy awareness and influence the adaptive behaviours related to energy usage (Day & Gunderson, 2015; Wagner et al., 2018). Besides, one's cultural belonging or certain lifestyle is another factor that affects human cognition and would alter the user behaviour (Delzende et al., 2017). All in all, perception and preference of comfort are highly interrelated with the socio-personal traits, thus these factors are significant influencers on the user experience.

5.1.2 Personal Needs

The factors mentioned in this category cover the main psychological elements in terms of users' needs and stressors that affect users in positive or negative ways.

Security

The need for security is a factor that influences the experience both directly and indirectly. According to *Vischer*, health and safety are part of the physical comfort parameters that are the first step of the habitability pyramid (*Vischer*, 2007). Additionally, the feeling of safety and security is a significant psychological factor that affects the indoor environmental satisfaction of the users (*Russell et al.*, 2013; *Zagreus et al.*, 2004). In terms of adaptive behaviours, in residential or working places, the act of window opening and closing is influenced by the means of providing security (*O'Brien & Gunay*, 2014; *Roulet et al.*, 2006). To indicate whether someone is outside, adjusting window blinds could also be another adaptive behaviour that is influenced by the feeling of security (*Deme Belafi et al.*, 2018).

Privacy

The need for privacy is another psychological factor (like security) that both directly and indirectly affects users' experience in a working environment (*Vischer*, 2007). The need for privacy applies to both visual and acoustical environments (*Kim & de Dear*, 2012). Especially for open-plan offices, communication privacy is an important parameter that affects the level of satisfaction and productivity in the physical work environment (*Al horr et al.*, 2016; *Samani*, 2015). For visual privacy, controlling the shading elements could be listed as the main influenced adaptive user behaviour, which applies to homes as well as offices (*Deme Belafi et al.*, 2018; *Lee et al.*, 2013).

Hygiene

The need for hygiene is one of the basic human needs as a part of physical comfort (*Vischer*, 2007). Cleanliness of the working space and maintenance of the building directly influence occupants' level of satisfaction and productivity in the work environment (*Huizenga et al.*, 2006; *Kim & de Dear*, 2012; *Roulet et al.*, 2006; *Samani*, 2015; *Zagreus et al.*, 2004). Although there is no mention in the literature about it triggering an adaptive behaviour, by means of protecting the indoor environment it may be interpreted that there is an indirect effect on the window closing action.

View

The need for a view is mentioned in relation to outside view, visual quality, and aesthetic appearance, which would influence the level of satisfaction with the working environment (*Samani*, 2015). Architectural features of the space, colours, textures, materials, and components affect the sense of aesthetics and positively influence the seeing experience (*Delzendeh et al.*, 2017). In addition, view out is one of the significant factors that affects visual comfort. Lack of view to outside may cause eye tiredness (*Day & Gunderson*, 2015), but having a pleasant view like a green landscape positively influences the overall satisfaction (*Kim & de Dear*, 2012). After sunlight levels, quality of view is the next main factor that triggers the window blind controls (*Bakker et al.*, 2014; *Kwon et al.*, 2019; *O'Brien & Gunay*, 2014; *Vischer*, 2007; *Wagner et al.*, 2018).

5.2 ENVIRONMENTAL FACTORS

Apart from the human factors, the conditions of the environment surrounding the users directly affect their comfort, both physically and psychologically (Vischer, 2007). As the barrier between the exterior and interior environments, façades undertake multiple functions with the main goal of providing a comfortable indoor environment (Klein, 2013). Therefore, its design is surfaced with regard to external conditions and it is the main element that shapes the internal conditions. Besides, other design characteristics related to the functionality of the building, referred to as spatial conditions, would also be factors that affect users' comfort in their environment. Effects of environmental factors on users' comfort and behaviours are a more commonly studied aspect, therefore the information presented in this section is a brief mention within the context of the mechanism of change. Table 2 below represents the relationship of each factor with each adaptive behaviour and user experience.

5.2.1 External Factors

The factors mentioned in this category are the main climate-related factors that depend on the geographic location and show variety for each season, time of year, or time of day.

Outdoor Temperature

Outdoor temperature is one of the main factors that affects thermal comfort. In different seasons, it influences the window opening/closing behaviours of the users, as well as the adjustment of window blinds and heating/cooling units (Al horr et al., 2016; Bakker et al., 2014; Brager et al., 2004; Buso et al., 2015; Day & Gunderson, 2015; Delzende et al., 2017; Fabi et al., 2012; Frontczak & Wargocki, 2011; Haldi & Robinson, 2008; Wagner et al., 2018; Zhang et al., 2018)

Solar Access

Solar access, depending on the orientation of the building, is one of the main factors that affects visual comfort. Along with the time of the day, the intensity of the daylight and sky conditions are mainly effective on the shading elements opening/closing behaviours of the users and turning on/off artificial lighting. Besides, the effect of sunlight may cause overheating which is related to thermal comfort. In terms of temperature adjustment, closing window blinds or altering the HVAC systems could also be listed as other influenced adaptive actions (Day & Gunderson, 2015; Delzende et al., 2017; Fabi et al., 2012; Huizenga et al., 2006; Wagner et al., 2018; Zhang et al., 2018).

TABLE 2 The environmental factors that affect user experience in a mechanism of change

IMPULSE (Influencer / Agent)		MECHANISM (Action / Behaviour)				RESPONSE (Effect / Change)				RELATED EXPERIENCE				
ENVIRONMENTAL FACTORS		Opening / Closing window	Adjusting window blind	Adjusting HVAC	Turning on/off lights	Air exchange rate	Sunlight transmittance	Indoor temperature	Illumination level	Seeing	Feeling	Hearing	Controlling	Overall
External Factors	Outdoor Temperature	+	+	0	-	+	+	+	0	0	+	-	+	0
	Solar Access	+	+	0	+	+	+	+	+	+	+	-	+	0
	Wind/Rain	+	-	-	-	+	-	+	-	-	+	-	0	0
	Relative Humidity	+	-	0	-	+	-	+	-	-	+	-	0	0
	Outdoor Noise Level	0	-	-	-	0	-	0	-	-	-	+	0	+
Internal Factors	Indoor Temperature	+	+	+	-	+	+	+	0	0	+	-	+	+
	Lighting Conditions	0	+	-	+	0	+	0	+	+	0	-	+	+
	Air quality	+	-	0	-	+	-	0	-	-	+	-	0	+
	Relative Humidity	+	-	0	-	+	-	0	-	-	+	-	0	+
	Indoor Noise Level	0	0	0	-	0	0	0	0	-	-	+	0	+
Spatial Factors	Building Function	+	+	+	+	+	+	+	+	0	0	0	0	+
	Building Layout	+	+	0	0	+	+	+	+	+	+	+	0	0
	Façade Characteristics	+	+	0	0	+	+	+	+	+	+	0	+	0
	Service Systems	0	0	+	+	0	0	+	+	+	+	0	+	+

(+) Direct mention in the literature, (o) Interpreted from the literature, (-) Not mentioned in the literature

Wind and Rain

Wind and rain conditions are listed together as factors that affect the window opening/closing behaviours of the users. Due to their effect, it results in changes in the indoor air quality and it also affects thermal comfort (Delzende et al., 2017; Fabi et al., 2012; Haldi & Robinson, 2008; Zhang et al., 2018).

Relative Humidity

The outdoor relative humidity is linked with thermal comfort and indoor air quality, in relation to the window opening behaviour and if there is an active ventilation system, by means of adjusting its air flow (Al horr et al., 2016; Delzende et al., 2017; Deme Belafi et al., 2018; Zhang et al., 2018).

Outdoor Noise Levels

Outdoor noise levels have a direct effect on acoustical comfort, and the resulting hearing experience, and they are also mentioned as one of the factors that influence window closing behaviour (Day & Gunderson, 2015; Haldi & Robinson, 2008; Roulet et al., 2006; Vischer, 2007)

5.2.2 Internal Factors

The factors mentioned in this category are the main quantifiable/measurable conditions of the indoor environment.

Indoor Temperature

Indoor temperature is one of the main factors that affects thermal comfort. Its effects could be investigated under two main sub-categories: mean radiant temperature and temperature variability created by the air movement, in other words, draught (Frontczak & Wargocki, 2011). Due to different needs, it influences the window opening/closing behaviours of the users as well as the adjustment of window blinds and heating/cooling units (Al horr et al., 2016; Bakker et al., 2014; Boerstra et al., 2012; Boerstra, 2016; Bordass et al., 1993; Brager et al., 2004; D'Oca et al., 2016; Day & Gunderson, 2015; Delzendeh et al., 2017; Deme Belafi et al., 2018; Fabi et al., 2012; Fanger, 1970; Frontczak & Wargocki, 2011; Haldi & Robinson, 2008; Holopainen et al., 2014; Huizenga et al., 2006; Kim & de Dear, 2012; Kwon et al., 2019; Nicol & Humphreys, 2002; O'Brien & Gunay, 2014; Roulet et al., 2006; Samani, 2015; Wagner, 2018; Zagreus et al., 2004; Zhang et al., 2018)

Lighting Conditions

Lighting conditions are the primary indicator of visual comfort. It covers the level of illumination within the space, homogeneity of the brightness, and formation of glare. It is affected by the external conditions, mainly solar access, and regulated initially by adjusting the window blinds and later by means of artificial lighting. In relation to the outside view and sunlight's overheating capability, it is linked with the window opening behaviour as well as the adjustment of window blinds (Bakker et al., 2014; Boerstra et al., 2012; Boerstra, 2016; Bordass et al., 1993; D'Oca et al., 2016; Day & Gunderson, 2015; Delzendeh et al., 2017; Deme Belafi et al., 2018; Fabi et al., 2012; Kim & de Dear, 2012; Kwon et al., 2019; O'Brien & Gunay, 2014; Roulet et al., 2006; Samani, 2015; Vischer, 2007; Wagner, 2018).

Air Quality

Indoor air quality refers to the CO₂ concentration of the air, odours, and air composition as in the content of dust/electrical particles/microorganisms. It is related to the feeling experience and affects the window opening/closing behaviours of the users (Bakker et al., 2014; Boerstra et al., 2012; Boerstra, 2016; Bordass et al., 1993; D'Oca et al., 2016; Deme Belafi et al., 2018; Fabi et al., 2012; Fanger, 1970; Haldi & Robinson, 2008; Huizenga et al., 2006; Kim & de Dear, 2012; Kwon et al., 2019; Roulet et al., 2006; Samani, 2015; Zagreus et al., 2004; Zhang et al., 2018).

Relative Humidity

The indoor relative humidity, similarly to the external conditions, influences thermal comfort and indoor air quality, in relation to the window opening behaviour and if there is an active ventilation system, by means of adjusting its air flow (Al horr et al., 2016; Day & Gunderson, 2015; Deme Belafi et al., 2018; Holopainen et al., 2014; Huizenga et al., 2006; Kwon et al., 2019; Roulet et al., 2006; Zhang et al., 2018).

Indoor Noise Levels

Indoor noise levels is one of the main factors that creates discomfort in a working environment. It directly affects acoustical comfort. Depending on the source of the noise - if it is from the outside it impacts window closing behaviour, and if it is an operational sound interfering the window blinds and/or HVAC systems, operations would be influenced (Boerstra, 2016; Day & Gunderson, 2015; Kim & de Dear, 2012; Roulet et al., 2006; Samani, 2015; Vischer, 2007; Zagreus et al., 2004).

5.2.3 Spatial Factors

The factors mentioned in this category are the properties related to the design of the space and its function.

Building Function

The function of the building is one of the main factors that defines the user requirements. It defines the function of the space and its spatial needs for comfortable usage. Therefore, it influences all adaptive behaviours in various ways and could be linked with all the user experiences (Al horr et al., 2016; Boerstra, 2016; Brager et al., 2004; Delzende et al., 2017; Frontczak & Wargocki, 2011; Huizenga et al., 2006; Kwon et al., 2019; Nicol & Humphreys, 2002; Roulet et al., 2006; Samani, 2015; Vischer, 2007; Wagner, 2018).

Building Layout

Building layout is the other factor that covers a wide range of design aspects like private or open-plan working environments, area of workspace per person, and position of each user within the space. It may affect all experiences in terms of seeing, feeling, and hearing. Users' interactions with their façade vary due to their distance from it, hence building layout is listed as one of the influential factors for opening/closing windows and adjusting shading elements behaviours (Kwon et al., 2019; Luna-Navarro et al., 2021). In addition to that, as was also mentioned under the socio-personal traits, being in a private or shared office may alter ones adaptive behaviours by creating social pressure (Bakker et al., 2014; Boerstra, 2016; Brager et al., 2004; Buso et al., 2015; D'Oca et al., 2016; Day & Gunderson, 2015; Delzende et al., 2017; Fabi et al., 2012; Huizenga et al., 2006; Kim & de Dear, 2012; O'Brien & Gunay, 2014; Roulet et al., 2006; Samani, 2015; Vischer, 2007; Wagner, 2018; Zagreus et al., 2004; Zhang et al., 2018).

Façade Characteristics

Façade characteristics refer to window size and position, wall to window ratio, mass, robust or dynamic character, and other design aspects of the façade. In the case of adaptive façades, it is clearly a factor that influences the controlling experience of the users (Tabadkani et al., 2021). The level of manual or automated control of the openings and shading units influence the level of user interactions and along with that effect the visual and thermal comfort of the occupant (Bakker et al., 2014; Buso et al., 2015; Fabi et al., 2012; Kwon et al., 2019; Vischer, 2007; Zhang et al., 2018).

Service systems refer to the active, mechanical units of the building, which have a great influence on shaping the indoor environment. Their design is outside the context of this paper; however, their control and feedback mechanisms can be mentioned as one of the factors that influences the controlling experience of the users (O'Brien et al., 2020). Alterations made by engaging with the HVAC systems or lighting element can also affect the visual, thermal, and overall comfort of the occupant (Brager et al., 2004; Buso et al., 2015; Delzendeh et al., 2017; Fountain et al., 1996; Huizenga et al., 2006; Kwon et al., 2019; Nicol & Humphreys, 2002; Wagner, 2018; Zhang et al., 2018).

6 DISCUSSION

In the previous section, an overview of the factors that affect user experience is systematically presented over the mechanism of change. According to the findings, it could be said that the most affected experience by the human factors is *feeling*. There is a direct effect, mainly related to the *perception of thermal comfort*, and an indirect effect as a result of being triggered by users' interactions. Among these, the most commonly investigated adaptive behaviour is found to be *opening/closing windows*, followed by *adjusting HVAC*. Both of these actions are in relation to the changes in the *air exchange rate* and/or *indoor temperature*, hence associated with the feeling experience. Other commonly affected experiences are *seeing* and *controlling*. Related to these experiences, the indirect effect of *adjusting window blind* behaviour needs to be further investigated, in terms of user-façade interactions. From the listed human factors, *type of job* and *socio personal traits* covered a wide range of factors, therefore it was an expected outcome to see that these titles are in relation to all the listed adaptive behaviours and experiences. Even though, with a holistic perspective, it was possible to gather information regarding the influences of human factors on user experience, the number of studies with this focus is limited and research targeted on the experience was found to be especially scarce.

As for the environmental factors, there was more research in the literature investigating direct or indirect effects on user experience. From the listed external factors, *solar access* is found to be the most influential one that could trigger all the issued adaptive behaviours. It directly and indirectly affects the *seeing* and *feeling* experience, and, related to the mechanism of change, could also be associated with the *controlling* experience. It is followed by the *outdoor temperature*, and from the internal factors, *indoor temperature*. From the listed spatial factors, the *function of the building* shows a clear relationship with all the adaptive behaviours and is related with the *overall* experience. However, based on the existing literature, it is difficult to define a direct effect caused by the building's function on each experience. On the other hand, studies show direct and indirect effects of *building layout* on *seeing*, *feeling*, and *hearing* experiences. By looking at the results of the review, studies investigating the effects of the environmental factors in relation to hearing experience seems to be lacking. Considering the fact that outside or inside sound levels are indicated as some of the main causes for discomfort, the indirect effects of these factors in relation to the mechanism of change need to be explored in a deeper way. Besides, *controlling* experience requires a more targeted study, where indirect effects on the experience would be investigated when the façade systems are fully or partially left to the users' control or fully automated. In addition to that, *façade* and *service systems characteristics* needs to be further explored in terms of their direct effects on each user experience. As a final remark on the review, the collective effect of different parameters is another issue that needs to be further investigated in terms of user experience.

The presented overview shows that the adaptive mechanisms related to the façade, like opening/closing windows and adjusting window blinds, are highly influenced by human factors. It could be said that the users' intention behind adaptive behaviours is the reflection of their adaptive comfort needs and adaptive control expectations. A similar outcome could be drawn for the behaviours related to the building service systems. Each adaptive behaviour is performed to overcome a certain discomfort and/or to enhance the user experience. Therefore, users' adaptive actions reflect their way of thinking. With a human centred approach, if the adaptive façades are to be designed in harmony with its users, users' anticipations of their indoor environment, as they relate to their experiences, require further research. Transferring this information from the occupancy to the design stage is crucial for developing occupant-centric control and operation systems, predicting the building's energy consumption, and enhancing users' positive interactions with their surroundings, with the ultimate aim of reaching the full potentials of the adaptive façades.

7 CONCLUSION

An overview of human-centred design and user experience in the context of working environments is presented in this paper. With a holistic perspective, all of the factors affecting users' experience are investigated through a literature review process. A mechanism of change is defined to explain the dynamic cycle of the user experience with respect to users' interactions with the building façade and service systems. According to the findings, factors that trigger a change mechanism by influencing an adaptive user behaviour are identified and categorized under two main groups: *human* and *environmental* factors.

Human factors are divided into two sub-groups: (1) *age, gender, country of origin, education level, type of job, and socio-personal traits* as personal descriptors; (2) *security, privacy, hygiene, and view* as personal needs. Environmental factors are divided into three sub-groups: (1) *outdoor temperature, solar access, wind/rain, relative humidity, and outdoor noise level* as external factors, (2) *indoor temperature, lighting conditions, air quality, relative humidity, and indoor noise level* as internal factors, (3) *building function, building layout, façade characteristics, and service systems* as spatial factors. The main adaptive behaviours are identified as (1) opening/closing windows, (2) adjusting window blinds (shading elements), (3) adjusting HVAC systems, (4) turning on/off lighting, and the change effects that these actions would result in are listed as (1) air exchange rate, level of (2) light transmittance, value of (3) indoor temperature, and (4) illumination level. Through these impulse, mechanism, and response relationships, the direct or indirect effects of each factor on user experiences are distinguished. Where the *user experiences* are defined as *seeing, feeling, hearing, and controlling*, they are therefore not only focused on the concept of comfort but also cover all human senses, emotions, behaviours, and interactions.

Based on the outcomes, in the simplest terms, it could be said that every user has different needs, perceptions, and thus, different behaviours. With a human-centred point of view, adaptive façades with their changeability feature, offer great potential to deal with these diverse needs and to keep the indoor environment in its preferred condition with a reduced level of energy consumption. An understanding of the users' relationships with the façade is essential in creating an ideal way of interaction, thus improving the user experience. In order to achieve that goal, the relationship between the human factor, as an agent of change, and automation systems of the adaptive façades, as the actor in the mechanism of change, is pointed out as the missing link. Therefore, relevant issues and further research areas towards a human-centred adaptive façade design approach

are introduced. The information presented in this paper could serve researchers in the field as a starting point, and show façade designers the adaptive nature of the users, hence transferring the knowledge on the dynamics of occupancy to the design phase.

Acknowledgments

Presented study is a part of Mine Koyaz's ongoing PhD Thesis, currently named as "Human Centred Adaptive Facades", at Construction Sciences Program, Istanbul Technical University. Research presented in this paper is carried during and after her visit at Architectural Engineering and Technology Department, Delft University of Technology as a Guest Researcher. The scholarship support from Istanbul Bilgi University for this visit is also acknowledged.

References

- Abras, C., Maloney-Krichmar, D., & Preece, J. (2004). User-centred design. *Bainbridge, W. Encyclopedia of Human-Computer Interaction*. <https://doi.org/10.1045/january2005-editorial>
- Addington, M. (2009). Contingent Behaviours. *Architectural Design*, 79(3), 12–17. <https://doi.org/10.1002/ad.882>
- Aelenei, L., Aelenei, D., Romano, R., Mazzucchelli, E. S., Brzezicki, M., & Rico-Martinez, J. M. (Eds.). (2018). Case Studies – Adaptive Façade Network. In *COST Action TU 1403 Adaptive Façade Network*. Tu Delft Open.
- Ajzen, I. (1991). The Theory of Planned Behaviour. *ORGANIZATIONAL BEHAVIOUR AND HUMAN DECISION PROCESSES*, 50, 179–211. https://doi.org/10.1922/CDH_2120VandenBroucke08
- Al-Obaidi, K. M., Azzam Ismail, M., Hussein, H., & Abdul Rahman, A. M. (2017). Biomimetic building skins: An adaptive approach. *Renewable and Sustainable Energy Reviews*, 79(May), 1472–1491. <https://doi.org/10.1016/j.rser.2017.05.028>
- Al horr, Y., Arif, M., Katafygiotou, M., Mazroei, A., Kaushik, A., & Elsarrag, E. (2016). Impact of indoor environmental quality on occupant well-being and comfort: A review of the literature. *International Journal of Sustainable Built Environment*, 5(1), 1–11. <https://doi.org/10.1016/j.ijbsbe.2016.03.006>
- Alavi, H. S., Verma, H., Papinutto, M., & Lalanne, D. (2017). Comfort: A coordinate of user experience in interactive built environments. *Lecture Notes in Computer Science (Including Subseries Lecture Notes in Artificial Intelligence and Lecture Notes in Bioinformatics)*, 10515 LNCS, 247–257. https://doi.org/10.1007/978-3-319-67687-6_16
- Attia, S., Garat, S., & Cools, M. (2019). Development and validation of a survey for well-being and interaction assessment by occupants in office buildings with adaptive façades. *Building and Environment*, 157(April), 268–276. <https://doi.org/10.1016/j.buildenv.2019.04.054>
- Attia, S. (2017). Evaluation of Adaptive Façades: The case study of Al Bahr Towers in UAE - Essay UK Free Essay Database. *QScience Proceedings*. <http://www.essay.uk.com/essays/architecture/evaluation-adaptive-facades/>
- Attia, S., Luna-Navarro, A., Juaristi, M., Monge-Barrio, A., Gosztonyi, S., & Al-Doughmi, Z. (2018). Post-Occupancy Evaluation for Adaptive Façades. *Journal of Façade Design & Engineering Volume*, 6(3), 1–9. <https://doi.org/10.7480/jfde.2018.3.2464>
- Bakker, L. G., Hoes-van Oeffelen, E. C. M., Loonen, R. C. G. M., & Hensen, J. L. M. (2014). User satisfaction and interaction with automated dynamic façades: A pilot study. *Building and Environment*, 78, 44–52. <https://doi.org/10.1016/j.buildenv.2014.04.007>
- Bluyssens, P. M. (2019). Towards an integrated analysis of the indoor environmental factors and its effects on occupants. *Intelligent Buildings International*, 0(0), 1–9. <https://doi.org/10.1080/17508975.2019.1599318>
- Boerstra, A., Beuker, T., Loomans, M., & Hensen, J. (2012). Impact of perceived control on comfort and health in European office buildings. *10th International Conference on Healthy Buildings 2012*, 1(April), 370–375.
- Boerstra, A. C. (2016). *Personal Control over Indoor Climate in Offices: Impact on Comfort, Health and Productivity*.
- Böke, J., Knaack, U., & Hemmerling, M. (2020). Automated adaptive façade functions in practice - Case studies on office buildings. *Automation in Construction*, 113(February), 103113. <https://doi.org/10.1016/j.autcon.2020.103113>
- Bordass, B., Bromley, K., & Leaman, A. (1993). *User and Occupant Controls in Office Buildings*. February.
- Brager, G. S., Paliaga, G., & de Dear, R. (2004). Operable Windows, Personal Control, and Occupant Comfort (RP-1161). *ASHRAE Transactions*, 110(December 2015), 17–35.
- Buso, T., Fabi, V., Andersen, R. K., & Corgnati, S. P. (2015). Occupant behaviour and robustness of building design. *Building and Environment*, 94, 694–703. <https://doi.org/10.1016/j.buildenv.2015.11.003>
- Capeluto, G., & Ochoa, C. E. (2017). *Intelligent Envelopes for High-Performance Buildings*. Springer International Publishing. <https://doi.org/10.1007/978-3-319-39255-4>
- Chammas, A., Quaresma, M., & Mont'Alvão, C. (2015). A Closer Look on the User Centred Design. *Procedia Manufacturing*, 3(Ahfe), 5397–5404. <https://doi.org/10.1016/j.promfg.2015.07.656>
- D'Oca, S., Corgnati, S., Pisello, A. L., & Hong, T. (2016). Introduction to an occupant behaviour motivation survey framework. *Clima 2016, February*. <http://datos.bancomundial.org/indicador/SL.TLF.CACT.FE.ZS>
- Damodaran, L. (1996). User involvement in the systems design process- a practical guide for users. *Behaviour & Information Technology*, 15(6), 363–377.
- Day, J. K., & Gunderson, D. E. (2015). Understanding high performance buildings: The link between occupant knowledge of passive design systems, corresponding behaviours, occupant comfort and environmental satisfaction. *Building and Environment*, 84, 114–124. <https://doi.org/10.1016/j.buildenv.2014.11.003>
- Delzendeh, E., Wu, S., Lee, A., & Zhou, Y. (2017). The impact of occupants' behaviours on building energy analysis: A research review. *Renewable and Sustainable Energy Reviews*, 80(August), 1061–1071. <https://doi.org/10.1016/j.rser.2017.05.264>

- Deme Belafi, Z., Hong, T., & Reith, A. (2018). A critical review on questionnaire surveys in the field of energy-related occupant behaviour. *Energy Efficiency*, 11(8), 2157–2177. <https://doi.org/10.1007/s12053-018-9711-z>
- Fabi, V., Andersen, R. V., Corgnati, S., & Olesen, B. W. (2012). Occupants' window opening behaviour: A literature review of factors influencing occupant behaviour and models. *Building and Environment*, 58, 188–198. <https://doi.org/10.1016/j.buildenv.2012.07.009>
- Fanger, P. O. (1970). *Thermal Comfort: Analysis and Applications in Environmental Engineering*. McGraw-Hill.
- Favoino, F., Loonen, R. C. G. M., Doya, M., Goia, F., Bedon, C., & Babich, F. (Eds.). (2018). Building Performance Simulation and Characterisation of Adaptive Façades – Adaptive Façade Network. In *COST Action TU 1403 Adaptive Façade Network*. Tu Delft Open.
- Fisk, W. J. (2000). Health and Productivity Gains from Better Indoor Environments and their Relationship with Building Energy Efficiency. *Annual Review of Energy and the Environment*, 25(1997), 537–566.
- Fountain, M., Brager, G., & De Dear, R. (1996). Expectations of indoor climate control. *Energy and Buildings*, 24(3), 179–182. [https://doi.org/10.1016/S0378-7788\(96\)00988-7](https://doi.org/10.1016/S0378-7788(96)00988-7)
- Frontczak, M., & Wargocki, P. (2011). Literature survey on how different factors influence human comfort in indoor environments. *Building and Environment*, 46(4), 922–937. <https://doi.org/10.1016/j.buildenv.2010.10.021>
- Haldi, F., & Robinson, D. (2008). On the behaviour and adaptation of office occupants. *Building and Environment*, 43(12), 2163–2177. <https://doi.org/10.1016/j.buildenv.2008.01.003>
- Heydarian, A., McIlvennie, C., Arpan, L., Yousefi, S., Syndicus, M., Schweiker, M., Jazizadeh, F., Risetto, R., Pisello, A. L., Piselli, C., Berger, C., Yan, Z., & Mahdavi, A. (2020). What drives our behaviours in buildings? A review on occupant interactions with building systems from the lens of behavioural theories. *Building and Environment*, 179(November 2019), 106928. <https://doi.org/10.1016/j.buildenv.2020.106928>
- Hoffman, R. R., Ford, K. M., Feltovich, A., Woods, D. D., Feltovich, P. J., & Klein, G. (2002). A Rose by Any Other Name...Would Probably Be Given an Acronym. *IEEE Intelligent Systems*, 17(4), 72–80. <https://doi.org/10.1109/MIS.2002.1024755>
- Holopainen, R., Tuomaala, P., Hernandez, P., Häkkinen, T., Piira, K., & Piippo, J. (2014). Comfort assessment in the context of sustainable buildings: Comparison of simplified and detailed human thermal sensation methods. *Building and Environment*, 71, 60–70. <https://doi.org/10.1016/j.buildenv.2013.09.009>
- Hong, T., Yan, D., D'Oca, S., & Chen, C. fei. (2017). Ten questions concerning occupant behaviour in buildings: The big picture. *Building and Environment*, 114, 518–530. <https://doi.org/10.1016/j.buildenv.2016.12.006>
- Huizenga, C., Abbaszadeh, S., Zagreus, L., & Arens, E. (2006). Air quality and thermal comfort in office buildings: Results of a large indoor environmental quality survey. *Proceeding of Healthy Buildings 2006*, 3, 399–397. <https://doi.org/10.12659/PJR.894050>
- Humphreys, M. A. (2005). Quantifying occupant comfort: Are combined indices of the indoor environment practicable? *Building Research and Information*, 33(4), 317–325. <https://doi.org/10.1080/09613210500161950>
- IDEO.org. (2015). *The Field Guide To Human Centred Design*.
- ISO 9241-210. (2010). *Ergonomics of human-system interaction : Human-centred design for interactive systems*.
- Jia, M., Srinivasan, R. S., & Raheem, A. A. (2017). From occupancy to occupant behaviour: An analytical survey of data acquisition technologies, modeling methodologies and simulation coupling mechanisms for building energy efficiency. *Renewable and Sustainable Energy Reviews*, 68(June 2016), 525–540. <https://doi.org/10.1016/j.rser.2016.10.011>
- Kaasinen, E., Kymäläinen, T., Niemelä, M., Olsson, T., Kanerva, M., & Ikonen, V. (2013). A user-centric view of intelligent environments: User expectations, user experience and user role in building intelligent environments. *Computers*, 2(1), 1–33. <https://doi.org/10.3390/computers2010001>
- Khalid, H. M. (2006). Embracing diversity in user needs for affective design. *Applied Ergonomics*, 37(4 SPEC. ISS.), 409–418. <https://doi.org/10.1016/j.apergo.2006.04.005>
- Kim, J., & de Dear, R. (2012). Nonlinear relationships between individual IEQ factors and overall workspace satisfaction. *Building and Environment*, 49(1), 33–40. <https://doi.org/10.1016/j.buildenv.2011.09.022>
- Klein, T. (2013). Integral Façade Construction : Towards a new product architecture for curtain walls [TU Delft]. In *Architecture and the Built Environment*. <https://doi.org/10.7480/abe.2013.3>
- Knaack, U., Klein, T., Bilow, M., & Auer, T. (2014). *Façades: Principles of Construction* (2nd editio). Birkhäuser Verlag GmbH.
- Kwon, M., Remøy, H., van den Dobbelaere, A., & Knaack, U. (2019). Personal control and environmental user satisfaction in office buildings: Results of case studies in the Netherlands. *Building and Environment*, 179, 428–435. <https://doi.org/10.1002/bdra.20073>
- Lassen, N., Josefsen, T., & Goia, F. (2021). Design and in-field testing of a multi-level system for continuous subjective occupant feedback on indoor climate. *Building and Environment*, 189(October 2020), 107535. <https://doi.org/10.1016/j.buildenv.2020.107535>
- Law, E. L. C., Roto, V., Hassenzahl, M., Vermeeren, A. P. O. S., & Kort, J. (2009). Understanding, scoping and defining user experience: A survey approach. *Conference on Human Factors in Computing Systems - Proceedings*, 719–728. <https://doi.org/10.1145/1518701.1518813>
- Lazarova-Molnar, S., & Mohamed, N. (2017). On the complexity of smart buildings occupant behaviour: Risks and opportunities. *ACM International Conference Proceeding Series, Part F1309*(November). <https://doi.org/10.1145/3136273.3136274>
- Lee, E. S., Fernandes, L. L., Coffey, B., McNeil, A., Clear, R., Webster, T., Bauman, F., Dickerhoff, D., Heinzerling, D., & Hoyt, T. (2013). A Post-Occupancy Monitored Evaluation of the Dimmable Lighting, Automated Shading, and Underfloor Air Distribution System in The New York Times Building *Building Technology and*.
- Luna-Navarro, A., Fidler, P., Law, A., Torres, S., & Overend, M. (2021). Building Impulse Toolkit (BIT): A novel IoT system for capturing the influence of façades on occupant perception and occupant-façade interaction. *Building and Environment*, 193(November 2020), 107656. <https://doi.org/10.1016/j.buildenv.2021.107656>

- Luna-Navarro, A., Loonen, R., Juaristi, M., Monge-Barrio, A., Attia, S., & Overend, M. (2020). Occupant-Façade interaction: a review and classification scheme. *Building and Environment*, 177, 106880. <https://doi.org/10.1016/j.buildenv.2020.106880>
- Maguire, M. (2001). Methods to support human-centred design. *International Journal of Human Computer Studies*, 55(4), 587–634. <https://doi.org/10.1006/ijhc.2001.0503>
- Masoso, O. T., & Grobler, L. J. (2010). The dark side of occupants' behaviour on building energy use. *Energy and Buildings*, 42(2), 173–177. <https://doi.org/10.1016/j.enbuild.2009.08.009>
- Naqvi, N., Shiv, B., & Bechara, A. (2006). The Role of Emotion in Decision Making: A Cognitive Neuroscience Perspective. *Current Directions in Psychological Science*, 15(5), 260–264. <https://doi.org/10.1111/j.1467-8721.2006.00448.x>
- Nicol, J. F., & Humphreys, M. A. (2002). Adaptive thermal comfort and sustainable thermal standards for buildings. *Energy and Buildings*, 34(6), 563–572. [https://doi.org/10.1016/S0378-7788\(02\)00006-3](https://doi.org/10.1016/S0378-7788(02)00006-3)
- Norman, D. A. (1988). *The psychology of everyday things*. Basic Books.
- Norman, D. A. (2013). *The design of everyday things*. Basic Books, A Member of the Perseus Books Group All. <https://doi.org/10.5860/choice.51-5559>
- O'Brien, W., & Gunay, H. B. (2014). The contextual factors contributing to occupants' adaptive comfort behaviours in offices - A review and proposed modeling framework. *Building and Environment*, 77, 77–87. <https://doi.org/10.1016/j.buildenv.2014.03.024>
- O'Brien, W., Wagner, A., Schweiker, M., Mahdavi, A., Day, J., Kjærsgaard, M. B., Carlucci, S., Dong, B., Tahmasebi, F., Yan, D., Hong, T., Gunay, H. B., Nagy, Z., Miller, C., & Berger, C. (2020). Introducing IEA EBC annex 79: Key challenges and opportunities in the field of occupant-centric building design and operation. *Building and Environment*, 178(May), 106738. <https://doi.org/10.1016/j.buildenv.2020.106738>
- Ortiz, M. A. (2019). *Home Occupant Archetypes: Profiling home occupants' comfort and energy-related behaviours with mixed methods*. [TU Delft]. <https://doi.org/10.7480/abe.2019.5>
- Ortony, A., Norman, D. A., & Revelle, W. (2005). Affect and Proto-Affect in Effective Functioning. In *Who Needs Emotions* (pp. 173–202). <https://doi.org/10.1093/acprof>
- Pee, L. G., Woon, I. M. Y., & Kankanhalli, A. (2008). Explaining non-work-related computing in the workplace: A comparison of alternative models. *Information and Management*, 45(2), 120–130. <https://doi.org/10.1016/j.im.2008.01.004>
- Perino, M., & Serra, V. (2015). Switching from static to adaptable and dynamic building envelopes: A paradigm shift for the energy efficiency in buildings. *Journal of Façade Design and Engineering*, 3(2), 143–163. <https://doi.org/10.3233/fde-150039>
- Roulet, C. A., Flourentzou, F., Foradini, F., Bluysen, P., Cox, C., & Aizlewood, C. (2006). Multicriteria analysis of health, comfort and energy efficiency in buildings. *Building Research and Information*, 34(5), 475–482. <https://doi.org/10.1080/09613210600822402>
- Russell, R., Guerry, A. D., Balvanera, P., Gould, R. K., Basurto, X., Chan, K. M. A., Klain, S., Levine, J., & Tam, J. (2013). Humans and Nature: How Knowing and Experiencing Nature Affect Well-Being. In *Ssrn*. <https://doi.org/10.1146/annurev-environ-012312-110838>
- Samani, S. A. (2015). The Impact of Personal Control over Office Workspace on Environmental Satisfaction and Performance. *Journal of Social Sciences and Humanities*, 1(3), 163–172. <http://www.aiscience.org/journal/jssh>
- Sanders, L. (2008). An evolving map of design practice and design research. *ACM — Interactions*, XV.6(November + December), 1–7. <https://doi.org/10.1093/beheco/arw006>
- Schweiker, M., Hawighorst, M., & Wagner, A. (2016). The influence of personality traits on occupant behavioural patterns. *Energy and Buildings*, 131, 63–75. <https://doi.org/10.1016/j.enbuild.2016.09.019>
- Stern, P. C. (1992). What Psychology Knows About Energy Conservation. *American Psychologist*.
- Tabadkani, A., Roetzel, A., Li, H. X., & Tsangrassoulis, A. (2021). A review of occupant-centric control strategies for adaptive façades. *Automation in Construction*, 122(May 2020), 103464. <https://doi.org/10.1016/j.autcon.2020.103464>
- Triandis, H. C. (1977). *Interpersonal Behaviour*. Brooks/Cole Pub.Co.
- van der Bijl-Brouwer, M., & Dorst, K. (2017). Advancing the strategic impact of human-centred design. *Design Studies*, 53, 1–23. <https://doi.org/10.1016/j.destud.2017.06.003>
- Verbeek, P.-P., & Slob, A. (2006). *User Behaviour and Technology Development: Shaping Sustainable Relations Between Consumers and Technologies*. Springer.
- Verplanken, B., & Aarts, H. (1999). Habit, Attitude, and Planned Behaviour: Is Habit an Empty Construct or an Interesting Case of Goal-directed Automaticity? *European Review of Social Psychology*, 10(1), 101–134. <https://doi.org/10.1080/14792779943000035>
- Vischer, J. C. (2007). The effects of the physical environment on job performance: Towards a theoretical model of workspace stress. *Stress and Health*, 23, 175–184. <https://doi.org/10.1002/smi.1134>
- Visser, F. S., Stappers, P. J., van der Lugt, R., & Sanders, E. B.-N. (2005). Contextmapping: experiences from practice. *CoDesign*, 1(2), 119–149. <https://doi.org/10.1080/15710880500135987>
- Wagner, A. (2018). Occupant behaviour-centric building design and operation EBC Annex 79. In *IEA EBC* (Issue October).
- Wagner, A., O'Brien, W., & Dong, B. (Eds.). (2018). *Exploring Occupant Behaviour in Buildings*. Springer International Publishing AG. <https://doi.org/10.1007/978-3-319-61464-9>
- Wigginton, M., & Harris, J. (2002). *Intelligent skins*. Butterworth-Heinemann.
- Yan, D., & Hong, T. (Eds.). (2018). Definition and Simulation of Occupant Behaviour in Buildings. In *IEA, EBC Annex 66 Final Report* (Issue May).
- Yan, D., O'Brien, W., Hong, T., Feng, X., Burak Gunay, H., Tahmasebi, F., & Mahdavi, A. (2015). Occupant behaviour modeling for building performance simulation: Current state and future challenges. *Energy and Buildings*, 107, 264–278. <https://doi.org/10.1016/j.enbuild.2015.08.032>
- Zagreus, L., Huizenga, C., Arens, E., & Lehrer, D. (2004). Listening to the occupants: a Web-based indoor environmental quality survey. *Indoor Air*, 14(s8), 65–74. <https://doi.org/10.1111/j.1600-0668.2004.00301.x>

- Zhang, T., & Dong, H. (2008). Human-centred design: an emergent conceptual model. *Include2009 Proceedings, 2008*, 7. <https://doi.org/10.1.1.426.5107>
- Zhang, Y., Bai, X., Mills, F. P., & Pezzey, J. C. V. (2018). Rethinking the role of occupant behaviour in building energy performance: A review. *Energy and Buildings, 172*, 279–294. <https://doi.org/10.1016/j.enbuild.2018.05.017>
- Zoltowski, C. B., Oakes, W. C., & Cardella, M. E. (2012). Students' Ways of Experiencing Human-Centred Design. *Journal of Engineering Education, 101*(1), 28–59. <https://doi.org/10.1002/j.2168-9830.2012.tb00040.x>

Exploring the Impact of Geometry and Fibre Arrangements on Daylight Control in Bistable Kinetic Shades

Elena Vazquez ^{*1,2}, Jose Duarte ¹

* Corresponding author

1 The Pennsylvania State University, Department of Architecture, United States of America

2 University of North Carolina at Charlotte, School of Architecture, United States of America, e.vazquez@uncc.edu

Abstract

Bistable laminates are composite structures that exhibit more than one static configuration, showing a "snap-through" behaviour that results from residual stresses generated during the curing process. This study focuses on finding adequate fibre and laminate arrangements for bistable laminates used in functional kinetic shadings. We present a study with a mixed-methods approach, combining experimental prototyping and performance simulation studies. We fabricated and analysed the geometry of a series of prototypes, conducting daylight studies to assess the performance of different laminates and fibre arrangements and showing how specific fibre arrangements can help control daylight throughout the day. We concluded that controlling fibre arrangements of bistable laminates could increase the functionality of bistable kinetic shadings in terms of daylight control, leading to more differentiated shapes between their two stable states, which corresponds to the open and closed positions of the shadings. Increasing such a difference increases the range of system configurations and, therefore, the ability to respond to various external lighting conditions and internal user requirements.

Keywords

kinetic architecture, bistability, snap-through, carbon-fibre laminates, kinetic shading

DOI

<http://doi.org/10.47982/jfde.2022.1.03>

1 INTRODUCTION

In recent years, there has been an increasing interest in designing more efficient building envelopes. Kinetic shadings adjust their configuration to shifting environmental conditions, thereby improving a building's environmental performance (Fiorito et al., 2016). There are several ways to describe kinetic systems like the one described in this research, including terms such as Adaptive Envelopes and Climate Adaptive Facades (Barozzi et al., 2016; Juaristi et al., 2018). For this study, kinetic shades are defined as solar-shading elements that can change their shape configuration. Daylight control is critical for designing energy-efficient buildings, which can be regulated with kinetic shading structures. One of the main obstacles to developing kinetic shading systems is the cost of production and maintenance of sophisticated mechanical systems that these have traditionally relied upon. In this context, bistability—a phenomenon observed in daily life in snap bracelets and measuring tapes—can be considered a promising approach to designing lightweight kinetic shape-morphing shading devices. However, little is known about incorporating bistable laminates in shading devices; therefore, we must first investigate what suitable shapes and forms can be obtained with bistable laminates for functional kinetic shades.

The use of bistable laminates as shape-morphing structures has attracted researchers' attention because they do not require continuous power to remain in either of their states (Emam & Inman, 2015). These laminates can keep their static configuration and transition on demand by supplying a small external force as needed. Bistability has been implemented in shape-morphing structures for multiple functionalities. Still, it has yet to be studied in architectural design as a potential strategy that can be used for developing kinetic facades. An architectural application of such laminates requires the design and study of prototypes with shapes and dimensions suitable for use at the building scale, the analysis of their shape-morphing range and their usefulness for daylight control, and the optimization of their configuration. Bistable systems could be used for automated kinetic systems where the user does not need to operate the shading device, which is particularly important for spaces with multiple users. They could also provide a wide variety of design forms and shapes and increase the granularity of shading devices. This study is motivated by the desire to attend to both performance needs (daylight control) and design needs (aesthetics, flexibility).

The research described in this article is part of a larger research agenda, the goal of which is the design and fabrication of kinetic shading screens that can increase the control of daylight being captured and filtered to interior spaces. This research includes several steps: (1) to identify adequate design forms for bistable laminates used in a kinetic screen, (2) to study suitable actuation mechanisms for bistable laminates using smart materials, and (3) to assess the performance of a bistable kinetic screen in a full-scale test. This paper is focused on the first step, whose goal is to identify configurations of the bistable flaps used in the shading screen with an increased difference between the open and closed positions to improve the capacity of the screen to control the filtering of daylight. In this step of the research, the only performance metric was light intensity. Future steps of the research will be concerned with activating the bistable laminates using smart materials, including glare as an additional lighting requirement, and optimizing daylight capture, considering the lighting requirements for the activities assigned to the space.

This study focuses on finding adequate fibre and laminate arrangements for bistable laminates used in functional kinetic shadings with a mixed-methods approach that combines experimental prototyping and performance simulation studies. In the first step, a set of bistable laminate designs are compared in terms of their curvature and impact on light capture performance, considering

a north-facing façade orientation, where diffuse light is prevalent. After this initial evaluation, the selected bistable laminate is used to explore the effects of changing fibre orientation to achieve material configurations that permit increased control over how sunlight enters the building. We show how prototypes with the same base geometry but different fibre arrangements could help maintain a daylight performance target throughout the day. The study shows the potential of bistable systems as an alternative to current shading solutions, showing possible shapes and opening patterns, and manipulating fibre arrangements to control curvature deflections, thereby diversifying kinetic shade design.

2 BACKGROUND

2.1 KINETIC BUILDING ENVELOPES

Kinetic or dynamic building envelopes are hardly a new concept in architectural design, albeit few built examples exist worldwide. Unlike kinetic devices in aviation or automotive industries, Kinetic systems in architecture are usually custom-designed and manufactured for every application, making them very costly. Some well-known icons of kinetic façades are the Institute du Monde Arabe (1987) and the Al-Bahr tower in Abu Dhabi (2012). Barozzi et al. (2016) present a review of several built examples of kinetic façades, classifying the different design approaches based on case studies. Researchers have also sought to characterize kinetic systems' performance by developing building performance simulation workflows that can potentially inform the design of such façades (Loonen et al., 2017) while maintaining high levels of indoor environmental quality. The development of such innovative materials and technologies, as well as their real-world implementation, can be enhanced with the use of building performance simulation (BPS). However, the current trend is to create kinetic systems that do not require mechanical actuation (Fiorito et al., 2016; Yi & Kim, 2021). Research in this area has sought to develop shape-changing mechanisms and study how smart materials can actuate such mechanisms. This paper focuses on finding adequate shape-changing forms of bistable composite laminates for kinetic façades, which can be used in combination with smart materials for actuation. A few studies have focused on developing shape-changing forms, for instance, Flectofin®, an elastic mechanism developed for façade shading systems inspired by the movement of plants (Lienhard et al., 2011).

In addition, there has been increasing interest over the past two decades in developing kinetic systems using smart materials. Recent advances in smart materials and methods have allowed designers to envision lighter and more efficient shape-changing façades that can change according to existing environmental conditions (Addington & Schodek, 2005). A recent review (Vazquez, Duarte, & Randall, 2019) identified different design and fabrication strategies used by researchers and designers over the past twenty years to develop kinetic envelopes using smart materials. There are two main strategies for incorporating smart materials into kinetic façades: passive and active actuation. In passive actuation, kinetic systems rely on changing environmental conditions to change shape, for instance, hygromorphic wood structures (Wood et al., 2016; Vazquez, Gürsoy, & Duarte, 2019), and structures made with thermo-bimetals (Sung, 2016), or Shape Memory Alloys (Denz et al., 2021; Sigmund, 2016). In active actuation, kinetic systems can be activated on demand, for instance, in designs with electroactive materials (Kretzer & Rossi, 2012) or with shape memory alloys activated with joule heating (Khoo, Salim, & Burry, 2012). While passive systems can be highly advantageous, relying only on shifting temperature and humidity to change their shape,

active systems are preferred when the system's on-demand user control is required, or specific performance metrics are needed. We argue that bistable composite laminates can be used in combination with smart materials with on-demand actuation to develop novel kinetic architectural façade systems. While actuation is not the focus of this study, a basic diagram of the proposed system is shown in the Conclusions section of the paper. Combining bistable mechanisms with smart materials for shape transformation is not new in fields other than architectural design, as will be discussed in the next section.

2.2 BISTABLE SHAPE-CHANGING SYSTEMS

Bistable mechanisms exhibit more than one static configuration and are a well-established research area with over thirty years of development (Emam & Inman, 2015). Current research trends focus on developing applications for such structures, both for actuation and energy harvesting functionalities. As actuators, studies include morphing aircraft structures (Mattioni et al., 2008) and wind turbine blades (Lachenal, Daynes, & Weaver 2013), allowing them to change shape according to operational or environmental requirements. Thin asymmetric laminates—used in this study—are a bistable mechanism that can assume large deflections from one static configuration to another with only a small input of energy (Emam & Inman, 2015). The low energy use and substantial shape transformation make them particularly promising for architectural applications, where energy efficiency is critical. Table 1 compares measured values for critical loads needed to transition between stable states. These values were obtained through experimental and modelling studies. While critical force values depend on boundary conditions, they estimate the required force to transition between states. The results confirm the practicality of combining bistable carbon fibre laminates with smart materials as actuators for kinetic shading systems. The critical loads are very low (~0.4 N) for the type of carbon-epoxy prepregs utilized in this study. To transition from one state to another, researchers have studied the use of smart materials such as piezoelectrics (PZT) and other smart materials (Schultz & Hyer, 2003). As an example, a study by Kim et al. (2010) presented a flytrap robot combining bistable laminates and shape memory alloy (SMA) springs. Together, these studies indicate two main characteristics of bistable laminates that make them appealing for building applications: a large shape-morphing motion and low energy requirements to snap through different stages.

TABLE 1 Critical force to allow snap-through of bistable laminates

BISTABLE LAMINATE MATERIAL	CRITICAL FORCE – N	SIZE	REFERENCE	NOTE
Carbon-epoxy prepregs	~0.4 N	Modules of 130 x 62 mm	(Lele et al., 2019)	0.075mm thick
Carbon-epoxy prepregs	5.8 N	120x100 mm	(Cantera et al., 2015)	0.44 mm thick
Graphite-epoxy prepreg	2.37 N	152.4 x 152.4 mm	(Tawfik et al., 2007)	0.1 mm thick. The critical force depends on the aspect ratio

Instability is not typically the desired feature in architectural design, primarily associated with structural malfunctions. Nevertheless, some studies utilize bistable principles in designing kinetic architectural elements. Seminal research in the area is the work of Song et al. (2018), who presented a prototype for a snapping façade that exploits instability for a shading device.

The bistable components utilized are snapping beams that offer a mechanical behaviour similar to elastic springs. Polyester membranes are then attached to the snapping beams with a Miura-ori folding pattern, and the device is designed to be operated manually. In a similar approach, Vander Werf (2009) developed a shading system using snapping beams made with carbon fibre plastics, covered with a textile membrane, and actuated with a metallic coil actuated with heat. Both studies rely on snapping beams and secondary materials to develop kinetic shades successfully, demonstrating the potential of using bistability as a design principle for kinetic architecture. Researchers, however, have not yet considered the use of another type of bistable element, bistable laminates, as a material for kinetic architecture. As opposed to bistable beams, bistable laminates present two stable states in the form of surfaces, which can be used as the skin itself in kinetic architecture applications. We argue that bistable laminates—which remain virtually unexplored in architecture—present significant potential for developing kinetic shading systems. Figure 1 shows the schematics of bistable laminates in two stable cylindrical shapes and a diagram showing the potential energy of bistable systems, which have two zero energy states corresponding to the stable shapes.

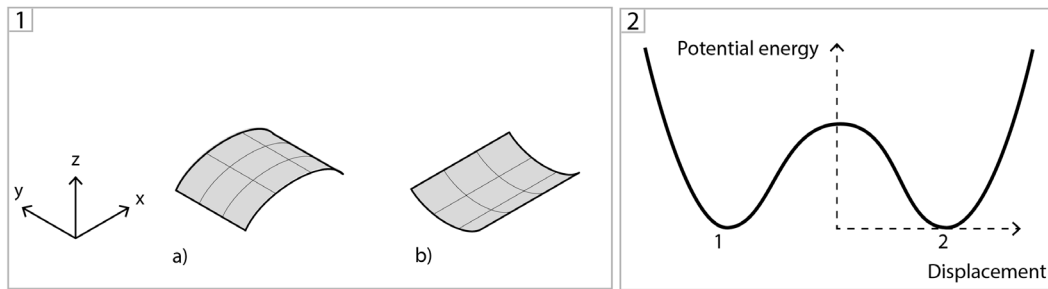


FIG. 1 The two stable states of a bistable composite laminate 2) a diagram depicting the potential energy of bistable systems, redrawn from Noh et al. (2021).

The bistable carbon fibre laminates in this study are fabricated following the method described by Yang et al. (2018) using prepreg carbon fibre sheets and a three-step process are summarized as follows. The first step is freezing and cutting, in which the carbon fibre prepreps are cooled in a freezer to $\sim 0^{\circ}\text{C}$ and then cut into the desired shapes. The freezing step avoids putting any additional stress on the samples. The next step is to layer the composites and assemble them in a vacuum bag. Two consecutive layers of carbon fibre prepreps are placed on an aluminium plate covered with mould release wax. These layers have fibre arrangements orthogonal to each other, i.e., 90° - 180° , 45° - 135° , and so on. A layer of perforated plastic sheet, followed by a polyester sheet and a breather fabric layer, goes on top of the uncured carbon prepreps. A vacuum bag film seals all the layers and is fixed to the aluminium plate with high-temperature tape. The entire package is vacuumed using a vacuum pump that is turned on during the whole curing process. The bag is then placed in the oven at 135°C for one hour, then slowly cooled down by turning off the oven until it reaches room temperature. When taken out of the vacuum bag, the prototypes are already settled in one of their two stable states. The authors explain that the prototypes' heating up and cooling down creates internal thermal stresses that generate the laminates' bistable behaviour.

2.3 DAYLIGHT PERFORMANCE AND KINETIC BUILDING SHADES.

Shading devices significantly impact both energy consumption and daylight performance of internal building spaces (Bellia et al., 2014). Static shades, however, present some limitations in terms of daylight and thermal performance in that they cannot adjust to shifting environmental conditions (Al-Masrani et al., 2018). Researchers have recently investigated the potential of kinetic shades in improving daylight performance, radiation, and even natural ventilation (Vazquez et al., 2019). This study focuses on daylight control because it is one of the main performance aspects that can be improved with kinetic shades. In a review by Al-Masrani & Al-Obaidi (2019), eleven out of the twenty studies were concerned with kinetic screen's daylight performance. Therefore, this study adds to the growing body of literature on kinetic building shades interested in daylight performance, with a focus on bistable elements. The study forms part of a larger research agenda aimed at characterizing the performance of bistable kinetic screens, addressing daylight performance in this first step.

3 METHODS AND MATERIALS

In recent studies, researchers have used experimental methods to develop kinetic façade systems, relying mostly on prototyping and testing cycles, aided by digital design and fabrication strategies. Ahlquist et al. (2013) characterize this research model as a material-centred approach, where a sequence of experimentations in increasing levels of complexity inform the introduction of new engineered materials into architectural design. Research into new materials in architecture has mostly relied on such experimental inquiry models. For example, Yoon (2019) develops kinetic façades using shape memory polymers by proposing design solutions and evaluating them through fabrication and performance simulation. Similarly, Sung (2016) argues that her research into smart materials for responsive shading is at the middle point between "scientific reduction and aesthetic expression."

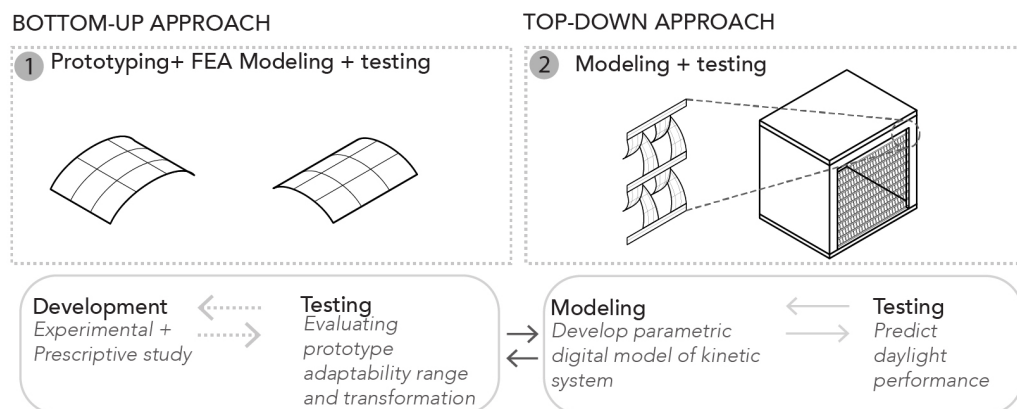


FIG. 2 Methods: A combined bottom-up and top-down approach. The bottom-up approach combines FEA modelling and testing. The obtained forms are then used in the top-down approach to conduct daylight studies.

This research adopts a mixed-methods approach that combines experiments and simulation studies. The methodology implemented is summarized in Figure 2. A bottom-up approach is concerned with prototyping at a smaller scale and evaluating the resulting deflection by measuring physical prototypes and comparing them to FEA modelling results. From the bottom-up explorations, we

obtain the geometry of the two stable states. These geometries are tested later in the top-down approach. The iterative development and analysis of prototypes permit the selection of promising configurations. A complementary top-down approach simulates the performance of the fabricated prototypes in terms of daylight. We developed a digital model of the kinetic system to assess the performance and defined a test room for conducting digital simulation studies. From the top-down approach, we obtain daylight performance data. Combining these two approaches aims to find adequate shapes and configurations for bistable laminates that enhance their performance as architectural elements. The prototypes are evaluated on their potential as architectural elements and ranked according to a design decision matrix. The most promising solutions then enter the subsequent rounds of prototyping and simulation studies.

In terms of digital simulations, we developed two different models: a daylight model that simulates the performance of the bistable shading device and an FEA model that simulates the cured state of bistable laminates. The daylight model was developed using the DIVA plugin for Grasshopper, which relies on Radiance as the simulation engine. The simulation was conducted in Rhinoceros. The FEA model was developed in ABAQUS, using the thick shell element SR4. The model uses the Standard/Explicit model, where the geometry is defined as a composite laminate of two plies of 0.12 mm thickness placed at 90 degrees from each other. The development of the FEA model includes two steps. First, defining the mesh geometry of the shell, identifying the composite layup, and setting the boundary conditions—for this experiment, the composite is fixed at the geometric centre, and second, establishing a temperature field to simulate the uniform heating of the samples followed by the cooling down of the samples. The nonlinear behaviour that results in the accurate cylinder shapes instead of saddle shapes (Schultz & Hyer, 2003) is implemented in the model with the NIgeom function. For further details on the FEA model, readers can refer to Pirrera et al. (2010).

In addition, the main material used in the experimental component of this study is the prepreg carbon fibre sheets, which were obtained from Rockwest composites. The prepregs utilized are 0.11684 mm thick with standard modulus and a unidirectional fibre arrangement. Table 2 lists the material properties of the carbon fibre prepregs. Figure 3 shows photos of the fabrication process, including layering carbon fibre prepregs and curing them in the oven under a vacuum.

TABLE 2 Material properties of the carbon fibre prepregs

PROPERTY	VALUE	PROPERTY	VALUE
Thickness	0.11684 mm	Epoxy	Newport 301
Pattern	Unidirectional	Curing temperature	250-300°F
Material	Standard Modulus Carbon (Graftil TR50S)	Tensile strength (0-90)	2950 MPa-79MPa
		Tensile modulus (0-90)	142 GPa-9GPa

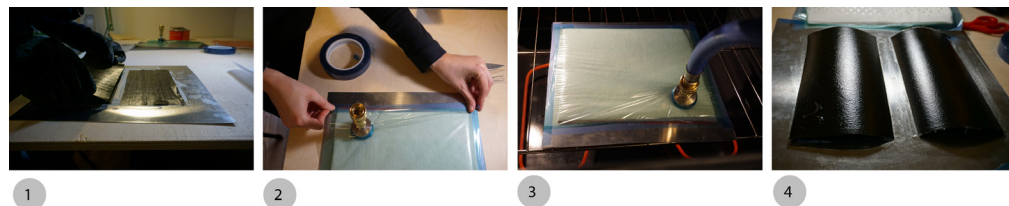


FIG. 3 Fabrication process. From left to right: 1) Placing the two layers of prepreg carbon fibres, 2) arranging the vacuum bag, 3) curing process in the oven, 4) prototypes after cooled in one of the stable states.

Numerous variables need to be considered in the design and fabrication of bistable composite laminates: fabrication variables, material variables, actuation variables, and design variables (Figure 4). Fabrication variables describe the manufacturing conditions, i.e., curing temperature and time, vacuum strength, and so on. Material variables relate to the carbon fibre properties and the resin utilized to layer the laminates. This study uses thin prepreg carbon fibre sheets to achieve a very lightweight structure that does not require much force to transition between states (the thicker the material, the more strength required to change states). Actuation variables refer to the snapping conditions that make the prototypes transition from one state to another. This study focuses only on two bistable laminates' design variables, the geometry of the composite and fibre arrangement, to determine the configurations that lead to their increased daylight functionality as part of a kinetic architectural shading device through experimental prototyping and daylight performance evaluation. These variables are selected because we hypothesize that these could significantly impact the daylight performance of the kinetic bistable screen. As such, the composites' shape and size are considered to determine how different shapes translate into different shading configurations. The fibre arrangement is also considered to explore its potential to enlarge the dynamic systems design's solution space by systematically changing the fibre angle of the prototypes. The layer order is not considered since a preliminary study did not show any significant statistical difference in the resulting bistable states' average curvature when changing the layer order in the prototypes. Layer count is also not considered since the goal is to have thin laminates with only two layers, since increasing the number of layers would decrease the curvature of the two stable states.

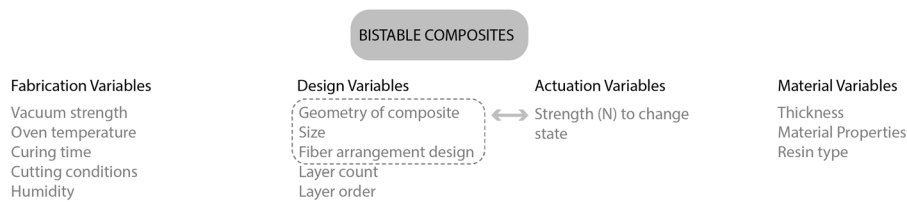


FIG. 4 Bistable laminate variables. The design variables considered for this study are highlighted.

4 RESULTS

4.1 DESIGN AND FABRICATION OF PROTOTYPES

The first set of prototypes was aimed at exploring different kinetic shading designs that could be constructed with three basic units: a rectangle (w, l), a triangle (b, h, a°), and a trapezoid (b_1, b_2, h). These initial shapes were defined through preliminary design exploration, following examples of other shape-changing architectural skins that rely on quadrilateral shapes (Worre Foged & Pasold, 2015) and triangles (Correa et al., 2015). The quadrilateral shapes also remain inside the 1-3 aspect ratio, over which Tawfik et al. (2007) found that shapes cannot go back to their original position. Figure 5 shows geometric designs A, B, and C, —whose basic shapes are a rectangle, triangle, and trapezoid, respectively, their predicted 'open' and 'closed' positions, and design ideas for overall configuration options. Note that the two stable states are named 'open' and 'closed' due to the predicted morphology that these will adopt. The open state is when the laminates k curvature is transversal to the prototype's longest side, and the closed state is when the laminates

k_2 curvature is parallel to the longest side. The overall configuration options are shown with their parameters, which can be adjusted according to specific design requirements on a case-by-case basis. Although many other arrangements exist, two possible design configurations are displayed for each prototype. As this study is not focused on the overall configuration design, these are shown to illustrate the potential to create various bistable screen designs from the three basic shapes considered in the study.

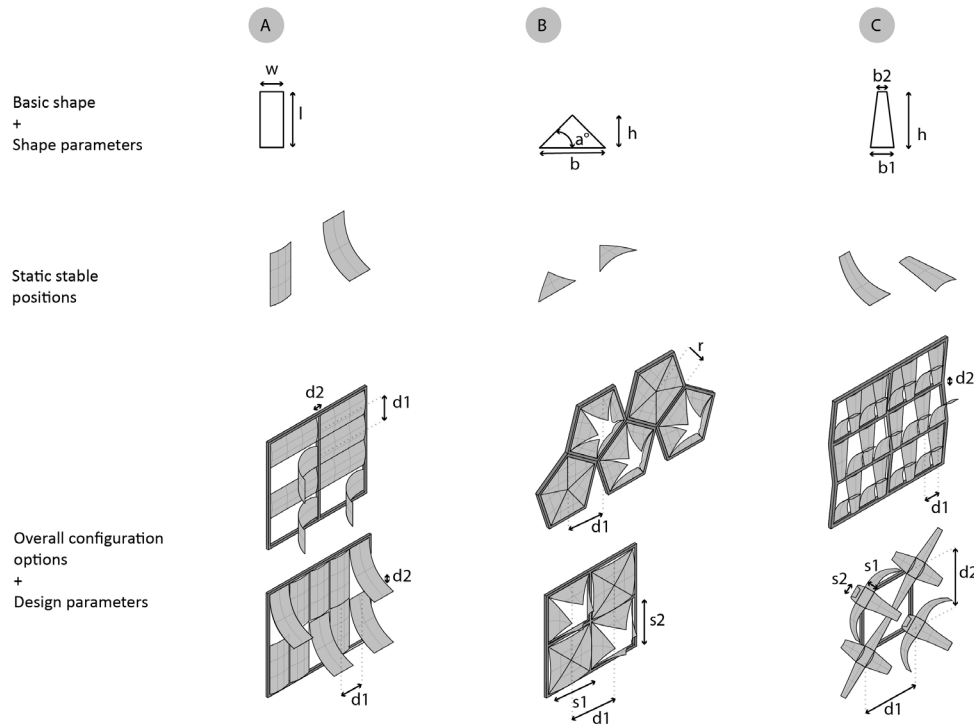


FIG. 5 Designs with basic shape, predicted open and closed positions, and overall configuration options

The three basic prototypes A, B, and C, were fabricated using the manufacturing method described in the previous section. In the initial prototypes, the dimensions were as follows: prototype A, $w=7.62$ cm $l=15.24$ cm; prototype B, $b=30.5$ cm $h=15.24$ cm $a^\circ=45^\circ$; and prototype C, $b_1=7.62$ cm, $b_2=3.81$ cm and $h=15.24$ cm. All the prototypes had a $0-90^\circ$ fibre angle arrangement parallel to the lines that conform to the basic shapes. In prototype A, the two layers had the carbon fibres aligned with the width and length of the rectangle, the triangle had the fibres aligned to its base and height, and the trapezoid had the prepreg fibres aligned with its base and height. After the layering, curing, and cooling procedures, the prototypes were 3D scanned with a 3D Systems SENSE scanner. After scanning the prototypes, the resulting meshes were edited, and the surface was rebuilt to simplify the geometry and obtain the curvature k values. The modelling of the two bistable positions also allowed us to determine the adaptability range of each prototype.

Figure 6 shows the fabricated prototypes and the scanned surfaces corresponding to their open and closed positions. In Figure 6-1, we overlaid pictures of the two positions. Note that in prototype B the two positions are not significantly different. Furthermore, the most significant curvature k is parallel to the longest side, resulting in a configuration different from that initially anticipated, drawn, and shown in Figure 5. Results show that the height must be longer than the base to obtain a unit with

a more significant curvature k , parallel to the triangle's height, provided all other variables remain unchanged. In prototypes A and C, the open position is also the one with curvature k parallel to the longest side. However, unlike in prototype B, the difference between the two positions is such that it would work for a shading device, as shown in Figure 6-1. Figure 6-3 compares the FEA model with the 3d scanned prototype. The curvature values from both are within a 10% difference, which can be considered acceptable. The FEA model is used in this study to predict the cured state of different bistable laminates and analyse the deflection shape and curvature of the built prototypes. The FEA model also provides the digital models of the prototypes used in the simulation studies.

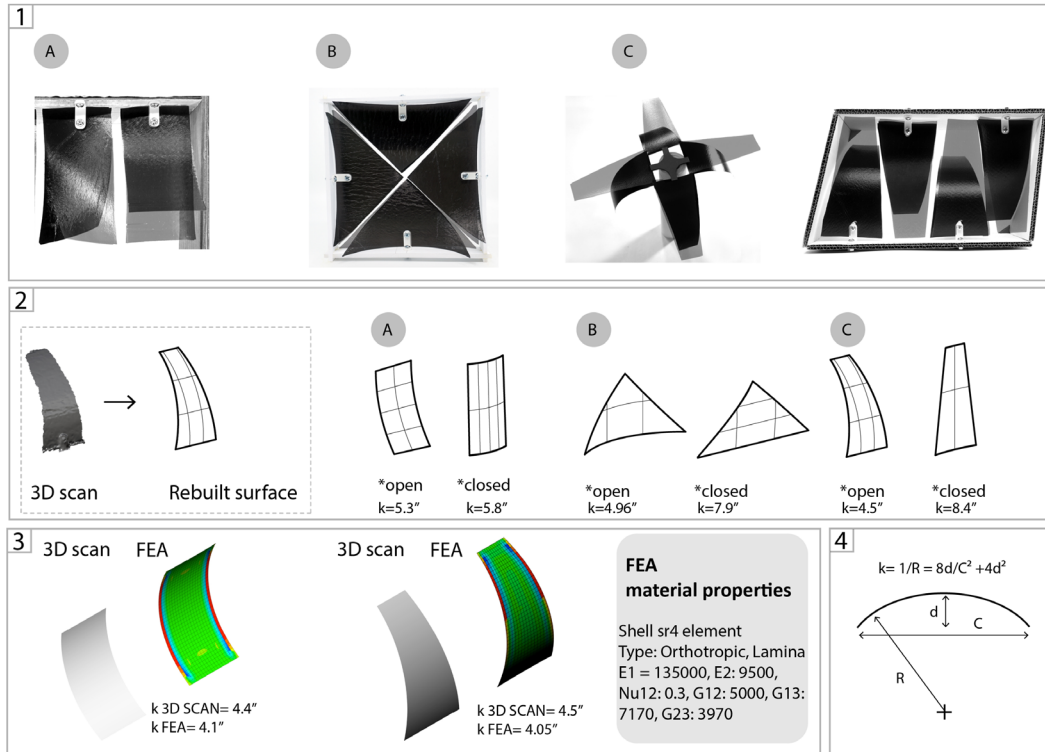


FIG. 6 Prototype fabrication with different geometries. 1) Built prototypes 2) Scanned and rebuilt surfaces with curvature value. 3) Compared curvature values from 3d scans and the FEA model. 4) Curvature formula.

The second set of studies aimed to assess the impact of changing the fibre arrangement on the prototypes. Changing the fibre arrangement made it possible to obtain two stable states that enhanced the units' potential use as shading devices, enriching the design space, and thereby increasing the possibility of achieving aesthetically pleasing architectural skins. The fibres were angled 45-135° with respect to the main lines used to construct the rectangle, triangle, and trapezoid. The manufacturing process mainly remained the same, except that the prototypes needed to be cut with particular attention given to the fibre orientation. The layer order, in which the 45° or 135° carbon fibre laminates are placed first on the aluminium plate, did not seem to affect the stable states' resulting curvature.

Figure 7 shows the prototypes fabricated with a 45-135° fibre arrangement; 7-1 shows the prototypes in their two stable positions by overlaying two photos; and 7-2 shows the scanned and rebuilt digital prototypes. All three basic shapes—rectangle, triangle, and trapezoid—were fabricated with the same initial measurements. The prototypes were also scanned, and the geometries were rebuilt to obtain the curvature k values and study the adaptability range of both stable states. One main difference in this set of prototypes is that instead of having ‘open’ and ‘closed’ positions, the stable states can be characterized as position one and position two due to their present geometry, as depicted in Figure 7-2. As seen in Figure 7-1, the two states for Prototypes A and C are distinct and appear promising for a shading device design since they could direct sunlight in two different directions. This hypothesis is tested in the next section of this paper. On the other hand, Prototype B with the 45-135° fibre arrangement does not present distinct positions in its two stable states. Modifying the triangle’s boundary condition could yield better results for skin design.

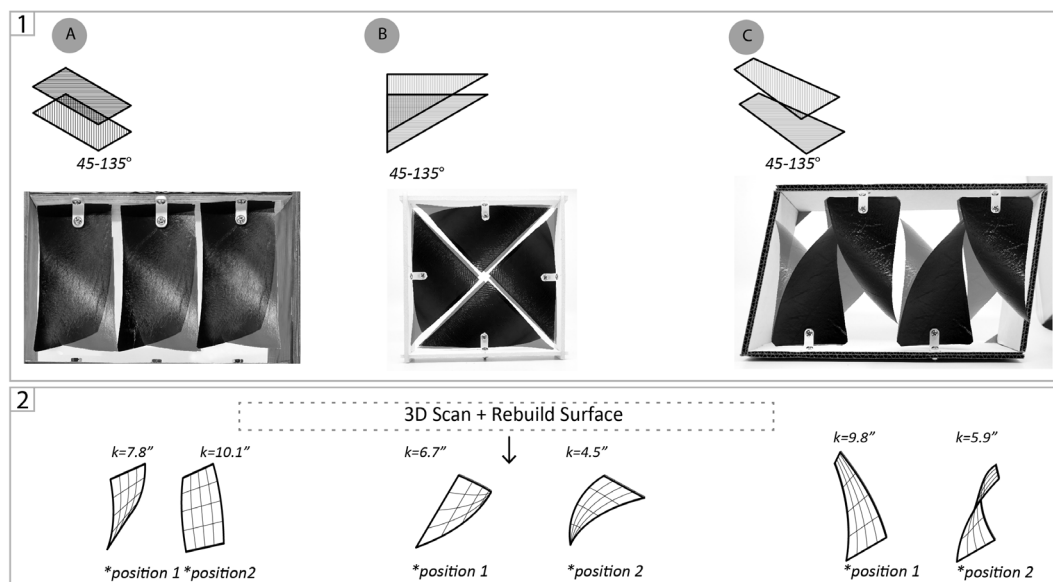


FIG. 7 Prototype fabrication with changing fibre arrangement 45-135°

4.2 DAYLIGHT PERFORMANCE EVALUATION OF FABRICATED PROTOTYPES

As mentioned before, this study combines bottom-up experimental prototyping with top-down studies to simulate the performance of the kinetic shading systems and assess their functionality as environmental control elements. The prototypes described in the previous section were scanned and rebuilt in modelling software. To evaluate the different prototypes’ performance, we developed a digital model of the kinetic system and defined a simple test room to perform daylight simulation studies. This study aims to measure the amount of daylight that enters a test room in the screen’s open and closed positions. For this study, a larger difference in daylight performance between open and closed positions is better, since this would provide a broader range for daylight needs. In contrast, if there is not much of a difference between the open and closed positions, the kinetic screen is not functional for the purpose of this study. The test room measures 2.1 x 2.5 m, and has a large window opening of 1.7 x 1.86 m. The shading screen is placed 12.7 cm behind the window’s

glass pane to avoid the bistable flaps colliding with the glass facing north. North-facing windows in the northern hemisphere receive little direct sunlight, so we selected this orientation for the study. To assess the difference between daylight with the screens in their all open and all closed positions. Details of the materials and enclosure are shown in Figure 8-3.

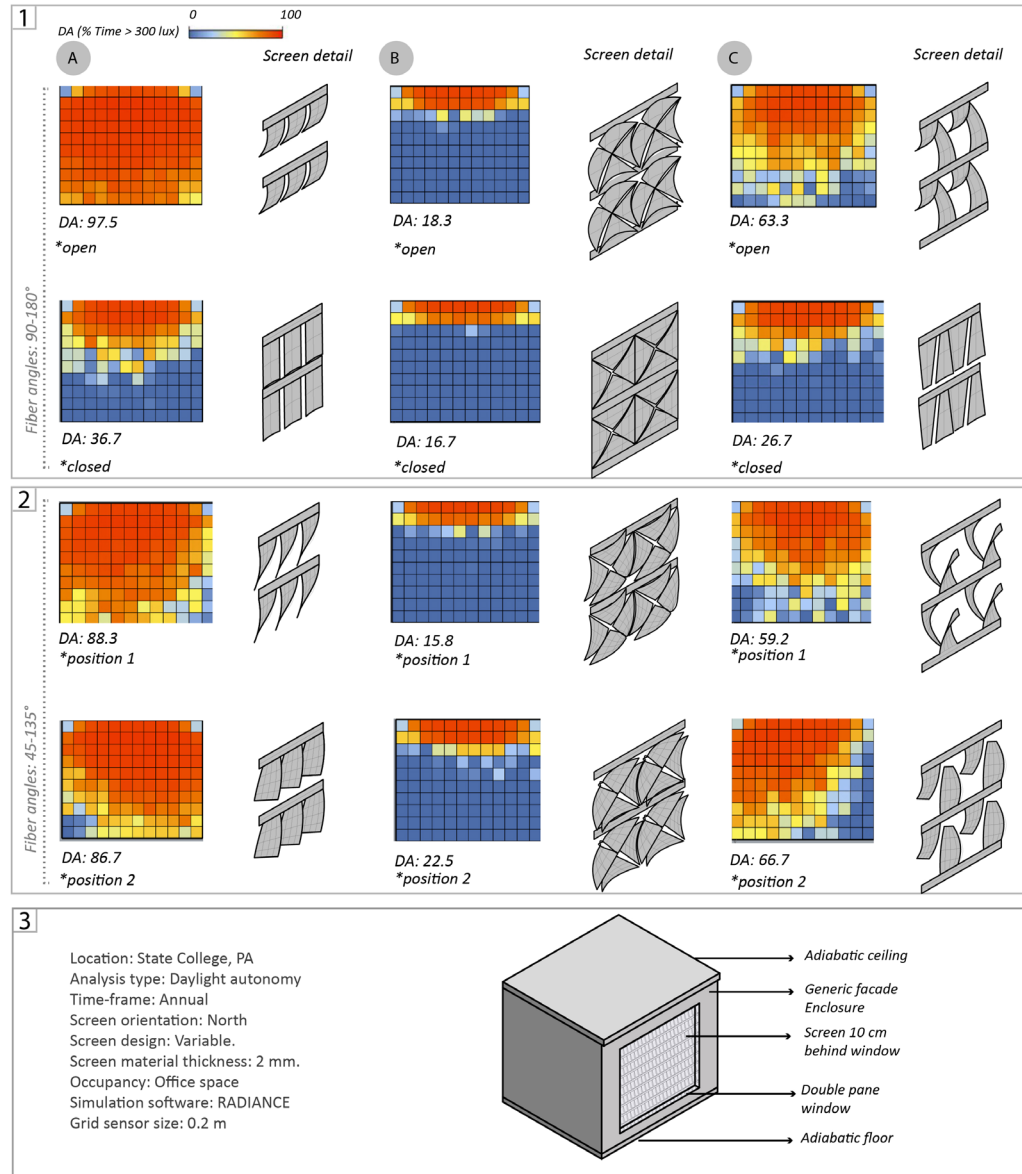


FIG. 8 Daylight simulation studies

Prototypes A, B, and C were simulated with two different fibre arrangements, 90-180°, and 45-135°. Again, it is noted that only prototypes with a 90-180° fibre arrangement have differentiated 'open' and 'closed' positions. Annual daylight autonomy analysis studies were conducted for State College, PA, to compare the screen's performance in its two stable states. The main advantage of kinetic shape-morphing systems is that each unit that forms the screen can adopt different positions during the day to achieve enhanced environmental performance. However, in this first set of simulations,

the shading screen was assumed to remain stable for the entire year. This is because this study's goal was to assess where there was a significant difference in daylight performance when the prototypes were in one stable state versus the other, i.e., when screens are open versus closed, position one versus position two. With the second set of simulation studies, we aimed to find optimal screen configurations and states for achieving specific daylight targets throughout the day.

Figure 8-1 shows daylight simulation results for designs with a 90-180° fibre arrangement. Notice how Prototypes A and C present distinct daylight performances in their open and closed positions, decreasing from ~98 % to 36% and from ~63% to 27% daylight autonomy. This result indicates that the two stable states of the bistable laminates are enough to impact daylight performance significantly and could be manipulated to achieve specific daylight requirements. On the other hand, Prototype B does not present significantly different daylight values for its two stable states, changing only from ~18 to 17% annual daylight autonomy. This result indicates that these prototypes need to be redesigned to increase the design's adaptability range and utilize them as units in a functional shading device. Figure 8-2 shows the simulation results of prototypes with a 45-135° fibre arrangement. Visual inspection of the daylight results shows that screen designs A and C direct daylight to either the right or left sides of the room, having distinct daylight performances. Although these results concern annual daylight values, they show the potential of designing different fibre arrangements of bistable laminates to achieve specific functional requirements, such as regulating daylight throughout the day. Prototype B, however, does not show distinct performance metrics for the two stable states. As mentioned above, the basic unit's proportions and design could be rethought to enhance its functionality as a shading device unit in terms of its potential for daylight control.

4.3 RANKING DESIGNS

The results from the experimental prototyping and simulation studies discussed above presented different criteria for evaluating the designs and selecting the most promising ones regarding their functionality as shading screens. While daylight performance was limited in scope, it indicates how distinct the performance that the two states of the prototypes generate is. Prototypes A, B, and C were evaluated according to the following criteria in a design decision matrix shown in Figure 9: 1) ability to easily maintain two states; 2) adaptability range; 3) adaptability range with other fibre arrangements; and 4) daylight performance in different states. The design decision matrix compares design alternatives from multiple points of view, where each attribute is assigned a score based on the scale. The prototypes' ability to maintain their two states was assessed empirically by handling the prototypes and referring to the amount of force needed to transition from one state to another. Since these prototypes are asymmetric, i.e., have one side longer than the other, the stresses in one direction are not the same as the other direction's stresses. Therefore, more considerable forces are needed to transition from position 1 to position 2 than from position 2 to position 1—position 1 being the one in which the curvature is parallel to the longer side. If this difference is too big, it becomes a problem to use them in a shading screen because the actuator would have to be measured up to the largest force, thus decreasing the system's efficiency. These findings are consistent with Tawfik et al. (2007), who found that prototypes required a decreasing force to snap through to position 1 as the length to width ratio got higher until the prototypes stopped exhibiting two stable states. Prototypes B and C required a large force to transition from position 1 to position 2, but a small force to transition back, making them unappealing for kinetic skin applications as any unintended force (air current) might make the laminates transition between states. The adaptability range was assessed by overlaying the pictures of their two stable positions and visually inspecting the two states' differences. The third criterion, fibre arrangement and adaptability range, was also evaluated

through visual analysis of the overlaid photos. The last criteria, daylight performance in different states, was assessed through daylight performance studies. Figure 9 shows the design decision matrix with the scores assigned to each prototype. Prototype A was selected as the most promising one. Therefore, the third set of experimental prototyping and the second round of simulation studies focused only on Prototype A.

	Typology A	Typology B	Typology C
Able to maintain states	5	1	1
Adaptability range ON/OFF state	5	1	5
Adaptability range with different fiber arrangements	5	2	5
Daylight performance in different states	5	2	5

Ability to maintain states: 5) Two similar forces are needed to snap from one position to the other to 1) The difference between the forces is so large that the prototype maintain only one position. Adaptability range: 5) There is a large difference in the shape of position 1 versus position 2 assessed visually to 1) There is not much difference in the shape of position 1 versus position 2. Adaptability range with different fiber arrangement (same as previous scale). Daylight performance in different states: 5) There is a 50+ percentage difference in daylight autonomy assessment to 1) There is a 10+ percentage difference in daylight autonomy assessment

FIG. 9 Evaluating the prototypes

4.4 FABRICATING PROTOTYPES WITH MULTIPLE FIBRE ARRANGEMENTS

The third set of studies focused only on Prototype A, as it was selected as the most promising one to use in a kinetic shading device. This study aimed to explore the potential of multiple fibre arrangements to increase the design space of kinetic shading systems while potentially enhancing functionality by tailoring fibre arrangements to targeted performance requirements. The second aim of this study was to characterize the geometry of the two stable states resulting from designed fibre arrangements. Six different prototypes were built with dimensions $w=7.62$ cm $l=15.24$ cm. The prototypes had different fibre arrangements, namely, $0-90^\circ$, $15-105^\circ$, $30-120^\circ$, $45-135^\circ$, $60-150^\circ$, and $75-165^\circ$. The angles were selected to test a gradient of options from 0 to 90 degrees. The prototypes were cured in a single aluminium plate to decrease any possible variability derived from different fabrication conditions (temperature, humidity) in multiple rounds.

Figure 10-1 shows the photograph of the prototypes in both states. At first glance, it is apparent that Prototypes 1 through 4 present a significant adaptability range, while prototypes 5 and 6 do not present states that are easily differentiated from each other. Also, the scanning and modelling of the prototypes and comparing them with FEA results gave more accurate information on the adaptability range. Figure 10-1 characterizes the geometry of all six prototypes, regardless of the individual fibre arrangement. The geometry is derived from a straight generatrix l and a curved directrix m . The angles of l and m with the main geometric lines of the prototypes change according to the designated fibre arrangement. Figure 10-3 shows the curvature $k1$ and $k2$ of the different prototypes, corresponding to position 1 and 2 states. Curvature $k1$ (position 1) presents a shorter radius—meaning it is more curved—in all the prototypes. Prototypes 1 through 6 have a shorter curvature radius parallel to the longest side of the rectangle in position 1, which indicates that the curing process generates more stress in that direction due to the fibres being longer in that direction. With

both the scanned prototypes and the FEA results, the modelling and geometric characterization allow one to construct accurate digital models that can be used to predict their performance as functional shading devices. In general, the directions of the fibres determine the directrix of the curved states, and the curvature radii appear to be smaller in the direction of the longer fibres.

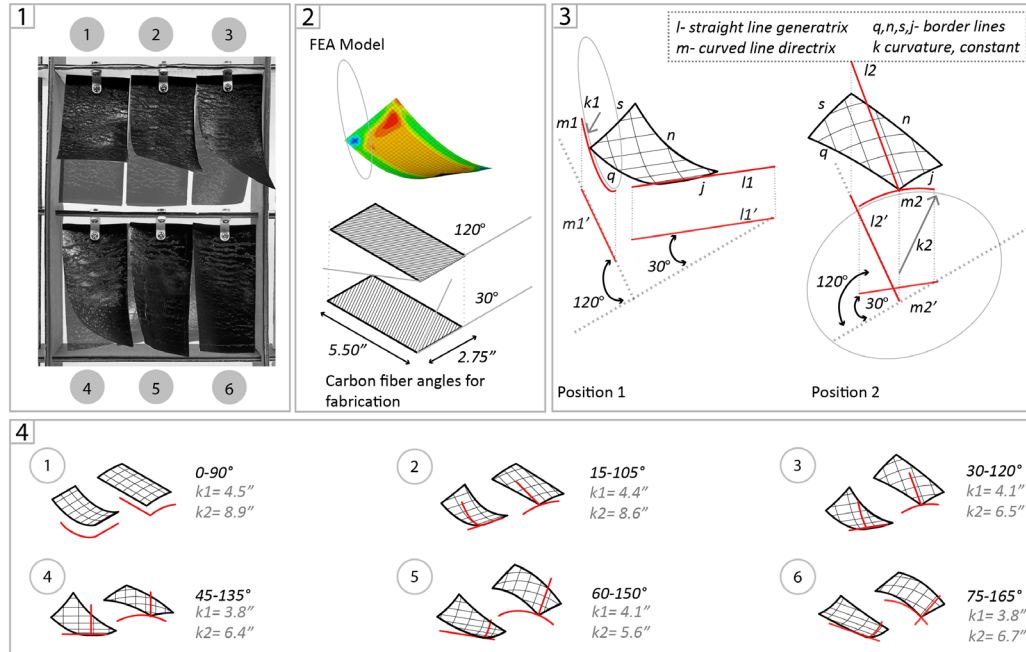


FIG. 10 Impact of fibre arrangement on the two states of the prototypes

4.5 OPTIMIZING KINETIC SHADING CONFIGURATIONS

The advantage of kinetic screens relies on being able to adapt their configuration according to changing environmental conditions. The first simulation studies compared daylight performance between the kinetic shades' different states, disregarding dynamic features. A second simulation study was then conducted to test the efficiency of Prototype A ($w=7.62$ cm $l=15.24$ cm), in two variations, in helping to maintain a certain level of daylight throughout the day. Prototype A.1 has fibres at angles of $90-0^\circ$, and Prototype A.2 has fibres at angles of $45-135^\circ$. The idea is that the kinetic shading system adopts multiple configurations throughout the day to guarantee a targeted performance, which, in this case, was to maintain an average of 500 lux in the space—appropriate for office work. It may be recalled that one of the benefits of having kinetic systems with active actuation is that they can be adjusted on demand to meet functionality requirements. Optimization algorithms were used to find the optimal screen states in two-hour intervals for the year's longest day—June 20. The objective of the study is the average lux value in the space: The algorithms seek to minimize the difference between the obtained average lux and the target average lux of 500. The variables are the values for each row (0: row is open, 1: row is closed). The room settings were the same as those adopted in the first simulation study. They were also conducted using Radiance as the simulation engine, with the DIVA plugin for Grasshopper 3D. The optimization problem was solved using Galapagos, a plugin for Grasshopper that utilizes genetic algorithms to minimize or maximize a function. Each row of the screen could adopt either one of the two stable positions modelled

according to the study on fibre arrangement. The selected fibre arrangements to test were 90-0° and 45-135°, which displayed wide adaptability ranges and tight curvature values in both states.

Figure 11-3 shows the performance of the optimized solution, which indicated that the screen with Prototype A.1 (90-0° fibres)—in optimized configurations—can keep a targeted daylight average of 500 lux throughout the day. The optimization algorithm found the best configuration to achieve an average value close to the targeted daylight value. As shown in the graph, prototype A.1 is more successful in maintaining the target daylight due to its shape in both states. For instance, at 2pm, the optimized configuration for the screen with Prototype A.1 is to have all the rows in Position 1, blocking the high sun rays at that time of day. Prototype A.2, on the other hand, can only achieve an average of ~1000 lux even in its optimal configuration at noon. The study showed that between two designs, A.1 and A.2, which only differ in their fibre arrangement, the optimal configuration of one design (A.1) performs better than the optimal configuration of the other. The optimization results suggest that selecting adequate fibre arrangement for kinetic bistable screens yields designs with better daylight performance.

The screen adopts a different configuration every two hours to maintain the targeted daylight. The study was performed every two hours due to the time (~10 hours) that the optimization takes. The possible kinetic shading configurations were also limited; we limited the number of possible screen configurations by establishing that all laminates on the same row must adopt the same position at a given time, which was decided based on the high position of the sun at the selected date, as shown in Figure 11.1. Future studies could allow each screen unit to move independently, enhancing daylight control and creating more complex aesthetic design solutions. Nevertheless, finding optimal screen configurations with such an ample design space and possible individuals in the optimization problem would require other heuristics to reduce computation time. Furthermore, finding the optimal configuration for the kinetic shadings would probably have to be done a priori, since real-time optimization does not seem feasible due to long computation times.

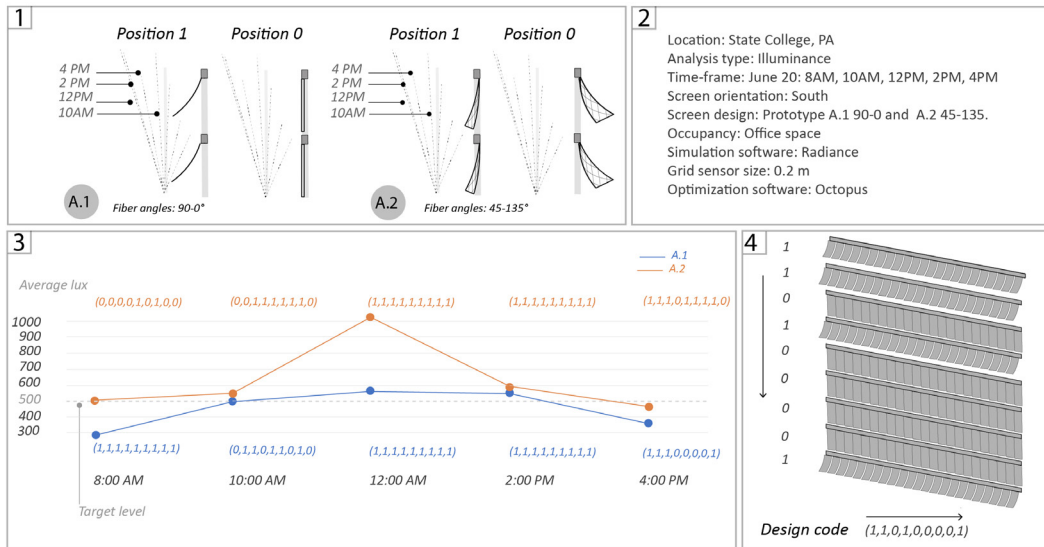


FIG. 11 Daylight simulation studies conducted to optimize screen configuration. 1) Sunray angles for both prototypes 2) Optimization settings 3) Optimization results, and 4) Design code for results.

5 CONCLUSION

This paper presents a comprehensive investigation of using bistable composite laminates for kinetic building shading devices. Following experimental prototyping, we analysed a series of bistable units with different geometrical configurations, aiming at different design solutions for kinetic shading devices. The analysis of such prototypes allowed us to identify the most promising units by assessing their adaptability range and studying their forms in the two equilibrium states, using an FEA model and scanned digital models. A series of annual daylight simulation studies were then conducted to compare the performance between the two states. We selected one prototype (Prototype A, a rectangle of $w=7.62$ cm $l=15.24$ cm) as the most promising unit to continue the investigation using a design decision matrix. In the second round of experimental studies, we explored the effects of changing fibre arrangement on the resulting stable states and characterized its impact on the units' geometry. The presented strategy for designing the fibre alignment increases the range of possible design configurations of the shading units, thereby increasing their potential as shape-morphing elements. The proposed strategy enhances their functionality as architectural elements by offering designers important insights for designing with bistable materials. Finally, we compared the effectiveness of a kinetic shading system using Prototype A with two fibre arrangements ($90-0^\circ$ and $45-135^\circ$) in maintaining target daylight throughout the day.

The first set of simulation studies demonstrated the impact of geometry on the resulting two stable states and its effect on daylight performance. Results show that some base geometries, such as rectangles, have a more distinct open and closed shape configuration and therefore are better suited to use in the design of kinetic shading devices for various daylight needs. The second set of simulation studies shows that the proposed system facilitates keeping daylight within the desired range. Research results indicate that fibre arrangement has an impact on the difference between the open and closed position of the bistable flaps, which is important to improve the daylight performance of the shading screens. Therefore, fibre arrangements and overall geometry are important design variables in achieving specific daylight targets.

This study argues that bistable kinetic systems could be introduced as an alternative to conventional shading solutions, with increased design potential in shape variety and shape morphing range of motions. This system offers increased granularity (resolution) by having smaller shading modules than in conventional systems, thereby allowing increased control of daylighting in terms of level. The main advantage of bistable systems for kinetic applications is their ability to maintain two stable states without additional input energy. Nevertheless, bistable laminates still have some limitations that need to be addressed: the non-manual actuation, the high cost of the carbon fibre prepregs, and the unknown impact carbon fibre has on the environment after its use. The design space of kinetic bistable shades increases when considering fibre arrangements, as shown with the different prototypes of this research.

A limitation of this study is that we only considered geometry, size, and fibre arrangement as design variables for the proposed kinetic shading system using bistable composite laminates. Other variables such as material thickness and mechanical properties, and optical values (reflection, absorption) were not explored. Considering that fatigue, durability, overall robustness, and human factors are critical for building-scale applications. Also, we only considered daylight in evaluating the performance of the shading devices; future research could also consider metrics such as glare, radiation, energy performance, and solar heat gain coefficient. Furthermore, this study assumes that the proposed kinetic systems can be actuated with a smart material actuator. We base that assumption on both the studies that have demonstrated the feasibility of combining bistable

materials and smart actuators and the low energy required to transition between states that previous studies, described in the literature review, reported using the same material in this study—carbon fibre prepregs. Future studies will combine bistable composite laminates with smart actuators, as shown in Figure 12. Notwithstanding these limitations, the study suggests that the geometric configurations that bistable composite laminates express render them a promising material for developing novel and functional kinetic systems for buildings.

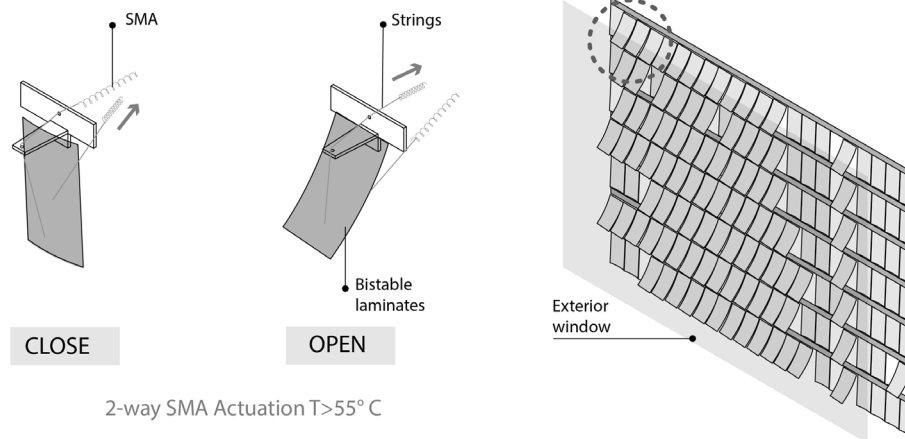


FIG. 12 Actuation mechanism schema, bistable laminates combined with two-way shape memory alloy springs.

Acknowledgments

This work was supported by the American Institute of Architects Upjohn Research Initiative, and the Architectural Research Centers Consortium Research Incentive Award.

References

- Addington, M., & Schodek, D. (2005). *Smart Materials and New Technologies - For architecture and design professions*. In Elsevier. Architectural Press.
- Ahlquist, S., Thün, G., Newell, C., & Velikov, K. (2013). Toward a Pedagogy of Material Systems Research Toward a Pedagogy of Material Systems Research. *TxA Interactive*, November 2013, 22–33.
- Al-Masrani, S. M., & Al-Obaidi, K. M. (2019). Dynamic shading systems: A review of design parameters, platforms and evaluation strategies. *Automation in Construction*, 102, 195–216. <https://doi.org/10.1016/j.autcon.2019.01.014>
- Al-Masrani, S. M., Al-Obaidi, K. M., Zalin, N. A., & Isma, M. I. A. (2018). Design optimisation of solar shading systems for tropical office buildings: Challenges and future trends. *Solar Energy*, 170, 849–872. <https://doi.org/https://doi.org/10.1016/j.solener.2018.04.047>.
- Barozzi, M., Lienhard, J., Zanelli, A., & Monticelli, C. (2016). The Sustainability of Adaptive Envelopes: Developments of Kinetic Architecture. *Procedia Engineering*, 155, 275–284. <https://doi.org/10.1016/j.proeng.2016.08.029>
- Bellia, L., Marino, C., Minichiello, F., & Pedace, A. (2014). An overview on solar shading systems for buildings. *Energy Procedia*, 62, 309–317. <https://doi.org/https://doi.org/10.1016/j.egypro.2014.12.392>
- Canera, M. A., Romera, J. M., Adarraga, I., & Mujika, F. (2015). Modelling and testing of the snap-through process of bi-stable cross-ply composites. In *Composite Structures* (Vol. 120, pp. 41–52). <https://doi.org/10.1016/j.compstruct.2014.09.064>
- Correa, D., Papadopoulou, A., Guberan, C., Jhaveri, N., Reichert, S., Menges, A., & Tibbits, S. (2015). 3D-Printed Wood: Programming Hygroscopic Material Transformations. *3D Printing and Additive Manufacturing*, 2(3), 106–116. <https://doi.org/10.1089/3dp.2015.0022>
- Denz, P.-R., Sauer, C., Waldhör, E. F., Schneider, M., & Vongsingha, P. (2021). Smart Textile Sun-Shading: Development of Functional ADAPTEX Prototypes. *Journal of Façade Design and Engineering*, 9(1), 101–116.
- Emam, S. A., & Inman, D. J. (2015). A review on Bistable Composite Laminates for Morphing and Energy Harvesting. *Applied Mechanics Reviews*, 67(6). <https://doi.org/https://doi.org/10.1115/1.4032037>
- Fiorito, F., Sauchelli, M., Arroyo, D., Pesenti, M., Imperadori, M., Masera, G., & Ranzi, G. (2016). Shape morphing solar shadings: A review. *Renewable and Sustainable Energy Reviews*, 55, 863–884. <https://doi.org/10.1016/j.rser.2015.10.086>

- Khoo, C. K., Salim, F., & Burry, J. (2012). Designing Architectural Morphing Skins with Elastic Modular Systems. *International Journal of Architectural Computing*, 09(04), 397–419. <https://doi.org/10.1260/1478-0771.9.4.397>
- Kim, S. W., Koh, J. S., Cho, M., & Cho, K. J. (2010). Towards a bio-mimetic flytrap robot based on a snap-through mechanism. *2010 3rd IEEE RAS and EMBS International Conference on Biomedical Robotics and Biomechatronics, BioRob 2010*, 534–539. <https://doi.org/10.1109/BIOROB.2010.5627994>
- Kretzer, M., & Rossi, D. (2012). ShapeShift. *Leonardo*, 45(5), 480–481. https://doi.org/https://doi.org/10.1162/LEON_a_00451
- Lachenal, X., Daynes, S., & Weaver, P. M. (2013). Review of morphing concepts and materials for wind turbine blade applications. *Wind Energy*, 16(2), 283–307. <https://doi.org/https://doi.org/10.1002/we.531>
- Lele, A., Deshpande, V., Myers, O., & Li, S. (2019). Snap-through and stiffness adaptation of a multi-stable Kirigami composite module. *Composites Science and Technology*, 182(May). <https://doi.org/10.1016/j.compscitech.2019.107750>
- Lienhard, J., Schleicher, S., Poppinga, S., Masselter, T., Milwich, M., Speck, T., & Knippers, J. (2011). Flectofin: A hingeless flapping mechanism inspired by nature. *Bioinspiration and Biomimetics*, 6(4). <https://doi.org/10.1088/1748-3182/6/4/045001>
- Loonen, R. C. G. M., Favoino, F., Hensen, J. L. M., & Overend, M. (2017). Review of current status, requirements and opportunities for building performance simulation of adaptive façades†. *Journal of Building Performance Simulation*, 10(2), 205–223. <https://doi.org/10.1080/19401493.2016.1152303>
- Mattioni, F., Weaver, P. M., Potter, K. D., & Friswell, M. I. (2008). The application of thermally induced multistable composites to morphing aircraft structures. *Industrial and Commercial Applications of Smart Structures Technologies*, 6930, 693012. <https://doi.org/https://doi.org/10.1117/12.776226>
- Pirraera, A., Avitabile, D., & Weaver, P. M. (2010). Bistable plates for morphing structures: a refined analytical approach with high-order polynomials. *International Journal of Solids and Structures*, 47(25–26), 3412–3425. <https://doi.org/https://doi.org/10.1016/j.ijsolstr.2010.08.019>
- Schultz, M. R., & Hyer, M. W. (2003). Snap-through of unsymmetric cross-ply laminates using piezoceramic actuators. *Journal of Intelligent Material Systems and Structures*, 14(12), 795–814. <https://doi.org/https://doi.org/10.1177%2F104538903039261>
- Sigmund, B. (2016). Solar Curtain – Sonnenschutz durch Formgedächtniseffekt (Solar Curtain - sun shading through shape memory effect). *DETAIL Research*.
- Song, J. Y., Heo, S., & Shim, J. (2018). Snapping Façades: Exploring Elastic Instability for the Building Envelope. *Technology Architecture and Design*, 2(1), 45–54. <https://doi.org/10.1080/24751448.2018.1420964>
- Sung, D. (2016). Smart Geometries for Smart Materials : Taming Thermobimetals to Behave Smart Geometries for Smart Materials. *Journal of Architectural Education*, 4883. <https://doi.org/10.1080/10464883.2016.1122479>
- Tawfik, S., Tan, X., Ozbay, S., & Armanios, E. (2007). Anticlastic stability modeling for cross-ply composites. *Journal of Composite Materials*, 41(11), 1325–1338. <https://doi.org/https://doi.org/10.1177%2F0021998306068073>
- Vander Werf, B. (2009). *Elastic Systems for Compliant Shading Enclosures*. University of Arizona.
- Vazquez, E., Gürsoy, B., & Duarte, J. P. (2019). Formalizing shape-change: Three-dimensional printed shapes and hygroscopic material transformations. *International Journal of Architectural Computing*. <https://doi.org/10.1177/1478077119895216>
- Vazquez, Elena, Randall, C., & Duarte, J. P. (2019). Shape-changing architectural skins: a review on materials, design and fabrication strategies and performance analysis. *Journal of Façade Design and Engineering*, 7(2), 91–102. <https://doi.org/https://doi.org/10.7480/jfde.2019.2.3877>
- Wood, D., Correa, D., Krieg, O. D., & Menges, A. (2016). Material computation-4D timber construction: Towards building-scale hygroscopic actuated, self-constructing timber surfaces. *International Journal of Architectural Computing*, 14(1), 49–62. <https://doi.org/10.1177/1478077115625522>
- Worre Foged, I., & Pasold, A. (2015). Thermal Activated Envelope : Development of a Method and Model for Programming Material Behaviour in a Responsive Envelope. In B. Martens, G. Wurzer, G. T. W. Lorenz, & R. Schaffranek (Eds.), *Proceedings of the 33rd eCAADe Conference - Volume 2, Vienna University of Technology, Vienna, Austria, 16-18 September 2015* (pp. 449–458). Vienna University of Technology.
- Yang, Y., Dias, M. A., & Holmes, D. P. (2018). Multistable kirigami for tunable architected materials. *Physical Review Materials*, 2(11), 1–6. <https://doi.org/10.1103/PhysRevMaterials.2.110601>
- Yi, H., & Kim, Y. (2021). Self-shaping building skin: Comparative environmental performance investigation of shape-memory-alloy (SMA) response and artificial-intelligence (AI) kinetic control. *Journal of Building Engineering*, 35(October 2020), 102113. <https://doi.org/10.1016/j.jobe.2020.102113>
- Yoon, J. (2019). SMP Prototype Design and Fabrication for Thermo- responsive Façade Elements. *Journal of Façade Design and Engineering*, 7(1), 41–62. <https://doi.org/10.7480/jfde.2019.1.2662>

Circular, biomimicry-based, and energy-efficient façade development for renovating terraced dwellings in the Netherlands

Ana Luíza Binow Bitar ^{*1,2,4}, Ivar Bergmans ¹, Michiel Ritzen ^{1,3}

* Corresponding author, albinowbitar@gmail.com

1 Zuyd University of Applied Sciences, Academy Built Environment, Netherlands

2 Universidade Federal de Viçosa, Civil Engineering Department, Brazil

3 VITO, Unit Smart Energy and Built Environment, Belgium

4 Deerns Nederland BV, Building Physics and Energy, Netherlands

Abstract

Many studies concerning lowering the Operational Energy (OE) of existing dwellings have been conducted. However, those studies barely cover its collateral Embodied Energy (EE). As the Circular Economy is gaining momentum and the balance between OE and EE is shifting, the Life Cycle Energy Performance (LCEP) is becoming increasingly relevant as an indicator. LCEP accounts for all the OE and EE a building consumes during its lifespan. However, clear insights into the LCEP are still to be investigated. This study focuses on developing a circular and energy-efficient renovation solution for a common terraced dwelling typology in the Netherlands. The energy-efficient renovation is based on three circular strategies: Biomimicry, Urban Mining, and Design for Disassembly (DfD), covering the aspects of EE and future reuse of building materials and components. The developed renovation solution reduces 82% of the LCEP compared to the existing scenario. With additional photovoltaic (PV) modules, the dwelling reduces 100% of the LCEP. Applying biomimicry, urban mining, and DfD-based renovation can significantly lower the overall LCEP and its collateral environmental impacts to achieve a Life Cycle Zero Energy circular renovation.

Keywords

Circular Façade Design, Open-joint ventilated façade, Circular Energy Renovation, Biomimicry, Design for Disassembly, Urban Mining, Life Cycle Energy Performance.

DOI

<http://doi.org/10.47982/jfde.2022.1.04>

1 INTRODUCTION

Buildings are responsible for up to 40% of Operational Energy (OE) consumption in the European Union (EU) (Poel et al., 2007), and more than 60% of this energy comes out of fossil fuels, with an alarming collateral carbon emission rate (Martins et al., 2018). OE can be defined as the energy required to maintain comfort conditions and the building itself, such as lighting, heating and cooling systems (Li et al., 2020).

Therefore, to lower OE consumption as a path to reduce carbon emissions, policies and developments are underway to achieve a nearly Zero Energy Building (nZEB). An nZEB is a building with high energy performance in which the low amount of energy required is covered by energy generation from renewable sources on-site or nearby, such as photovoltaic (PV) modules (Chesné et al., 2012; European Commission, 2016). By 2021, all new buildings in the EU should be nZEB, and by 2050 the complete building stock should achieve this target (European Commission, 2010).

LIST OF ABBREVIATIONS

CDW	Construction and Demolition Waste
DfD	Design for Disassembly
EC	European Commission
ECO2	Embodied Carbon
EE	Embodied Energy
EU	European Union
LCEP	Life Cycle Energy Performance
nZEB	nearly Zero Energy Building
OE	Operational Energy
PV	Photovoltaic
ZEB	Zero Energy Building

The façade plays an essential role in OE reduction, as most heat and light transfers occur through it (Tokuç et al., 2018). Therefore, the façade design strategy highly influences the thermal performance of a building. A commonly adopted solution towards an energy-efficient building is the addition of inorganic fibrous materials and organic foamy materials, such as polyurethane and extruded polystyrene insulation throughout the façade (Papadopoulos, 2005). Reused and bio-based insulation materials are less applied, and their full potential and effect on LCEP are still to be thoroughly investigated.

A significant amount of studies has been conducted related to energy-efficient buildings' façades design, such as ventilated façades (Ahmed et al., 2015; Balocco, 2002; De Gracia et al., 2013; Fantucci et al., 2013, 2020; Gratia & De Herde, 2003; Medved et al., 2019; Sanjuan et al., 2011; Zhou & Chen, 2010), showing a decrease of up to 87% of the energy consumption during summer (Rasca, 2014). However, these studies barely cover the energy consumption related to the building's construction, demolition, disposal phases, and raw material consumption, which is covered in this research.

Of all extracted materials, 50% is attributed to buildings (Cottafava et al., 2020), and according to the European Commission (EC), construction waste accounts for over 35% of all waste generated in the EU, with its collateral Embodied Energy (EE) (European Commission, 2020c). The EE is defined as the energy required in buildings and their materials during the manufacturing, construction,

final demolition, and disposal phases (Dixit et al., 2010). Hence, the EC set up a long-term circular economy plan: the construction sector will be fully circular by 2050, and the intermediate goal is to have a 50% circular economy by 2030 (European Commission, 2020a).

Due to the growing progress toward a Zero Energy Building (ZEB), the shift between OE and the effect of building materials is becoming increasingly relevant for the environmental impact (BPIE, 2021; Sartori & Hestnes, 2007). It means that with OE reduction, the EE percentage tends to have a higher impact on the total energy consumption during the building's lifespan. Figure 1 visually expresses the balance shift between OE and EE for different energy profiles of dwellings. It shows that the better the energy efficiency of the dwelling (such as passive houses), the bigger the significance of EE. Therefore, the assessment of EE associated with the buildings' materials, and the buildings' energy performance by OE, are becoming equally vital to effectively evaluate the way to a sustainable built environment.

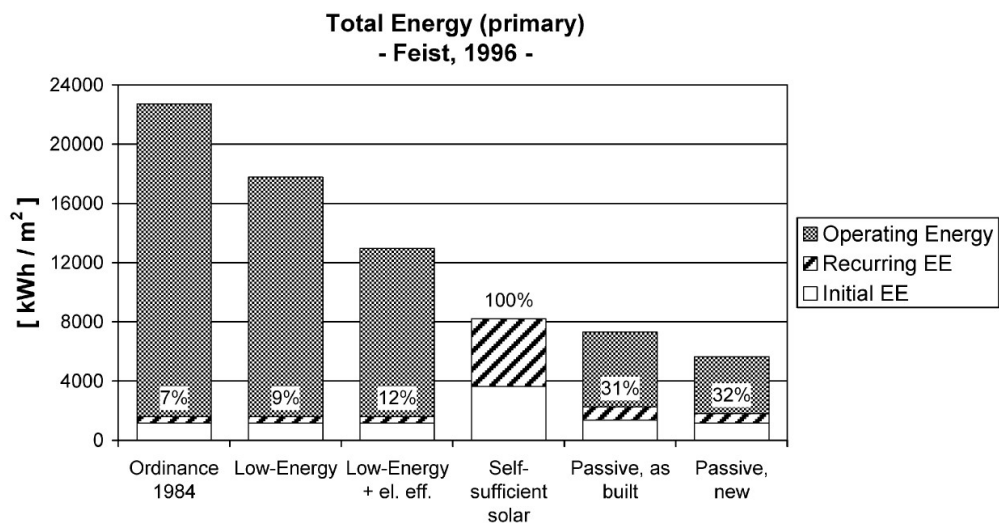


FIG. 1 Life cycle energy demand in different dwelling types (Source: (Feist, 1996))

In order to evaluate OE and EE at the same scale, this paper makes use of the Life Cycle Energy Performance (LCEP) analysis. The LCEP of a building corresponds to the summation of the total OE and EE consumption throughout its lifespan, enabling to address the total energy input and formulate strategies to reduce the primary energy use of the building and control emissions (Ramesh et al., 2010). In this sense, the LCEP should be as low as possible to reach the most sustainable building performance, assessing both EE and OE.

Accordingly to the EC, 85 to 95% of the existing buildings will remain standing by 2050 (European Commission, 2020b). This means that to achieve the mentioned goals, it is necessary to focus on the new buildings as well as on renovating existing ones. In this sense, the Renovation Wave comes as a strategy established by the EC in 2020 to double renovation rates in the next ten years and ensure higher energy and resource efficiency within the EU (European Commission, 2020b).

However, the total LCEP of building renovations has to be investigated as one path of the Renovation Wave to achieve the European plan using circular strategies and energy efficiency improvement. Therefore, this study aims to develop a circular and energy-efficient renovation of a common terraced dwelling type in the Netherlands, aiming at achieving a minimal LCEP, based on three strategies: firstly, “biomimicry” aiming at lowering the OE consumption and improving summer comfort; secondly, “urban mining” with maximum locally reused, recycled and bio-based materials to reduce the EE consumption; and thirdly, “Design for Disassembly” (DfD), aiming at multi-cycle circular solutions of building materials and components.

2 BACKGROUND ON THE STRATEGIES CONSIDERED IN THIS STUDY

2.1 BIOMIMICRY

Since nature has developed over aeons to provide sufficient solutions, it is the source of our sustenance and has the potential to be the source of answers to most of the challenges humankind faces. Therefore, analysing and mimicking natural strategies can also be a promising scenario for human design challenges. Biomimicry is the practice of designing and creating artificial replicas of natural phenomena to learn from them and improve upon or replace human-made counterparts.

Biomimicry has already been applied successfully in the built environment, bringing ample opportunities for innovation in engineering and architectural design (Badarnah, 2015). As an example, Figure 2 shows a building located in Harare, Zimbabwe, designed by architect Mick Pearce. Inspired by a termite mound system, this building is entirely cooled by natural ventilation.

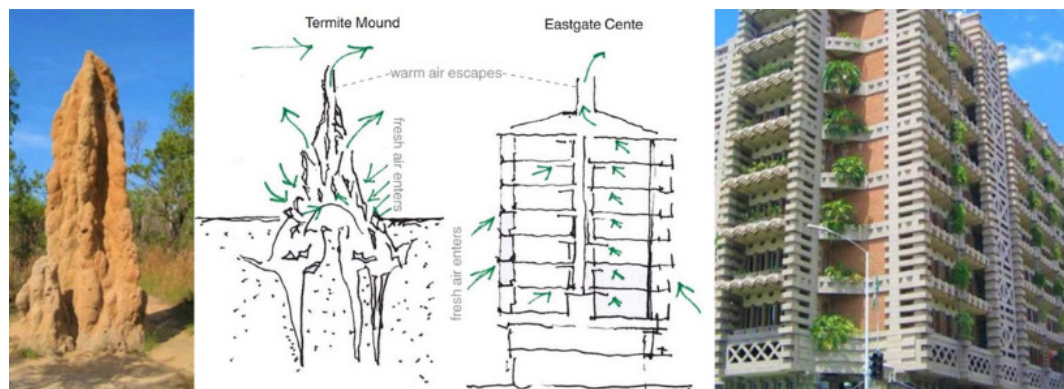


FIG. 2 Ventilation system in a termite mound vs a realised building (Source: (Aithal, 2020; Samimi, 2011))

Buildings' thermal performance, adaptability, and overall OE can all benefit from the application of functional biomimicry (Webb et al., 2018).

2.2 URBAN MINING

Urban mining first appeared with urbanist Jane Jacobs half a century ago. Jacobs estimated that if the metal content in rock continues to decline and the rate of metal resources extracted in the speedy mining increases, it would bring environmental problems and depletion of natural resources. Therefore, she penned the phrase “the cities are the mines of the future” and predicted a situation that is considerably more evident to perceive today (Graedel, 2011).

Even though the concept of urban mining kicked off with the metal extraction insight some time ago, it is widely extended to refer to the process of reclaiming components and elements previously used for buildings, infrastructure, and industries (Cossu & Williams, 2015).

The term “urban mining” is closely linked to the circular economy and offers an idea contrary to the classical “take-use-disposal” approach. It represents the process of recovering and reusing waste materials from urban areas once most of the materials incorporated into cities are disposed of in landfills, incinerated, or downcycled into products of much lower value at the end of their lifespan (Brunner, 2011).

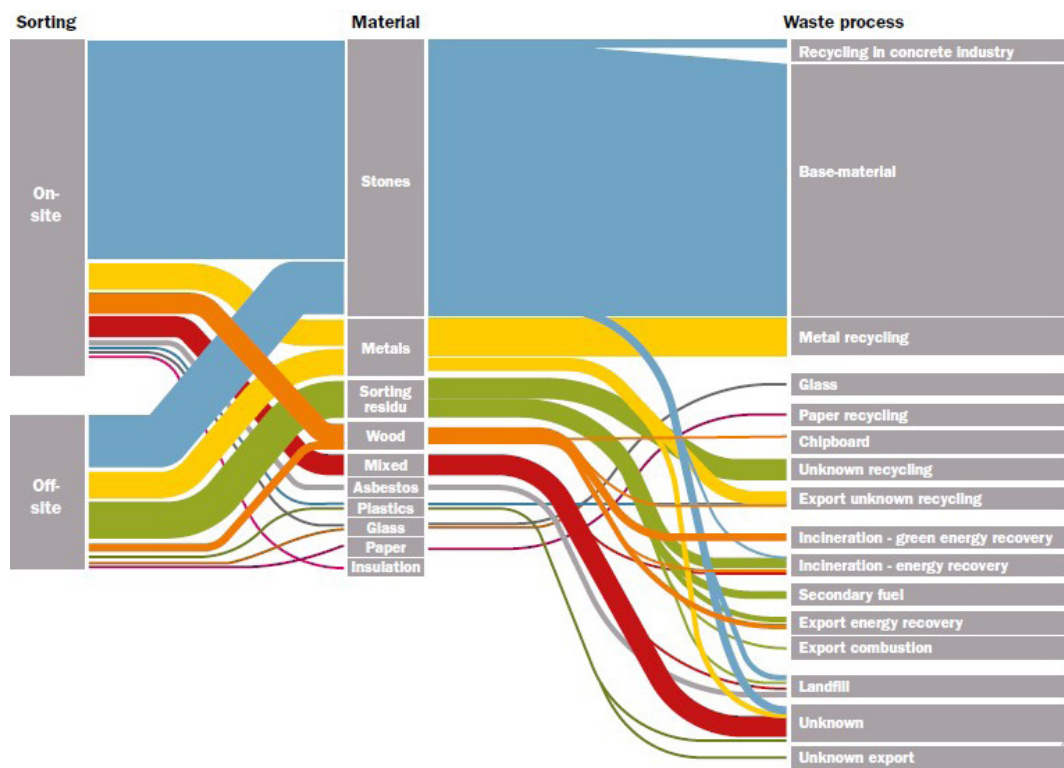


FIG. 3 Material End of Life Sankey diagram in the Netherlands (Source: (TNO, 2018))

In the Netherlands, about 85% of Construction and Demolition Waste (CDW) is downcycled into materials for building foundations, roads, or new residential areas and industrial estates, and only 3% of waste is recycled to construct new buildings (TNO, 2018), as visually represented in Figure 3 with the material end-of-life diagram. This overview reveals a critical improvement needed, and urban mining shows to be a promising strategy to upgrade these rates.

2.3 DESIGN FOR DISASSEMBLY

DfD is a key strategy that guides construction decisions and material selections, altering how elements are connected and structured to be simple, reversible, and resilient, ensuring that building components may be reused or recycled in the most effective manner possible at their end-of-life (Rasmussen et al., 2019). In the built environment, this strategy challenges the current processes, minimising the use of primary materials and maximising the rethinking of the shape of buildings by employing an easy assembly and disassembly technology for the reuse of components and materials.

Different tools have been developed to assess the disassembly level of building elements. For example, Alba Concepts (Mike van Vliet et al., 2019) has developed a methodology to measure the disassembly level. Moreover, the European Level(s) framework and the Belgium GRO framework show similar approaches (European Commission, 2021; GRO, 2022). They form a relevant basis for determining the environmental impact of entire or partial reuse and are directly in line with the end-of-life processing scenarios from LCA calculations.

Building components can only be recovered if they are easily connected to the surrounding building elements. Dry and mechanic connections, such as bolts and screws, are thus more effective than wet and chemical ones, such as glue and mortar (Galle, 2017). Therefore, easy assembly and disassembly design solutions are promising strategies to advance innovation towards a more circular built environment.

3 METHODOLOGY

This chapter is structured as follows: 3.1 describes the boundary conditions for the development of the renovation, such as the characteristics of the existing dwelling type and the available waste demolition materials for the application of urban mining; 3.2 describes the design methodology used throughout the development of the façade design; and 3.3 describes the methods used for assessing the renovation developed in terms of LCEP (3.3.1), such as EE and OE, and DfD (3.3.2).

3.1 BOUNDARY CONDITIONS

3.1.1 Existing dwelling design and structure

In the reconstruction period from 1946 to 1965, after World War II, terraced dwellings were rapidly built all around the Netherlands on a large scale. During that period, no regulations concerning energy performance were imposed (M. J. Ritzen et al., 2016). The choice of materials and design

strategies focused on reducing the costs as much as possible, while energy performance was not of significant relevance. According to the governmental Dutch Enterprise Agency (RVO.nl) of the Ministry of Economy, Innovation and Agriculture, 42% of all the dwellings in the Netherlands are terraced dwelling types (Agentschap NL, 2011).



FIG. 4 Existing terraced dwelling (Source: Google maps)

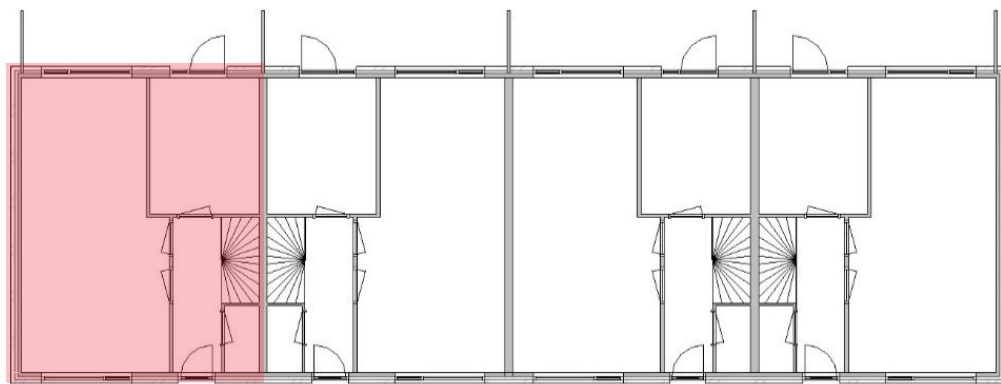


FIG. 5 Floorplan of the dwellings (analysed dwelling highlighted in red)

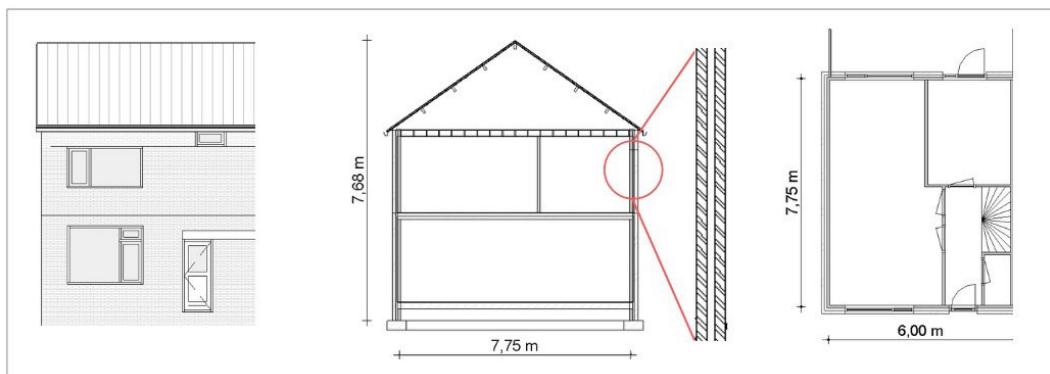


FIG. 6 Existing terraced dwelling: south façade, section, façade structure and floor plan

The selected dwelling for this study is a barely insulated two-floor residential dwelling, as indicated in Figures 4-6 and Table 1. The façade consists of two bricklayers with a ventilated air cavity between them, which does not efficiently insulate the dwelling, resulting in high energy consumption to maintain the inhabitants' thermal comfort. As an outcome, these terraced dwellings consume 41% of all primary energy intended for buildings in the Netherlands (Agentschap NL, 2011).

Moreover, terraced dwellings in the Netherlands are mainly social housing intended for people with lower incomes. Consequently, the reality of most of these houses is a lack of cooling systems, outdated heating systems, such as gas-heated radiators, and low insulation levels.

TABLE 1 Terraced dwelling: general characteristics.

GENERAL CHARACTERISTICS		
Total area	132	m ²
Heated area	81.25	m ²
Orientation front façade	Azimute 0	(North)
Building element	U-value (W/m ² K)	
External wall	2.70	
Roof	4.76	
Floors	1.96	
Windows	5.10	
Doors	3.40	

3.1.2 Available materials for renovation

The applicability of the urban mining concept in this study consists of reclaiming demolition materials from a region in the Netherlands called Parkstad, in the southeast of Limburg, Netherlands. The area faces a population decline, which causes a significant demolition assignment of approximately 10,000 dwellings and 150,000 m² utility and retail buildings (Stadhouders et al., 2021), resulting in a significant amount of waste materials, as indicated in Figure 7.

Among the materials presented in Figure 7, this study focuses on reusing wood. Firstly, because of the large quantity available (14kton). Secondly, wood has a high thermal resistance, is easy to separate from other building materials, has aesthetical appeal, and can be used in different building segments, such as insulation and construction structures.

Moreover, wood stores CO₂ and consequently can contribute to a low-carbon economy. The CO₂ stored in trees throughout their lifespan is retained in about 50% of the wood's dry weight in wood products. Therefore, the longer the wood remains in the application, the longer the CO₂ is removed from the atmosphere (Friedmann & Kelly, 2003; Petersen & Solberg, 2002; van der Lugt, 2012).

However, it is essential to highlight that critical issues occur when designing and constructing wooden façades, such as ageing treatment, suitable protection from various harmful effects, and fire protection (Herzog et al., 2005; Ivanović-Šekularac et al., 2016).

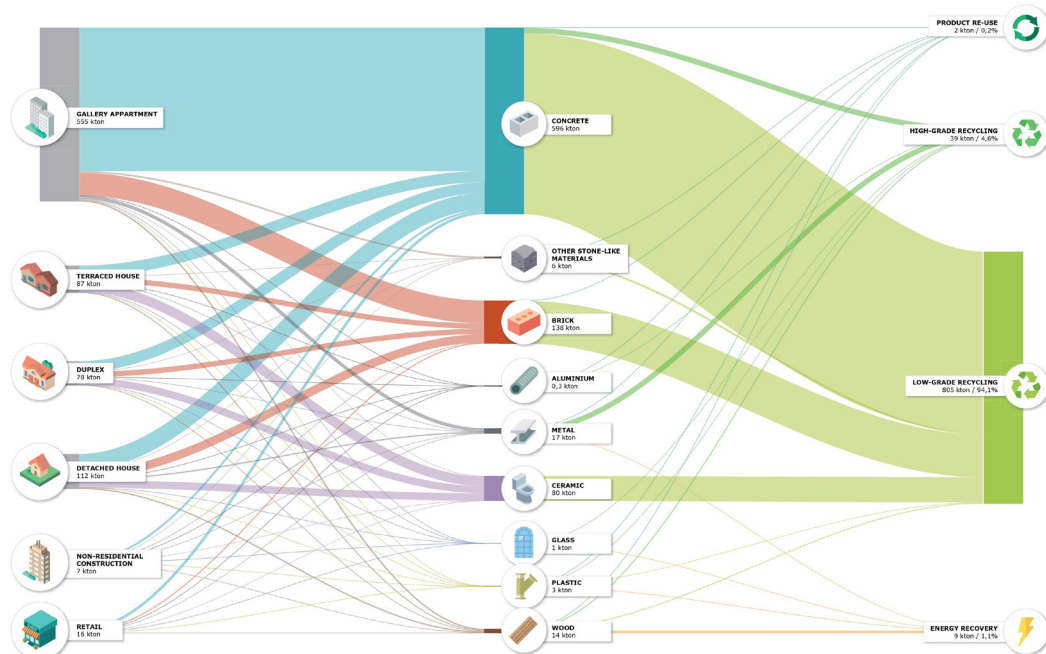


FIG. 7 Materials from demolition in Parkstad (Source: (Stadhouders et al., 2021))

3.2 DESIGN METHODOLOGY

The design methodology of this study follows the strategy of “Research by Design” (Biggs, 2002; Hauberg, 2011; Roggema, 2016; Zimmerman et al., 2007). Generally speaking, employing Research by Design means that the research and the design processes work intertwined; the design is not just a product of research but also a significant component of the research process.

According to Roggema (Roggema, 2016), the Research by Design process can be divided into three parts:

- Pre-design phase: this first stage of a Research by Design process is characterised by understanding;
- Design phase: this is the heart of the process, in which the research is continuously brought into the design process and deliberations;
- Post-design phase: the results are the final syntheses of the work, which must be coherently presented.

The applicability of this methodology strategy in the present study is shown in Figure 8.

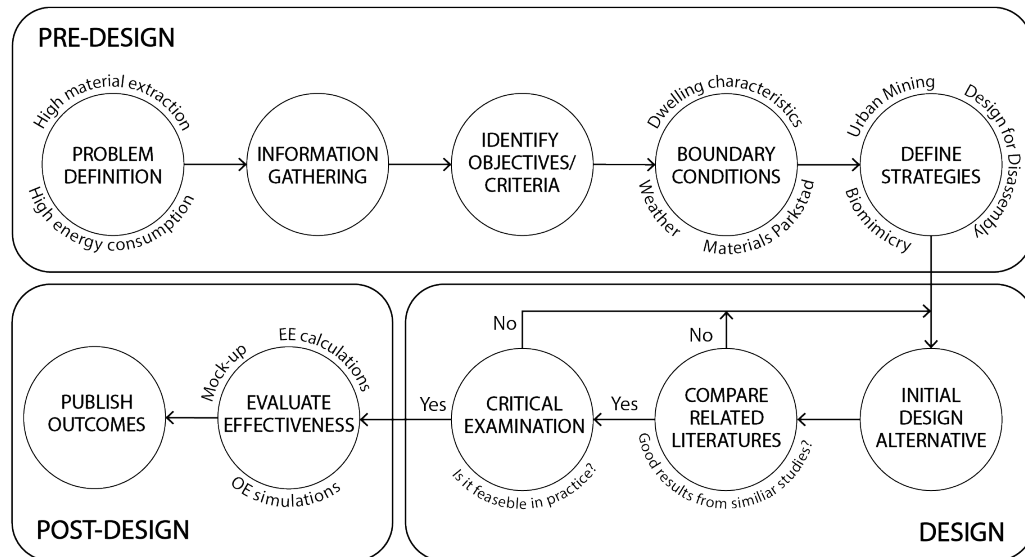


FIG. 8 Research by Design process

3.3 ASSESSMENT METHODOLOGY

This section describes the methodology for assessing the developed façade and the complete dwelling renovation. As previously mentioned, this paper uses the LCEP analysis to evaluate the designed renovation, addressing both the EE and OE (3.3.1) and assesses the developed DfD concept (3.3.2).

3.3.1 Life Cycle Energy Performance

In order to assess the LCEP of the developed renovation, the present study compares OE and EE in three different scenarios:

- **Scenario 1:** The existing dwelling before renovation (characteristics shown in section 3.1);
- **Scenario 2:** The renovated dwelling, implementing the developed façade design;
- **Scenario 3:** Scenario 2 with the addition of 25 m² PV modules on the south-orientated roof.

For comparing the three scenarios, a lifespan of 50 years was assumed. The lifespan of a building is both essential and difficult to predict. Generally, the lifespan ranges between 30 and 100 years (Mequignon et al., 2013). The choice of 50 years was based on previous buildings' life cycle studies (Barbara, R. et al., 2012; M. J. Ritzen et al., 2016; Van Ooteghem & Xu, 2012).

The minimal insulation value for façades in the Dutch standard is 4.5 m²K/W (Bowens et al., 2020). However, for comparison with existing products available on the market in subsequent steps of the research, this study is based on an insulation value of at least 7.10 m²K/W.

The conversion from kWh to MJ considered in this research was 5.22, based on system efficiency in the Netherlands (Bowens et al., 2020).

The OE and EE for scenarios 1, 2, and 3 are named OE₁, OE₂, OE₃, and EE₁, EE₂, EE₃, respectively.

3.3.1.1 Operational Energy

For the OE assessment, the present study used external literature and the programs *Uniec 2* (Uniec, n.d.) and Photovoltaic Geographical Information System (PVGIS) (European Commission, 2020).

Uniec 2 is an online tool that allows performing energy calculations for buildings based on Dutch regulations. The energy demand calculation is a multi-zone model, and the weather input file and occupancy and schedule for lighting and equipment were based on the NTA 7120. This makes it slightly more difficult to create a realistic picture of a situation but simplifies the program considerably. For the weather input file, *Uniec 2* uses an average and standard climate year, which is provided by NTA 7120. For the occupancy and schedules for lighting and equipment, NTA 7120 has different rules, some of which are related to the size of the building. The energy calculation only applies to building-related installations. Energy for household appliances, such as TVs, fridges, etc., is not included in the calculation. The infiltration load considered is 0.7 dm³/s per usable area (m²). As output, the total primary energy consumption of the building is revealed, and the percentage destined for heating, hot water, cooling, summer comfort, ventilation, and lighting is specified.

The energy intended for “summer comfort” provided by *Uniec 2* is a way to alert to the risks of overheating in the summer period. This energy refers to the energy required for cooling features to maintain the building’s summer comfort in overheating periods (Uniec, 2018).

PVGIS is an online free solar PV energy calculator to estimate the solar electricity production of a PV system. PVGIS has been developed by the European Commission Joint Research Centre to disseminate knowledge and data about PV performance and solar radiation. The tool employs high-quality satellite data on solar radiation, ambient temperature, and wind speed from climate reanalysis models. The PVGIS energy model is validated by the Joint Research Centre’s European Solar Test Installation (ESTI). Input data such as location, module type, slope, orientation, and peak PV power are entered into the tool. It then calculates the potential monthly and yearly electricity generation of the specified PV system.

Scenario 1

Firstly, the yearly OE₁ has been calculated using *Uniec 2*, following the characteristics described in 3.1.

Scenario 2

The OE₂ was divided into two parts: firstly, the renovation (without the developed ventilated façade addition) was calculated using *Uniec 2*. In this part, the glazings were changed from single to triple-glazed, and the external doors were changed to insulated wooden doors. Furthermore, 150 mm of insulation was added to the roof and ground floor and 240 mm to the exterior wall. The heating and hot water system were changed from a gas-heated radiator to an air heat pump. The U-values of the new building elements input in *Uniec* are shown in Table 2.

TABLE 2 U-value data input for energy simulation in Uniec.

U-VALUE (W/M ² K)		
Building element	Scenario 1	Scenario 2
External wall	2.70	0.14
Roof	4.76	0.13
Floors	1.96	0.21
Windows	5.10	1.10
Doors	3.40	2.00

Secondly, regarding the open-joint ventilated façade developed, due to the complexity of existing software, some values to analyse the effect of the ventilated façade on the buildings' energy consumption are based on previous research. Studies with similar designs and technologies present the scenarios' temperature differences, making the predictions of energy savings percentage for the complete building difficult (Sanjuan et al., 2011; Schabowicz & Zawislak, 2021). Therefore, a review study regarding ventilated façades (Ibañez-Puy et al., 2017) was used to define the expected energy percentage reduction destined for summer comfort with the addition of a ventilated façade.

Scenario 3

25 m² of PV modules (320 Wp/panel or 200 Wp/m² (Innodura, 2021)) on the south-orientated roof was included, corresponding to the available area of the south-oriented roof, resulting in a peak PV power of 5 kWp. The output energy per year from the PV modules implementation was calculated using PVGIS and discounted from the OE₂.

3.3.1.3 Embodied Energy

The EE of the three different phases of renovation were calculated through a cradle-to-gate assessment, which is an analysis of a portion of the product life cycle, starting with the resource extraction (cradle) and ending at the factory gate (before transportation to the consumer) (C.Cao, 2017). It is considered the energy spent for material extraction or harvest and the energy spent for the manufacturing process, as shown in Figure 9. Therefore, this study did not consider the energy used for the transportation of the material, the energy spent during the building assembly, the energy used for maintenance during the usage phase, and the energy consumption related to the end-of-life phase.

Firstly, the three scenarios were accurately modelled in *Autodesk Revit*, with the precise dimensions of the components, and the volumes of each material used in the models were calculated by Revit. Secondly, after having the density and materials' volume in the three scenarios, the EE in MJ/kg of each material was determined by gathering information from material suppliers, literature reviews, and the "ICE database".

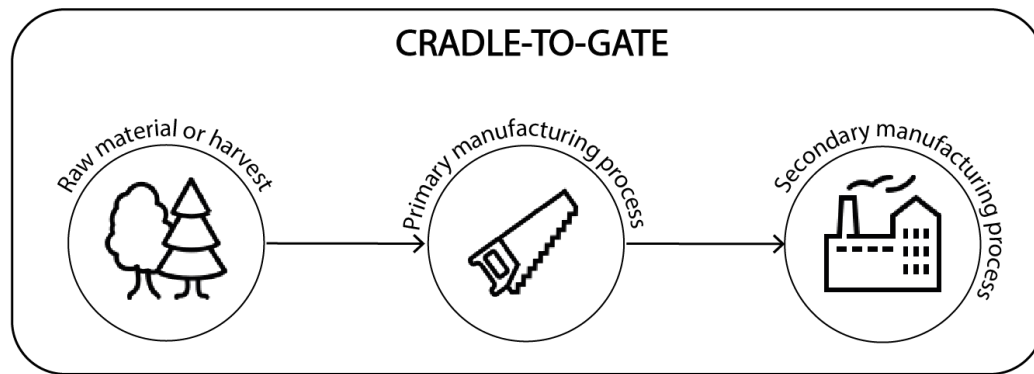


FIG. 9 Cradle-to-gate assessment scheme

The ICE database is a spreadsheet format developed by Geoff Hammond and Craig Jones from the Sustainable Energy Research Team (SERT) of the Department of Mechanical Engineering of the University of Bath (UK) (SERT, 2011), which compares different alternatives and calculates the environmental impact of components. It includes LCA information on the material or component levels and provides the EE [MJ/kg] and ECO_2 [kgCO_2/kg] of the most common construction materials utilised in the built environment (Bach & Hildebrand, 2018) based on the cradle-to-gate assessment. The database was selected by the consortium of a European research project.

The total EE from scenario 1 (EE_1) is the total of all EE from all materials that compose the existing terraced dwelling. The EE in scenario 2 (EE_2) is EE_1 discounting all the EE referent to the components demolished or changed in the renovated scenario, plus the energy related to the manufacturing of façade components. The calculation of EE in scenario 3 (EE_3) is the sum of EE_2 and the EE required for the PV modules extraction, manufacturing, and construction ($\text{EE}_{\text{PV modules}}$).

3.3.2 Design for Disassembly

The methodology adopted to assess the DfD index of the proposal was based on Alba Concepts (Mike van Vliet et al., 2019) and ISSO assessment (ISSO, 2021).

This method assesses the DfD index of a product, both in the end-of-life and the maintenance scenarios, by analysing the connections within its components based on four aspects: connection type, accessibility of the connection, piercing, and inclusion.

The “end-of-life” scenario refers to a situation where the complete structure is either demolished or disassembled. It evaluates the element’s potential to be reused for a new application in a new building. It depends on the product quality after use and how damage-free the product can be removed (disassembly). For that, the elements are assessed by their type and accessibility of connections.

The “maintenance” scenario refers to a situation in which one or more components of the structure will be removed or replaced during the lifespan of the building. It is assumed that every element will be removed individually. Therefore, besides the connection’s type and accessibility, the piercing and inclusion in its original positions in the building are also considered.

A connection can be valued at 0.1 - 1.0 according to its characteristics, with 0.1 giving the lowest rating for DfD and 1.0 the highest, as shown in Table 3. The average of these four scores determines the DfD level of the element in question. The weighted average of all the elements used in a building together constitutes the DfD Index of a building.

TABLE 3 Ranking for scoring an element connection for the DfD assessment.

TYPE OF CONNECTION		SCORE
Dry connection	Dry connection	1
Click connection	Dry connection	1
Velcro connection	Dry connection	1
Magnetic connection	Dry connection	1
Bolt and nut connection	Connection with added elements	0.8
Spring connection	Connection with added elements	0.8
Corner connection	Connection with added elements	0.8
Screw connection	Connection with added elements	0.8
Connection with added elements	Connection with added elements	0.8
Pin connection	Direct integral connection	0.6
Nail connection	Direct integral connection	0.6
Lute connection	Soft chemical bond	0.2
Foam connection (PUR)	Soft chemical bond	0.2
Glue connection	Hard chemical bond	0.1
Pouring joint	Hard chemical bond	0.1
Welded connection	Hard chemical bond	0.1
Cement bound connection	Hard chemical bond	0.1
Chemical anchors	Hard chemical bond	0.1
Hard chemical bond	Hard chemical bond	0.1
Accessibility of connection		score
	Freely accessible	1
	Accessible with actions that don't cause damage	0.8
	Accessible with actions that cause repairable damage	0.4
	Not accessible - irreparable damage to objects	0.1
Inclusion		score
	Open, no inclusion	1
	Overlap	0.8
	Closed (on one side)	0.2
Piercing		score
	No piercing	1
	Piercing by one or more objects	0.4
	Full integration of objects	0.1

4 RESULTS

This chapter is structured as follows: 4.1 discusses the design process (clarifying the reasons for each choice) and describes the final façade design; 4.2 reports the assessment in terms of LCEP of the three different scenarios; 4.3 shows the DfD assessment of the developed façade design.

4.1 FAÇADE DESIGN

The first part of the energy renovation proposal for the existing dwelling consists of added insulation on the façade structure. The proposed insulation addition does not only focus on improving the energy performance of the building but also on reusing the materials from demolition (urban mining) in its manufacturing process. In other words, this study defines the available materials at the demolition site that can potentially be transformed into an insulation material, which filtered the analyses between the use of glass (fibreglass) or wood (cellulose fibre and wood fibre). These options were then compared in terms of thermal conductivity, EE, and fire class, as indicated in Table 4.

TABLE 4 List of insulation materials and properties to be compared.

INSULATION MATERIALS			
Material	λ (W/mK)	EE (MJ/kg)	Fire Class
Cellulose Fibre	0.041	0.94 - 3.3	B
Wood Fibre	0.038	10.8	D
Fibreglass	0.033	28	B

Firstly, cellulose fibre shows the best results in terms of EE. However, the current manufacturing process of cellulose fibre is based on downcycling newspapers, and the process of reusing cellulose fibre from wood waste is not yet developed. As this study focuses on reusing the available materials from demolition waste, this option was discarded.

Regarding fibreglass insulation, it is the best among the options in terms of thermal conductivity, and glass is one of the listed materials available at the demolition site. However, its EE is the highest among the materials analysed.

Thus, wood fibre insulation has shown to be the best option. If it can be made from wood waste from demolition (available at a rate about 14 times higher than glass), it has an outstanding performance in terms of thermal conductivity (around 0.038 W/mK), and its EE is almost three times lower than that of fibreglass. An ambitious alternative for the production process of wood fibre insulation could be the reuse of the sawdust produced during the manufacturing of the wooden structure.

However, since this material has fire class D, some strategies should be adopted to improve the fire resistance of the whole construction. Most of the alternatives to overcome this hindrance are related to adding chemicals into the insulation material, such as boric acid (Veitmans & Grinfelds, 2016), contradicting the idea of the circular analysis, bringing harmful consequences into the environment, and carrying high collateral EE (An & Xue, 2014; Cusenza et al., 2021). As a potential alternative, using fire-resistant boards (such as fibre cement) on the outsides of the insulation material was the chosen solution for this research.

After defining the insulation material to be used, the discussion relates to how this wood fibre insulation would be placed on the existing façade. As presented previously, the current façade consists of two brick layers with an air cavity between them. Therefore, the insulation material could be applied in three ways in the cavity wall, as shown in Figure 10.

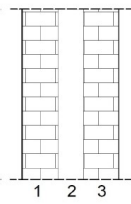
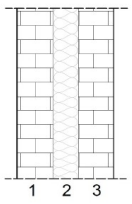
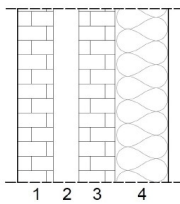
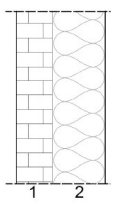
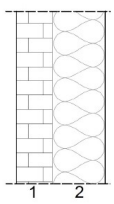
	CURRENT CONDITION		POSSIBILITIES				
Wall Structure							
	1 Brick 2 Ventilated air cavity 3 Brick	100 mm 70 mm 100 mm	1 Brick 2 Insulation 3 Brick	100 mm 70 mm 100 mm	1 Brick 2 Ventilated air cavity 3 Brick 4 Insulation	100 mm 70mm 100 mm 240mm	1 Brick 2 Insulation
Thickness (mm)	270		270		510	340	
Rc (m²K/W)	0.37		2.27		7.14	7.14	
U (W/m²K)	2.70		0.44		0.14	0.14	

FIG. 10 Comparison of different insulation settlements

Firstly, it could be placed between the two brick layers; however, the void of 70 mm is not enough to reach the Dutch standard of $4.5 \text{ m}^2\text{K/W}$ as a minimal Rc (Bowens et al., 2020). Secondly, the insulation could be placed in front of the double-brick façade; however, the wall would be very thick and unrealistic from a practical perspective. Therefore, the option that would meet the requirements consists of demolishing the external brick layer and placing the insulation outside of the single brick layer. The red and green cells in Figure 10 represent the values that do not meet the requirements and those that meet the requirements, respectively.

Thus, 240 mm of wood fibre insulation was placed on the outer part of the single-brick wall, and 150 mm of insulation was added to the roof and ground floors, as shown in Figure 11.

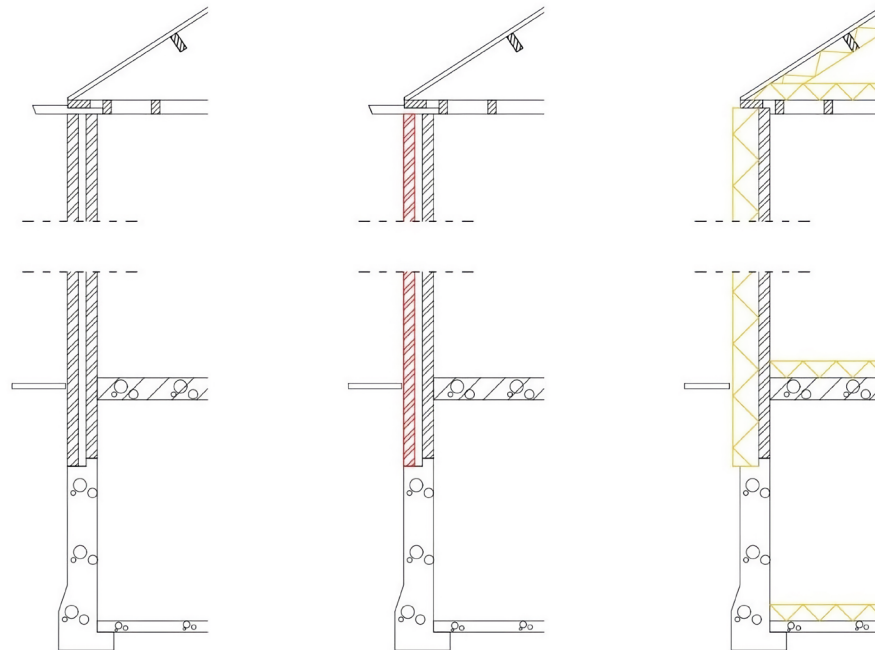


FIG. 11 Insulation addition and structure of renovated wall (existing façade in grey, the brick layer to be demolished in red, and the new insulation addition in yellow)

However, this arrangement raises the need to think about a structure to which this insulation can be attached. When analysing the demolition site, a significant number of wooden beams from existing roof structures will be discarded after demolition in Parkstad.

Aiming at reusing these wooden beams in the least processed manner possible, this study proposes sawing the beams into two parts and using them directly as the structure for the insulation material. The proposed process from the roof structure (waste from demolition) to the insulation structure is shown in Figure 12.

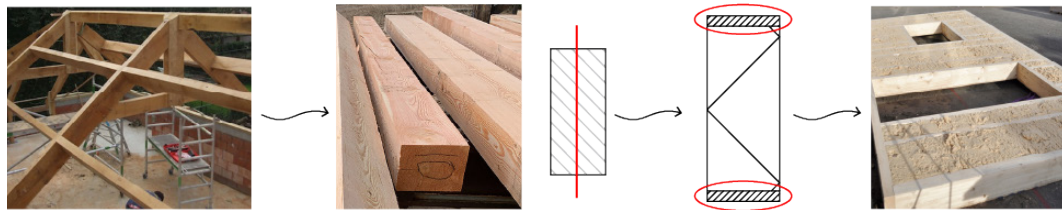


FIG. 12 Urban mining process: wooden structure for insulation

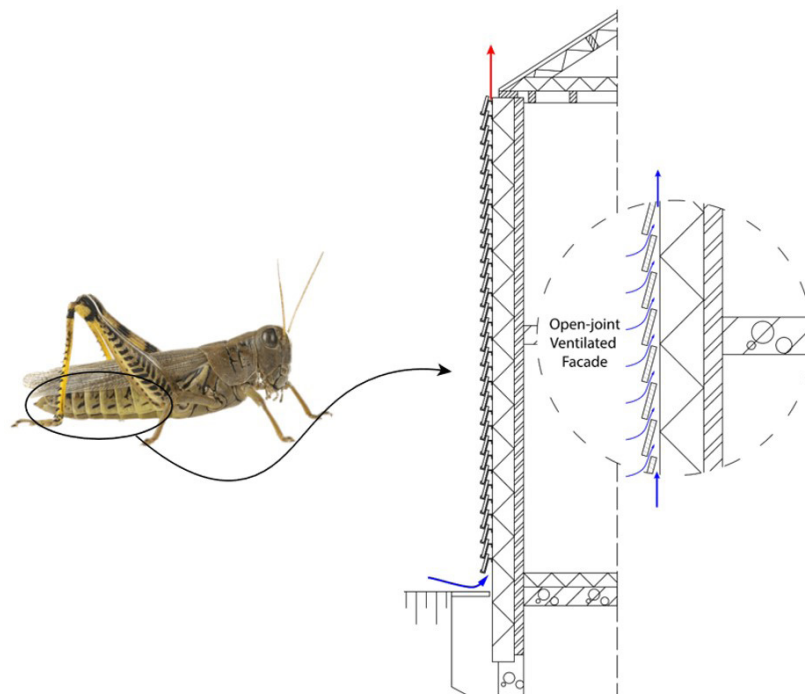


FIG. 13 Final concept of façade design inspired by cricket's openings

After developing an insulation application based on the urban mining strategy, an open-joint ventilated façade based both on the urban mining and biomimicry concepts was developed in this study.

Ventilated façades work as follows: the cool air enters through the bottom opening, and air pressure pushes out the hot air through the top opening. The developed open-joint ventilated façade works similarly. However, in the developed ventilated façade, openings were applied throughout the height of the façade, as the design was inspired by the openings of the cricket's respiratory system, as

shown in Figure 13. Thus, the façade's final structure consists of a single brick layer, an insulation element and structure, an air cavity, and an additional external wooden skin.

Moreover, following the urban mining concept, the external skin of the ventilated façade was developed by reusing the wooden beams from demolition. As shown in Figure 14, the wooden beams from the roof structure were sawed into two parts, and the wooden slabs were placed along the façade length with a space between them for air circulation.

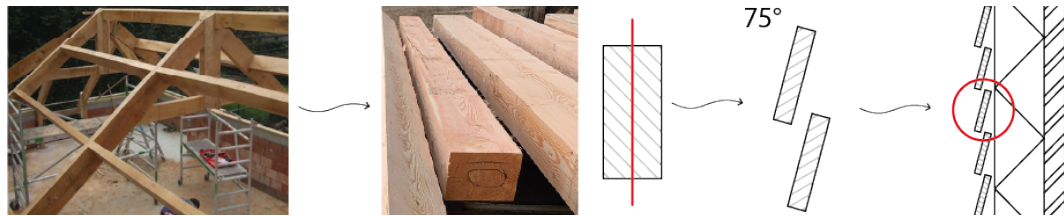


FIG. 14 Urban mining process: ventilated façade

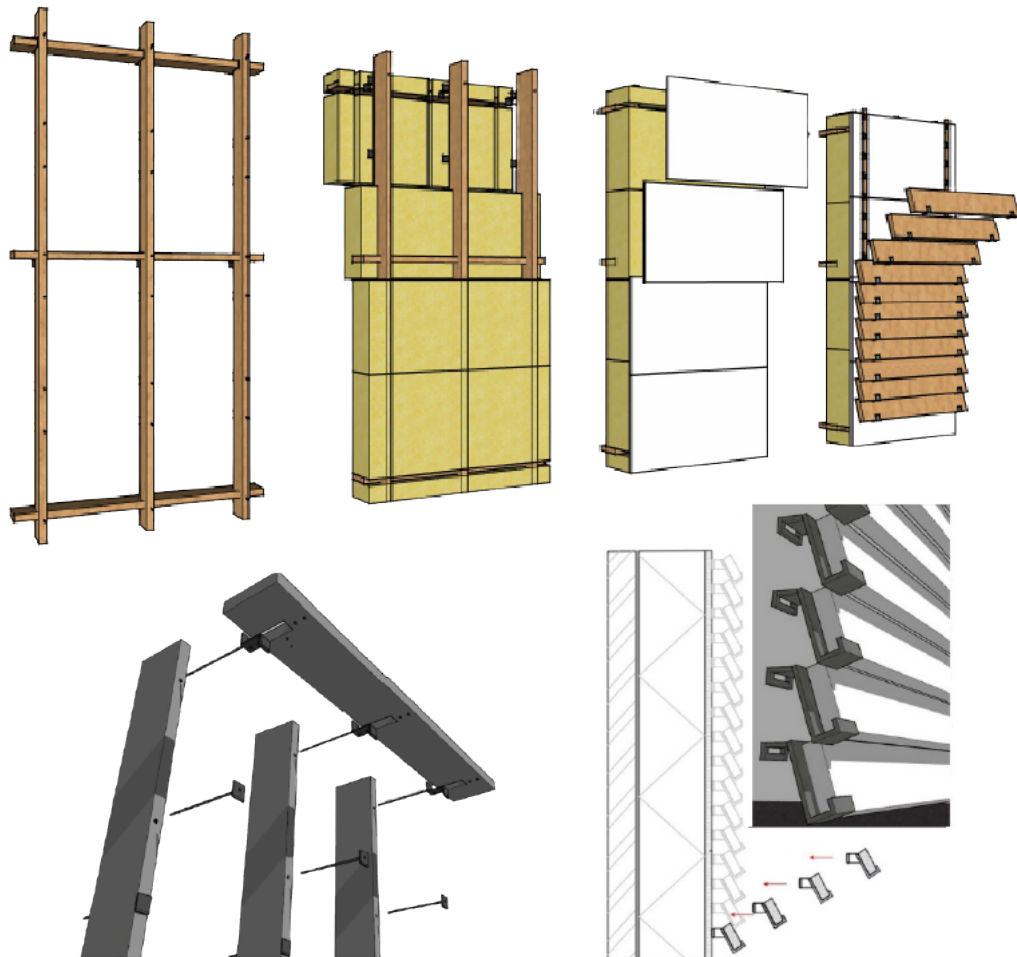


FIG. 15 Easy and dry assembly, based on the concept of DfD

Nevertheless, using wood as a cladding material has several problems due to its exposure to external weather conditions, such as accelerated ageing and mould infestation. With a focus on avoiding the use of chemicals in preventing these harmful effects, the study proposes using heat treatment for ageing and moisture control. As reviewed by (Esteves & Pereira, 2008), the heat treatment enhances the wood's resistance to insects and increases durability.

Finally, the whole façade renovation was also based on the previously discussed concept of DfD, with an easy assembly and disassembly method to reduce tenants and neighbourhood disturbance as much as possible, guarantee a fast and clean construction, and enable the reuse of components.

The strategy consists of using a pre-moulded insulation structure fastened with screws. The cladding material for the ventilated façade will be placed using a hook system, avoiding any use of glue or mortar. The assembly method is shown in Figure 15.

4.2 LCEP CALCULATIONS

4.2.1 Operational Energy

In scenario 1, the yearly energy calculations performed using *Uniec* indicated that the OE of the existing dwelling is 1.38E+05 MJ/year, as shown in Figure 16. Thus, **OE1 = 6.88E+06 MJ** over a lifespan of 50 years.

This result is equivalent to 324.20 kWh/m²/year, considering a kWh to MJ conversion of 5.22 and the previously mentioned heated area of 81.25 m².

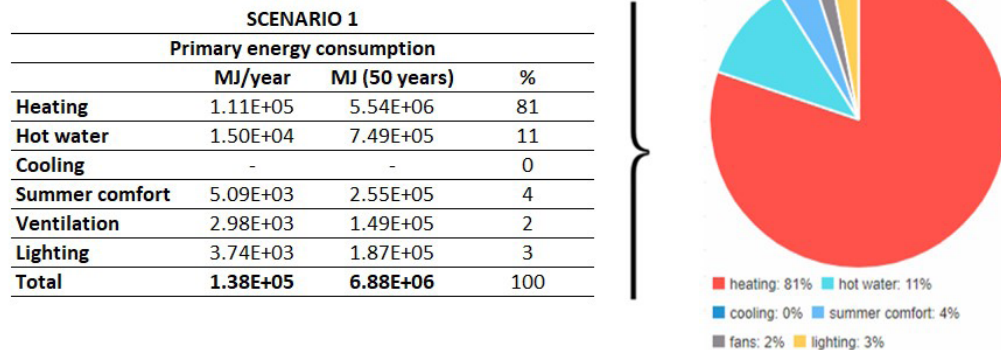


FIG. 16 Scenario 1: OE consumption and the percentage calculated in *Uniec*

In scenario 2, before considering the ventilated façade, the *Uniec* simulation indicates an OE consumption of 2.07E+04 MJ/year, which reduces 81.8% of the OE₁. The percentage distribution of the energy use is shown in Figure 17. The total energy consumed per dwelling is approximately **1.03E+06 MJ** over 50 years.

SCENARIO 2			
Primary energy consumption			
	MJ/year	MJ (50 years)	%
Heating	4.86E+03	2.43E+05	23
Hot water	9.46E+03	4.73E+05	46
Cooling	-	-	0
Summer comfort	2.10E+03	1.05E+05	10
Ventilation	5.17E+02	2.59E+04	2
Lighting	3.74E+03	1.87E+05	18
Total	2.07E+04	1.03E+06	100

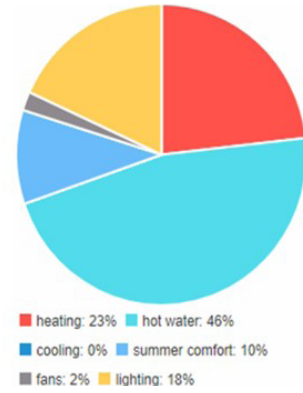


FIG. 17 Scenario 2: OE consumption and the percentage calculated by Uniec

After simulating the energy required in scenario 2 without the ventilated façade, the effect of the ventilated façade is considered. The summer comfort corresponds to 10% of all the energy consumption in scenario 2, as shown in Fig 17. As reviewed by (Ibañez-Puy et al., 2017), the ventilated façade studies typically include energy savings in summer periods exceeding 40%. Therefore, considering a 40% reduction of summer comfort energy, there will be a reduction of 840 MJ/year and **4.20E+04 MJ** over 50 years. Thus, the total OE of scenario 2 corresponds to:

$$OE_2 = 1.03E+06 - 4.20E+04$$

$$OE_2 = 9.88E+05$$

This result is equivalent to 46.78 kWh/m²/year, considering a kWh to MJ conversion of 5.22 and the previously mentioned heated area of 81.25m².

Finally, in scenario 3, the output energy was calculated considering the PV technology Crystalline Silicon, as indicated in Table 5.

TABLE 5 Scenario 3: Energy output from PV modules

PV PANELS - ENERGY GENERATION					
Orientation	PV size	Output Energy		Lifespan	TOTAL
	(m ²)	(kWh/year)	(MJ/year)	(years)	(MJ)
South (180)	25	5.12E+03	2.67E+04	50	1.34E+06

The energy output from the PV modules is discounted in the OE from scenario 2. As a result, the total OE associated with scenario 3 is:

$$OE_3 = OE_2 - OE_{PV\ modules} = 9.88E+05 - 1.34E+06$$

$$OE_3 = - 3.52E+05 MJ$$

This result is equivalent to -16.60 kWh/m²/year, considering a kWh to MJ conversion of 5.22 and the previously mentioned heated area of 81.25m².

A negative OE means that the building generates more energy than it consumes. In other words, the energy generated from the PV modules installed in the building is higher than the energy required for maintaining the building, such as lighting, heating, cooling, and hot water. However, for a complete overview of the building's LCEP and to analyse whether this scenario does indeed generate more energy than it consumes over 50 years, EE should also be addressed.

4.2.2 Embodied Energy

For scenario 1, Table 6 lists all the materials in the terraced dwelling, its volume, and associated EE following the previously discussed methodology. The calculations result in a total $EE_1 = 2.60E+05$ MJ for the existing scenario.

TABLE 6 Scenario 1: Calculation of existing EE.

BUILDING COMPONENT	MATERIALS	QUANTITY	DENSITY	TOTAL AMOUNT OF MATERIALS	DATA FROM ICE INVENTORY	
	Description of each material	Amount Revit (4 dwellings) [m ³]	Unit of measure [kg/m ³]	Per dwelling [kg]	Embodied Energy [MJ/kg]	Embodied Energy [MJ]
Foundation	Basement walls (0,03m thick)	1.97E+01	2.40E+03	1.18E+04	9.90E-01	1.17E+04
	Basement floor (0,08m thick)	4.12E+00	2.40E+03	2.47E+03	9.90E-01	2.45E+03
	Foundation slabs 600x300mm	1.19E+01	2.40E+03	7.11E+03	7.10E-01	5.05E+03
	Foundation slabs 300x300mm	1.16E+00	2.40E+03	6.96E+02	7.10E-01	4.94E+02
Opaque façades	Internal bricks	3.07E+01	1.70E+03	1.30E+04	3.00E+00	3.91E+04
	External bricks	3.17E+01	1.90E+03	1.50E+04	3.00E+00	4.51E+04
Roof	2 wall plates (50x155mm)	3.69E-01	5.10E+02	4.70E+01	1.00E+01	4.70E+02
	1 ridge purlin (80x180mm)	3.50E-01	5.10E+02	4.46E+01	1.00E+01	4.46E+02
	6 purlins (65x165mm)	1.57E+00	5.10E+02	2.00E+02	1.00E+01	2.00E+03
	Roof underlayment (18mm thickness)	4.37E+00	5.10E+02	5.57E+02	1.00E+01	5.57E+03
	Roof beams (25x38mm)	9.37E-01	5.10E+02	1.19E+02	1.00E+01	1.19E+03
	Roof tiles ceramic (12mm thickness)	2.91E+00	2.00E+03	1.45E+03	1.00E+01	1.45E+04
Frames, doors, windows	Wooden frames for windows and doors (façades)	1.41E+00	5.10E+02	1.80E+02	1.00E+01	1.80E+03
	Internal wooden sill	8.02E-01	5.10E+02	1.02E+02	1.00E+01	1.02E+03
	Internal doors and frames	2.58E+00	5.10E+02	3.29E+02	1.20E+01	3.94E+03
	Glass panels 3.2mm thick	2.80E-01	2.50E+03	1.75E+02	1.50E+01	2.63E+03

>>>

TABLE 6 Scenario 1: Calculation of existing EE.

BUILDING COMPONENT	MATERIALS	QUANTITY	DENSITY	TOTAL AMOUNT OF MATERIALS	DATA FROM ICE INVENTORY	
	Description of each material	Amount Revit (4 dwellings) [m ³]	Unit of measure [kg/m ³]	Per dwelling [kg]	Embodied Energy [MJ/kg]	Embodied Energy [MJ]
Internal ground floor	Internal ground floor concrete (200mm thick)	3.40E+01	2.40E+03	2.04E+04	7.50E-01	1.53E+04
	Floor finish ("plasterboard") 20mm thick	3.10E+00	1.90E+03	1.47E+03	4.51E+00	6.65E+03
Internal first-storey floor	Internal first-storey floor concrete (200mm thick)	3.40E+01	2.40E+03	2.04E+04	7.50E-01	1.53E+04
	Floor finish ("plasterboard") 20mm thick	3.10E+00	1.90E+03	1.47E+03	4.51E+00	6.65E+03
Internal second floor	Wooden floor structure	2.06E+00	5.10E+02	2.63E+02	1.00E+01	2.63E+03
	Floor finish ("wooden floor") 18mm thick	2.90E+00	5.10E+02	3.70E+02	1.00E+01	3.70E+03
Internal walls	Internal bricks wall (200mm thick)	3.26E+01	1.70E+03	1.39E+04	3.00E+00	4.16E+04
	Internal bricks wall (100mm thick)	1.19E+01	1.70E+03	5.05E+03	3.00E+00	1.51E+04
	Internal bricks wall (70mm thick)	8.32E+00	1.70E+03	3.54E+03	3.00E+00	1.06E+04
Stairs	Wooden structure	3.47E+00	5.10E+02	4.42E+02	1.00E+01	4.42E+03
1. Dutch demonstrator (surface: 132.82 m²)					EE1 =	2.60E+05

In scenario 2, the EE calculation considers EE_1 and discounts the changes promoted by the wall demolition, wooden frames, insulation material, ventilated façade, heating and hot water systems, and new windows and frames.

Firstly, since the external façade brick layer is demolished and the windows and frames are changed, the EE from the external brick layer ($4.51E+04$), glass panels ($2.63E+03$), and façade frames ($1.80E+03$) shown in Table 6 were not considered in the "Existing" phase of EE_2 , resulting in $2.10E+05$.

Secondly, for calculating the EE associated with the wooden structure, the energy necessary to saw the wood was considered. According to (Nwuba & Kaul, 1987), the energy required to saw the wood with a power chain is 3.8kJ/min. The sawing process takes approximately four hours, resulting in a consumption of 0.91MJ.

Regarding the wood fibre insulation material, the values from the ICE database were considered: EE of 10.8 MJ/kg and density of 40kg/m^3 . The total volume of insulation necessary is 41.26m^3 , resulting in an EE of 17,825.18 MJ.

As previously mentioned, for the cladding material of the ventilated façade, the beams from the demolition site undergo a sawing and heat treatment process, both of which are included in the calculation. Firstly, the energy required for sawing the wood was considered the same for sawing the wooden structure (0,91MJ). The heat treatment was considered a thermal modification, with the volume of wood about 3.32 m³. According to (Candelier & Dibdiakova, 2021), the EE associated with this treatment is 2830 kWh/m³, based on kWh to MJ conversion of 5.22 (Bowens et al., 2020), corresponding to 14,772.60 MJ/m³, resulting in 48,999.18 MJ.

The new heating and hot water system adopted is the air heat pump. The energy required for this system is calculated in Table 7.

TABLE 7 EE calculation of air heat pump.

EE - AIR HEAT PUMP			
Material	Amount (kg)	EE (MJ/kg)	Total EE (MJ)
Low alloyed steel	32	56.7 ¹	1814.4
Reinforced steel	120	56.7 ¹	6804
Copper	36.6	57 ¹	2086.2
Elastomere	16	102.1 ¹	1633.6
Polyvinylchloride	1.6	77.2 ¹	123.52
Polyolester oil	2.7	37.28 ²	100.656
HDPE	0.5	76.7 ¹	38.35
R-134a (20 yrs)	13.3	26.508 ³	352.5564
Total			1.30E+04

¹ ICE database 2011

² Energy Demand and Greenhouse Gases Emissions in the Life Cycle of Coffee Harvesters lubricant oil

³ 1430 kg CO₂; International Energy Agency / Evaluation of Embodied Energy and CO_{2,eq} for Building Construction (Annex 57); 6,6 kg CO₂; From mine to refrigeration: a life cycle inventory analysis of the production of HFC-134a

The energy values associated with the new windows and frames are provided by the manufacturer. Thus, Table 8 shows the final EE of scenario 2, considering all the processes and materials mentioned for this scenario.

TABLE 8 Scenario 2: EE calculation.

RENOVATED SCENARIO		
2.1	Existing	2.10E+05
2.2	Wooden frames	9.12E-01
2.3	Insulation	1.78E+04
2.4	Ventilated façade	4.90E+04
2.5	Heating and hot water system	1.30E+04
2.6	Windows, door, frames	1.11E+04
	TOTAL EE2 (MJ)	3.01E+05

Finally, for scenario 3, the EE associated with the PV modules is indicated in Table 9.

TABLE 9 EE from PV modules (Source: (Michiel J. Ritzen, 2017)).

EE - PV MODULES				
EE extraction (MJ/m ²)	EE manufacturing (MJ/m ²)	EE construction (MJ/m ²)	Area (m ²)	TOTAL EE (MJ)
600	1488	13	25	5.25E+04

Thus, the EE of scenario 3 is the sum of the previous EE₂ and the EE of the PV modules:

$$EE_3 = EE_2 + EE_{PV\ modules} = 3.01E+05 + 5.25E+04$$

$$EE_3 = 3.53E+05 \text{ MJ}$$

4.2.3 Total LCEP

After calculating the OE and EE for each scenario, the total LCEP per scenario can be calculated and compared based on:

$$\text{Life Cycle Energy} = \text{Embodied Energy} + \text{Operational Energy}$$

Figure 18 and Table 10 show the values calculated of EE and OE from each scenario, with the reduction percentage compared to the existing situation (scenario 1).

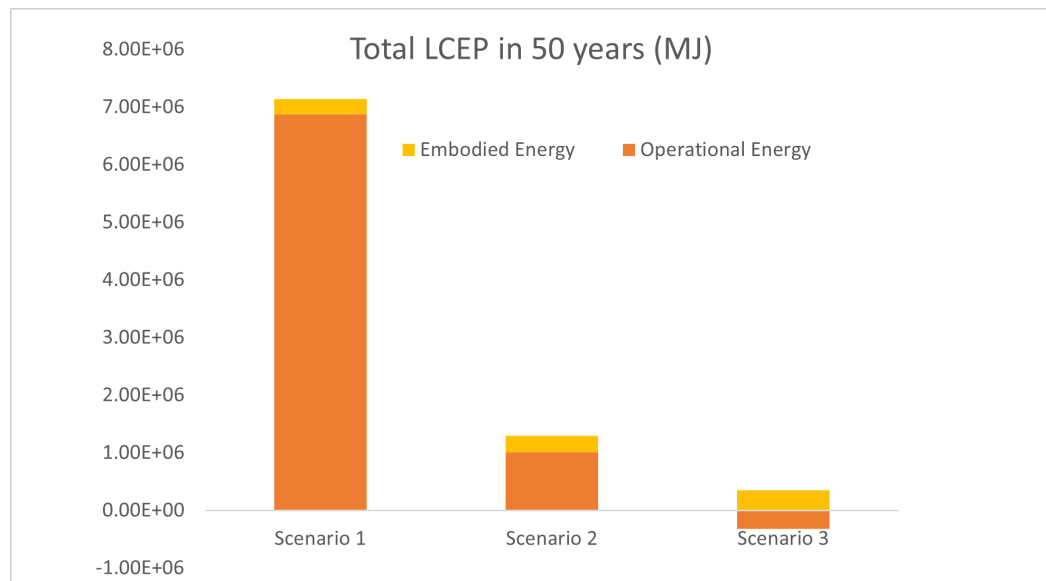


FIG. 18 Total LCEP of each scenario, accounting for OE and EE

TABLE 10 Total LCEP of each scenario, accounting for OE and EE, with the reduction percentage.

TOTAL LCEP IN 50 YEARS (MJ)			
	Scenario 1	Scenario 2	Scenario 3
Operational Energy	6.88E+06	9.88E+05	-3.49E+05
Embodied Energy	2.60E+05	3.01E+05	3.53E+05
Total LCEP	7.13E+06	1.29E+06	4.82E+03
Reduction	0%	81.9%	99.9%

4.3 DESIGN FOR DISASSEMBLY ASSESSMENT

The DfD index calculated for end-of-life and maintenance results in 0.86/1.0 and 0.95/1.0, respectively, as shown in Figure 19.

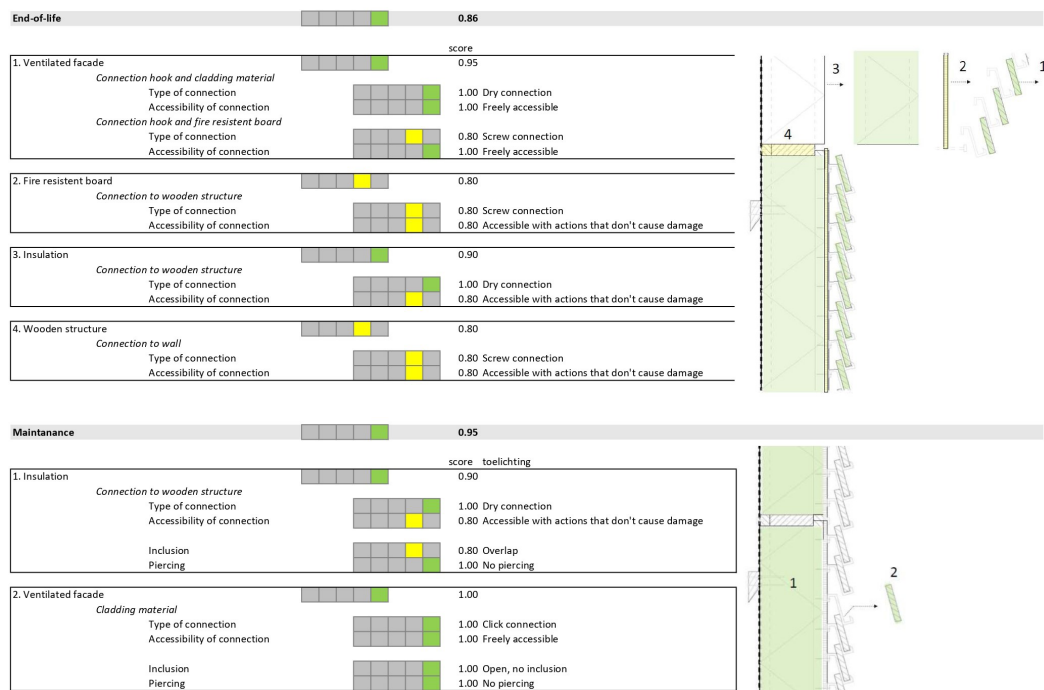


FIG. 19 DfD index of developed façade design

5 DISCUSSIONS

Renovating the building stock is a potential key aspect toward an energy-neutral built environment. Literature shows that the OE has a more significant effect on the overall LCEP. However, with the increasing attention and improvements regarding this concern, the EE is becoming increasingly relevant. Therefore, OE and EE, in conjunction, are vital indices in assessing the complete environmental impact of a building.

Concerning the EE calculations and the use of the ICE database, some limitations and uncertainties exist since the ICE dataset refers to the United Kingdom, and the version applied is not up-to-date. However, as this is a comparative study in an international context, this is not a very relevant shortcoming. If an absolute answer is needed, a national database such as Nationale Milieudatabase (NMD, 2020) could be used in a particular context.

Regarding the wood fibre insulation, there was a lack of information concerning the fire resistance treatment in a circular and/or bio-based way. Through literature reviews, the options were mainly related to using chemicals with high EE to improve the fire class of the material.

Furthermore, reusing the wood straight from the demolition site to produce the wood fibre insulation is still very theoretical, and studies concerning the process of upscaling still need to be investigated.

Since scenario 1 of this paper corresponds to approximately 42% of the dwellings in the Netherlands, the importance of this research is related to the possibility of upscaling the renovation of these dwellings. It would bring significant energy savings and, consequently, a significant reduction in CO₂ emission rates.



FIG. 20 Mock-up developed for results validation

As the next step in this research, a mock-up has been developed to validate the results, as shown in Figure 20. In this mock-up, the designed façade is compared with already existing ventilated façade products in the market and the existing façade (as scenario 1). In this mock-up, the circular aspects related to the reuse of wood from demolition and the DfD strategies are fully considered, also working to evaluate the urban mining and the assembling and disassembling processes.

6 CONCLUSIONS

As a result of the complete design, scenario 2 presents a reduction of 82% in the total LCEP, and scenario 3 shows a 100% reduction in the LCEP. This means that the Zero Energy Building was achieved with the renovation proposed in scenario 2 and the addition of PV modules in scenario 3. Nevertheless, the developed ventilated façade does not bring positive results for the LCEP when applied in combination with the complete building renovation (scenario 2) and in the Dutch weather characteristics. Contrariwise, the results show an EE of the ventilated façade ($4.90E+04$ MJ) higher than the OE savings due to the ventilated façade ($4.20E+04$ MJ) in a lifespan of 50 years. It signifies that the energy spent for manufacturing the ventilated façade was higher than its effect on the energy reduction and, therefore, not beneficial for the conditions applied in scenario 2.

There are two ways to analyse this result: firstly, in the renovated scenario (scenario 2), the energy destined for summer comfort is a small percentage of the overall building's energy consumption (10%). It means that the ventilated façade would bring better results in scenarios where the energy for maintaining summer comfort is higher, such as in countries with warmer weather and in a future perspective due to climate change and temperature increment.

Secondly, suppose the developed ventilated façade is added separately to the existing dwelling (scenario 1). In that case, the OE savings due to the ventilated façade ($40\% * 2.55E+05$ MJ = $1.02E+05$ MJ) is greater than the energy required for manufacturing ($4.90E+04$ MJ). Thus, if the developed ventilated façade is applied individually to an existing dwelling with low energy performance, the results are positive even in the Dutch scenario.

The DfD index for the developed façade design presents high results for the end-of-life (0.86/1.0) and maintenance (0.95/1.0) analysis. This indicates that the developed ventilated façade technology and wooden structure can be an innovative alternative to strengthen the circular built environment concept and deal with construction and demolition waste. However, future research should still study the trade-off between LCEP and DfD.

Acknowledgements

First of all, I would like to express my immense gratitude to all Drive 0 team members, especially the Dutch Drive 0 team, which jointly assisted with the study: Wendy Broers, John van Oorschot, and Joost van der Veer.

Furthermore, I would like to thank the Living Lab Biobased Brazil program for the exchange opportunity in the Netherlands and the assistance from Marliene Bos throughout the process. Moreover, I would like to thank Kyle Smeets and Carsten de Bruyn for their previous studies' contributions. Finally, my gratitude to Jérôme De Vreede for closely collaborating on the Revit model, José Maria Franco de Carvalho for advising throughout the study, and Leo Gommans for helping with the *Uniec* energy simulations.

The DRIVE 0 project has received funding from the European Union's Horizon 2020 research and innovation programme under grant agreement No. 841850.

Michiel Ritzen has received funding from the Dutch Organisation for scientific research (NWO) grant number HBOPD.2018.02.025.

References

- Agentschap NL. (2011). *Voorbeeldwoningen 2011 -Bestaande bouw. 1975–1991*.
- Ahmed, M. M. S., Abel-Rahman, A. K., & Ali, A. H. H. (2015). Development of Intelligent Façade Based on Outdoor Environment and Indoor Thermal Comfort. *Procedia Technology*, 19, 742–749. <https://doi.org/10.1016/j.protcy.2015.02.105>
- Aithal, H. (2020). *What is Biomimetic Architecture and why young Architects should know about it*. <https://www.re-thinkingthefuture.com/fresh-perspectives/a539-what-is-biomimetic-architecture-and-why-young-architects-should-know-about-it/>
- An, J., & Xue, X. (2014). Life cycle environmental impact assessment of borax and boric acid production in China. *Journal of Cleaner Production*, 66, 121–127. <https://doi.org/10.1016/j.jclepro.2013.10.020>
- Bach, R., & Hildebrand, L. (2018). *A Comparative Overview of Tools for Environmental Assessment of Materials. - RWTH AACHEN UNIVERSITY Cycle oriented construction - English. June*. <https://www.rb.rwth-aachen.de/go/id/hpdo/tidx/1/file/749772>

- Badarnah, L. (2015). A Biophysical Framework of Heat Regulation Strategies for the Design of Biomimetic Building Envelopes. *Procedia Engineering*, 118, 1225–1235. <https://doi.org/10.1016/j.proeng.2015.08.474>
- Balocco, C. (2002). A simple model to study ventilated facades energy performance. *Energy and Buildings*, 34(5), 469–475. [https://doi.org/10.1016/S0378-7788\(01\)00130-X](https://doi.org/10.1016/S0378-7788(01)00130-X)
- Barbara, R., Anne-Françoise, M., & Reiter, S. (2012). Life-cycle assessment of residential buildings in three different European locations, case study. *Building and Environment*.
- Biggs, M. (2002). The role of the artefact in art and design research. *International Journal of Design Sciences and Technology*, November.
- Bowens, C., Gommans, L., Linden, K. van der, Nieman, H., Alders, N., Vries, K. de, Weele, H. van, & Wordragen, R. van. (2020). *Energie Vademecum*. Delft Digital Press.
- BPIE. (2021). Whole-Life Carbon: Challenges and Solutions for Highly Efficient and Climate-Neutral Buildings. *Buildings Performance Institute Europe (BPIE)*, May. <https://www.bpie.eu/>
- Brunner, P. H. (2011). Urban mining A contribution to reindustrializing the city. *Journal of Industrial Ecology*, 15(3), 339–341. <https://doi.org/10.1111/j.1530-9290.2011.00345.x>
- C.Cao. (2017). *Sustainability and life assessment of high strength natural fibre composites in construction* (pp. 529–544).
- Candelier, K., & Dibdiakova, J. (2021). A review on life cycle assessments of thermally modified wood. *Holzforschung*, 75(3), 199–224. <https://doi.org/10.1515/hf-2020-0102>
- Chesné, L., Duforestel, T., Roux, J. J., & Rusaouën, G. (2012). Energy saving and environmental resources potentials: Toward new methods of building design. *Building and Environment*, 58, 199–207. <https://doi.org/10.1016/j.buildenv.2012.07.013>
- Cossu, R., & Williams, I. D. (2015). Urban mining: Concepts, terminology, challenges. *Waste Management*, 45, 1–3. <https://doi.org/10.1016/j.wasman.2015.09.040>
- Cottafava, D., Ritzen, M., & Oorschot, J. van. (2020). *Drive 0 Report: D6.1 Report on benchmarking on circularity and its potentials on the demo sites* (Issue 841850).
- Cusenza, M. A., Gulotta, T. M., Mistretta, M., & Cellura, M. (2021). Life cycle energy and environmental assessment of the thermal insulation improvement in residential buildings. *Energies*, 14(12), 1–21. <https://doi.org/10.3390/en14123452>
- De Gracia, A., Castell, A., Navarro, L., Oró, E., & Cabeza, L. F. (2013). Numerical modelling of ventilated facades: A review. *Renewable and Sustainable Energy Reviews*, 22, 539–549. <https://doi.org/10.1016/j.rser.2013.02.029>
- Dixit, M. K., Fernández-Solís, J. L., Lavy, S., & Culp, C. H. (2010). Identification of parameters for embodied energy measurement: A literature review. *Energy and Buildings*, 42(8), 1238–1247. <https://doi.org/10.1016/j.enbuild.2010.02.016>
- Esteves, B. M., & Pereira, H. M. (2008). Wood modification by heat treatment: A review. *BioResources*, 4(1), 370–404. <https://doi.org/10.15376/biores.4.1.370-404>
- European Commission. (2020). *PVGIS Photovoltaic Geographical Information System*. https://re.jrc.ec.europa.eu/pvg_tools/en/
- European Commission. (2010). Directive 2010/31/EU of the European Parliament and of the Council on the Energy Performance of Buildings. *La Presse Médicale*.
- European Commission. (2016). The European Construction Sector. *European Union*, 16. <http://ec.europa.eu/growth/sectors/construction/>
- European Commission. (2020a). *2050 long-term strategy*. https://ec.europa.eu/clima/policies/strategies/2050_en#:~:text=The EU aims to be,action under the Paris Agreement.
- European Commission. (2020b). A Renovation Wave for Europe - greening our buildings, creating jobs, improving lives. *European Commission, COM(2020)*, 1–26.
- European Commission. (2020c). Circular economy action plan. *European Commission, March*, 28. <https://doi.org/10.2775/855540>
- European Commission. (2021). *Levels(s): A Guide to Europe's New Reporting Framework for Sustainable Buildings*. 1–12.
- Fantucci, S., Serra, V., & Carbonaro, C. (2020). An experimental sensitivity analysis on the summer thermal performance of an Opaque Ventilated Façade. *Energy and Buildings*, 225, 110354. <https://doi.org/10.1016/j.enbuild.2020.110354>
- Fantucci, S., Serra, V., Carbonaro, C., Gratia, E., De Herde, A., Medved, S., Begelj, Ž., Domjan, S., Šuklje, T., Černe, B., Arkar, C., Gratia, E., De Herde, A., de Gracia, A., Castell, A., Navarro, L., Oró, E., Cabeza, L. F., Sanjuan, C., ... Chen, Y. (2013). Experimental study of a ventilated facade with PCM during winter period. *Energy and Buildings*, 58(2), 324–332. <https://doi.org/10.1016/j.enbuild.2012.10.026>
- Feist, W. (1996). Life-cycle energy balances compared: low-energy house, passive house, self-sufficient house. *Proceedings of the International Symposium of CIB W67*.
- Friedmann, S. J., & Kelly, W. (2003). *Storing Carbon in*. *March*, 16–20.
- Galle, W. (2017). *Design for Change towards a circular economy in construction (handout) What is design and*. *March*, 44. <https://doi.org/10.13140/RG.2.2.23275.75041>
- Graedel, T. (2011). The prospects for urban mining. *Bridge*, 41(1), 43–50.
- Gratia, E., & De Herde, A. (2003). Natural ventilation in a double-skin facade. *Energy and Buildings*, 36(2), 137–146. <https://doi.org/10.1016/j.enbuild.2003.10.008>
- GRO. (2022). *GRO: Towards future-oriented construction projects*. <https://www.vlaanderen.be/vlaamse-overheid/werking-van-de-vlaamse-overheid/bouwprojecten-van-de-vlaamse-overheid/gro-op-weg-naar-toekomstgerichte-bouwprojecten>
- Hauberg, J. (2011). Research by Design – a research strategy. *Architecture & Education Journal, March*, 46–56.
- Herzog, T., Krippner, R., & Werner Lang. (2005). *Facade Construction Manual*.
- Ibañez-Puy, M., Vidaurre-Arbizu, M., Sacristán-Fernández, J. A., & Martín-Gómez, C. (2017). Opaque Ventilated Façades: Thermal and energy performance review. *Renewable and Sustainable Energy Reviews*, 79, 180–191. <https://doi.org/10.1016/j.rser.2017.05.059>
- Innodura. (2021). *Zonnepanelen 320wp*. <https://www.innodura.nl/lp/zonnepanelen-320wp>
- ISSO. (2021). *Circularity into detail*. *March*.

- Ivanović-Šekularac, J., Čikić-Tovaročić, J., & Šekularac, N. (2016). Application of wood as an element of façade cladding in construction and reconstruction of architectural objects to improve their energy efficiency. *Energy and Buildings*, 115, 85–93. <https://doi.org/10.1016/j.enbuild.2015.03.047>
- Li, C. Z., Lai, X., Xiao, B., Tam, V. W. Y., Guo, S., & Zhao, Y. (2020). A holistic review on life cycle energy of buildings: An analysis from 2009 to 2019. *Renewable and Sustainable Energy Reviews*, 134(April), 110372. <https://doi.org/10.1016/j.rser.2020.110372>
- Martins, F., Felgueiras, C., & Smitková, M. (2018). Fossil fuel energy consumption in European countries. *Energy Procedia*, 153, 107–111. <https://doi.org/10.1016/j.egypro.2018.10.050>
- Medved, S., Begelj, Ž., Domjan, S., Šuklje, T., Černe, B., & Arkar, C. (2019). The dynamic thermal response model and energy performance of multi-layer glass and BIPV facade structures. *Energy and Buildings*, 188–189, 239–251. <https://doi.org/10.1016/j.enbuild.2019.02.017>
- Mequignon, M., Adolphe, L., Thellier, F., & Ait Haddou, H. (2013). Impact of the lifespan of building external walls on greenhouse gas index. *Building and Environment*, 59, 654–661. <https://doi.org/10.1016/j.buildenv.2012.09.020>
- Mike van Vliet, A. C. J. van, Grinsven, A. C. J. T., & Alba Concepts. (2019). *Circular Buildings - Measurement methodology detachability*. NMD. (2020). *Nationale Milieu Database*. <https://milieudatabase.nl/>
- Nwuba, E. I., & Kaul, R. N. (1987). Energy requirements of hand tools for wood cutting. *Journal of Agricultural Engineering Research*, 36(3). <https://www.sciencedirect.com/science/article/abs/pii/0021863487900746>
- Papadopoulos, A. M. (2005). State of the art in thermal insulation materials and aims for future developments. *Energy and Buildings*, 37(1), 77–86. <https://doi.org/10.1016/j.enbuild.2004.05.006>
- Petersen, A. K., & Solberg, B. (2002). Greenhouse gas emissions, life-cycle inventory and cost-efficiency of using laminated wood instead of steel construction. Case: Beams at Gardermoen airport. *Environmental Science and Policy*, 5(2), 169–182. [https://doi.org/10.1016/S1462-9011\(01\)00044-2](https://doi.org/10.1016/S1462-9011(01)00044-2)
- Poel, B., van Cruchten, G., & Balaras, C. A. (2007). Energy performance assessment of existing dwellings. *Energy and Buildings*, 39(4), 393–403. <https://doi.org/10.1016/j.enbuild.2006.08.008>
- Ramesh, T., Prakash, R., & Shukla, K. K. (2010). Life cycle energy analysis of buildings: An overview. *Energy and Buildings*, 42(10), 1592–1600. <https://doi.org/10.1016/j.enbuild.2010.05.007>
- Rasca, S. (2014). *Dynamic Facade Systems*. Lund University.
- Rasmussen, F., Birkved, M., & Birgisdóttir, H. (2019). Upcycling and Design for Disassembly LCA of buildings employing circular design strategies. *IOP Conference Series: Earth and Environmental Science*, 225, 012040. <https://doi.org/10.1088/1755-1315/225/1/012040>
- Ritzen, M. J., Haagen, T., Rovers, R., Vroon, Z. A. E. P., & Geurts, C. P. W. (2016). Environmental impact evaluation of energy saving and energy generation: Case study for two Dutch dwelling types. *Building and Environment*, 108(2016), 73–84. <https://doi.org/10.1016/j.buildenv.2016.07.020>
- Ritzen, Michiel J. (2017). *Environmental impact assessment of building integrated photovoltaics: numerical and experimental carrying capacity based approach*. 217.
- Roggema, R. (2016). Research by Design: Proposition for a Methodological Approach. *Urban Science*, 1(1), 2. <https://doi.org/10.3390/urbansci1010002>
- Samimi, N. (2011). *Adaptive reuse of agrivaal building* [University of Pretoria]. <https://repository.up.ac.za/bitstream/handle/2263/27833/00front.pdf?sequence=1&isAllowed=y>
- Sanjuan, C., Suárez, M. J., González, M., Pistono, J., & Blanco, E. (2011). Energy performance of an open-joint ventilated façade compared with a conventional sealed cavity façade. *Solar Energy*, 85(9), 1851–1863. <https://doi.org/10.1016/j.solener.2011.04.028>
- Sartori, I., & Hestnes, A. G. (2007). Energy use in the life cycle of conventional and low-energy buildings: A review article. *Energy and Buildings*, 39(3), 249–257. <https://doi.org/10.1016/j.enbuild.2006.07.001>
- Schabowicz, K., & Zawiślak, L. (2021). Numerical Comparison of Thermal Behaviour between Ventilated Facades. *Studia Geotechnica et Mechanica*, 42(4), 297–305. <https://doi.org/10.2478/sgem-2019-0044>
- SERT. (2011). *Sustainable Energy Research Team*. <https://www.bath.ac.uk/teams/sustainable-energy-research-team/>
- Stadhouders, M., Loef, J., Ritzen, M., Eggels, N., & Consten, P. (2021). *Material and energy flows in the demolition stock of Parkstad*. TNO. (2018). Circulair bouwen in perspectief. *Circulair, Bouwmaterialen*, 37, 1–37. <http://ir.obihiro.ac.jp/dspace/handle/10322/3933>
- Tokuç, A., Özkaban, F. F., & Çakır, Ö. A. (2018). Biomimetic Facade Applications for a More Sustainable Future. *Interdisciplinary Expansions in Engineering and Design With the Power of Biomimicry*. <https://doi.org/10.5772/intechopen.73021>
- Uniec. (n.d.). *Uniec 2*. Retrieved December 8, 2020, from <https://uniecc2.nl/>
- Uniec. (2018). *BENG – meer aandacht voor zonwering*. <https://uniecc3.nl/beng-meer-aandacht-voor-zonwering/>
- van der Lugt, P. (2012). Carbon Storage Utilising Timber Products. *Environment Industry Magazine*, 2012(6), 76–80. <https://www.accoya.com/wp-content/uploads/2013/09/Carbon-Storage-using-Timber-Products.pdf>
- Van Ooteghem, K., & Xu, L. (2012). The life-cycle assessment of a single-storey retail building in Canada. *Building and Environment*, 49, 212–226. <https://doi.org/10.1016/j.buildenv.2011.09.028>
- Veitmans, K., & Grinfelds, U. (2016). Wood Fiber Insulation Material. *Research for Rural Development*, 2, 91–98.
- Webb, M., Aye, L., & Green, R. (2018). Simulation of a biomimetic façade using TRNSYS. *Applied Energy*, 213(August 2017), 670–694. <https://doi.org/10.1016/j.apenergy.2017.08.115>
- Zhou, J., & Chen, Y. (2010). A review on applying ventilated double-skin facade to buildings in hot-summer and cold-winter zone in China. *Renewable and Sustainable Energy Reviews*, 14(4), 1321–1328. <https://doi.org/10.1016/j.rser.2009.11.017>
- Zimmerman, J., Forlizzi, J., & Evenson, S. (2007). Research through design as a method for interaction design research in HCI. *Conference on Human Factors in Computing Systems - Proceedings, January*, 493–502. <https://doi.org/10.1145/1240624.1240704>

Process Automation to Improve the Building Engineering Design Analysis of Non-Repetitive Façade Geometries

Jacopo Montali ^{*}1, Thomas Henriksen ^{*}1

* Corresponding authors, jacopo@henriksenstudio.com, thomas@henriksenstudio.com

1 Henriksen Studio ltd

Abstract

This paper evaluates how parts of the building engineering design processes can be automated using software automation, with a focus on the analysis of thermal bridges in façades. Reduced repetition in façade design requires the automation of routine tasks that would otherwise be performed manually. Because full software automation is seldom achievable, a preliminary decision-making process that considers both the effort to create automation and the benefit to exploit it is required. A methodology is presented to achieve beneficial trade-offs between effort and benefits, by using heuristic knowledge. The knowledge was gathered by interviews with façade professionals. The methodology was tested on two case studies based on the analysis of the expected thermal bridge heat loss of two large-scale and low-repetition buildings. The results of the automated process described in the methodology were compared against information obtained from traditional approach, where the engineer/consultant performs each individual task manually. The results shows that the introduction of automation leads to time savings of 44%, if compared to the manual approach.

Keywords

Façade design, process automation, thermal bridges, building physics, heuristic knowledge, software development

DOI

<http://doi.org/10.47982/jfde.2022.1.05>

1 INTRODUCTION

Façade engineering requires many routine tasks to be performed on façade types or interfaces, especially when repetition in the project is minimal. With architectural expression growing in ambition, and with increasing performance requirements that need to be coordinated with many different engineering disciplines, this aspect becomes a source of risk due to the lack of precision in the expected performance, requiring analysis of the most critical parts of the project and leading to product over-engineering and, therefore, less sustainable solutions.

Façade design automation is a current topic of interest in the sector as it provides ways of streamlining the design of complex systems, while capturing the underlying mechanisms that govern the design of the product (Henriksen et al., 2016; Montali et al., 2017). The paradigm is fostered by recent advances in software programming languages, propelled in turn by the growth of data and advances in web technologies in the last decades.

An opportunity therefore emerges in combining software automation and façade engineering to achieve a better understanding of the expected performance when designing non-repetitive façades. The traditional use of software via graphical user interface (GUI), requiring manual mouse and keyboard interaction on every single task to be performed, is currently being replaced by more sophisticated software applications based on programming interfaces (API). Commercially available, off-the-shelf software applications like Rhinoceros (Robert McNeel & Associates, 2021) or Revit ("Revit," 2021) nowadays provide users with access to the same GUI objects via API that can be controlled via commonly-available programming languages (such as Python or C#). Such API normally extend the functionality the software's GUI.

Excluding human labour from repetitive tasks, while leaving a supervising role to people who would otherwise perform the tasks in question, simplifies processes and provides opportunities for increasing productivity and creativity. To this end, research has shown that there is no clear solution on how to manage repetitive tasks manually as they prove intrinsically challenging. For instance, it has been shown that interruptions in repetitive tasks provide benefits (Back et al., 2010). But, if exceedingly short and unwanted, they can reduce productivity and lead to more human errors (Altmann et al., 2014). It has also been shown that a key role is played by how the GUI is built and its level of user-friendliness (Tsai & Byrne, 2007) computer-based routine procedural tasks involving execution of multiple steps. Differences were found in error frequencies at particular steps between the three tasks, a result that is consistent with predictions derived from Altmann and Trafton's (2002). As Israeli Nobel prize winner Daniel Kahneman would say: "humans are noisy", hinting that the same person will produce different outputs (some of which incorrect) by performing the same task repetitively. Computer automation thus allows for more time to be spent on value-adding and less error-prone activities, and partly addresses the construction sector "productivity imperative" (McKinsey & Company, 2015).

In this paper, a method is presented to show how to implement software solutions for task automation. The method builds upon existing literature in the field of knowledge management (Milton, 2007), as well as optimization techniques (Ashby, 2011) that prioritise which tasks to automate first in order to minimise the initial cost of software implementation. A case study of the total heat loss calculation through the envelope for two UK-based, large-scale Passivehaus projects will be used to demonstrate the validity of the proposed method.

The choice of the heat loss through the building envelope for energy-efficient buildings as a case study is driven by recent international ambitions to tackle the energy crisis. It is estimated that the incorrect incorporation of thermal bridges can lead to an underestimation of the heating peak power by 29% and of the annual energy demand by 37% in passive houses (Berggren & Wall, 2011). Furthermore, the adoption of a fixed percentage increasing the centre-of-pane building envelope thermal loss to account for thermal bridges was proven not suitable in cold climates (Berggren & Wall, 2013). Therefore, a more in-depth analysis of the actual thermal bridging is required, and automation can be a valuable instrument in this regard.

The present study is structured as follows. First, the methods will be shown, along with a description of the two case-study projects. The paper will follow with the application of the method to the above-mentioned projects, while it will end with discussions of the results and conclusions and final remarks.

2 METHODS

The method is based on the technique described in Milton (2007), and adapted by selecting specific steps (in particular step numbers 7, 28, 32, 33) to reduce the time required to complete and to streamline the automation process. An overview of the method is shown in Figure 1 in a BPMN ("BPMN," 2017) view.

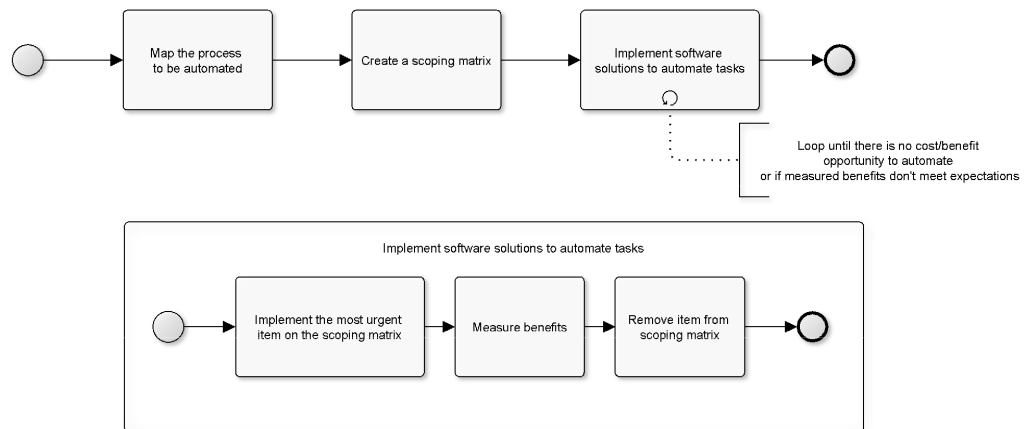


FIG. 1 BPMN view of the method adopted.

The method consists in the following tasks:

1 Map the process to be automated

This task requires to create a detailed process map showing each individual task required. Each task is a detailed and individual operation that is normally performed manually and whose automation will be evaluated. See Figure 3 in the results section for an example. BPMN ("BPMN," 2017) can be used as it is a widely used formal process mapping language, although any process mapping style is valid.

2 Create a scoping diagram

The automation of each task from the process map created at the step above is then evaluated in terms of benefits and cost. For this purpose, two tables are produced (example in Table 1): one addressing the benefits and another one the cost of automating each task (table rows). Each task is evaluated against a series of topics (table columns), which depend on the project and may differ between the two tables. The evaluation score could be a number ranging from 1 to 5, where 1=lowest score and 5=highest score. The topics are weighted in case the relative importance of topics differs. An example of a topic for evaluating costs can be "time required", while an example for evaluating benefits could be "increased quality". Each task is then given a weighted average, calculated as a linear combination of the scores and the weightings. The weighted average represents the overall cost or benefit in automating a specific task. See Table 3 and Table 4 in the results section for a practical example.

TABLE 1 Example of table for capturing cost or benefits in automating a specific task

	Topic 1	Topic 2	Weighted average
Weighting	2	1	
Task 1	1	1	3.0
Task 2	2	2	6.0
Task 3	3	3	9.0

The evaluation scores in each diagram are normally based on heuristics. The matrices can be completed by one or more expert people. If more than one person is required to complete the assessment, either individual tasks (rows) or aspects (columns) are assigned to each person. In the case of a multitude of people contributing to a single task/topic entry, a simple average can be used. Once the two tables are prepared, each task is prioritised via a scoping diagram (Figure 2). Given that each task presents two weighted scores, a diagram ("scoping diagram", named after the "scoping matrix" in Milton (2007)) can be drawn to prioritise the tasks to be automated. As the diagram presents benefits and costs on the axes, a point in the diagram identifies a task. The optimal tasks, i.e., tasks laying on the Pareto front (Sawaragi et al., 1985), are those that have the priority in terms of implementation as they improve in both cost and benefit at least another task. For this reason, optimal tasks are also referred to as "non-dominated", while the remaining are defined "dominated" (Sawaragi et al., 1985).

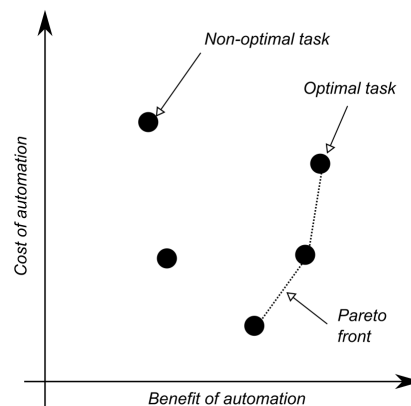


FIG. 2 Scoping diagram showing which tasks shall be automated first

3 Implement software solutions to automate tasks

The third step consists of an iterative process where the most urgent task from the scoping diagram is automated first via software implementation. Given that all tasks on the Pareto front have the same level of priority, an expert judgment may be required. Depending on the inclination of the front, it is possible to start with the task with the lowest cost (nearly vertical front) or largest benefit (nearly horizontal front). Alternatively, it is possible to transform the problem from multi-objective to single-objective via a penalty function approach, by determining the appropriate exchange coefficient, if possible (Ashby, 2011). In this case, the most urgent task is the task with the minimum penalty function value.

Once the task is chosen, both the time required to implement the software solution and an assessment of the time required to manually perform the task are produced. If the assessment proves that the automation of the task increases productivity (e.g., by showing that the time required to implement the software and run it is lower than what measured in a manual approach) or quality (e.g., by counting the number of typos/errors in the final output), then the team marks the step as completed and proceeds with a second iteration. The second iteration will automate the second most urgent item between those on the Pareto front in the scoping diagram.

3 DATA

The data used in the results section are taken from two real-world projects currently under development in London, UK. Both projects present miscellaneous end uses, such as student accommodation, office, and retail and are pursuing the Passivhaus certification.



FIG. 3 Render images of the two projects used to test the automated process. Courtesy of Alford Hall Monaghan Morris, Apt and Urbanest.

The two projects are characterized by a series of tower blocks and a podium area at ground level. The tower blocks are mainly student accommodations, while the podiums present a mixed use. Both projects present two additional levels below ground. The total GFA area of the projects is approximately 25000 m² and 60000 m².

The Passivhaus certification required in-depth evaluation of the total heat loss through the building, including thermal bridging. All thermal bridges related to the curtain wall façade were excluded in the present analysis as analysed separately in the U_{cw} as per BS EN 12631. Therefore, only thermal bridges at roof and basement levels were considered in this study, including those at the interface between roofs/slabs and curtain walls (a.k.a. non-façade thermal bridge types). The number of non-façade thermal bridge types identified in the two projects and analysed in this paper was 77 and 109.

4 RESULTS

4.1 MAP THE PROCESS TO BE AUTOMATED

The first step comprised mapping the process by defining all individual tasks. In this case, the process consisted of automating the calculation of the lengths and number of thermal bridges for the two projects investigated. This process was deemed to contain repetitive and error-prone activities as it required the determination of the length and count of a large number of different types of thermal bridges. For this reason, the process was first performed manually for a few representative examples and then represented in a process map as shown in Figure 4.

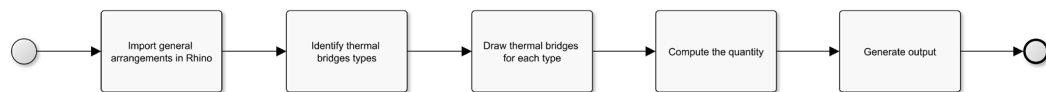


FIG. 4 BPMN process map for determining all thermal bridges lengths and number.

The individual tasks of the process were:

Import general arrangements in Rhino: in this step, the architectural plans in CAD format were retrieved and imported in Rhinoceros. The process consisted in using the "Import..." function for each general arrangement imported.

Identify thermal bridge types: all possible thermal bridges were identified by inspecting the above general arrangements. When a new thermal bridge type was identified, a new layer in Rhino was generated with the following naming convention:

XXX-YYY-L00-TB123-0_0_0_0-Description-H123-V123

Where the hyphen-separated fields are:

XXX is the project code

YYY is an additional descriptor field

L00 identifies the project level at which the thermal bridge refers

TB123 is the thermal bridge code where:

- TB identifies the thermal bridge type and can be PT (point), LH (linear horizontal), LV (linear vertical)
- 123 is a progressive number for numbering the thermal bridge

0_0_0_0_0 is the ratio of the thermal bridge heat loss to a specific project zone/area. For instance, a 0.1_0_0.9 code assigns 10% of the heat loss to the first project zone, zero to the second, and 90% to the third. This field is useful in case of projects requiring the total heat loss calculation for different zones/areas of the same building, such as in Passivhaus certifications.

Description is a natural language description of the thermal bridge in question

H123 is a mandatory field for LV thermal bridge types, representing only their lengths, as this is not captured in plan views, where 123 is the thermal bridge length in metres.

V123 is the value of the thermal bridge loss, where 123 is either in W/K for point thermal bridges (χ) or W/m²K otherwise (φ)

- Draw thermal bridges for each type: each of the identified thermal bridges were drawn in Rhinoceros as either points (for "PT" or "LV" types) or lines (for "LH" for linear horizontal types)
- Compute the quantity: per each thermal bridge type, the total quantity is calculated by determining the number of point thermal bridges or the total length of linear thermal bridges.
- Generate output: the output consists of determining the total heat loss $Q_i[\frac{W}{K}]$ for each thermal bridge type i :

$$Q_i = \varphi_i \cdot \sum l_{j,i}$$

$$Q_i = \chi_i \cdot \sum j$$

Where $\sum l_{j,i}$ is the sum of all individual length of a specific linear thermal bridge type i and $\sum j$ is the count of all point thermal bridges of type i , as calculated from the step above. The values of φ_i and χ_i are determined via separate FEM modelling or tabular data.

4.2 CREATE A SCOPING DIAGRAM

The purpose of this step is to assess the cost/benefit of automating the above tasks by creating a scoping diagram. For each task from the process map, two tables were created to independently assess benefits and cost.

Table 2 defines the benefits of automation and it was evaluated against two possible aspects: time savings and increased quality. In this instance, the former was given a weight of 2, while increased quality was assigned a weight of 1, indicating that the benefit of automation was expected to have more of an impact on productivity than quality, if compared to a manual approach.

TABLE 2 Assessment of the benefits in automating each step

	Time saving	Increased quality	Weighted average
Weighting	2	1	
Import general arrangements in Rhino	1	1	1.0
Identify thermal bridges types	2	2	2.0
Draw thermal bridges for each type	3	3	3.0
Compute the quantity	3	1	2.3
Generate output	3	1	2.3

Similarly, Table 3 was used to assess the cost of automating each task from the process map. Two cost aspects were analysed: time required to automate i.e., time to produce code, and cost in terms of additional specialist people i.e., the task requires advanced techniques to be used, such as machine learning.

TABLE 3 Assessment of the cost of automating each step

	Time required to produce code	Specialist people required	Weighted average
Weighting	2	1	
Import general arrangements in Rhino	1	1	1.0
Identify thermal bridges types	5	3	4.3
Draw thermal bridges for each type	5	2	4.0
Compute the quantity	1	1	1.0
Generate output	2	1	1.7

In this case, both tables were completed by experts in the field. All tasks are then given a weighted average both in terms of cost and benefit, which were represented in the scoping diagram shown in Figure 5. The scoping diagram evaluates all individual tasks (triangles) against their cost/benefit, with the best tasks to automate being the ones that have lower costs and greater benefits.

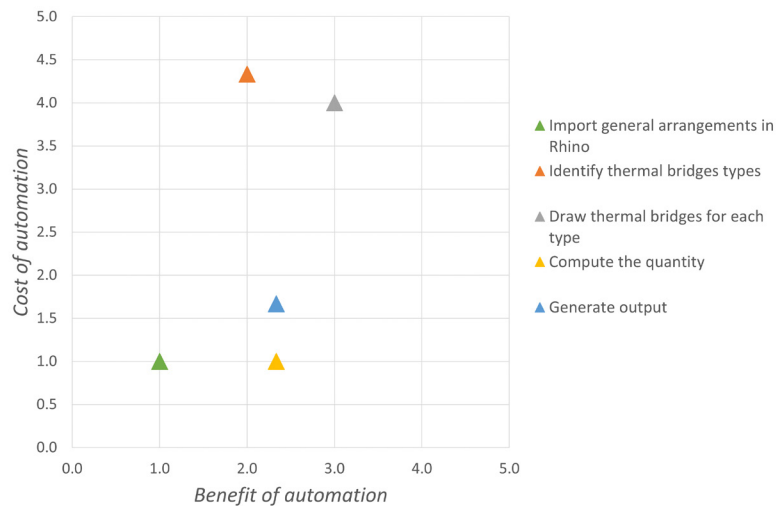


FIG. 5 Scoping diagram (Milton, 2007) for the investigated process. The scoping diagram evaluates all individual tasks (triangles) against their cost/benefit, with the best tasks to automate being the ones which have lower costs and larger benefits.

4.3 IMPLEMENT SOFTWARE SOLUTIONS TO AUTOMATE TASKS

This step is an iterative as it requires the identification of the most urgent tasks from the process map at step 1). The iteration is terminated when there is no cost/benefit opportunity or if, after having implemented a specific task, measured benefits don't meet the expected results.

The most urgent item on the scoping diagram is chosen from the subset of optimal tasks, i.e., those lying on the Pareto front. In this case, there are three out of five tasks that are optimal and they are, in ascending order of cost of automation: "Compute the quantity", "Generate output", and "Identify thermal bridge types". In this case, the task with the lowest cost of automation was chosen, as all three Pareto front tasks seemed to have similar values in terms of benefit (vertical Pareto front).

Iteration 1

The "Compute the quantity" task was chosen to be the most urgent as it was the one with the lowest cost of those in the Pareto front. The task was implemented via custom C# scripting by creating dedicated classes of objects that represented the thermal bridges (Figure 6). Note that the naming convention of the Rhinoceros layers containing thermal bridges of the same type can be interpreted as a serialised version of the objects in Figure 6, in that it includes all object properties except for the read-only properties "TotalQuantity" and "HeatLoss". The former is calculated as the sum of all thermal bridge quantities (either number or length), while the latter is equal to the product between the two properties *Value* and *TotalQuantity*. There is also an array of thermal bridges quantities "Quantities" which is excluded from the layer-naming convention as it is a property that gets generated at runtime and serves to determine the "TotalQuantity".

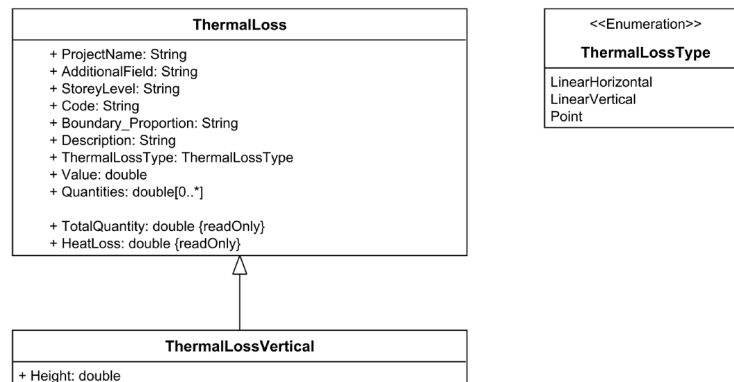


FIG. 6 UML class diagram representing the taxonomy of the thermal bridges in the software application.

The benefits were measured by comparing the time to perform the task manually with the time to implement the software solution and run it. For this task, an average of 15s per element to be measured (if a Rhino point, adding it to the count, whereas if a Rhinoceros line, by reading the length and reporting it onto an Excel spreadsheet, including a 10 minute break every hour of work) was determined. The time required to automate the task was measured to be 4 hours, while the time to run it required approximately 1 ms per task. For the two projects, the total number of Rhinoceros elements was 1756.

Figure 7 represents the obtained results, showing that the time required to complete the task manually is 440 minutes. As task automation required overall 240 minutes (time to run the automation was negligible in this case), the increase in productivity was positive and it was thus possible to move to the next task automation.

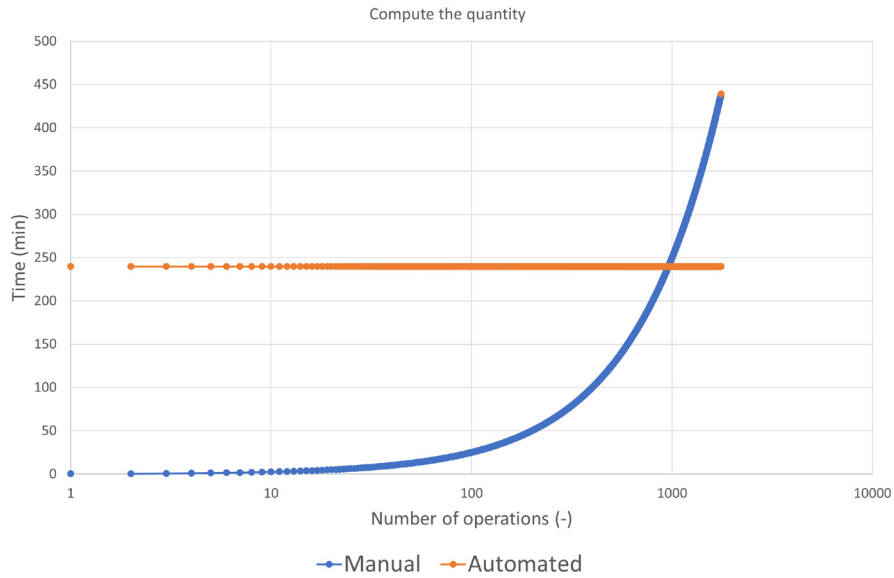


FIG. 7 Measured benefits from the automation of the task “Compute the quantity”.

Iteration 2

The second iteration involved the automation of the “Generate output” task. Due to project requirements, it was necessary to both report the total heat loss per each individual thermal bridge and their location in plan view. As the number of identified thermal bridge types was larger than 100, a plan view of each thermal bridge and their location was required. An example of the expected output is shown in Figure 8.



FIG. 8 Expected output for the two projects investigated. Left: summary of total heat loss per each thermal bridge. Right: example of the location of a thermal bridge in plan view (courtesy of Allford Hall Monaghan Morris).

Building upon the code from iteration 1 and the classes shown in Figure 5, first an extension of the C# code was made to export results into an Excel table automatically. This code was used to generate the clustered bar chart on the left of Figure 9. Then, additional code was produced to automatically take screenshots of each thermal bridge and the Rhinoceros entities representing coloured in red, along with the project general arrangements shown in the background in a lighter colour, as shown on the right of Figure 9.

Once the code was implemented, results were measured and compared. It was measured an average of 5 minutes per thermal bridge, if the task were to be performed manually. This value considers the act of turning all Rhinoceros layers off except those identifying the thermal bridge and the background general arrangements, setting the right layer colours and including a 10-minute break every hour of work. The time to create and use the automation was measured to be 240min and 1ms/task, respectively.

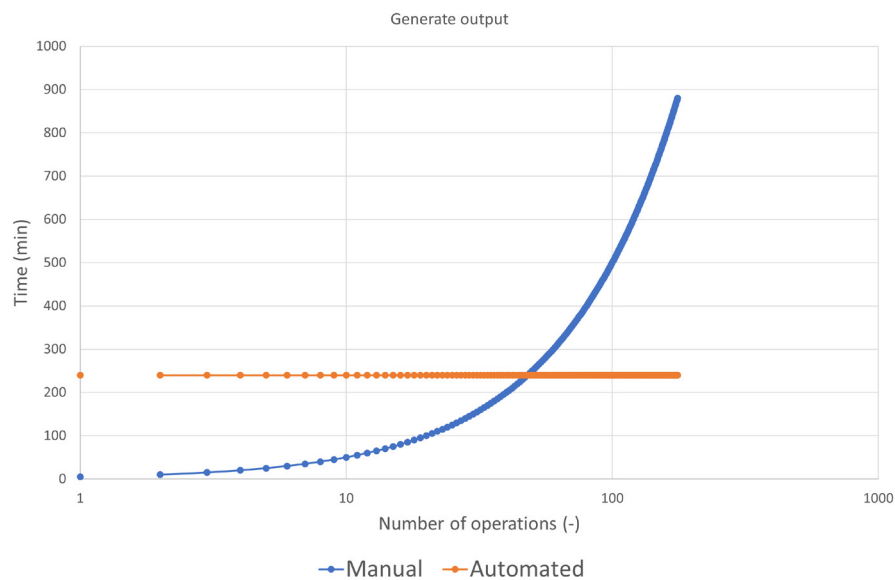


FIG. 9 Measured benefits from the automation of the task "Generate output".

The measured benefits arising from automating this task are shown in Figure 6. While the manual approach would require approximately 880 minutes of work, the automated task would slightly exceed 240 minutes.

Iteration 3

The third iteration would involve the automation of the "Draw thermal bridges for each type" task. This would mean automating a task with a software solution capable of recognizing complex concepts such as "building", "thermal bridge" and even more abstract ones, such as representing a thermal bridge with a line on a building's general arrangement plan view. While these concepts would be quite elementary to be performed manually by an experienced professional, it is harder to embed them into a software application such as an artificial intelligent agent via, for instance, machine learning. For this reason, the iteration was stopped and the rest of the tasks were performed manually.

5 DISCUSSION

The proposed method was used to automate part of the calculation of the total heat loss through the building envelope on two large-scale UK projects. The method was proven to produce a series of results that increased productivity. First, it demonstrated how to identify bottlenecks in a manual engineering task. For the two projects analysed, these were the tasks associated with counting the number and length of thermal bridges, generating the output, and identifying thermal bridge types on architectural drawings. Second, the time required to perform a large number of repetitive operations was significantly reduced. By comparing the time required to perform the two tasks requiring automation, a 63% reduction was measured (Figure 10). Overall, the time required to perform all tasks from Figure 3 was calculated to be 1893 minutes for the fully manual approach and 1054 minutes for the semi-automated route, thus leading to a global 44% reduction in time (Figure 11).

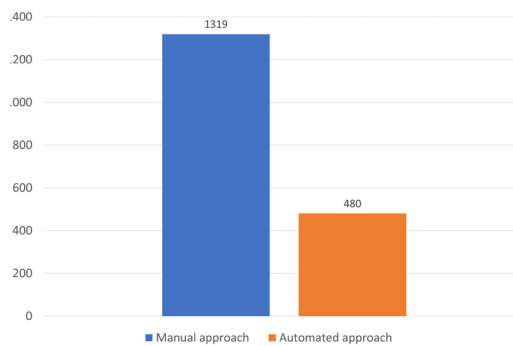


FIG. 10 Time (in minutes) to perform "Compute the quantity" and "Generate output" tasks.

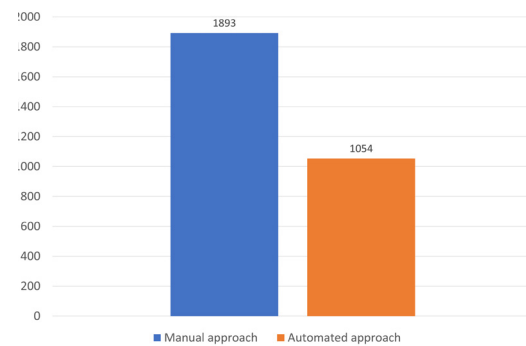


FIG. 11 Time (in minutes) to perform all tasks.

Lastly, given the repetitiveness of the tasks being automated, there is an expectation that quality would be increased. It is envisaged that human repetition may lead to random errors, such as incorrect reporting of thermal bridges lengths/counts onto an Excel spreadsheet or when generating graphical output. While quality may prove challenging to measure and/or assess, the authors believe that automation of repetitive and easy-to-automate tasks produces high-quality results. Producing experiments where people are required to complete a repetitive task, to be then reviewed in terms of number of errors against what is produced by a machine, may be a possible route. As these types of experiments fall outside of the expertise of the authors, further research in this field by design engineers and psychologists is required.

The assessment of the quality in automation is deemed to be both a point in favour and a limitation of this study. Other limitations consist of the inability to automate tasks requiring complex reasoning, such as the above-mentioned "Draw thermal bridges for each type" task. Novel computer science techniques, appropriately implemented in off-the-shelf software libraries, are required by construction professionals.

6 CONCLUSION

The present paper has proposed a method to analyse and prioritise manual tasks in a typical façade engineering process for successive software process automation. The method consisted of three major tasks, requiring process mapping, the subsequent evaluation of the tasks to be automated with the largest priority, and a final part where automation is implemented iteratively on each task. The method was applied concurrently to two large-scale UK projects for the assessment of the total heat loss through the building envelope via a large number of thermal bridges. Results have shown that the time to complete the engineering tasks can be reduced up to 44%, if appropriate automation on the most urgent tasks is implemented. The tasks that were automated in this study suggested that the more repetitive the task, the higher the likelihood of running into errors when performing it manually. This aspect is as crucial as it is complex to demonstrate and assess in advance. Further research requires methods to assess the expected increase in quality, as this aspect plays a fundamental role in increasing productivity in the engineering design of façades.

REFERENCES

- Altmann, E. M., Trafton, J. G., & Hambrick, D. Z. (2014). Momentary interruptions can derail the train of thought. *Journal of Experimental Psychology: General*, 143(1), 215–226. <https://doi.org/10.1037/a0030986>
- Ashby, M. F. (2011). *Materials Selection in Mechanical Design*.
- Back, J., Brumby, D. P., & Cox, A. L. (2010). Locked-out: Investigating the effectiveness of system lockouts to reduce errors in routine tasks. *Conference on Human Factors in Computing Systems - Proceedings*, 3775–3780. <https://doi.org/10.1145/1753846.1754054>
- Berggren, B., & Wall, M. (2011). Thermal bridges in passive houses and nearly zero-energy buildings. In *4th Nordic Passive House Conference, 2011*.
- Berggren, B., & Wall, M. (2013). Calculation of thermal bridges in (Nordic) building envelopes - Risk of performance failure due to inconsistent use of methodology. *Energy and Buildings*, 65, 331–339. <https://doi.org/10.1016/j.enbuild.2013.06.021>
- BPMN. (2017). Retrieved from <http://www.bpmn.org/>
- Henriksen, T., Lo, S., & Knaack, U. (2016). A new method to advance complex geometry thin-walled glass fibre reinforced concrete elements. *Journal of Building Engineering*, 6, 243–251. <https://doi.org/10.1016/j.jobe.2016.04.002>
- McKinsey & Company. (2015). The construction productivity imperative. Retrieved from www.mckinsey.com/industries/capital-projects-and-infrastructure/our-insights/the-construction-productivity-imperative
- Milton, N. R. (2007). *Knowledge Acquisition in Practice: A Step-by-step Guide* (1st ed.). Springer-Verlag London. <https://doi.org/10.1007/978-1-84628-861-6>
- Montali, J., Overend, M., Pelken, P. M., & Sauchelli, M. (2017). Towards facades as Make-To-Order products - The role of knowledge-based-engineering to support design. *Journal of Facade Design and Engineering*, 5(2). <https://doi.org/10.7480/jfde.2017.2.1744>
- Revit. (2021). Retrieved from <https://www.autodesk.com/products/revit/overview>
- Robert McNeel & Associates. (2021). Rhinoceros webpage. Retrieved from <https://www.rhino3d.com/>
- Sawaragi, Y., Nakayama, H., & Tanino, T. (1985). *Theory of multi-objective optimization*. Academic Press.
- Tsai, J., & Byrne, M. D. (2007). Evaluating systematic error predictions in a routine procedural task. *Proceedings of the Human Factors and Ergonomics Society*, 2, 817–821. <https://doi.org/10.1177/154193120705101209>

Empirical validation of co-simulation models for adaptive building envelopes

Esther Borkowski^{*1,2}, **Alessandra Luna-Navarro**^{3,4}, **Michalis Michael**³, **Mauro Overend**⁴,
Dimitrios Rovas¹, **Rokia Raslan**¹

* Corresponding author, esther.borkowski.12@ucl.ac.uk

1 University College London, Institute for Environmental Design and Engineering, United Kingdom

2 ETH Zurich, Institute of Technology in Architecture, Architecture and Building Systems, Switzerland

3 University of Cambridge, Department of Engineering, Glass and Façade Technology Research Group, United Kingdom

4 Delft University of Technology, Faculty of Architecture and the Built Environment, The Netherlands

Abstract

The thermal performance of adaptive building envelopes can be evaluated using building performance simulation tools. Simulation capabilities and accuracy in predicting the dynamic behaviour of adaptive building envelopes can be enhanced through co-simulation. However, it is unclear how accurately co-simulation can predict the performance of adaptive building envelopes and how the accuracy of adaptive building envelope models created in co-simulation setups can be assessed and validated. Therefore, this study presents new evidence on the empirical validation of co-simulation setups for adaptive building envelopes by establishing an assessment framework to determine the extent to which they can accurately represent the real world. The framework was applied to a case study to validate a co-simulation setup for a blind automation system using monitored data from MATELab, a full-scale outdoor test facility with realistic indoor and outdoor conditions. The validation of the co-simulation model of MATELab resulted in a median CV-RMSE index, a measure of model accuracy, of 5.9%. This indicates that the simulated data points have a small variance relative to the measured data points, showing a good model fit. In the future, modellers from the façade community can use the assessment framework for their co-simulation setups.

Keywords

Adaptive building envelope, Empirical validation, Co-simulation, Outdoor test facility, In-situ characterisation.

DOI

<http://doi.org/10.47982/jfde.2022.1.06>

1 INTRODUCTION

Adaptive building envelopes can improve thermal building performance by dynamically adapting their behaviour over time to changing environmental conditions (Loonen, Favoino, Hensen, & Overend, 2017). For example, adaptive building envelopes may significantly reduce energy demand for lighting, heating and cooling by conveniently modulating the incoming solar radiation (Favoino, Fiorito, Cannavale, Ranzi, & Overend, 2016).

Despite the rapid development of novel adaptive building envelope technologies, they are hardly adopted in practice. One reason is that capital costs for adaptive building envelopes are typically higher than for static building envelopes due to additional components – involving more raw materials and higher investment costs. However, operating costs for energy consumption and maintenance may be lower throughout the life cycle of adaptive building envelopes and are rarely considered by designers and clients (Attia et al., 2018; Loonen, Trčka, Cóstola, & Hensen, 2013). Another reason is a lack of evidence in real-world applications of the benefits that can arise from these technologies or the lack of benchmarks, standards and testing procedures for evaluating adaptive building envelope performance (Hensen, Loonen, Archontiki, & Kanellis, 2015). The latter is in part attributed to uncertainty in predictions of adaptive building envelope performance when using existing building performance simulation (BPS) tools. BPS tools are software tools for predicting building performance by dynamically solving a set of mathematical equations. The main barriers to an accurate performance prediction of adaptive building envelopes in BPS tools are: (i) the limited modelling capabilities of existing BPS tools in simulating different types and ranges of control algorithms, on which the performance of adaptive building envelopes during operation largely depends (Loonen et al., 2017), (ii) the limited integration of multi-domain influences (Tabadkani, Tsangrassoulis, Roetzel, & Li, 2020) and (iii) the lack of occupant behaviour models that can successfully estimate the impact of users (Luna-Navarro, Gaetani, Anselmo, Law, & Overend, 2021). This limits the capability of BPS tools to adequately capture the influence of the control algorithm on the dynamic behaviour of adaptive building envelopes, which in turn increases the uncertainty about accurately predicting adaptive building envelope performance.

Taveres-Cachat, Favoino, Loonen, & Goia (2021) suggest that the co-simulation of adaptive building envelope models is a valuable approach to overcome the limitations discussed above. Co-simulation stands for *cooperative simulation* and refers to the joint simulation of separate models developed in different tools. The models are executed in individual simulators and are allowed to cooperate (Hafner et al., 2012; Trčka, Wetter, & Hensen, 2009). While the tools communicate and synchronise outputs, such as variables or status information, at certain points in time, each tool independently solves one part of the coupled problem between the communication points. A particular challenge in co-simulation is the time synchronisation and orchestration of the heterogeneous models and their individual solvers. To enable synchronisation and interactions across sub-simulators, co-simulation uses a coordinator-worker concept. The worker simulates sub-problems, and the coordinator initiates the start of the simulation and is responsible for coordinating the overall simulation and the data transfer between the tools (Broman et al., 2013). An earlier study by Borkowski, Donato, Zemella, Rovas, & Raslan (2019) proposed a modelling approach for the co-simulation of adaptive building envelopes. According to Attia, Hensen, Beltrán, & De Herde (2012), BPS tools should provide the flexibility to integrate guidance to influence design decisions, e.g. through optimisation of design solutions. However, many BPS tools lack such capabilities, and the modelling approach by Borkowski et al. (2019) integrates additional functionalities, such as optimisation, to support the design decision-making process.

It is still unclear whether co-simulation tools can accurately predict the thermal performance of adaptive building envelopes, albeit accurate adaptive building envelope models are crucial (Loonen et al., 2017). The accuracy of BPS tools is usually systematically tested through diagnostic methods, such as the Building Energy Simulation Test method, which allows comparison of the predictions of BPS tools with analytical solutions (Neymark et al., 2002). However, it is generally difficult to establish a common diagnostic method for co-simulation setups, as there is no one-size-fits-all approach to co-simulation, with the end product often being case-dependent (Trčka et al., 2009).

Despite the importance of assessing the accuracy of co-simulation setups for adaptive building envelopes, there is currently only one study that shows the empirical validation of a co-simulation setup for adaptive building envelopes, and that is a study by Taveres-Cachat & Goia (2020). In this study, a fully controlled test facility was used to validate a co-simulation setup for predicting the thermal and daylighting performance of a highly flexible parametric model of an external louvred shading system. The study by Taveres-Cachat & Goia (2020) does not take into account that the end products of co-simulation setups are very different and strongly depend on the respective co-simulation task. For example, they can differ depending on the internal routines of the tools used or the degree of complexity required to describe the task. This case dependency means that an approach for the validation of co-simulation of adaptive building envelopes is required that can be used for the different co-simulation setups. Therefore, the aim of the present study is to provide new evidence on how to validate co-simulation setups for thermal and control models of adaptive building envelopes. Since access to expensive calorimetric test facilities is often a barrier to providing empirical evidence for co-simulation setups, a full-scale non-calorimetric test facility was used. In addition, the approach by Taveres-Cachat & Goia (2020) has been extended through the use of an in-situ characterisation and a sensitivity analysis (SA), and details of each step of the assessment framework are provided for modellers from the façade design and engineering community to determine the accuracy of their own co-simulation setups.

To achieve these objectives, the present study adopted a twofold validation technique. On the one hand, empirical validation, which compares the outcomes of a tool with measured data, was used to test the solution process and appropriateness of the modelling approach within (i) its domain of applicability (Sargent, 2013) and (ii) the range of experimental uncertainty (Coakley, Raftery, & Keane, 2014). On the other hand, comparative testing, which compares the outcomes of a tool with the outcomes of another tool, was used to identify and diagnose sources of error or inaccuracy in the modelling approach. However, conducting comparative testing, which requires the use of a tool commonly accepted to represent the state-of-the-art, was complicated by the challenging representation of control algorithms for adaptive building envelopes in existing BPS tools. To still be able to perform comparative testing, only control algorithms that could be modelled in existing BPS tools were used in the present study.

The remaining part of the paper proceeds as follows: the next section (Section 2) provides an overview of the challenges of using non-controlled real-world facilities, such as MATELab, an outdoor test cell for occupant-façade interaction in the United Kingdom (UK) (Luna-Navarro & Overend, 2021), to empirically validate co-simulation setups. MATELab is a 30.0 m² office-like test facility designed to investigate occupant responses to different adaptive building envelope technologies. It has a modular glazed building envelope oriented to the east, south and west for testing different building envelope bays per orientation (Figure 2). Each bay has a maximum dimension of 1.5 m by 2.3 m and was designed to be easily installed and replaced, thereby allowing different building envelope technologies to be investigated in a relatively short period of time. In addition, each of the bays can be covered with obscuring cover panels made of highly insulated external and corresponding

internal plasterboard to generate a broad range of glazing orientation scenarios. Section 3 describes the co-simulation setup that is empirically validated and the assessment framework adopted for its validation. The results of the validation are then reported in Section 4 and discussed in Section 5.

2 CHALLENGES OF ADOPTING NON-CONTROLLED TEST FACILITIES FOR EMPIRICAL VALIDATION OF ADAPTIVE BUILDING ENVELOPE CO-SIMULATION MODELS

The thermal performance of building envelopes is usually measured in indoor calorimetric facilities, as the British Standards Institution describes in BS ISO 19467 (BSI, 2017b). In recent years, the performance of adaptive building envelopes has been increasingly tested in outdoor test facilities (e.g. Cattarin, Causone, Kindinis, & Pagliano, 2016). However, since they do not present full control of environmental parameters or calorimetric conditions, the thermal performance of these test facilities tends to be less accurate and controlled than traditional outdoor test cells for adaptive building envelopes.

Compared to real buildings, the modelling and calibration of not fully controlled outdoor test cells share some challenges but also bring benefits (Cattarin et al., 2016). Of key importance are the challenges discussed hereafter. The first challenge is that boundary conditions, thermal bridges and air infiltrations have a larger impact on the performance, given the smaller size of these test cells. In this sense, the detection of individual heat transfer paths is required, as recommended by Annex 58 of the International Energy Agency's Energy in Buildings and Communities (IEA EBC) programme (Roels, 2012). Thermal bridges and air infiltration rates also tend to be non-negligible due to the large surface-to-volume ratio.

The second challenge is the measurement and modelling of boundary conditions, which is particularly important as boundary conditions are not fully controlled. Monitoring and modelling of weather conditions are also important, especially the fraction of direct, diffuse and ground-reflected solar radiation (Judkoff & Neymark, 2006). Solar gains can have a large impact due to the larger surface of the transparent envelope relative to the total volume. The heat transfer coefficient of the surface must therefore be accurately selected from the large number of available empirical correlations to better describe the specific boundary conditions, such as wind velocity in the proximity of the building envelope (Moinard & G.Guyon, 1999).

If the thermal inertia of the building envelope is low, a third challenge is the unwanted oscillations in indoor air temperature compared to highly controlled test cells. Loutzenhiser et al. (2007) highlighted that predictions of cooling performance obtained through simulations are more sensitive to boundary conditions when performed on lightweight buildings compared to massive buildings due to the low thermal mass (and time constant) of the former case.

Lastly, real-world non-controlled test facilities typically include building automation systems for controlling heating, cooling, ventilation, lighting or window systems. These building automation systems usually have sensors, but they are not easily accessible or programmable to take measurements with the accuracy or frequency required for the calibration process of a BPS tool (Saelens & Reynders, 2016).

3 CO-SIMULATION SETUP AND ASSESSMENT FRAMEWORK FOR VALIDATION IN A NON-CONTROLLED TEST FACILITY

This section provides an overview of the co-simulation setup and the assessment framework used to validate it.

3.1 CO-SIMULATION SETUP

The co-simulation setup used the modelling approach developed by Borkowski et al. (2019) to model the blind automation system of MATELab. The modelling approach was specifically developed to accurately predict the thermal performance of control algorithms for adaptive building envelopes. To represent adaptive building envelopes, the modelling approach uses the following software:

- *EnergyPlus*: Integration of EnergyPlus v8.9.0 (National Renewable Energy Laboratory, 2018) to create the thermal model of the building and the building envelope.
- *Dymola*: Integration of Dymola v2020x (Dassault Systèmes, 2018), a commercial simulation programme based on the object-oriented, multi-domain modelling language Modelica (Modelica Association, 2017), to create the model of the control algorithm.
- *FMI Standard*: Integration of the Functional Mock-up Interface (FMI) Standard v2.0 (MODELISAR, 2014), an open middleware developed to facilitate communication and information exchange in co-simulation setups, to exchange information at each simulation timestep between EnergyPlus and Dymola.

Dymola is used as a coordinator simulation tool, and EnergyPlus as a worker simulation tool, as shown in Figure 1. This means that the EnergyPlus model is encapsulated and shared as a Functional Mock-up Unit (FMU) for co-simulation, which enables EnergyPlus to exchange information at each timestep with Dymola. The software package EnergyPlusToFMU v3.0.0 (Nouidui, Lorenzetti, & Wetter, 2020) is invoked to create the FMU, which is then manually imported into Dymola, the co-simulation coordinator, and connected to the control algorithm model. In the present study, the solar irradiance was measured in MATELab and provided as an input to the model to compute the blind position, which was then provided as an input for the FMU.

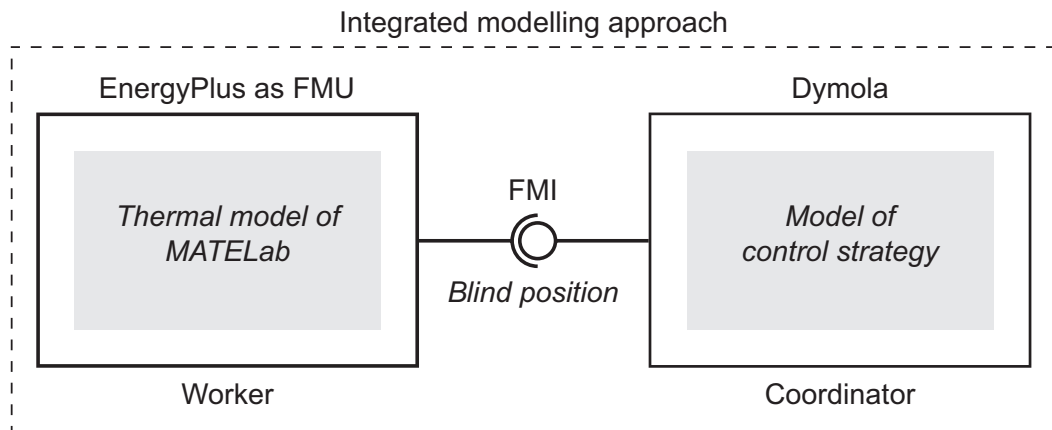


FIG. 1 Schematic of the co-simulation process: the control algorithm for the blind automation system in Dymola was coupled to the model of MATELab through the FMI Standard for information exchange at each zone timestep.

The co-simulation was automated through a script written in Python v3.8.5 (Python Software Foundation, 2020), which covered three basic steps: (i) export of the thermal model of MATELab as an FMU to be used in the co-simulation setup by calling EnergyPlusToFMU through the *Subprocess.call()* function; (ii) co-simulation of the entire model of MATELab through the *Simulator.simulate()* function of the BuildingsPy package (Lawrence Berkeley National Laboratory, 2019) and (iii) extraction and storage of data in CSV format for analysis. All simulations required for the validation were performed using the standard Dassi solver of Dymola with the default solver tolerance of 10^{-4} on a 2015 MacBook Pro with a dual-core Intel Core i5 processor of 2.7 GHz and with 16 GB of memory running Ubuntu 20.04 in a virtual machine.

3.2 ASSESSMENT FRAMEWORK

Table 1 describes the assessment framework to validate co-simulation setups for adaptive building envelopes used in non-controlled calorimetric test facilities. MATELab was chosen as a case study for a non-controlled and non-calorimetric test facility to collect the empirical data. The following sections describe the actions taken in each step of the framework's application and the rationale for the specific procedures and techniques used to identify, collect and analyse information.

TABLE 1 Steps involved in the validation of co-simulation setups for control algorithms of adaptive building envelopes

Step	
1	Definition of the validation scenario according to the purpose of the present study.
2	In-situ characterisation of the thermal properties of the validation scenario.
3	Collection of empirical data for the validation.
4	Creation of a reduced-complexity thermal model of the validation scenario in EnergyPlus based on the available facility construction documentation and the in-situ characterisation results.
5	Undertaking of a SA to identify key input variables for the calibration.
6	Calibration of the reduced-complexity thermal model of the validation scenario.
7	Creation of an adaptive building envelope model in the co-simulation setup by extending the model from Step 6 with a control algorithm for the building envelope.
8	Validation of the co-simulation setup by comparing the predicted data with the experimental data and identification of potential sources of error.

3.3 VALIDATION SCENARIO

The first step in the validation of the co-simulation setup was to define the validation scenario according to the purpose of the study. For the present study, MATELab was used with the east and west glazing panels covered with the obscuring cover panels internally and externally, thereby generating a south-facing glazed building envelope scenario. The south-oriented glazing consisted of two high-performance double-glazed units and internal automated Venetian blinds, as shown in Figure 3. This setup resulted in a window-to-wall ratio of approximately 0.5 on the south-oriented building envelope. The validation scenario's characteristics are reported in Appendix A.



FIG. 2 Exterior views of MATELab: a. View of the south-west building envelope; b. View of the east building envelope with cover panels.

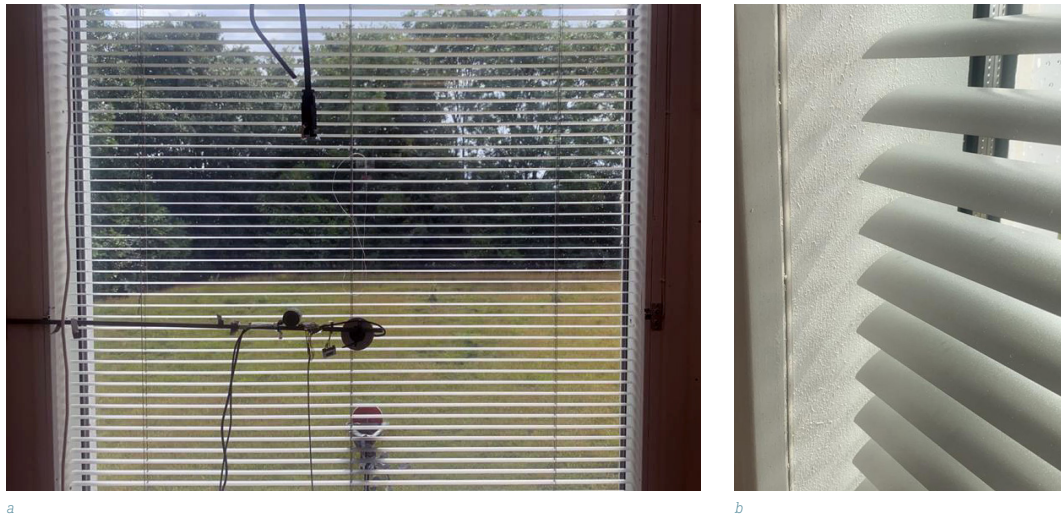


FIG. 3 Views of blind installed in MATELab: a. View from inside to outside through blind with installed sensors; b. Detailed view of blind slats.

MATELab was unoccupied and operated in a free-running mode during this study, i.e. the underfloor air distribution (UFAD) system was switched off. This eliminated uncertainties arising from occupant behaviour and operation of the heating, ventilation and air-conditioning (HVAC) system, as suggested by previous work (Lomas, Eppel, Martin, & Bloomfield, 1997). It resulted in a simpler and more controlled validation scenario and facilitated the identification of inaccuracy or error in the building envelope and in the basic setup of the model.

Table 2 shows the control algorithm of the automated Venetian blinds that was implemented for the validation of the co-simulation setup. It was a rule-based control algorithm whose input and output were the solar irradiance, the time delay and the position of the blind.

TABLE 2 Control algorithm for MATELab's blind automation system

Input	$I_{sol,sky}$: global horizontal solar irradiance in W/m ²
Output	$I_{sol,south}$: global vertical solar irradiance on south surface in W/m ²
Algorithm	<pre> set $I_{sol} = 1/3 \times I_{sol,sky} + 1.0 \times I_{sol,south}$ if $I_{sol} > 250 \text{ W/m}^2$ and $t > 15 \text{ min}$ then $u_{blind} = 1.0$ else $u_{blind} = 0.0$ end if </pre>

Due to the challenges of modelling a test facility such as MATELab, it was initially necessary to model a reduced-complexity model of MATELab, i.e. the thermal model with a static building envelope, allowing for a better understanding of the model dynamics. Accordingly, for the reduced-complexity model (Step 4), the blind automation system was turned off, so the building envelope was static. In addition, the blinds remained down all the time to minimise solar gain effects. In contrast, in the co-simulation model (Step 7), the blind automation system was turned on, so the building envelope was adaptive. Details of both models are reported in Table 3.

TABLE 3 Building envelope setup of models in validation scenario

Step	Model	Mode of operation	Position of blinds	Measurement period
4	Reduced-complexity model	Static	Down	14-21 May 2020
5	Co-simulation model	Adaptive	Alternating depending on control algorithm	8-16 August 2020

3.4 IN-SITU CHARACTERISATION OF THERMAL CHARACTERISTICS

In the second step, the thermal characteristics of the validation scenario were characterised. The thermal performance of the building envelope is often considered a major source of uncertainty in thermal building models, as the actual performance may differ from the performance estimated during design. For this reason, this methodology proposed the characterisation of the building envelope through in-situ measurements. The in-situ characterisation included the evaluation of the most important thermal properties of the building envelope: the thermal transmittance and the solar factor of the glass façade, the thermal bridges and the air infiltration flow rate. Further details of the calculations and procedures are given in Appendix B.

3.4.1 In-situ measurements of U- and g-values

According to ISO Standard 13790 (International Organization for Standardization Technical Committee 163/SC 2, 2008), the thermal characterisation of the building envelope is done by evaluating the air tightness, as recommended in BS EN 13829 (BSI, 2001), and by measuring two simplified parameters: (i) the thermal transmittance, i.e. the U-value (W/m²K), and, if glazed, the solar factor, i.e. the g-value (-). These two parameters are usually measured under steady-state conditions either by laboratory tests or by software tools integrating databases of glass panes. However, due to the simplified approach in evaluating these parameters, they may not correspond to the actual thermal and solar performance (Goia & Serra, 2018). For example, there may be a discrepancy between the boundary conditions registered in situ and the standardised conditions

used during laboratory characterisation. Therefore, the simplified approach can lead to significant differences between the calculated and in-situ energy performance of the glazing system. Since there are no calorimetric conditions in non-controlled, non-calorimetric test facilities to assess the performance of the building envelopes, this framework used the in-situ characterisation based on the work by Goia and Serra (2018). The framework measures the U- and g-values through empirical measurements under non-calorimetric conditions. The measurements for the characterisation of the in-situ performance of the building envelope were taken as shown in Figure 4.

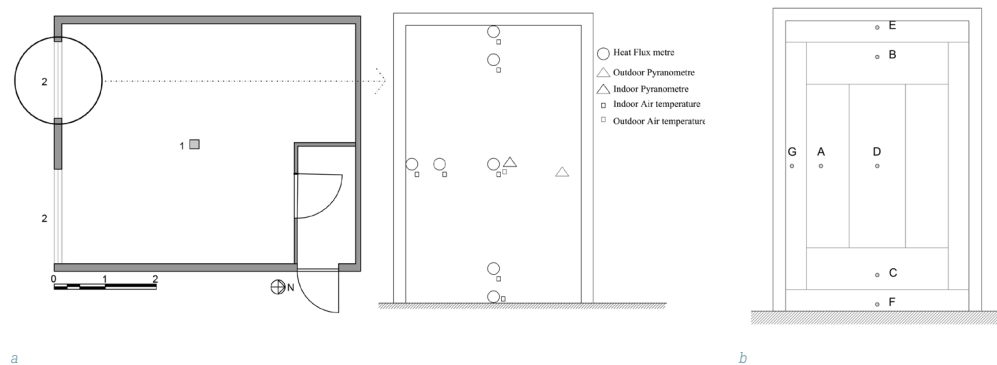


FIG. 4 Experimental setup in MATELab: a. Plan view with the indoor sensors at the centre of the facility (1) and at the building envelope (2); b. Experimental setup at the building envelope with indication of the sensors used (sensor details are reported in Appendix B); c. Area-weighting for the calculation of the U-value..

3.4.2 Air tightness of building envelope

The air tightness of the building envelope can be characterised in situ by a blower door test (BDT) according to BS EN 13829 (BSI, 2001). This standard describes two types of test methods, depending on the purpose of the application. Method A (testing of a building in use) is applied during the heating or cooling season, while Method B (testing of the building envelope) assumes that intended openings in the building envelope are closed or sealed and the HVAC system is switched off. In a BDT, a specific range of pressure differences is created in the building envelope, and the airflow through the fan is monitored to assess the level of air tightness of the building envelope. Method B was chosen in this study since the goal of the air tightness test was to evaluate the performance of the building envelope. Therefore, all openings of the test facility were closed or sealed, including the air conditioning grills and vents, and the UFAD system was switched off. The indoor and outdoor temperatures were the same. The BDT was performed on a day when the meteorological wind speed was within the recommended range of BS EN 13829 (BSI, 2001).

After performing the BDT, the data were processed according to the Technical Memoranda TM23 by the Chartered Institution of Building Services Engineers (CIBSE, 2000) to determine the air tightness.

3.4.3 Thermal bridges assessment

If the validation scenario has a large ratio of external surface area to internal volume, thermal bridges can significantly affect the thermal model of the test facility and must be evaluated accordingly. Thermography provides a rapid and non-destructive means of assessing the thermal performance of building envelopes in situ (Asdrubali, Baldinelli, & Bianchi, 2012). Applications include (i) detection of missing or defective insulation, (ii) detection of air leaks and moisture and (iii) investigation of thermal discontinuities in the building envelope and thermal bridges. Thermographic tests should be carried out in accordance with BS EN 13187 (BSI, 1999) and BS EN ISO 6781-3 (BSI, 2015). When using thermography to identify thermal bridges, the temperature difference between the inside and outside of the building should be at least 10 °C. To minimise the effect of solar radiation on the results, in-situ thermographic tests are usually carried out during the night. In this study, the method proposed by Asdrubali et al. (2012) was used to quantify the effect of thermal bridges.

3.5 DATA COLLECTION PROCEDURES

The third step was to collect empirical data for the validation. During the measurement periods, the parameters described below were measured based on the available sensors for undertaking the model calibration and validation. After the data collection, the values were compiled and averaged over 1 minute. Details on the measurement campaign are reported in Appendix C.

3.5.1 Outdoor environmental parameters

Outdoor environmental parameters were needed to create the weather file for the validation of the model of MATELab. Weather data, specifically the dry bulb air temperature and the global horizontal solar irradiance, were collected using the weather station of MATELab, located on its roof at a height of approximately 3.0 m above ground level. It was assumed that these data were of particular importance for predicting MATELab's performance, in particular the aspects listed in Table 4.

TABLE 4 Effects of measured outdoor environmental parameters on the performance of MATELab

Parameter measured	Measurement instrument used	Performance aspects affected by parameter
Dry bulb air temperature	Weather station	Exterior surface convection Infiltration/ventilation sensible heat transfer
Global solar irradiance	Weather station	Fenestration heat gains Exterior surface heat balance Control algorithm

3.5.2 Indoor environmental parameters

Indoor environmental parameters were needed to assess the accuracy of the model during validation. The thermal performance indicator used was the indoor temperature, which was measured at the centre of the facility by a 1.0 m high sensing station (1 in Figure 4a).

3.5.3 Parameters related to control actions of blind automation system

Another data point required for the validation was the control actions of the blind automation system, namely the position of the blind. It was an important data point for the cross-validation of model outcomes, as the performance of adaptive building envelopes largely depends on the control algorithm during operation.

3.6 CREATION OF A REDUCED-COMPLEXITY THERMAL MODEL

The reduced-complexity thermal model was developed in the fourth step in EnergyPlus, which was chosen because it can represent the building envelope with sufficient accuracy (Attia et al., 2018). This offers the possibility to simulate and explore the performance of adaptive building envelope technologies constructed in MATELab in future studies. Furthermore, EnergyPlus allows the calculation of the thermal performance under non-stationary conditions, which is important in the present study as MATELab has a low thermal mass and is free-running. In the model, three thermal zones were implemented: (i) a supply air plenum under the raised floor, (ii) a return air plenum over the suspended ceiling and (iii) an occupied space. Further simulation parameters of the thermal model of MATELab are reported in Appendix D.

The models of the building envelopes were initially created based on the specifications received from the manufacturers of the building components. In a second iteration, the U- and g-values measured in Step 2 were incorporated. This was followed by a third iteration in which the U-values of the opaque building components were modified to capture the effects of the thermal bridges as measured in Step 2. Thermal bridges were included by increasing the conductivity of each building component by the corresponding value.

Data from outdoor environmental conditions were then used to create a new weather file for the study periods with Elements (Big Ladder Software & Rocky Mountain Institute, 2016), a free and open-source software tool for creating and editing custom weather files. Further details are reported in Appendix D.

3.7 SENSITIVITY ANALYSIS TO INFORM THE CALIBRATION

In the fifth step, a SA was carried out to identify key input variables for the calibration. The evaluation of the uncertainties is a fundamental step in the calibration process of BPS tools to confirm that a model was implemented correctly (de Wit & Augenbroe, 2002). In the present study, this was achieved by identifying and quantifying the degree of uncertainty of the most important input variables of the model of MATELab and then fine-tuning uncertain input variables to minimise discrepancies between measured and predicted data points. Possible sources of uncertainty in the model of MATELab are listed in Table 5.

TABLE 5 Possible sources of uncertainty in the model of MATELab

Type of uncertainty	Description
Specification uncertainty	Inaccurate or incomplete building and system specifications, such as geometry, material and blind properties and internal heat gains.
Modelling uncertainty	Simplifications and inaccurate assumptions of the physical processes, such as infiltration and ground heat transfer characteristics, in the computational simulation.
Numerical uncertainty	Errors introduced in the numerical analysis of the computational simulation.
Scenario uncertainty	Inaccurate representation of external conditions imposed on the building, such as climate conditions and occupant behaviour.

Detailed audits and in-situ characterisation are effective instruments to reduce the first source of uncertainty and should be carried out where possible. This includes in-situ measurements of actual geometrical characteristics as well as HVAC and lighting systems and schedules. Such in-situ characterisations are relatively easy to perform in outdoor test facilities that are not fully controlled (as described in Step 1), so that uncertainties due to inaccurate or incomplete building specifications become negligible.

To determine the most important input variables, the next step of the calibration process consisted of undertaking a SA (Chong and Menberg 2018). In this study, a global approach to SA was adopted, taking into account the interactions between variables by varying input variables simultaneously over the whole input sample space. The approach to global SA adopted was a Monte Carlo sensitivity analysis (MCSA), a variance-based method that measures the sensitivity of the output to the input variable by the amount of variance in the output caused by that input (Tian, 2013). It uses random samples from a given distribution, and this study selected the Latin hypercube sampling (LHS) method to generate the sample due to its efficient stratification properties. Figure 5 shows the schematic of the processes involved in the MCSA.

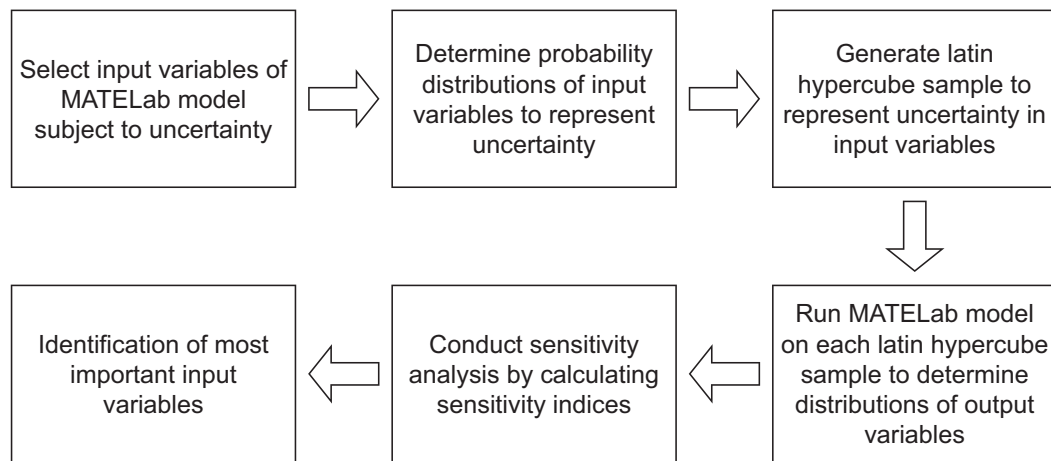


FIG. 5 Workflow diagram showing the processes involved in the MCSA.

In the MCSA, numerous sets of input-output variables were generated by running the model of MATELab on the input sample. The uncertain inputs considered in the MCSA are listed in Appendix E. Correlation-based methods were then applied to measure the strength of the input and output variables and to rank the input variables from 1 (the most important variables) to 8 (the least important variable). The two indices applied were: (i) the Pearson correlation coefficient (S_{Pear}) to measure the strength of the linear relationship between each of the input variables and the indoor temperature and (ii) the Spearman rank-order correlation coefficient (S_{Spear}) to measure the strength of the monotonic relationship between each of the input variables and the indoor temperature. Both indices had to be applied to capture information in the case of a non-linear relationship between input and output variables. The ranking was then used to generate plots for an initial qualitative evaluation of key input variables using the Python package Matplotlib (Hunter, 2007): (i) tornado plots to compare the relative importance of the input variables and (ii) scatter plots to show the relationships between the variables.

Given that sensitivity indices are estimated based on a limited sample, SA methods are subject to uncertainty (Yang, 2011). To get good estimations nonetheless, Monte Carlo simulations require many iterations depending on the complexity of the model and the number of parameters. The present work used the bootstrap technique (Yang, 2011), plotting the estimated statistic against the gradually increasing base sample size. Convergence is assumed as soon as there is no significant variation for each sensitivity index.

As the MCSA required many iterations and thus a lot of computing power, a research computing cluster was used to run the MCSA, which was completely automated through a Python script. To keep the computational time as short as possible, the MCSA only utilised the previously created reduced-complexity model. This required the use of EnergyPlus alone, which helped to reduce the computational intensity of the MCSA.

3.8 CALIBRATION OF A REDUCED-COMPLEXITY THERMAL MODEL

The reduced-complexity model was calibrated in the sixth step. Previous work on model calibration of outdoor test facilities suggested using an uncertainty analysis (UA) in the calibration of a thermal model (Jensen, 1995). An UA was described as 'the process of determining the degree of confidence in the true value when using a measurement procedure(s) and/or calculation(s)' by the American Society of Heating, Refrigerating and Air-Conditioning Engineers (ASHRAE, 2014, p. 10). It measures the acceptable level of model accuracy using uncertainty indices. The index applied in this part of the study was the coefficient of variation of root mean square error (CV-RMSE) index, which measures the variability of the errors between measured and simulated data points, thereby indicating the model's ability to fit the data

$$CV - RMSE = \frac{1}{\bar{m}} \sqrt{\frac{\sum_{i=1}^n (m_i - s_i)^2}{n - p}} \times 100$$

Equation 1

where \bar{m} is the average of the measured data points, m_i is the measured data point for each model instance i , s_i is the simulated data point for each model instance i , n is the number of measured data points, and p is the number of adjustable data points, which is suggested to be zero for a calibration.

The IEA EBC Annex 58 developed a comprehensive framework and guidelines for reliable in-situ dynamic testing to characterise the actual energy performance of building components and whole buildings (Roels, 2012). This study applied the framework proposed in IEA EBC Annex 58 by using an automated method to calibrate the model once the experimental data collection has been performed. The automated calibration was implemented by using jEPlus (Zhang, 2012), a parametric tool for EnergyPlus, and an automated optimisation script in Python. It calculated the CV-RMSE index for each design option and selected the minimum CV-RMSE index as the final calibration solution. The parameters for the calibration were selected based on the results of the MCSA.

ASHRAE and other organisations (e.g. ASHRAE, 2014; Federal Energy Management Program, 2008; International Organization for Standardization Technical Committee 163/SC 2, 2008) specify

the maximum values for model calibration depending on whether the model was calibrated with hourly or monthly data. Furthermore, it should be noted that current calibration criteria only refer to the predicted energy consumption and do not account for uncertainties or inaccuracies of input parameters or the accuracy of the simulated environment (e.g. temperature profiles). This study used the hourly CV-RMSE index, which should be less than 30.0% for a model considered calibrated (ASHRAE, 2014). In previous work, calibrated models of outdoor test facilities have achieved low CV-RMSE values, such as 2.0% (Taveres-Cachat & Goia, 2020) or 3.4% (Martínez, Erkoreka, Eguía, Granada, & Febrero, 2019).

3.9 CREATION OF CONTROLLER MODELS

To model alternative dynamic controls of the adaptive building envelope, the previously created EnergyPlus model of MATELab was connected to a controller model in the seventh step. The controller model was developed in (i) the Energy Management System (EMS) feature of EnergyPlus and (ii) Dymola in the co-simulation setup. The controller model in the EMS feature was used (i) for the SA and (ii) to generate outputs of a tool that is generally accepted as state-of-the-art to identify and diagnose sources of error or inaccuracy in the co-simulation setup (Neymark et al., 2002). The co-simulation model was then used to test the accuracy of the adaptive building envelope model's predictions coupled with the modelling approach, a co-simulation setup developed in previous work.

3.9.1 Controller model in EMS feature of EnergyPlus

The EMS feature uses the EnergyPlus runtime language (Erl), a simple scripting language, to describe control algorithms (DOE 2018). EnergyPlus interprets and executes the control sequence implemented in Erl as the model is being run. In the present study, the EMS feature was used to provide high-level supervisory control to override the *WindowProperty:ShadingControl* object in EnergyPlus. Without the EMS feature, MATELab's control algorithm could only have been modelled in fragments, as blind control algorithms within EnergyPlus are either preset or time-scheduled. This might have had a negative impact on the model outcome (BSI, 2017a). To model a control algorithm that is based on boundary conditions or simulation state variables instead, the EMS feature must be used. Even though two aspects of the control algorithm were particularly complex to model in the EMS feature (Appendix D), it was implemented in the *EnergyManagementSystem:Program* object in EnergyPlus, as shown in Figure 6.

```

EnergyManagementSystem:Program,
  setyblind,                !- Name
  SET solrad_log_1 = @TrendValue solrad_log 1,    !- Program Line 1
  SET solrad_log_2 = @TrendValue solrad_log 2,    !- Program Line 2
  SET solrad_log_3 = @TrendValue solrad_log 3,    !- Program Line 3
  SET solrad_log_4 = @TrendValue solrad_log 4,    !- Program Line 4
  SET blind_on = Shade_Status_Interior_Blind_On,  !- Program Line 5
  SET blind_off = Shade_Status_Off,              !- Program Line 6
  IF (solrad_log_1 >= 250) && (solrad_log_2 >= 250) && (solrad_log_3 >= 250),  !- Program Line 7
  SET yblind_left = blind_on,                    !- Program Line 8
  SET yblind_right = blind_on,                   !- Program Line 9
  ELSEIF (solrad_log_1 < 250) && (solrad_log_2 < 250) && (solrad_log_3 < 250),  !- Program Line 10
  SET yblind_left = blind_off,                   !- Program Line 11
  SET yblind_right = blind_off,                  !- Program Line 12
  ENDIF;                                         !- Program Line 13

```

FIG. 6 Control algorithm for MATELab's blind automation system in the EMS feature of EnergyPlus.

3.9.2 Controller model in co-simulation setup

To link the EnergyPlus model to the Dymola model, the external interface of EnergyPlus had to be activated. With the *ExternalInterface* object present, the values listed in the object received their inputs from the FMI Standard at each zone timestep. The software package EnergyPlusToFMU was used to export the EnergyPlus model of MATELab as an FMU for co-simulation. The FMU was then imported into Dymola, where it appeared as an input/output block and was connected to the controller model. Figure 7 represents the model of the control algorithm in Dymola, with (i) the input data of the monitored solar irradiance, (ii) the control algorithm and (iii) the FMU.

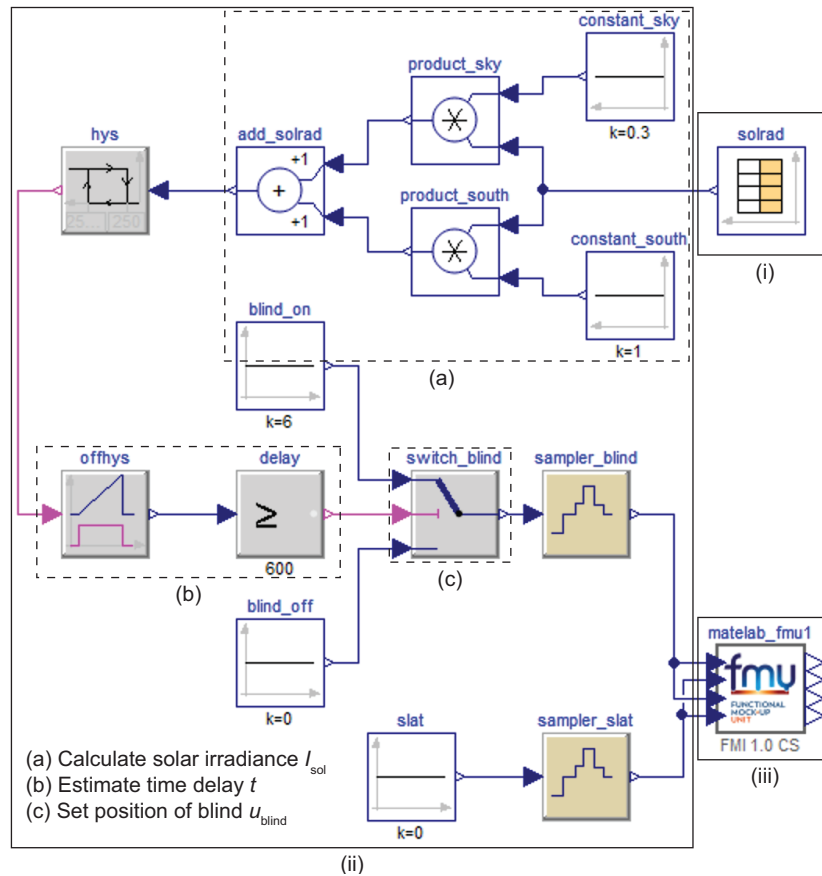


FIG. 7 Graphical representation of the control algorithm model for MATELab's blind automation system in Dymola.

3.10 ANALYSIS OF VALIDATION RESULTS

When analysing the validation results in the eighth step, there could be large discrepancies between measured and simulation-predicted data points. Another UA was therefore carried out to quantify how well the model of MATELab described the variability in the measured data, hence decreasing the model's uncertainty and increasing the level of confidence in it. The uncertainty indices used in this part of the study to evaluate the accuracy were the normalised mean bias error (NMBE) and the CV-RMSE (as in Step 6, see Section 3.6.2). The NMBE index gives the global difference between measured and simulated data points by normalising the average of the errors of a sample space and dividing it by the mean of the measured data points (\bar{m}).

$$\text{NMBE} = \frac{1}{\bar{m}} \times \frac{\sum_{i=1}^n (m_i - s_i)}{n - p} \times 100$$

Equation 2

where m_i is the measured data point for each model instance i , s_i is the simulated data point for each model instance i , and n is the number of measured data points. p is the number of adjustable data points, which is suggested to be zero for the validation.

Although the NMBE index is a good measure of model accuracy, its main problem is the cancellation error, where the sum of positive and negative values reduces the value of the NMBE index (Ruiz & Bandera, 2017). Consequently, using this index alone is not recommended, and the CV-RMSE index was used as a further measure of model accuracy.

As outlined in Figure 8, an iterative process was applied to reduce discrepancies between measured and predicted data points. The model's output variable of interest used to calculate the uncertainty indices was the indoor temperature, and the acceptable range of accuracy should be in accordance with ASHRAE Guideline 14-2014 (ASHRAE, 2014). According to the guideline, the hourly NMBE index is required to be less than 10.0%, and the hourly CV-RMSE index less than 30.0% to evaluate a model as validated.

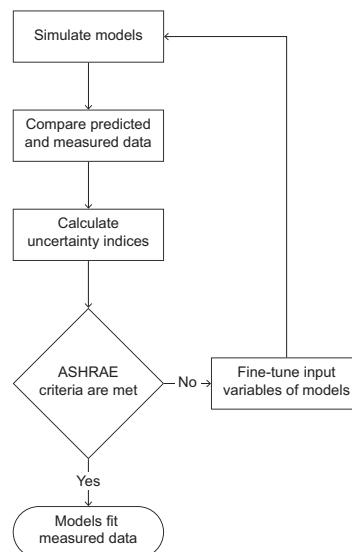


FIG. 8 Iterative process for the reduction of discrepancies between measured and predicted data.

4 RESULTS AND DISCUSSION

This section discusses the results that emerged from this study. It begins by presenting the results related to the in-situ measurements and the results of the MCSA. It then moves on to analyse the calibration of the reduced-complexity model of MATELab and the validation of the co-simulation model of MATELab.

4.1 IN-SITU MEASUREMENTS

Figure 9a shows the linear regression leading to the determination of the in-situ thermal transmittance for the measurement points A, B, C and D given in Figure 4, while Figure 9b shows the linear regression leading to the evaluation of the U-values at the edge of the glass, corresponding to the measurement points E, F and G in Figure 4. The resulting U-values are reported in Table 15 in Appendix F. The total U-value was then evaluated by calculating a weighted average of each zone corresponding to the areas of influence in Figure 4. The total U-value was assessed as 1.2 W/Km², which is higher than the U-value of 1.1 W/Km² originally obtained from the manufacturer's specifications. The total U-value was adjusted accordingly in the model of the construction elements of the thermal model.

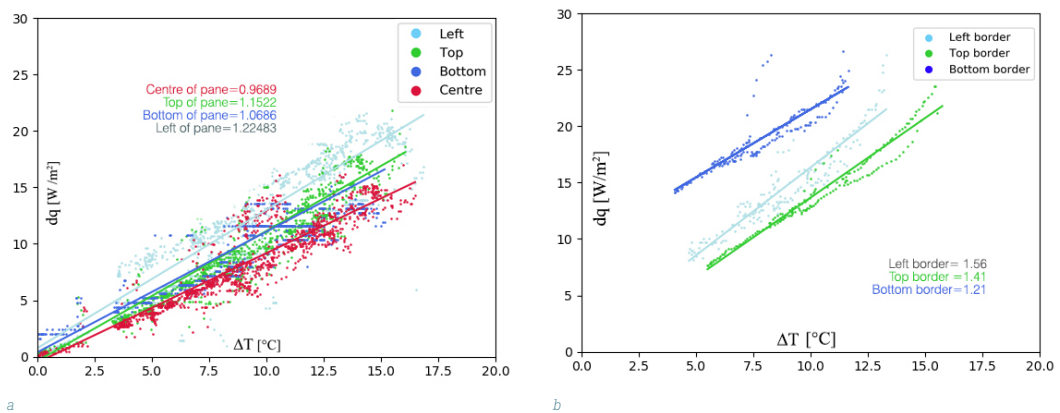


FIG. 9 Results from the U-value monitoring: a. Linear regressions leading to the computing of the U-values closer to the centre of the glass pane; b. U-values at the edge of the glass pane.

Figure 10 shows the results of the g-value monitoring and the corresponding linear regression for the empirical evaluation of the g-value. It can be seen that the g-value of 0.4 is higher than the originally assumed 0.3 in the first iteration of the model. This was adjusted accordingly in the second iteration.

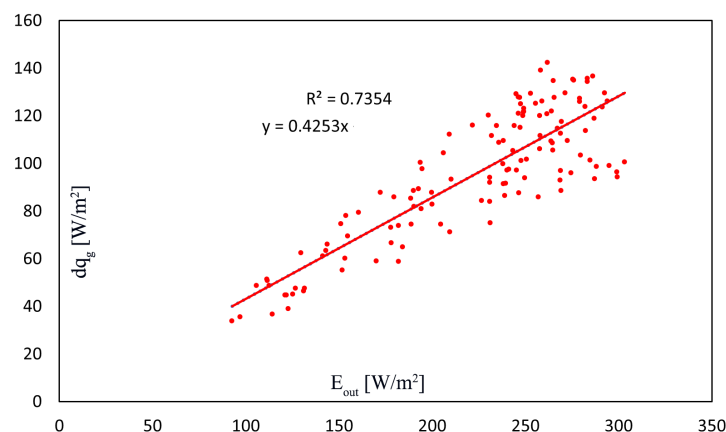


FIG. 10 Linear regression leading to the evaluation of the g-value.

The results of the BDT are shown in Figure 11, which plots the characteristic curve of the air infiltration in MATELab. The air permeability of the building envelope was found to be 2.3 air changes per hour at 50.0 Pa. This value is within the recommended maximum limit of the UK Part L regulation for fuel and power conservation (Office of the Deputy Prime Minister, 2006). The value of the flow coefficient C was determined to be 0.0084, which was then used as an input in the *ZoneInfiltration:FlowCoefficient* object in EnergyPlus. A schedule of 24/7 and a conventional pressure exponent of 0.7 were used. For the stack coefficient, the value recommended by ASHRAE Fundamentals for a one-storey building with a typical shelter for a rural house was used, corresponding to 0.000145 (ASHRAE, 2017).

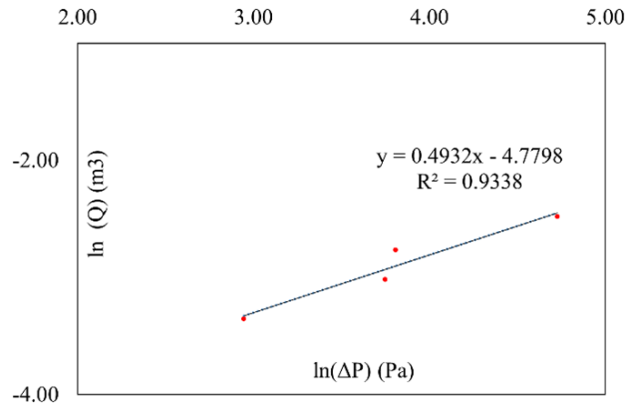


FIG. 11 Characteristic curve of the air infiltration of MATELab.

Finally, the thermal images in Figure 12 show the temperature distribution of the outdoor surface temperature of MATELab. The even colouring of the walls around the windows indicates a uniform installation of the thermal wall insulation. The temperature distribution also shows that there are no significant thermal bridges in the building envelope, except for the expected thermal bridges at the interface between two different materials (e.g. glass-frame) and at geometrical discontinuities.

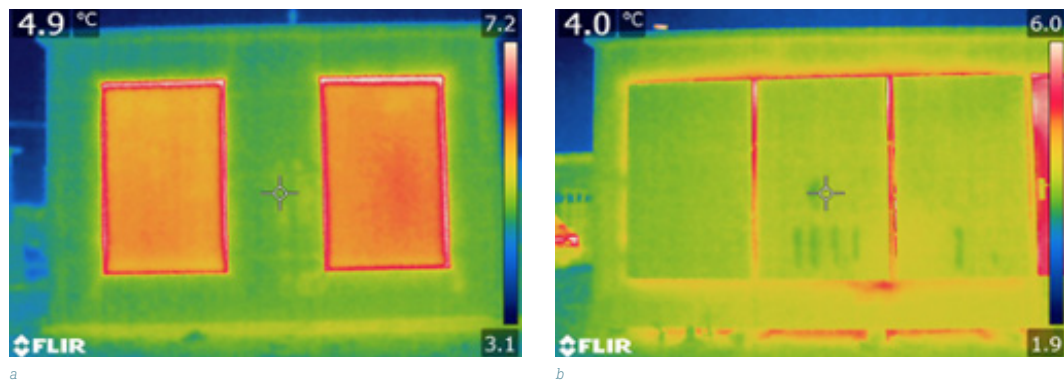


FIG. 12 Thermographic images of two different building envelopes of MATELab, taken from the outside: a. South-facing glass façade; b. East building envelope with opaque covers on glass.

4.2 MONTE CARLO SENSITIVITY ANALYSIS

The aim of the MCSA was to determine the most important input variables in the validation scenario by using the sensitivity indices S_{Pear} and S_{Spear} to evaluate the relationships between the input variables and the indoor air temperature T_{ai} .

As discussed above, this study adopted the bootstrap technique to achieve convergence. S_{Pear} and S_{Spear} were plotted against the gradually increasing number of iterations N , and convergence was assumed as soon as there was no significant variation for each sensitivity index. Figure 13 shows that the indices reveal a clear distinction between the two most important input variables – the internal heat gains Q_{int} and the infiltration flow rate Q_{inf} – and the other six variables after a few hundred iterations ($N = 750$). Internal heat gains describe the heat emitted within MATELab from internal sources, especially computer equipment, resulting in a temperature increase within the facility, and infiltration describes the unintended flow of outside air into MATELab, typically caused by cracks in the building envelope.

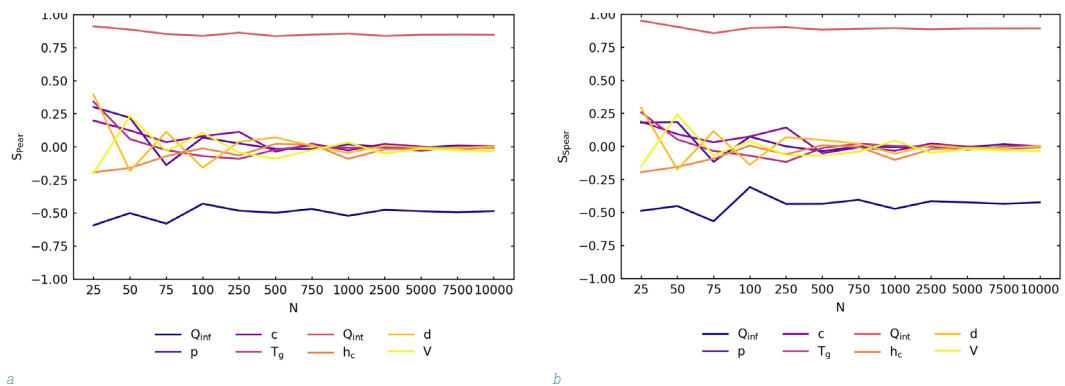


FIG. 13 Convergence of S_{Pear} and S_{Spear} for input variables and increasing base sample size expressed as number of iterations N .

While the indices started to converge at the base sample size of around 5000, only the two most important variables (Q_{int} and Q_{inf}) could be identified with certainty. The other six variables (p , c , T_g , h_c , d and V) had no noticeable effect on the model outcome compared to the internal heat gains and the infiltration flow rate. The data show that these six variables had a negligible correlation with S_{Pear} and S_{Spear} close to zero. This indicated that the relationship was random or non-existent. It would thus have been computationally ineffective to increase the number of iterations further. As a consequence, convergence was assumed.

This study applied two correlation-based methods to measure the strength of the input and output variables. From the data in Figure 14, it is apparent, however, that S_{Pear} and S_{Spear} were similar for each of the input variables, consequently leading to the same conclusions. The data also shows that the two most important input variables in relation to the indoor air temperature were the internal heat gains Q_{int} and the infiltration flow rate Q_{inf} . Therefore, variations in the indoor air temperature could largely be attributed to variations in the internal heat gains and the infiltration flow rate, and the internal heat gains and the infiltration flow rate were used to calibrate the model.

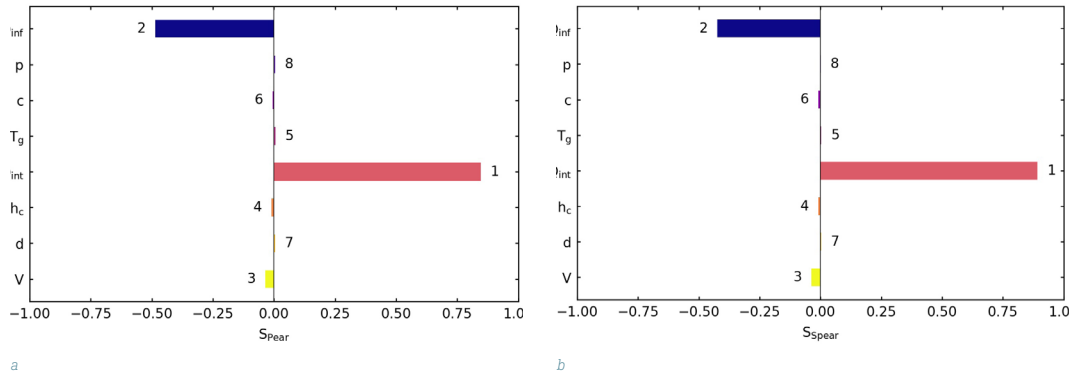


FIG. 14 Comparison of the relative importance of the input variables for $N = 10000$, with the rank of each input variable given next to the bar (1 is the highest rank).

4.3 CALIBRATION OF A REDUCED-COMPLEXITY THERMAL MODEL

The aim of calibrating the reduced-complexity model with the static building envelope was to minimise the error between the measured and predicted indoor air temperature T_{ai} . This was achieved by fitting the internal heat gains and the infiltration flow rate through the automated process described in Section 3.8. In this process, the model was calibrated by performing an automated parametric analysis and running 4,642 simulations varying the internal heat gains and the infiltration flow rate. The simulation scenario with the minimum CV-RMSE index was then selected, indicating a good model fit. Table 6 shows the CV-RMSE index and the correspondent internal heat gains and infiltration flow rate before calibration (predicted based on the construction documents and the results of the in-situ characterisation) and after calibration (predicted based on the results of the parametric analysis). Figure 15 compares the predicted indoor air temperature T_{ai} before and after calibration with the measured indoor air temperature. In addition, the following changes were made to the model:

- Since infiltration highly depends on outside wind conditions, measured wind data from MATELab's weather station were added to the weather file.
- Since MATELab's weather data were not measured at World Meteorological Organization standard conditions, the *Site:WeatherStation* object was added to EnergyPlus to specify the measurement conditions for the climatic data, such as the height above ground of the weather station.

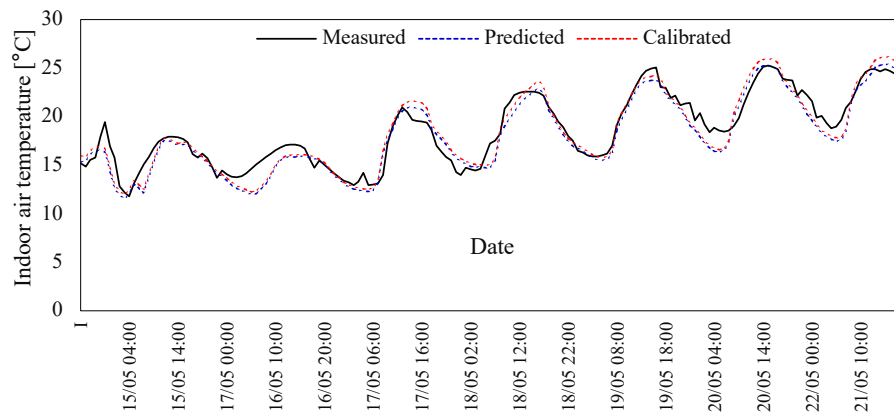


FIG. 15 Comparison of measured and predicted T_{ai} before and after calibration of the reduced-complexity model.

TABLE 6 Comparison of CV-RMSE index before and after calibration

Model	CV-RMSE (%)	Q_{int} (W/m ²)	Air infiltration
Before calibration	6.6	8.7	Q_{int} : 0.0008 m ³ /s m ²
After calibration	6.3	13.0	C: 0.0084

The results in this section indicate that the in-situ characterisation proved useful in improving the accuracy of the predicted data. This shows that including the non-calorimetric in-situ characterisation of the building envelope in the assessment framework may contribute to a more accurate prediction of the indoor air temperature. It should be noted that the original thermal model developed based on construction documents was already very accurate, with a CV-RMSE index of 6.6%, well below the ASHRAE requirement of 30.0%. The reason for this could be the authors' detailed knowledge of MATELab's construction details. The fact that the data collection was conducted shortly after the test facility was built may also have contributed to the accurate results, as the building components were largely unaffected by deterioration and maintenance factors. For example, the U-values were not significantly different from those published in the construction documents. Nevertheless, an in-situ characterisation is recommended in all cases because the performance of building components deteriorates over time. Therefore, it is important to measure their actual performance at the time of data collection. In addition, the use of non-stationary models to measure the actual performance of the building envelope may be considered.

4.4 VALIDATION OF A CO-SIMULATION MODEL OF MATELAB

The validation was undertaken to reduce the uncertainty of the model of MATELab created in a co-simulation setup. The control algorithm was modelled, in addition to Dymola, in the EMS scripting feature of EnergyPlus to identify and diagnose sources of error or inaccuracy in the co-simulation setup. Since the parameters of the thermal model and the weather file were identical for both models, the main difference between them was that the control algorithm was modelled in different tools. When comparing the predictions of the models of MATELab with the actual measured data, good agreement with the measured data was found. The data were analysed by descriptive statistics, and the summary statistics for the uncertainty indices NMBE and CV-RMSE are compared in Table 7. The data in the table shows that the NMBE minima (Dymola: -1.4%, EMS: -1.4%) and maxima (Dymola: 0.8%, EMS: 0.7%) were well below the ASHRAE requirement of 10.0% for hourly empirical data. With median values of -0.1% (Dymola) and -0.1% (EMS) for the NMBE indices, both Dymola and EMS models tended to slightly over-predict the measured data. However, NMBE indices close to zero indicate that there is only a small difference between the predicted and actual indoor air temperature and that the model has a sound goodness-of-fit. Similarly, the CV-RMSE minima (Dymola: 0.01%, EMS: 0.02%) and maxima (Dymola: 20.6%, EMS: 21.0%) were well below the AHREAE requirement of 30.0%, which was also suggestive of a good model fit.

TABLE 7 Summary statistics of uncertainty indices applied in validation

Type of error	Tool	Median	Standard deviation	Minimum	Maximum
NMBE (%)	Dymola	-0.1	0.5	-1.4	0.8
	EMS	-0.1	0.5	-1.4	0.7
CV-RMSE (%)	Dymola	6.3	4.0	0.01	20.6
	EMS	6.2	4.2	0.02	21.0

The results of the validation are also shown in Figure 16. When comparing the measured and predicted indoor air temperature data, the discrepancies between measured and predicted data become apparent, especially in the last three days when the weather quickly changed from sunny to cloudy. A possible explanation for this could be inaccuracies in the thermal mass (e.g. due to computer equipment inside MATELab). If the real test facility was lighter than the model, it gave back more thermal energy and cooled down faster when the environmental temperatures were cooler than the thermal mass.

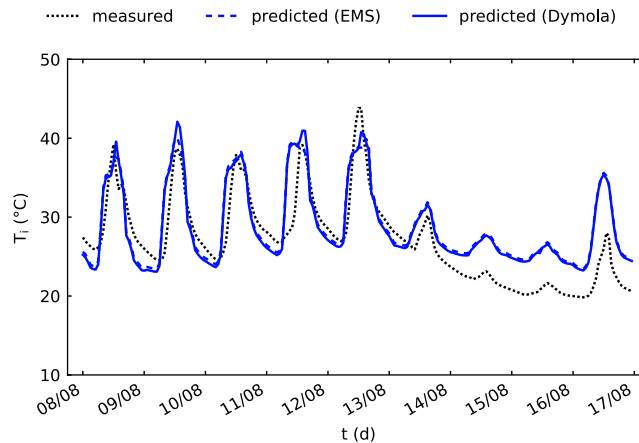


FIG. 16 Comparison of measured and predicted T_{ai} in the validation of the co-simulation model.

Interestingly, Dymola and the EMS feature predicted slightly different outcomes. Since the weather file and the parameters of the thermal model were identical, it can be assumed that the differences were due to the different models and solution techniques supported by each of the tools used to represent the control algorithm. For example, the EMS feature used the Erl programming language commands, such as IF-ELSEIF-ELSE-ENDIF statements and trend variables, and Dymola used the Modelica Standard Library (Modelica Association, 2016) model components, such as *Modelica.Blocks.Logical.Hysteresis* and *Modelica.Blocks.Logical.Switch*. But such small discrepancies were expected and are in line with earlier observations, e.g. by Trcka, Wetter, and Hensen (2009).

These different approaches to representing the control algorithm in the respective tools may have resulted in differences in how the output of the control algorithm was computed. A differently computed control algorithm could then have led not only to discrepancies in the predictions of the blind movements but also to discrepancies in the predictions of the indoor temperatures. Figure 17 compares the measured and predicted blind positions for two representative days. On 11 August (Figure 17a), the blinds closed at 13:10 (measured), while in Dymola they moved at 13:15 and in the EMS feature at 13:05. This error could be linked to data averaging during the analysis according to the 5-minute timestep of the simulation, but also to an inaccurate implementation of the time delay in either the real test facility or in the models. Furthermore, the EMS feature predicted to open the blinds at 16:15 (measured: 15:55, Dymola: 16:00). This inaccuracy could be due to the input data of the monitored solar irradiance for the control algorithm, which contained 15-minute interval data and was provided to EnergyPlus using values from an external CSV file as a schedule. The input data in Dymola were the same as in EnergyPlus. But whereas Dymola was able to interpolate the data so that they matched the measured data, EnergyPlus did not interpolate them but adopted the same value for 15 minutes. After 15 minutes, EnergyPlus moved on to the next value in the input file and adopted this value again for a period of 15 minutes.

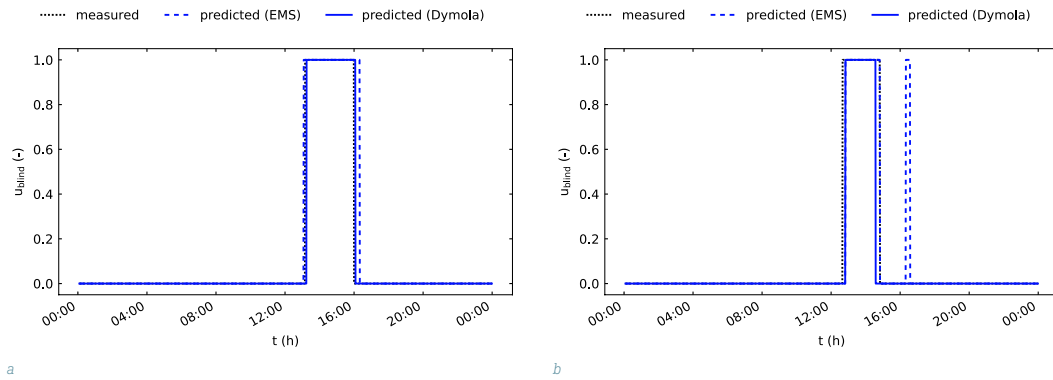


FIG. 17 Comparison of measured and predicted blind positions (0: blinds open, 1: blinds closed) for two representative days.

The blind behaviour discussed above also appeared on 12 August (Figure 17b). The EMS feature predicted a spike in the movement of the blinds for 15 minutes between 16:20 and 16:35. The reason for this was again the interpolation of the solar irradiance data. While there was one occurrence where the solar irradiance was greater than the control threshold of 250 W/m^2 , the blinds should not have moved, given the 15-minute time delay. Because of the interpolation error described above, the control algorithm in the EMS feature assumed that the solar irradiance was above the threshold for more than 15 minutes, resulting in the blinds being incorrectly closed.

These results indicate that both Dymola and the EMS feature of EnergyPlus were able to represent the control algorithm for MATELab's blind automation system. But it remains unclear whether or not the differences between the predicted and measured blind behaviours were due to an inaccurate implementation of the time delay in the real test facility. Although such imperfect knowledge of the experimental objects being simulated is common (Judkoff and Neymark, 2006), it is recommended to fully understand the implementation of a control algorithm in the real test facility to be able to model it correctly. Also, the results may provide some advice to other modellers on how to adapt the setup of similar models:

- Even though EnergyPlus was set to interpolate the values from the 15-minute interval input data to the 5-minute simulation timestep, this study found that EnergyPlus did not correctly interpolate the input data, resulting in inaccurate predictions. Future work should take this error into account and debug the EnergyPlus model to thoroughly determine its cause(s).
- A potential solution to resolve this error could be to provide solar irradiation data at 5-minute intervals to EnergyPlus. In this case, EnergyPlus would not need to interpolate the input data so that it could correctly (i) calculate the time delay and (ii) predict the positions of the blinds.

5 CONCLUSION

This research was undertaken to provide new evidence on how to validate co-simulation setups for adaptive building envelopes using a full-scale non-controlled and non-calorimetric test facility. The adaptive component of the building envelope in the case of the present study was MATELab's blind automation system. The results show that the validated model of MATELab accurately captured the building envelope controls and properties with median CV-RMSE indices of 5.9% for Dymola in the co-simulation setup and 6.1% for the EMS feature. This underlines the capability of the proposed assessment framework to validate both models to accurately reflect the variability in the measured data. Furthermore, the result suggests that the co-simulation setup can generally be used to validate

the behaviour of adaptive building envelopes, confirming the findings of Taveres-Cachat et al. (2021), who found that their co-simulation setup with Grasshopper had a CV-RMSE index of 2.0%, also well within the acceptable range of accuracy.

Nevertheless, it may be difficult to generalise these results because, on the one hand, empirical validation only tests 'whether the simulation model's output behaviour has the accuracy required for the model's intended purpose over the domain of the model's intended applicability' (Sargent, 2013, p. 18). The co-simulation setup consequently validated the behaviour of MATELab only for its intended application (i.e. rule-based control algorithm). Further testing is hence required to create a truth standard for other control algorithms and to validate the co-simulation setup over the complete domain of its intended applicability. On the other hand, empirical validation should never be used as the only validation method due to measurement uncertainty and experimental complexity (Cattarin et al. 2018). Consequently, there is abundant room for further progress in fully determining the accuracy of the co-simulation setup, e.g. by undertaking inter-model comparisons.

Despite its lack of generalisation, the assessment framework can be used by modellers from the façade design and engineering community to determine the accuracy of their own co-simulation setups. To enable them to use the framework, it is important to provide the key lessons learned:

- During the first set of measurements, the HVAC system of MATELab was turned on. Very soon, it became clear that the data were too complicated and hindered the understanding of the effects of, for example, the building envelope, the heat gains and the climate conditions on the building dynamics. Therefore, it was decided to perform the validation with data from the free-running MATELab to determine the cause of certain deviations in the data.
- The initial simulation results, which considered the manufacturers' specifications for the building components, differed from the measurements. To ensure that key input values, such as the infiltration rate, were entered correctly, it was decided to perform an in-situ characterisation.
- It sometimes proved difficult to compare predicted with measured data and especially to find output variables in the thermal EnergyPlus model suitable for comparison with the measured sensor variables. While the authors of this study were fortunate to have full access to the sensor variables in MATELab, this could complicate the validation of adaptive building envelopes in other studies. It is therefore recommended to ensure that appropriate empirical data are available for validation.
- Despite the high number of input variables, the MCSA accelerated the investigation of the effects of the input variables on the outcome of the MATELab model. Therefore, the MCSA was particularly useful in reducing the number of parameters to be adjusted during the calibration process. However, since a high number of simulations was necessary to achieve convergence, the use of the reduced-complexity model appeared to be critical to potentially reduce the time needed to run the MCSA.

By ensuring that the predictions of the co-simulation setups of modellers from the façade community are accurate, the assessment framework has the potential to lead to broader use of co-simulation in the industry. Co-simulation is a valuable approach to overcoming the limitations in accurately predicting the performance of adaptive building envelopes in BPS tools. This, in turn, can help façade designers and engineers to reliably evaluate the performance of adaptive building envelopes and integrate them more easily into building projects. In turn, more adaptive building envelopes may lead to more energy-efficient buildings, which may help achieve global climate change goals.

CRediT author statement

Esther Borkowski: Conceptualization, Methodology, Software, Validation, Formal Analysis, Investigation, Resources, Data curation, Writing – Original Draft, Writing – Review & Editing, Visualization, Project administration

Alessandra Luna-Navarro: Conceptualization, Methodology, Software, Validation, Formal Analysis, Investigation, Resources, Data Curation, Writing – Original Draft, Writing – Review & Editing, Visualization, Project administration

Michalis Michael: Methodology, Formal Analysis, Investigation, Data Curation, Writing – Original Draft, Visualization

Mauro Overend: Writing – Review & Editing, Supervision

Dimitrios Rovas: Writing – Review & Editing, Supervision

Rokia Raslan: Writing – Review & Editing, Supervision

Acknowledgements

The authors acknowledge the use of the UCL Myriad High Throughput Computing Facility (Myriad@UCL), and associated support services, in the completion of this work.

References

- American Society of Heating, Refrigerating and Air-Conditioning Engineers. (2014). *ASHRAE Guideline 14-2014: Measurement of Energy and Demand Savings*. Atlanta, GA, USA: ASHRAE.
- American Society of Heating, Refrigerating and Air-Conditioning Engineers. (2017). *2017 ASHRAE Handbook—Fundamentals (SI Edition)*. ASHRAE.
- Asdrubali, F., Baldinelli, G., & Bianchi, F. (2012). A quantitative methodology to evaluate thermal bridges in buildings. *Applied Energy*, 97, 365–373. <https://doi.org/10.1016/j.apenergy.2011.12.054>
- Attia, S., Bilir, S., Safy, T., Struck, C., Loonen, R., & Goia, F. (2018). Current trends and future challenges in the performance assessment of adaptive façade systems. *Energy and Buildings*, 179, 165–182. <https://doi.org/10.1016/j.enbuild.2018.09.017>
- Attia, S., Hensen, J., Beltrán, L., & De Herde, A. (2012). Selection criteria for building performance simulation tools: Contrasting architects' and engineers' needs. *Journal of Building Performance Simulation*, 5(3), 155–169. <https://doi.org/10.1080/19401493.2010.549573>
- Big Ladder Software & Rocky Mountain Institute. (2016). *Elements*. Retrieved from <https://bigladdersoftware.com/projects/elements/>
- Borkowski, E., Donato, M., Zemella, G., Rovas, D., & Raslan, R. (2019). Optimisation Of Controller Parameters For Adaptive Building Envelopes Through A Co-Simulation Interface: A Case Study. *Proceedings of Building Simulation 2019: 16th Conference of IBPSA*. Rome, Italy.
- British Standards Institution. (1999). *BS EN 13187:1999: Thermal performance of buildings. Qualitative detection of thermal irregularities in building envelopes. Infrared method*. British Standards Institution. Retrieved from <https://bsol.bsigroup.com/en/Bsol-Item-Detail-Page/?pid=000000000001569434>
- British Standards Institution. (2001). *BS EN 13829:2001: Thermal performance of buildings. Determination of air permeability of buildings. Fan pressurization method*. British Standards Institution. Retrieved from <https://bsol.bsigroup.com/en/Bsol-Item-Detail-Page/?pid=000000000019983036>
- British Standards Institution. (2015). *BS EN ISO 6781-3:2015: Performance of buildings. Detection of heat, air and moisture irregularities in buildings by infrared methods. Qualifications of equipment operators, data analysts and report writers*. British Standards Institution. Retrieved from <https://bsol.bsigroup.com/en/Bsol-Item-Detail-Page/?pid=000000000030259341>
- British Standards Institution. (2017a). *BS EN 15232-1:2017: Energy Performance of Buildings. Impact of Building Automation, Controls and Building Management. Modules M10-4,5,6,7,8,9,10*. British Standards Institution.
- British Standards Institution. (2017b). *BS ISO 19467: 2017: Thermal performance of windows and doors. Determination of solar heat gain coefficient using solar simulator*. British Standards Institution. Retrieved from <https://bsol.bsigroup.com/en/Bsol-Item-Detail-Page/?pid=000000000030294394>
- Broman, D., Brooks, C., Greenberg, L., Lee, E., Masin, M., Tripakis, S., & Wetter, M. (2013). Determinate composition of FMUs for co-simulation. *Proceedings of the International Conference on Embedded Software (EMSOFT)*, 1–12. Montréal, Canada: IEEE Press.
- Cattarin, G., Causone, F., Kindinis, A., & Pagliano, L. (2016). Outdoor test cells for building envelope experimental characterisation – A literature review. *Renewable & Sustainable Energy Reviews*, 54, 606–625. <https://doi.org/10.1016/j.rser.2015.10.012>

- Chartered Institution of Building Services Engineers. (2000). *Testing Buildings for Air Leakage - CIBSE Technical Memoranda TM23: 2000*. Chartered Institution of Building Services Engineers.
- Chartered Institution of Building Services Engineers. (2015). *CIBSE Guide A: Environmental design*. London, UK: Chartered Institution of Building Services Engineers.
- Coakley, D., Raftery, P., & Keane, M. (2014). A review of methods to match building energy simulation models to measured data. *Renewable and Sustainable Energy Reviews*, 37, 123–141. <https://doi.org/10.1016/j.rser.2014.05.007>
- Dassault Systèmes. (2018). *Dymola*. Lund, Sweden. Retrieved from <https://www.3ds.com/products-services/catia/products/dymola>
- de Wit, S., & Augenbroe, G. (2002). Analysis of uncertainty in building design evaluations and its implications. *Energy and Buildings*, 34(9), 951–958. [https://doi.org/10.1016/S0378-7788\(02\)00070-1](https://doi.org/10.1016/S0378-7788(02)00070-1)
- Department of Energy. (2018). *EnergyPlus v9.0.1 Documentation—Application Guide for EMS*. Department of Energy.
- Dervishi, S., & Mahdavi, A. (2012). Computing diffuse fraction of global horizontal solar radiation: A model comparison. *Solar Energy*, 86(6), 1796–1802. <https://doi.org/10.1016/j.solener.2012.03.008>
- Digital Technology Group. (n.d.). *DTG weather station*.
- Duffie, J. A. (2013). *Solar Engineering of Thermal Processes* (4th ed.). Somerset: John Wiley & Sons, Incorporated.
- Erbs, D. G., Klein, S. A., & Duffie, J. A. (1982). Estimation of the diffuse radiation fraction for hourly, daily and monthly-average global radiation. *Solar Energy*, 28(4), 293–302. [https://doi.org/10.1016/0038-092X\(82\)90302-4](https://doi.org/10.1016/0038-092X(82)90302-4)
- Favoino, F., Fiorito, F., Cannavale, A., Ranzì, G., & Overend, M. (2016). Optimal control and performance of photovoltaic switchable glazing for building integration in temperate climates. *Applied Energy*, 178, 943–961. <https://doi.org/10.1016/j.apenergy.2016.06.107>
- Federal Energy Management Program. (2008). *M&V Guidelines: Measurement and Verification for Federal Energy Projects (Version 3.0)*. Retrieved from https://www.hud.gov/sites/documents/DOC_10604.PDF
- Goia, F., & Serra, V. (2018). Analysis of a non-calorimetric method for assessment of in-situ thermal transmittance and solar factor of glazed systems. *Solar Energy*, 166, 458–471. <https://doi.org/10.1016/j.solener.2018.03.058>
- Hafner, I., Rössler, M., Heinzl, B., Körner, A., Breitenecker, F., Landsiedl, M., & Kastner, W. (2012). Using BCVTB for Co-Simulation between Dymola and MATLAB for Multi-Domain Investigations of Production Plants. *Proceedings of the 9th International Modelica Conference*. Munich, Germany. <https://doi.org/10.3384/ecp12076557>
- Hensen, J., Loonen, R., Archontiki, M., & Kanellis, M. (2015). Using building simulation for moving innovations across the 'valley of death'. *REHVA Journal*, 52(3), 58–62.
- Hunter, J. D. (2007). Matplotlib: A 2D Graphics Environment. *Computing in Science & Engineering*, 9(3), 90–95. <https://doi.org/10.1109/MCSE.2007.55>
- International Organization for Standardization Technical Committee 163/SC 2, C. methods. (2008). *Energy performance of buildings—Calculation of energy use for space heating and cooling* (2nd ed.: 2008-03-01). Geneva: ISO.
- Jensen, S. Ø. (1995). Validation of building energy simulation programs: A methodology. *Energy and Buildings*. [https://doi.org/10.1016/0378-7788\(94\)00910-C](https://doi.org/10.1016/0378-7788(94)00910-C)
- Judkoff, R., & Neymark, J. (2006). Model validation and testing: The methodological foundation of ASHRAE Standard 140. *ASHRAE Transactions*.
- Lawrence Berkeley National Laboratory. (2019). *BuildingsPy*. Retrieved from <http://simulationresearch.lbl.gov/modelica/buildingspy/>
- Lomas, K. J., Eppel, H., Martin, C. J., & Bloomfield, D. P. (1997). Empirical validation of building energy simulation programs. *Energy and Buildings*, 26(3), 253–275. [https://doi.org/10.1016/S0378-7788\(97\)00007-8](https://doi.org/10.1016/S0378-7788(97)00007-8)
- Loonen, R., Favoino, F., Hensen, J., & Overend, M. (2017). Review of current status, requirements and opportunities for building performance simulation of adaptive facades. *Journal of Building Performance Simulation*, 10(2), 205–223. <https://doi.org/10.1080/19401493.2016.1152303>
- Loonen, R., Trčka, M., Cóstola, D., & Hensen, J. (2013). Climate adaptive building shells: State-of-the-art and future challenges. *Renewable and Sustainable Energy Reviews*, 25, 483–493. <https://doi.org/10.1016/j.rser.2013.04.016>
- Loutzenhiser, P. G., Maxwell, G. M., & Manz, H. (2007). An empirical validation of the daylighting algorithms and associated interactions in building energy simulation programs using various shading devices and windows. *Energy*. <https://doi.org/10.1016/j.energy.2007.02.005>
- Luna-Navarro, A., Gaetani, I., Anselmo, F., Law, A., & Overend, M. (2021). The influence of occupant behaviour on the energy performance of single office space with adaptive facades: Simulation versus measured data. *Proceedings of Building Simulation Conference 2021*. Ghent, Belgium.
- Luna-Navarro, A., & Overend, M. (2021). Design and validation of MATELab: A novel full-scale test room for investigating occupant perception to and interaction with façade technologies. *Building and Environment*, 203, 108092. <https://doi.org/10.1016/j.buildenv.2021.108092>
- Madsen, H., Bacher, P., Bauwens, G., Deconinck, A.-H., Reynders, G., Roels, S., ... Lethé, G. (2016). *IEA EBC Annex 58, Report of Subtask 3, part 2: Thermal performance characterisation using time series data – statistical guidelines*. Leuven, Belgium: KU Leuven. Retrieved from https://www.iea-ebc.org/Data/publications/EBC_Annex_58_Final_Report_ST3b.pdf
- Martinez, S., Erkoreka, A., Eguia, P., Granada, E., & Febrero, L. (2019). Energy characterization of a PASLINK test cell with a gravel covered roof using a novel methodology: Sensitivity analysis and Bayesian calibration. *Journal of Building Engineering*, 22, 1–11. <https://doi.org/10.1016/j.jobe.2018.11.010>
- Modelica Association. (2017). *Modelica*. Linköping, Sweden. Retrieved from <https://www.modelica.org>
- MODELISAR. (2014). *FMI Standard for co-simulation*. Retrieved from <https://fmi-standard.org>
- Moinard, S., & Guyon, G. (1999). *IEA Task 22: Empirical validation of EDF ETNA and GENEC test-cell models*.
- National Renewable Energy Laboratory. (2018). *EnergyPlus*. Golden, CO, USA: DOE. Retrieved from <https://github.com/NREL/EnergyPlus>

- Neymark, J., Judkoff, R., Knabe, G., Le, H.-T., Dürig, M., Glass, A., & Zweifel, G. (2002). Applying the building energy simulation test (BESTEST) diagnostic method to verification of space conditioning equipment models used in whole-building energy simulation programs. *Energy and Buildings*, 34(9), 917–931. [https://doi.org/10.1016/S0378-7788\(02\)00072-5](https://doi.org/10.1016/S0378-7788(02)00072-5)
- Nouidui, T., Lorenzetti, D. M., & Wetter, M. (2020). *EnergyPlusToFMU*. Berkeley, CA, USA: LBNL. Retrieved from <http://simulationresearch.lbl.gov/fmu/EnergyPlus/export/index.html>
- Office of the Deputy Prime Minister. (2006). *Conservation of fuel and power: Approved Document L*.
- Python Software Foundation. (2020). *Python*. Wilmington, NC, USA. Retrieved from <https://www.python.org/>
- Roels, S. (2012). Annex 58—Reliable Building Energy Performance Characterisation Based on Full Scale Dynamic Measurements. *The International Energy Agency*.
- Ruiz, G. R., & Bandera, C. F. (2017). Validation of Calibrated Energy Models: Common Errors. *Energies*, 10(1587), 1–19. <https://doi.org/10.3390/en10101587>
- Saelens, D., & Reynders, G. (2016). *Report of Subtask 4b: Towards a characterisation of buildings based on in situ testing and smart meter readings and potential for applications in smart grids*.
- Sargent, R. G. (2013). Verification and validation of simulation models. *Journal of Simulation*, 7(1), 12–24. <https://doi.org/10.1057/jos.2012.20>
- Tabadkani, A., Tsangrassoulis, A., Roetzel, A., & Li, H. X. (2020). Innovative control approaches to assess energy implications of adaptive facades based on simulation using EnergyPlus. *Solar Energy*, 206, 256–268. <https://doi.org/10.1016/j.solener.2020.05.087>
- Taveres-Cachat, E., Favoino, F., Loonen, R., & Goia, F. (2021). Ten questions concerning co-simulation for performance prediction of advanced building envelopes. *Building and Environment*, 191, 107570-. <https://doi.org/10.1016/j.buildenv.2020.107570>
- Taveres-Cachat, E., & Goia, F. (2020). Co-simulation and validation of the performance of a highly flexible parametric model of an external shading system. *Building and Environment*, 182, 107111-. <https://doi.org/10.1016/j.buildenv.2020.107111>
- Tian, W. (2013). A review of sensitivity analysis methods in building energy analysis. *Renewable & Sustainable Energy Reviews*, 20, 411–419. <https://doi.org/10.1016/j.rser.2012.12.014>
- Trčka, M., Wetter, M., & Hensen, J. (2009). *An implementation of co-simulation for performance prediction of innovative integrated HVAC systems in buildings*. 724–731. Glasgow, Scotland: Lawrence Berkeley National Laboratory.
- Yang, J. (2011). Convergence and uncertainty analyses in Monte-Carlo based sensitivity analysis. *Environmental Modelling & Software*, 26(4), 444–457. <https://doi.org/10.1016/j.envsoft.2010.10.007>
- Zhang, Y. (2012). *Use jEPlus as an efficient building design optimisation tool*. Presented at the CIBSE ASHRAE Technical Symposium, London, UK. Retrieved from <http://www.jeplus.org/wiki/lib/exe/fetch.php?media=docs:072v1.pdf>

APPENDIX A BUILDING ENVELOPE CHARACTERISTICS

The test facility has internal dimensions of 5.0 m x 6.0 m x 2.5 m and is fully exposed to the outside. The required ventilation is provided by an UFAD system through a plenum below the finished floor level, and the exhaust air is extracted through the ceiling plenum. The construction and characteristics of the opaque building envelopes are shown in Table 8, and the characteristics of the transparent envelope are listed in Table 9. The internal walls are white and have a surface absorptance of approximately 0.3 and a surface emissivity of approximately 0.9.

TABLE 8 Characteristics of opaque building envelopes of MATELab

Component Total U-value	Layers	Thickness (m)	Density (kg/m ³)	Specific heat (J/kg*K)
Roof 0.10 W/Km ²	Steel sheet	0.002	8050	500
	Rock wool panel	0.30	22.0	1030
	Air layer	0.15	1.25	1000
	Steel PIR sandwich panel	0.040	37.0	1400
Floor 0.15 W/Km ²	Wood floor	0.030	350	2300
	Cavity	0.10	1.25	1000
	Wood panel	0.030	350	2300
	Steel	0.002	8050	500
	Cavity	0.15	1.25	1000
	Steel PIR sandwich panel	0.15	37.0	1400
External wall 0.175 W/Km ²	Wood panel	0.024	350	2300
	Air layer	0.020	1.25	1000
	Steel sheet	0.002	8050	500
	Steel PIR sandwich panel	0.10	37.0	1400
Internal wall 0.50 W/Km ²	Plasterboard	0.0125	600	1090
	Rock wool	0.050	22.0	1030
	Plaster board	0.0125	600	1090
Glass building envelope external panel	Steel PIR sandwich panel	0.15	37.0	1400
Glass building envelope internal panel	Wood	0.050	350	2300

TABLE 9 Characteristics of the transparent building envelopes of MATELab

Component	Characteristics	Value
Glass building envelope	U-value	1.10 W/Km ²
	Solar heat gain coefficient	0.31
	Visible transmittance	0.50
	Solar transmittance	0.27
Internal blind	Slat width	0.035 m
	Slat separation	0.030 m
	Solar reflectance	0.65

APPENDIX B IN-SITU CHARACTERISATION OF BUILDING ENVELOPE

The in-situ characterisation included the evaluation of the most important thermal properties of the building envelope. This appendix contains detailed information on the in-situ characterisation of (i) the thermal transmittance and the solar factor of the glass façade, (ii) the air leakage flow coefficient and (iii) the thermal bridges.

B.1 THERMAL TRANSMITTANCE AND SOLAR FACTOR OF GLASS FAÇADE

To formulate the thermal performance of the building envelope as a linear and stationary steady-state thermal model, the measured data were sub-sampled by averaging it over a sufficiently long period of time. In addition, the recommendation of Madsen et al. (2016) was followed, which indicates that measurements should be averaged over periods equal to the length of the sampling time. If the test facility has a low thermal mass, a low-frequency time (equal to or less than 6 hours) is suggested. Further details of the experimental setup of the in-situ characterisation are listed in Table 10.

TABLE 10 Measured environmental parameters with details of sensing devices and frequency of monitoring for the in-situ characterisation

Parameter	Location	Sensor	Frequency
Heat flux	Inner building envelope surface	Hukseflux Heat flux meter	1 min
Global Solar Irradiance	Inner and outer building envelope surface	Hukseflux Pyranometer	1 min
Air temperature	Outer and inner building envelope surface	Pt100 Lastem	1 min

Following Goia & Serra (2018), the U-value U was obtained by linear regression using the ordinary least squares method and calculated as:

$$U = \left[\sum_i^n (\Delta T \times dq_i) \right] \left[\sum_i^n (\Delta T_i^2) \right]^{-1}$$

Equation 3

$$\Delta T = [T_{\text{out}} - T_{\text{in}}]$$

Equation 4

where ΔT is the temperature difference between the outdoor environment T_{out} and the indoor environment T_{in} measured in the proximity of the building envelope. dq_i is the heat flux measured at the glass façade at each timestep i until the final timestep n . These measurements were taken at night to minimise the effect of solar radiation on the long-wave heat transfer.

The g-value g was calculated as:

$$g = \left[\sum_i^n (E_{\text{out},i} \times dq_{g,i}) \right] \left[\sum_i^n (E_{\text{out},i}^2) \right]^{-1}$$

Equation 5

$$dq_g = [E_{\text{in}} + dq_E]$$

Equation 6

$$dq_E = [dq - dq_{DT}]$$

Equation 7

$$dq_{\Delta T} = U \times \Delta T$$

Equation 8

where $E_{\text{out},i}$ is the solar radiation incident on the glass façade at each timestep and $dq_{g,i}$ is the solar energy transmitted through the glass, taking into account both the transmitted solar energy E_{in} and the energy transmitted by the glass due to the absorbed incident solar energy dq_E . To calculate dq_E , the heat transferred due to the difference in temperature between indoor and outdoor $dq_{\Delta T}$ must be subtracted from the total heat flow of the glass dq , which can be measured with a heat flux meter. dq can be calculated taking into account U and ΔT according to Equations 3 and 4.

B.2 AIR LEAKAGE FLOW COEFFICIENT

After performing the BDT, the data were processed according to CIBSE TM23 (CIBSE, 2000) to determine the air leakage flow coefficient C . The data obtained during the test included a series of flow rate values Q for pressure differences ΔP between indoors and outdoors:

$$Q = C(\Delta P)^n$$

Equation 9

where n is a coefficient that depends on the facility characteristics and can be determined from the experimental data. Transforming the above equation with natural logarithms, the following air leakage characteristic curve is obtained:

$$\ln(Q) = \ln(C) + n \times \ln(\Delta P)$$

Equation 9

The equation is obtained by linearising the data using natural logarithms and linear regression. The results must then be corrected to account for differences between actual test conditions and those of instrument calibration (CIBSE, 2000).

B.3 THERMAL BRIDGES

To quantify the effect of thermal bridges, the method proposed by Asdrubali et al. (2012) was used. This method is based on the evaluation of the incidence factor of the thermal bridges I_{tb} , which is defined as:

$$I_{tb} = \frac{U_{1D}(I_{tb} + I_{1D}) + \psi}{U_{1D}(I_{tb} + I_{1D})}$$

Equation 9

$$U_{corrected} = I_{tb} U_{1D}(I_{tb} + I_{1D})$$

Equation 9

where U_{1D} is the thermal transmittance without the thermal bridge, ψ is the linear thermal transmittance of the thermal bridge, l_{1D} is the length of the side of the wall perpendicular to the thermal bridge and unaffected by it, and l_{tb} is the length of the wall affected by the thermal bridge. The incidence factor of the thermal bridges, considering steady-state conditions and a constant convective coefficient, represents the ratio between the measured thermal loss, including the effect of the thermal bridge and the thermal loss of the same area of the wall without considering the effect of the thermal bridges. Therefore, the new corrected U-value $U_{corrected}$ is defined as shown in Equation 12.

The thermal images were taken for each of the locations indicated in Table 11. The images were taken at a distance of 30.0 cm from the thermal bridge to minimise possible errors due to an incorrect selection of the emissivity of the infrared camera. A FLIR T650 infrared camera was used for this assessment.

TABLE 11 Location of the thermal bridges assessed

Reference	Location
A	Bottom corners between south and east opaque walls and floor
B	Top corners between south and east opaque walls roof
C	Top corners between north and west opaque walls roof
D	Bottom corners between north and west opaque walls and floor
E	Junction between north and east, north and west walls
F	Junction between walls and floor
G	Junction between walls and ceiling
H	Junction between south and west, south and east walls

APPENDIX C DESCRIPTION OF MEASUREMENT CAMPAIGN

Due to ongoing research work, MATELab was only available for a limited period of time for data collection, and data were gathered between 14-21 May 2020 and 8-16 August 2020. During these periods, the parameters listed in the remainder of this appendix were collected: (i) outdoor environmental parameters, (ii) indoor environmental parameters and (iii) parameters related to the control algorithm.

C.1 OUTDOOR ENVIRONMENTAL PARAMETERS

The available weather station on MATELab's roof at the time of the experiment collected data on the dry bulb air temperature and the global solar irradiance. To evaluate the diffuse and direct components of the measured solar irradiance, a simplified approach was followed. The diffuse solar irradiance was approximated by the correlation model by Erbs, Klein, & Duffie (1982), whose accuracy was confirmed by Dervishi & Mahdavi (2012). This model calculates the ratio of the diffuse to the global solar irradiance as a function of the clearness index k_T . The average clearness index value for London, UK, in May and August was used (Duffie, 2013). Therefore, the diffuse component $I_{\text{sol,dif}}$ was evaluated as:

$$I_{\text{sol,dif}} = \left(0.9511 - 0.1604 k_T + 4.388 k_T^2 - 16.638 k_T^3 + 12.336 k_T^4 \right) \times I_{\text{sol,sky}}$$

Equation 13

where $I_{\text{sol,sky}}$ is the global horizontal solar irradiance. The direct solar irradiance was then derived from the difference between the global and the diffuse solar irradiance.

When values were missing in the weather data set, the data had to be interpolated. To verify the accuracy of the measured data, dry bulb air temperature data were compared with data from a nearby weather station located on the roof of the Cambridge Computer Laboratory by the Digital Technology Group (DTG, n.d.). Nonetheless, a larger weather dataset would have been preferable to accurately determine the local boundary conditions. Ideally, direct and diffuse solar irradiance data at the weather station level should also have been measured since the control algorithm relied on the solar irradiance data and, therefore, even short-term inaccuracies could lead to incorrect or time-shifted control actions.

These data were then supplemented with humidity and wind data from an existing weather file for Cambridge created with Meteonorm v6.0 (Meteotest 2007).

C.2 INDOOR ENVIRONMENTAL PARAMETERS

Additional monitoring stations were also available to measure the indoor environmental quality at several different locations in MATELab and on the building envelope. A typical setup to monitor the influence of building envelopes on indoor environmental quality is reported in previous work (Luna-Navarro & Overend, 2021). Table 12 reports information on the sensing devices per environmental parameter and the frequency and location of the measurement.

TABLE 12 Measured environmental parameters with details of sensing devices and frequency of monitoring for the validation

Parameter	Location	Sensor	Frequency
Indoor dry bulb air temperature	Centre of facility	Pt100 Lastem	10 min
Surface temperature (optional)	One location	Plate Pt100 Lastem	10 min
Direct and global solar radiation	Roof of the test facility or any unobstructed location in the proximity	Weather station	1 min
Outdoor dry bulb air temperature	In the proximity of the test facility and shielded by solar radiation	Weather station	10 min
Wind speed	In the proximity of the test facility but not obstructed by the test facility or other buildings	Weather station	10 min

C.3 PARAMETERS RELATED TO THE CONTROL ALGORITHM

The movements of the blinds were monitored by a control unit, which wrote a message in a log and stored it in an internal memory when an action of the actuator was registered, i.e. when the position of a blind changed. To evaluate the accuracy of the predicted control actions during validation, the data points related to the control actions of the blind automation system were downloaded and used directly from the computer that stored the actuator messages. Other indoor and outdoor parameters triggering control actions, e.g. solar radiation incident on the building envelope and indoor and outdoor temperatures, were also used to validate blind movements.

APPENDIX D MODELLING AND SIMULATION DETAILS

This appendix provides details on the modelling and simulation of the model of MATELab. In particular, it outlines (i) the modelling parameters of the thermal model, (ii) the simulation and measurement periods and (iii) the modelling challenges of the control algorithm in the EMS feature of EnergyPlus.

D.1 MODELLING PARAMETERS OF THE THERMAL MODEL

The thermal model of MATELab was created in EnergyPlus based on the parameters reported in Section 3.3 and in Table 13.

TABLE 13 Modelling parameters of MATELab

Parameter	Condition
Occupancy	None
Air conditioning	None
Infiltration flow rate	0.0008 m ³ /s per zone floor area
Internal heat gains	Lighting: 11.8 W/m ² Computer equipment: 10.0 W/m ²

D.2 SIMULATION AND MEASUREMENT PERIODS

Figure 18 shows the durations of the measurement periods (EMS: 14-21 May 2020, Dymola: 8-16 August 2020) and the simulation periods (EMS: 1-31 May 2020; Dymola: 1-31 August 2020). It highlights that the simulation periods began several days before the actual measurement periods, which was necessary to ensure that the initial conditions produced by the simulations matched those of the measured data. To determine the appropriate number of days needed to produce similar initial conditions, simulations and comparisons with the measured data were carried out in advance. In addition to the simulation period, the model was warmed up between 6 and 25 days, which was automatically determined by EnergyPlus and continued until the temperatures and heat flows in each zone converged, as described by the U.S. Department of Energy (DOE, 2018). The simulation timestep was 5 minutes.

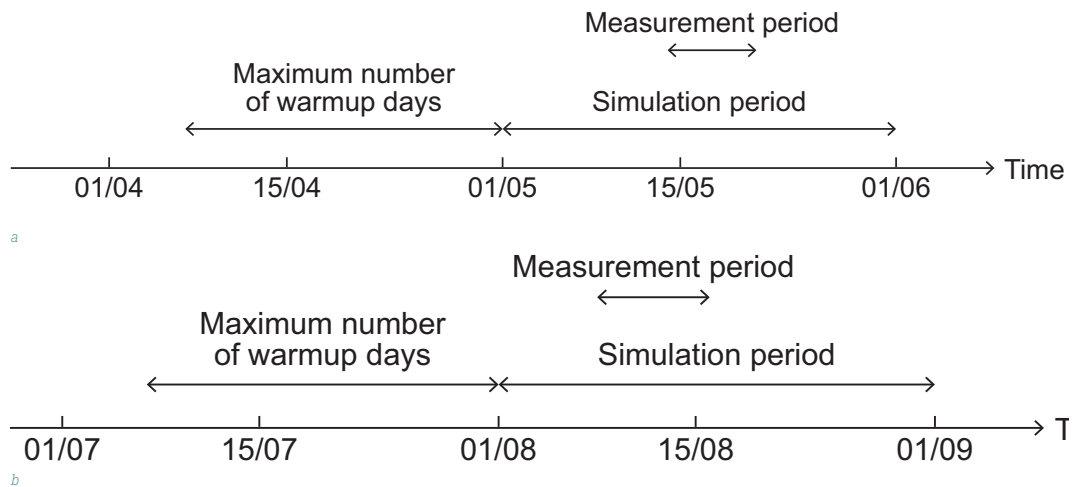


FIG. 18 Schematic of simulation and measurement periods: a. EMS feature; b. Co-simulation setup.

D.3 MODELLING CHALLENGES OF THE CONTROL ALGORITHM IN EMS FEATURE

Two aspects of the control algorithm were particularly complex to model in the EMS feature. Modelling these aspects was, however, important to reduce the modelling uncertainty and eventually obtain realistic predictions of the control actions for validation. Firstly, the monitored solar irradiance had to be used as an input to the control algorithm to ensure that the information provided to the control system was the same for the real and the predicted setup. This was achieved by using the *Schedule:File* object in EnergyPlus as a schedule, which read sub-hourly values from an external CSV file. While the input file contained 15-minute interval data, the *Interpolate to Timestep* field was set to interpolate values and use them at the appropriate minute in the hour. Secondly, the control algorithm had a time delay; since the blinds changed their position only when the solar irradiance was greater than 250 W/m^2 for more than 15 minutes. The time delay was modelled in the EMS feature through the use of trend variables, which are used to store the history of Erl variables.

APPENDIX E UNCERTAIN INPUTS USED IN MCSA

The model of MATELab had many input variables that could vary as a result of specification and modelling uncertainty. However, the variables that were likely to have an impact on the indoor air temperature – the performance indicator – were:

- 1 Infiltration flow rate
- 2 Density of building envelope cover panels
- 3 Specific heat capacity of building envelope cover panels
- 4 Ground temperature
- 5 Internal heat gains of equipment
- 6 Convective heat transfer coefficient of gap between MATELab and the ground
- 7 Thickness of internal partition
- 8 Volume of internal partition

The infiltration flow rate and the ground temperature (inputs 1 and 4) were based on measurements, and it was assumed that they follow standard normal distributions. Inputs 2 and 3 were based on the manufacturer's specifications in terms of nominal performance, which might differ from the actual performance in situ. Therefore, a standard normal distribution was assumed, and the minimum and maximum values found in the literature were used (CIBSE, 2015). The input variables 5 to 6 reflect variations in building specifications, for which only minima and maxima were known. They were also regarded as standard normal distributions where extreme values were less likely to be selected than values near the mean. Since the tails of a standard normal distribution extend indefinitely, the previously described LHS method may generate negative numbers that are usually not supported by EnergyPlus. They represented only a very small proportion of the total number of samples and were thus set to zero.

The last two input variables (7 and 8) were design parameters, which were defined by the authors and could be changed through interventions. Therefore, they were assumed to be uniformly distributed as they may be regarded as being equally probable. The sources used to inform the shape of the distributions can be seen in Table 14.

TABLE 14 Input variables used in MCSA, including their symbol, assumed distribution, type of variation and source

Input variable	Symbol (unit)	Distribution assumed	Uncertainty type	Source
Infiltration flow rate	Q_{in} (m ³ /s m ²)	$N(0.003,0.0008)$	Modelling uncertainty	Measured
Density	ρ (kg/m ³)	$N(1500,333)$	Specification uncertainty	Technical sheet from manufacturer
Specific heat capacity	c (J/kgK)	$N(5000,1000)$	Specification uncertainty	Technical sheet from manufacturer
Ground temperature	T_g (°C)	$N(20.0,1.7)$	Modelling uncertainty	Measured
Internal heat gains	Q_{int} (W/m ²)	$U(100,33.3)$	Modelling uncertainty	CIBSE (2015, Table 1)
Convective heat transfer coefficient of gap	h_c (W/m ² K)	$U(1.5,0.5)$	Modelling uncertainty	CIBSE (2015, Table 3.7)
Thickness	d (m)	$U(0.2,0.07)$	Specification uncertainty	Defined by authors
Volume	V (m ³)	$U(20.0,6.7)$	Specification uncertainty	Defined by authors

APPENDIX F RESULTS OF IN-SITU MEASUREMENTS

This appendix begins by presenting the results of the in-situ measurements of the U-values and then goes on to describe the analysis of the thermal bridges using infrared images.

TABLE 15 Results of the in-situ measurements of the U-values

ID	Zone	Area (m ²)	U-value (W/Km ²)	Total U-value (W/Km ²)
A	Left side	0.438	1.225	1.232
B	Top side	0.373	1.152	
C	Bottom side	0.373	1.069	
D	Centre side	0.578	0.969	
E	Top edge	0.246	1.410	
F	Bottom edge	0.246	1.210	
G	Left edge	0.321	1.559	
H	Right side	0.438	1.225	
I	Right edge	0.321	1.559	

Figure 19 shows the thermal bridge type F (Table 15) with the thermal image (Figure 18a) and the corresponding calculated temperature profile along a 0.77 m long line on the wall (Figure 18b). The results of the full thermal bridge assessment using infrared images are reported in Table 16. The average indoor air temperature was 22.6 °C, while the temperature in the homogeneous wall areas was around 22.1°C. The corresponding value of the incidence factor of the thermal bridge calculated from Equation 11 was 1.17, as reported in Table 16. To evaluate the total thermal losses taking into account the thermal bridge effect, the corrected U-value $U_{corrected}$ was calculated according to Equation 12, where I_{tb} was the weighted average of the several I_{tb} affecting each surface.

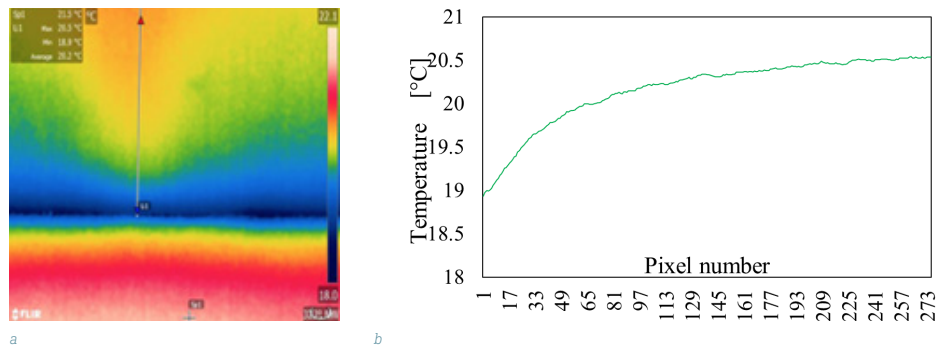


FIG. 19 Thermal bridge assessment for type F: a. Thermal image; b. Temperature profile across the wall.

TABLE 16 Quantitative analysis of infrared images

ID	Typology and description of thermal bridge	I_{tb}	Affected surfaces
A	Bottom corners on south building envelope (floor-wall-wall)	1.26	Floor and east, south and west walls
B	Top corners on south building envelope (roof-wall-wall)	1.12	Roof and east, south and west walls
C	Top corners on north building envelope (roof-wall-wall)	1.09	Roof and east, north and west walls
D	Bottom corners on north building envelope (floor-wall-wall)	1.18	Floor and east, north and west walls
E	Vertical corner lines wall-wall (wall-wall)	1.14	All walls
F	Horizontal corner lines wall-floor	1.17	Floor and wall
G	Horizontal corner lines wall-roof (roof-wall)	1.11	East and west walls
H	Vertical lines wall-wall interface (junction of 2 wall parts on south building envelope)	1.13	South wall

The acoustic and daylighting effects of external façade sun shading systems

Simone Secchi ¹, Patrizio Fausti ², Gianfranco Cellai ¹, Martina Parente ¹, Andrea Santoni ², Nicolò Zuccherini Martello ³

- * Corresponding author, simone.secchi@unifi.it
- 1 University of Florence, Department of Architecture, Italy
- 2 University of Ferrara, Department of Engineering, Italy
- 3 Formerly University of Ferrara, Department of Engineering, Italy

Abstract

External sun shading devices are increasingly used in sustainable buildings to reduce the greenhouse effect in the summer and the glare effect due to direct solar irradiation through transparent surfaces. The acoustic effects of these devices have been investigated in recent studies that suggest the possibility of optimising these elements to improve acoustic comfort in indoor environments, even with open windows. Nevertheless, there are few studies that analyse the combined effect of these devices on acoustic attenuation and improved daylighting.

In this paper, the results of acoustics and daylighting simulations are reported, considering different dimensions, distances of the louvres and orientations of the façade. The main results of previous works concerning the effect of lining the bottom side of each louvre with sound-absorbing material are also briefly summarised. The acoustic effects of different configurations of the louvres are evaluated in terms of Insertion Loss in the façade plane. For the lighting simulations (daylight factor, daylighting uniformity and daylight glare probability), the variation of the shielding effect is studied considering the spacing between the louvres and the orientation of the façade for different times and seasons for latitude in the South of Europe.

Keywords

Façade, Indoor comfort, Light shelves, Insertion Loss, Acoustic absorption, Daylighting

DOI

<http://doi.org/10.47982/jfde.2022.1.07>

1 INTRODUCTION

Solar shading systems installed on building façades are necessary to reduce the summer energy consumption of buildings, based on the technical standards EN 13363 (EN 13363-1, 2003) and EN 14501 (EN 14501, 2006), received within the Energy Performance Buildings Directive (EPBD) released in 2002 and revised in 2010 (Directive 2010/31/eu, 2010). These standards and the EU directive concern building construction techniques to achieve very high energy-efficient buildings, also known as nearly Zero Energy Buildings (nZEB); buildings that significantly reduce their environmental footprint.

Solar shading devices can influence visual comfort (Cellai, Carletti, Sciarpi, Secchi, Nannipieri & Pierangioli, 2014) (ECBCS Annex 29/SHC Task 21, 2010) negatively by diminishing daylight amount in inner spaces, but also positively by reducing glare effects and improving daylighting uniformity, especially with clear sky conditions. This paper evaluates the effect of variation in daylight availability in a specific period of the year in South Europe. The threshold parameters that define the quality and quantity of natural lighting are regulated by national laws and calculated by international standards such as EN 12464 (EN 12464-1, 2021), EN 14501 (EN 14501, 2005) and EN 17037 (EN 17037, 2018).

The assessment and management of environmental noise are also very important for the well-being of people (Directive 2002/49/ec, 2002). Poorly designed façade shading systems can lower the acoustic comfort and undermine the overall acoustic performance of the façade if the sound coming from the traffic is directed toward the windowpane. This negative effect can be suppressed and converted into a positive effect by proper louvre design that reflects the traffic noise away from the façade surface.

The acoustic performances of building façades have been considered in several studies, which investigated multiple aspects such as their shape (Busa, Secchi & Baldini, 2010), the presence of balconies (Li, Lui, Lau & Chan, 2003), the effects of a green envelope (Van Renterghem, Hornikx, Forssen & Botteldooren, 2013), the influence of the windows (Granzotto et al., 2017) and the flanking transmission (Secchi, Cellai, Fausti, Santoni & Zuccherini, 2015). A comprehensive review related to the acoustic performances of building façades was recently published (Hu, Zayed & Cheng, 2021), including studies on sound insulation, the effect of façade on street noise, and noise reduction techniques. On the other hand, the acoustic influence of façade shading systems has not been widely investigated. Sakamoto and Aoki (Sakamoto & Aoki, 2015) presented a numerical study to examine the sound reduction effects due to the presence of louvres mounted on the building façade, validating the results with experimental measurements on a 1:20 scale model. Numerical analysis and a 1:1 scale model were also used by Zuccherini et al. (Zuccherini, Fausti & Secchi, 2016) and Fausti et al. (Fausti, Secchi & Zuccherini, 2019) to analyse variations in the acoustic sound pressure field on the building façade, considering different sound source positions and changing the configuration of the louvres and their tilt angle. Further investigations of the acoustic effects of building façade shading systems, involving in-situ experimental measurements (Sakamoto, Lee, Ishii, Katayama, Iwase & Takahashi, 2017) (Zuccherini, Fausti, Santoni & Secchi, 2015) and evaluation of the related psychoacoustic effects (Zuccherini, Aletta, Fausti, Kang & Secchi, 2019), highlighted that the louvres can reduce the sound pressure levels across the building façade and the magnitude perception of the noise. The most common indoor shading devices were experimentally analysed by Catalina et al. (Catalina, Ene & Biro, 2019), assessing their influence on both the improvement of the sound insulation performance and the reverberation time of the room. However, in both cases, results showed negligible differences between different shading device systems.

At present, most studies deal with the effect of façade shape and shielding devices, with analyses referring only to acoustics or daylight, whereas the human reaction to sound and light stimuli are strongly correlated, as some studies show (Buratti, Belloni, Merli & Ricciardi, 2018) (Huang, Zhu, Ouyang & Cao, 2012) (Hangzi, Xiaoying, & Yue, 2020). The main aim and the novelty of this work are, therefore, the use of a multi-domain approach to evaluate the acoustic and daylight effects given by the presence of an external shading device made of shading louvres. This study was carried out by means of both simulations and measurements in a real building and in a scale model realised in an acoustic laboratory. In the follow-up to this work, questionnaire-based investigations will make it possible to analyse the reciprocal influence between the daylighting and acoustic parameters currently described by independent parameters and limit values.

A virtual mock-up building was designed as a reference for various evaluations. The building could be assimilated into an 8-storey office building with a flat façade. The shading system was simulated by evaluating various sizes of louvres and the spacing between them. Acoustic and daylight simulations were carried out on the same geometries.

The louvres' tilt angle was not considered in this work for daylight simulations because it was assumed that shading devices with horizontally oriented louvres constitute the best compromise between acoustic and daylight comfort: previous works have shown that louvres tilted towards sound sources can increase the sound pressure level on building façade, offering, on the other hand, the best shading to the building itself (Fausti et al., 2019) (Zuccherini et al., 2019).

Acoustic performances have been evaluated as sound pressure level differences (Insertion Loss – IL) on building façades, between a reference scenario, without shading devices on the façade, and with various shading systems. In previous works, a standard shading system was compared to an acoustically optimised one, having louvres with sound-absorbing properties on the bottom side (Zuccherini et al., 2016) (Fausti et al., 2019) (Zuccherini et al., 2015) (Zuccherini et al., 2019). The conclusions of these studies are assumed in the present work.

The daylighting effect of external louvres is evaluated in many studies for their importance in the reduction of thermal loads but also for the improvement of visual well-being (Technical Report of IEA SHC Task 50.C2, 2016) (Technical Report of IEA SHC Task 61.C1, 2019) (Ahmad, Kumar, Prakash & Amana 2020) (Carletti, Cellai, Pierangioli, Sciarpi & Secchi, 2017). Several parameters have been introduced to assess the quantity, quality and glare of light (Carlucci, Causone, De Rosa & Pagliano, 2015).

In this study, the daylighting effect is analysed with reference to three parameters, and the relevant results are compared with the corresponding recommended values. In particular, the amount of daylight is evaluated by means of the Daylight Factor (D), described in many national and international standards; the distribution of daylight is analysed with the Daylighting Uniformity (U), as defined in the standard EN 12665 (EN 12665, 2013); the daylighting glare effect is analysed by means of the Daylight Glare Probability (DGP), described in the standard EN 17037 (EN 17037:2018) (Galatioto & Beccali, 2016). Also, the Useful Daylight Illuminance (UDI) is an important parameter to analyse the probability of glare occurrence due to daylight. It is defined as the annual occurrence of illuminances across the work plane where all the illuminances are within the range 100 to 3000 lx; the degree to which UDI is not achieved because illuminances exceed the upper limit is indicative of the potential for occupant discomfort due to glare (Nabil & Mardaljevic, 2005). In any case, as has been shown (Mardaljevic, Andersen, Roy & Christoffersen, 2012), there is a strong correlation between the Useful Daylight Illuminance and the Daylight Glare Probability used in this study.

2 METHODOLOGY

2.1 DESCRIPTION OF THE CASE STUDY

The virtual mock-up considered in the present study is a 28 m tall building with 8 floors (ground floor + floors 1 to 7). Each floor is 3.1 m high, having 0.4 m slabs dividing two consecutive floors.

A road was set in front of the building façade, made up of two lanes (3.5 m each), lateral pavements/sidewalks and cycling paths, a total of 6.5 m wide (Figure 1). The sound source was set as a traffic lane, 8.25 m away from the building façade.

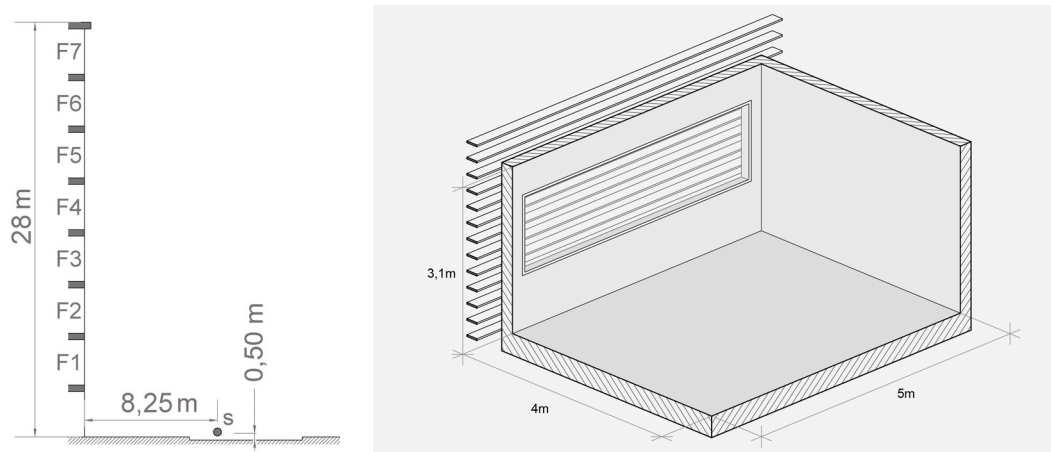


FIG. 1 LEFT: Section of the building façade. Dimensions are in meters (m). Each floor is 3.50 m high, including the thickness of the floor slab. The sound source S is placed at 8.25 meters from the building façade and 0.50 m from the ground, simulating the sound emission of a traffic lane. F1-7 indicates the floor level.

FIG. 2 RIGHT: Axonometry of the inner space. Dimensions in meters.

The third dimension of the test room was only considered with daylight simulations. The inner space was simulated as a room 5 m wide, 4 m long and 3.1 m high (Figure 2), with windows 4.6 m wide and 1.5 m high (34.5% of the floor surface).

Both the acoustic and the daylight simulations consider louvres 3 cm thick and variable between 20 / 30 / 40 cm in spacing.

2.2 ACOUSTIC SIMULATIONS METHODOLOGY

The acoustic effects of external louvres were investigated with a commercial Finite Element (FE) Solver (COMSOL® Multiphysics), whose detailed description is reported in (Fausti et al., 2019). This model was previously validated with reference to a 1:1 scale model analysed in a semi-anechoic chamber (Zuccherini et al., 2016) (Figure 3). The laboratory mock-up used in the cited work was characterised by tiltable louvres, sized 0.2 m x 2 m, 1.8 cm thick: the tilting possibility of the louvres helped study the variability of acoustic Insertion Loss (IL) associated with the tilt angle of sun shading louvres. The IL was calculated as the differences between the sound pressure level (SPL)

measured without the shading system (considered as the reference value) and the SPL measured with the shading devices. The IL was calculated first considering a traditional façade shading system (Figure 3 (b)) and then adding sound-absorbing material on the bottom faces of each louvre in the shading system (Figure 3 (c)).

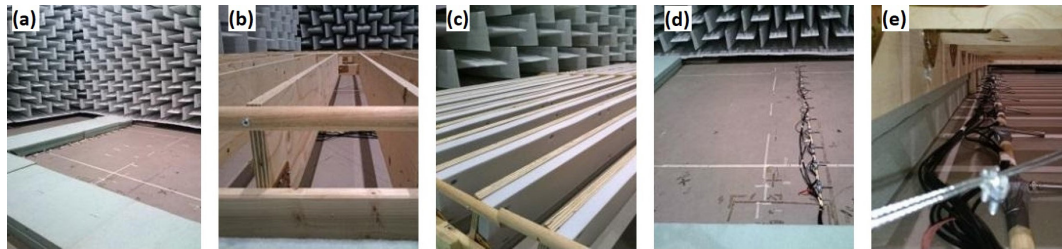


FIG. 3 (a) Empty floor of the semi-anechoic room simulating a flat building façade; (b) non-absorbing shading louvres; (c) sound absorbing louvres; (d) microphones used for measuring SPL without the shading device; (e) microphones used for measuring SPL with the shading devices.

Figure 4 shows measured values (EN ISO 10534-2, 2001) of the normal incidence sound absorption coefficient of the melamine foam used in the experiment.

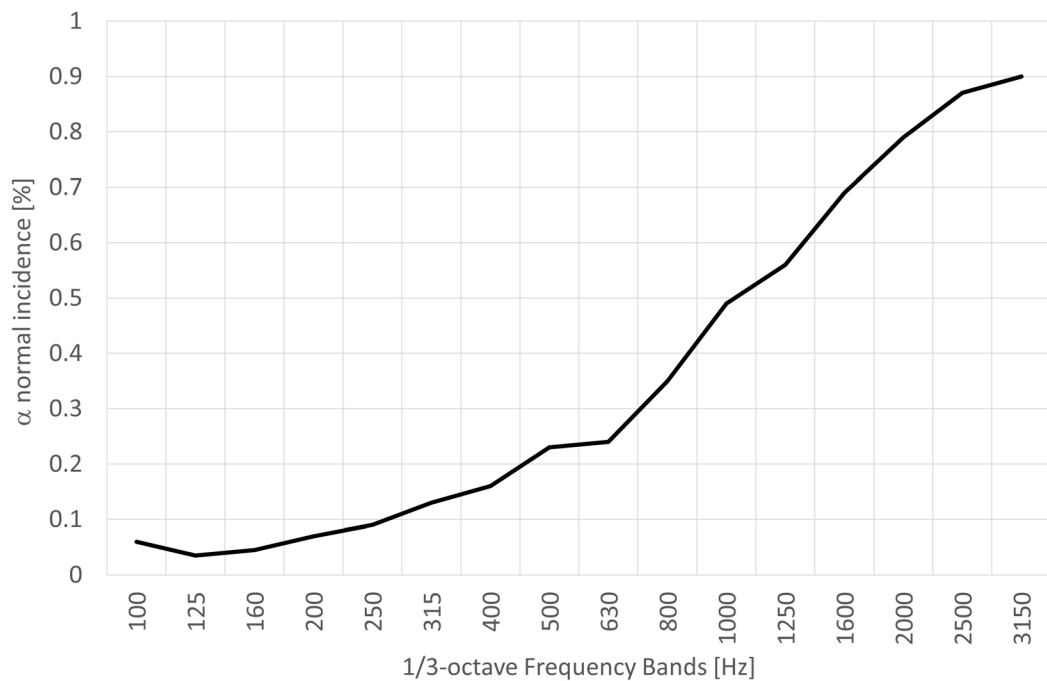


FIG. 4 Measured normal incidence sound absorption coefficient (α) of the material (expanded melamine foam) used in the mock-up.

A 2D FE model, representing the experimental mock-up in a semi-infinite acoustic domain, was first validated with laboratory measurements and then expanded to further investigations, simulating urban situations (Fausti et al. 2019).

To exactly reproduce the laboratory condition, the louvre system was modelled with the same geometry as the mock-up, backed by perfectly reflecting boundary conditions representing the

floor of the semi-anechoic chamber (as well as the glazing surface in real conditions). The acoustic fluid domain was modelled with a radius of 4.8 m and truncated by using perfectly matched layer (PML) elements to approximate the semi-infinite domain condition (Figure 5 a). The louvres in the standard condition (bare wood material with no sound-absorbing layer) were approximated as rigid boundaries of the fluid domain. The condition representing louvres lined with a layer of sound-absorbing material was simulated with the *Poroacoustic* built-in feature in COMSOL®, applied to sound-absorbing domains: a Delany-Bazley-Miki (DBM) (Delany & Bazley, 1970) (Miki, 1990) equivalent fluid model was used to replicate measured absorption properties.

After the validation of the model, further FE analyses were carried out using an extended model, as shown in Figure 5 b.

The sound source, which reproduced the experimental configuration, was implemented as a monopole (omnidirectional) point source (5 Pa) placed in the middle of the left lane, 0.5 m from the ground, 8.25 m from the building façade.

Although the section of the simulated road includes two traffic lanes, only one was simulated. The acoustic effects of the shading louvres were evaluated in terms of Insertion Loss (evaluation of the effects on a building façade facing the one with the shading louvres). Further details on this modelling approach can be found in the reference (Fausti et al., 2019).

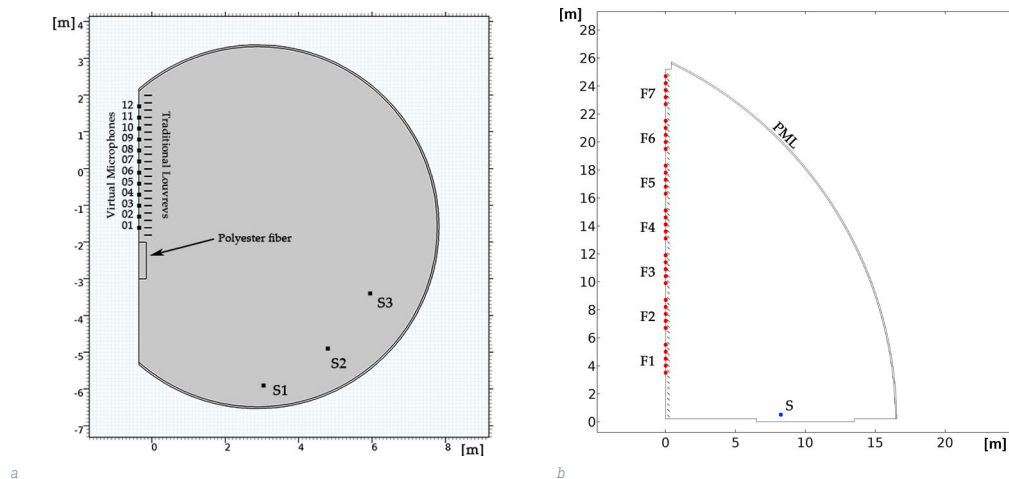


FIG. 5 (a) Bi-dimensional FEM Set-Up reproducing the experimental set-up. (b) Extended FEM model of an entire 7-storey building façade facing a traffic lane at ground level; red dots represent virtual pressure sensors to measure the sound pressure level.

2.3 DAYLIGHTING SIMULATIONS METHODOLOGY

The daylighting parameters described in section 1 (D, U and DGP) were calculated with RELUX® (www.relux.com), a software to simulate artificial light and daylight according to standards EN 12464-1:2021 and EN 17037:2018, one of the most used and advanced lighting simulation tools for daylight and lighting calculation (Maamari, Fontoynt, Adra, 2006) (Bhavani & Khan, 2011) (Kaempf et al., 2016). Relux® is validated (Bouroussis, Nikolaou & Topalis, 2019) regarding the methodology described by the technical report CIE 171:2010 (CIE 171, 2010) that defines and proposes a set of several test cases to validate the calculations accuracy of a lighting simulation software. An in-depth study of the validity of nine different software tools, including Relux®, showed that they can

simulate a standard room, also with louvres, with minimal percentage differences between them (Iversenet al., 2013).

In this work, simulations were performed with reference to the CIE sky types 1 (overcast sky, for daylight factor) and 12 (clear sky, low turbidity, for daylighting uniformity and daylight glare probability). The investigated solutions assessed the ability of the software to simulate the influence of an obstruction, like an external horizontal louvre, on the diffuse reflection and on the internal direct illuminance.

The analysed model was placed in a geographical location in the South of Europe with the correct North orientation. The calculation method uses radiosity algorithms to evaluate the lighting characteristics in discrete points of the environment after dividing each surface into meshes with homogeneous photometric properties. Radiosity algorithms require that all surfaces be ideal diffusers that follow Lambert's law.

The following summarises the main lighting properties of the surfaces and the calculation parameters.

- Reflection factor of walls and ceiling in gypsum plaster, white matt: 80%.
- Reflection factor of floor: 40%.
- Reflection factor of external louvres: 80%.
- Transmission factor of window glasses: 80%.
- Position of the calculation surface: 0.75 m from the floor and 0.5 m from the walls.
- Position of the case study: Florence, Central Italy (43° 46' N 011°15' E).
- Orientation of the case study: South and East (West façade in the morning is equal to East façade in the afternoon about the altitude of the sun; therefore, only the East façade has been evaluated).
- Sky conditions: standard CIE overcast sky for daylight factor simulations; standard CIE clear sky with sun and overcast sky for Uniformity factor and Discomfort Glare Probability simulations.
- Percentage of indirect light used in simulations: average.

Reflection factors of internal surfaces were taken from the acceptable ranges described by both EN 12645-1:2021 and EN 17037:2018 (0.7 to 0.9 for the ceiling, 0.5 to 0.8 for walls and 0.2 to 0.4 for the floor). Annex B of EN 17037 recommends using lower values of reflection factors in the above-reported range to take into account the presence of furniture. However, we considered the case of a room furnished with light-coloured furniture.

Simulation refers to the following parameters described in the introduction:

- Daylight factor D.
- Daylight Uniformity U.
- Daylight Glare Probability DGP.

The daylight factor, D, is believed to have been developed by Alexander Pelham Trotter towards the end of the nineteenth century (Mardaljevic, J., 2013) as the ratio of the internal horizontal illuminance to the unobstructed external horizontal illuminance, usually expressed as a percentage. Nowadays, the required levels of daylight factor range between 1% and 5%, depending on building types and activities, and it can be evaluated in standard overcast conditions as under various unobstructed skies (Danny et al., 2018) (Xu, Yuehong, Xin, 2014).

Daylighting uniformity, U, (EN 12665, 2013) is the ratio of minimum illuminance to average illuminance.

The daylight glare probability, DGP, (EN 17037, 2018) is the parameter used to analyse the daylight glare effect that considers both the illuminance at eye level and individual glare sources of high luminance to estimate the fraction of dissatisfied people. Both U and DGP are useful parameters to evaluate the effect of louvres in clear sky conditions (Kose & Kazanasmaz, 2020).

For daylighting purposes, the International Commission on Illumination, CIE, defines 15 different standard sky conditions (CIE S 011/E, 2003) (Darula & Kittler, 2014) that are described by functions, depending on the solar altitude, even when the sun is obscured. In this study, the analysis of the parameters U and DGP was performed with clear sky conditions (less than 30 % cloud cover or none) combined with sunny sky conditions; in this case, the sky distribution corresponds to the standard CIE clear sky condition with additional direct illumination from the sun. This model of the sky is useful when visual glare and thermal discomfort studies are performed (Suk & Kensek, 2011).

Standard EN 17037 (EN 17037, 2018) gives recommendations for the daylight factor D with reference to different locations. Table 1 shows the values of D to obtain a given target illuminance E_T (lx) from 100 (minimum target illuminance) to 750 lx (high target illuminance), referred to the median external diffuse illuminance $E_{v,d,med}$ of Florence and Rome for a fraction of daylight hours $F_{time,\%} = 50\%$.

As an example, in the case of Central Italy (Florence), the value D equal to 2% allows exceeding 300 lx for 50% of the time daylight hours.

TABLE 1 Values of D for daylight vertical openings to exceed an illuminance level from 100 to 750 lx for a fraction of daylight hours $F_{time,\%} = 50\%$

Place	Latitude (°)	Median external diffuse illuminance $E_{v,d,med}$ lx	D to exceed 100 lx	D to exceed 300 lx	D to exceed 500 lx	D to exceed 750 lx
Florence	43.46	15017	0.67%	2.00%	3.33%	5.00 %
Rome	41.80	19200	0.50%	1.60%	2.60%	3.90%

Table 2 shows the correspondence between values of Daylight Glare Probability and the statistical perception of glare according to the standard EN 17037.

TABLE 2 Recommended values of daylight glare probability according to annex E of EN 17037

Criterion	DGP value
Glare is mostly not perceived	$DGP \leq 0.35$
Glare is perceived but mostly not disturbing	$0.35 < DGP \leq 0.40$
Glare is perceived and mostly disturbing	$0.40 < DGP \leq 0.45$
Glare is perceived and mostly intolerable	$DGP \geq 0.45$

To assess daylight glare probability, the luminance distribution within the field of view and the size, intensity and location of the glare sources in regard to the line of sight have to be taken into account. Consequently, DGP values have been calculated for the three positions shown in Figure 6: DGP1 and DGP2 are symmetrical but facing the opposite walls, located 2.0 m from the façade and with a view direction parallel to the window, while DGP 3 is perpendicular to the façade and located 3 m away; all points are 1.2 m high from the floor.

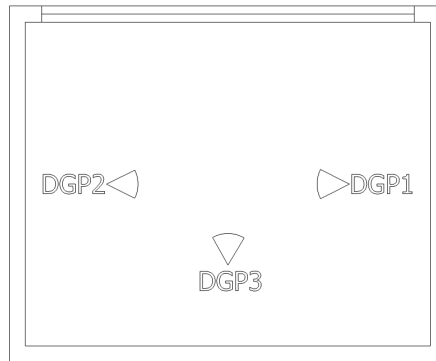


FIG. 6 Position of the points views for the calculation of DGP.

The analysis of DGP was carried out for different configurations of louvres for the same orientations of the façade (South and East), periods of the year (two solstices and equinox) and at the same hours of calculation (09:00, 12:00 and 15:00) as for the daylighting uniformity.

3 RESULTS AND DISCUSSION

3.1 ACOUSTIC RESULTS

Simulations were performed with the above-described FE software and method: they produced a detailed description of the sound distribution across the façade at different frequencies.

Figure 7 shows a sample result obtained by FE simulations: the sound pressure level at 1 kHz across the building façade portion is affected by the presence of the shading louvres; the sound pressure level also appears to be highly reduced by the presence of sound absorbing louvres, with respect to the traditional ones.

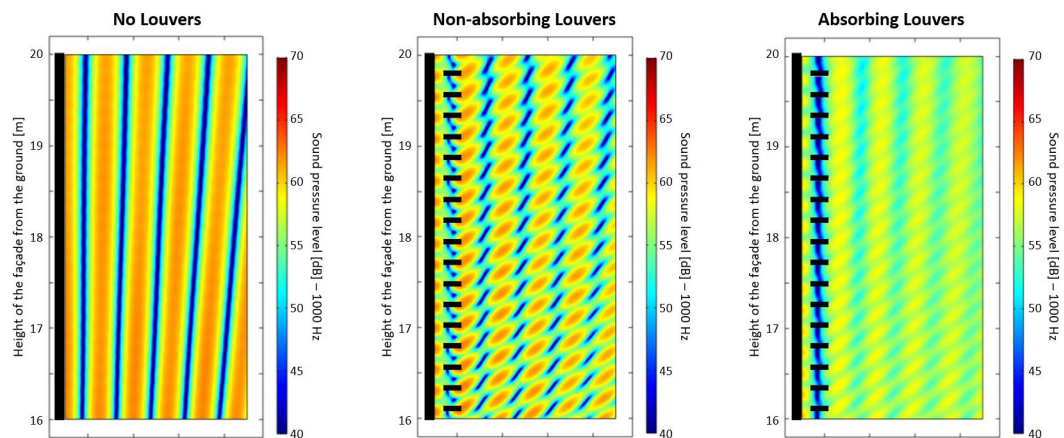


FIG. 7 Sound pressure level simulated in correspondence with the 4th floor of the simulated building façade. The solid thick black vertical line represents the façade surface. Left: without louvres. Center: non-absorbing louvres. Right: sound-absorbing louvres.

As shown in Figure 7, the sound pressure level with louvres present is far from uniform across the façade. The results of the simulations have therefore been further evaluated in terms of arithmetic averages of the Insertion Loss, with each average referring to a single floor. Simulations have been conducted considering five virtual measurement positions on each floor. Each average considers five measurement points across the virtual building façade.

In the FE acoustic model, the effect of the variation of the following parameters was studied:

- Louvres' tilt angle (0, -30°, -45°), considering: 0° for horizontal louvre; -45° for louvre tilted towards the soil and the sound source.
- Louvres' width (20, 30, 40 cm).
- Louvres' spacing (20, 30, 40 cm).

The following summarises the main results.

3.1.1 Tilt angle of louvres

The louvres' tilt angle with respect to the sound source has an impact on the acoustic Insertion Loss: it is shown that tilted louvres offer less acoustic protection than horizontal ones. Therefore, only horizontal louvres have been considered in further daylight analyses.

It is very clear how IL increases with respect to the building height: this consideration can be made while evaluating other geometrical aspects of the shading system.

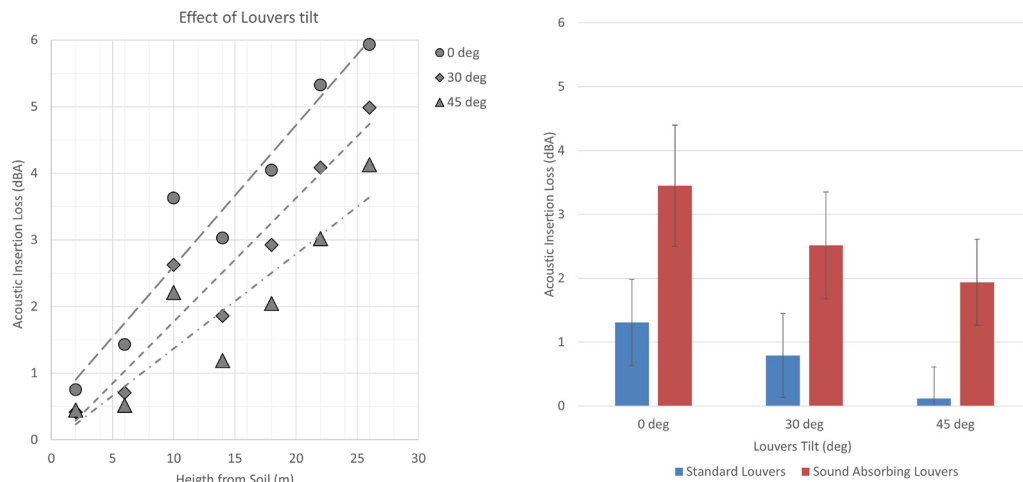


FIG. 8 LEFT: Average of IL in dB(A) considering sound-absorbing louvres' tilt angles (0°, 30°, 45°) with respect to building height. RIGHT: Overall evaluation of the effect of louvre tilt angle on IL: standard versus sound-absorbing louvres results are shown.

3.1.2 Louvre width

In this case, the width of the louvres varied between 20, 30 and 40 cm, with respect to the floor height and an overall average.

Results show that the louvres' section width is not relevant when acoustic IL in dBA is observed: it is important to mention that simulations have been executed considering the spacing between louvres being no shorter than their width. In other words, the ratio between the spacing and width of louvres has been kept equal to 1. This fact can partially explain the minor effects of louvre widths on the acoustic IL.

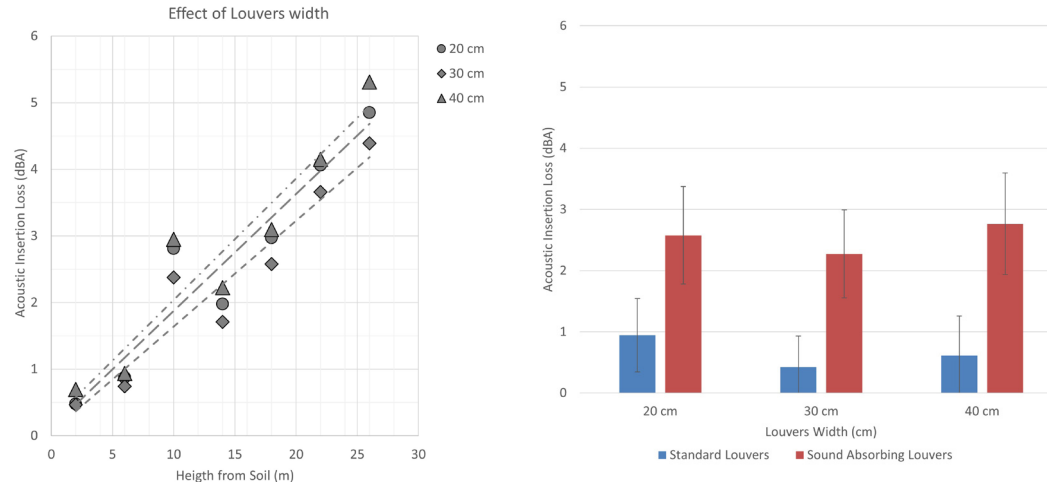


FIG. 9 LEFT: Average of the IL in dB(A) considering sound-absorbing louvres section width (20, 30 and 40 cm) with respect to building height. RIGHT: Overall evaluation of the effect of louvre section width on IL: standard versus sound-absorbing louvres results are shown.

3.1.3 Louvre spacing

Results showed that values of IL in dB(A) are affected by the louvres' spacing: wider distances between louvres give poorer sound protection to the building façade.

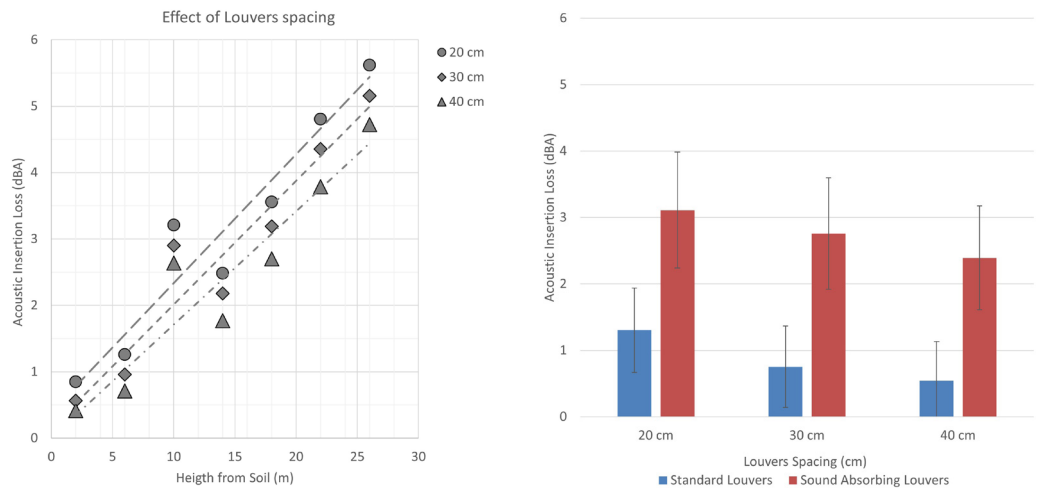


FIG. 10 LEFT: Average of IL in dB(A) considering the spacing between sound-absorbing louvres (20, 30 and 40 cm) with respect to building height. RIGHT: Overall evaluation of the effect of louvre section width on IL: standard versus sound-absorbing louvres results are shown.

3.1.4 Preliminary considerations on acoustic results

Figures 8, 9 and 10 indicate that the acoustic effect of the louvres is mainly influenced by the floor level and by their tilt angle and spacing.

Since these results are the starting point for daylighting analysis, it must be considered that the floor level does not influence the indoor daylighting for a building not obstructed by other buildings, as in the case study analysed. On the other hand, louvres tilted downward (30° or 45°) negatively affect both the reduction of the Insertion Loss and the Daylighting Factor. For this reason, daylighting simulations have been performed with reference to a typical floor level and horizontal louvres (0° of tilt angle) 20 cm wide, spaced 20, 30 and 40 cm from each other.

3.2 DAYLIGHTING RESULTS

Figure 11 shows the results with reference to the values of maximum, average and minimum daylight factor, D , calculated with standard CIE overcast sky, in the conditions expressed in paragraph 2. The second vertical axis in the same graph shows the fraction of the reference plane (F_{plane}) where the target daylighting level (500 lx) or the minimum target daylighting level (300 lx) are achieved, according to annex A of EN 17037:2018.

The reduction of the daylight factor is a consequence of the presence of the louvres and their spacing. With horizontal louvres 20 cm wide and spaced 20 cm from each other, the average daylight factor is 3.1%, and 47% of the reference plane (F_{plane}) reaches the target illuminance level of 500 lx, while 100% of the reference plane reaches the minimum target level of 300 lx for 50% of the daylight hours. According to EN 17037:2018, minimum values of F_{plane} should be 50% for the target level and 95% for the minimum target level. Therefore, it can be deduced that, for the latitude of Southern Europe, even with external louvres spaced 20 cm from each other, the minimum values of daylighting level are achieved with good approximation under overcast conditions (47% instead of 50% can be considered within the uncertainty margin of the method).

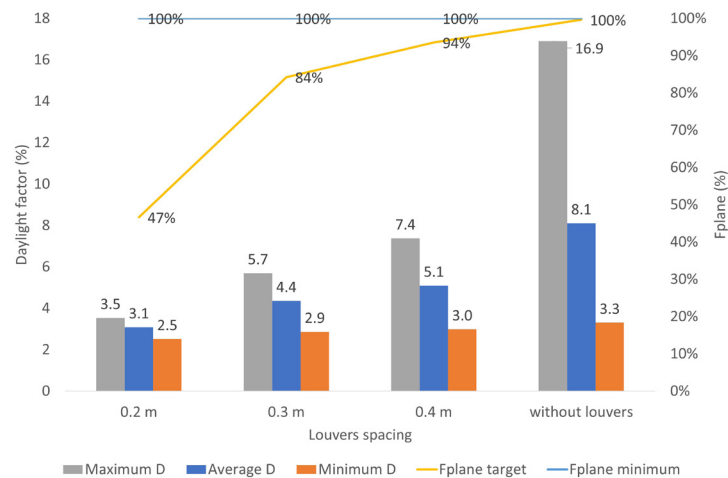


FIG. 11 Variation of the average Daylight Factor as a function of the louvres' spacing with overcast skies.

From Figure 12 it can be observed that the presence of the louvres spaced 20 cm improves the uniformity of daylighting, U , (E_{\min}/E_{avg}) with clear sky, at the latitude of Central Italy and with reference to a different orientation of the façade, the two solstices and the equinox, both in the morning and in the afternoon. An important exception to this is the South façade, without louvres, at 12:00 of the winter solstice, when the direct sun radiation involves all the evaluation area of the office. Here, the minimum and the average values of daylighting are very similar (very high uniformity factor). It can also be noted that at the equinox (21 March), the illuminance uniformity with louvres spaced 20 cm is much higher than with louvres more broadly spaced. This is due to the fact that with louvres spaced 20 cm, the direct solar radiation is completely intercepted by the louvres, as can be seen in Figure 13, which compares the luminances of the room surfaces with louvres spaced 20, 30 and 40 cm for 9.00 am on 21 March. We must consider, for this purpose, that the Eastern orientation of the sun's altitude at 9:00 corresponds to the Western orientation at 15:00, while the Eastern orientation at 15:00 corresponds to the Western orientation at 09:00. For this reason, the Western orientation is not considered in these evaluations.

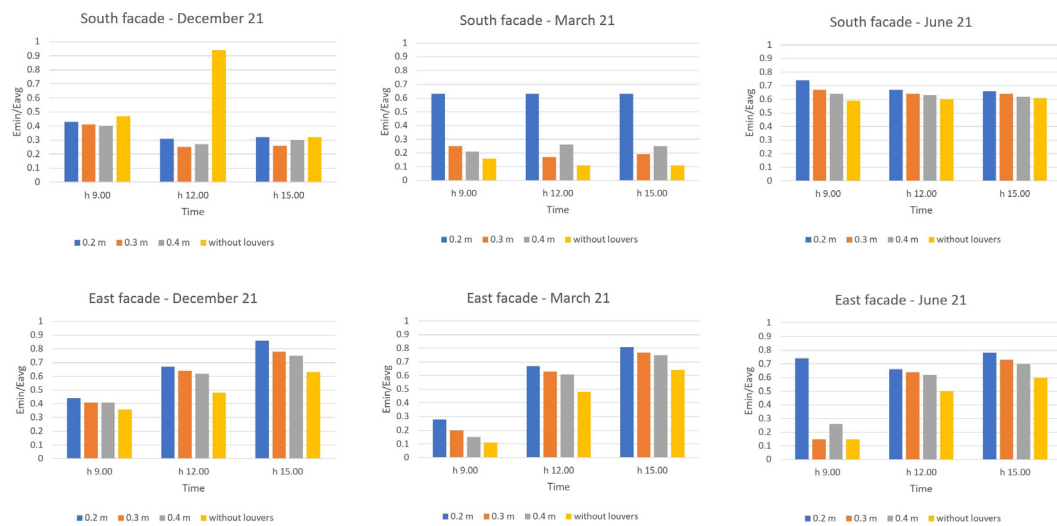


FIG. 12 Variation of the Uniformity factor as a function of the louvres' spacing with clear sky.

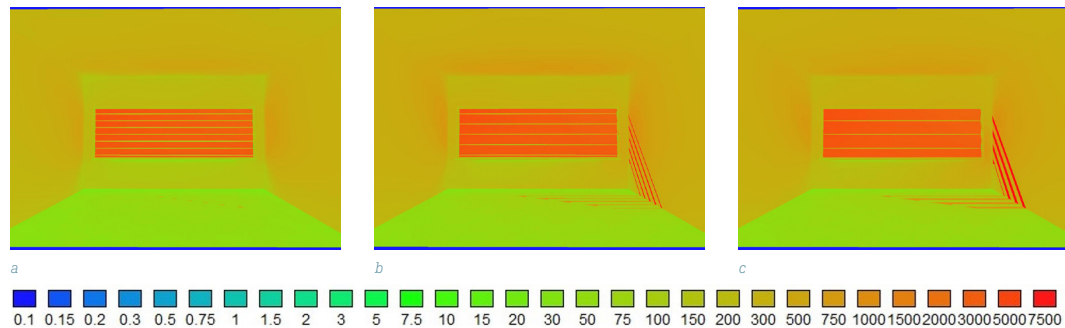


FIG. 13 Luminance values (cd/m^2) as a function of the louvres' spacing with clear sky. From left to right, louvres spaced 20, 30 and 40 cm.

Also, with overcast skies, when the orientation and the date and hour of the evaluation are irrelevant, a better uniformity factor is achieved with louvres' spacing of 20 cm (Figure 14).

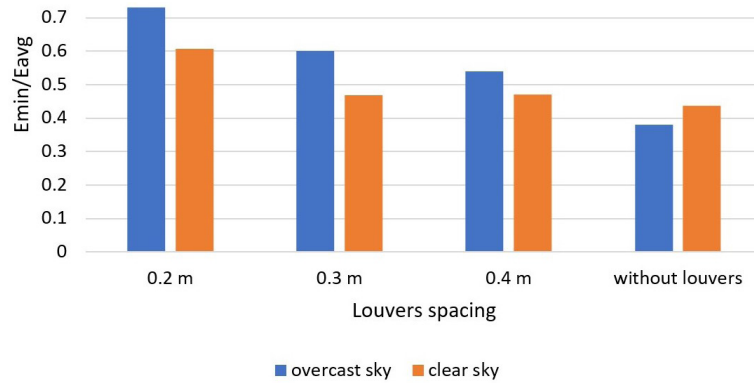


FIG. 14 Variation of the Uniformity factor as a function of the louvers' spacing with overcast and clear sky (average values over the year).

Tables 3 and 4 show the DGP values calculated for the three positions and for East and South exposure.

TABLE 3 Daylight Glare Probability for South orientation of the façade. The cell colours refer to DGP range of values in Table II

date	21-December				21-March				21-JUNE			
	0.20m	0.30m	0.40m	no louvers	0.20m	0.30m	0.40m	no louvers	0.20m	0.30m	0.40m	no louvers
DGP1												
h 9.00	0.28	0.29	0.29	0.3	0.36	0.4	0.42	0.46	0.31	0.37	0.4	0.45
h 12.00	0.22	0.23	0.23	0.23	0.23	0.24	0.24	0.26	0.23	0.24	0.24	0.24
h 15.00	0.19	0.19	0.19	0.2	0.19	0.2	0.2	0.21	0.19	0.2	0.2	0.21
DGP2												
h 9.00	0.28	0.29	0.3	0.31	0.37	0.41	0.42	0.46	0.32	0.37	0.4	0.45
h 12.00	0.22	0.22	0.23	0.23	0.24	0.24	0.25	0.25	0.23	0.24	0.24	0.24
h 15.00	0.19	0.19	0.19	0.2	0.2	0.2	0.2	0.21	0.2	0.2	0.2	0.21
DGP3												
h 9.00	0.37	0.39	0.39	0.41	0.49	0.55	0.57	0.62	0.41	0.5	0.55	0.62
h 12.00	0.28	0.29	0.29	0.29	0.31	0.31	0.31	0.34	0.31	0.31	0.32	0.32
h 15.00	0.21	0.21	0.22	0.23	0.22	0.23	0.23	0.25	0.22	0.23	0.23	0.25

TABLE 4 Daylight Glare Probability for East orientation of the façade. The colours of cells refer to DGP range of values in Table II

date	21-December				21-March				21-JUNE			
	0.20m	0.30m	0.40m	no louvers	0.20m	0.30m	0.40m	no louvers	0.20m	0.30m	0.40m	no louvers
DGP1												
h 9.00	0.86	0.87	0.88	0.89	0.28	0.31	0.33	0.35	0.24	0.25	0.25	0.26
h 12.00	0.49	0.53	0.54	0.57	0.32	0.37	0.4	0.45	0.25	0.26	0.27	0.34
h 15.00	0.33	0.35	0.35	0.37	0.28	0.32	0.35	0.39	0.23	0.24	0.24	0.29
DGP2												
h 9.00	0.28	0.29	0.3	0.31	0.26	0.3	0.32	0.35	0.22	0.23	0.23	0.27
h 12.00	0.4	0.44	0.44	0.48	0.31	0.36	0.4	0.45	0.25	0.26	0.27	0.35
h 15.00	0.33	0.34	0.35	0.4	0.3	0.34	0.36	0.4	0.24	0.25	0.26	0.29
DGP3												
h 9.00	0.37	0.39	0.39	0.41	0.34	0.4	0.44	0.49	0.29	0.3	0.3	0.36
h 12.00	0.54	0.58	0.59	0.63	0.41	0.5	0.55	0.61	0.31	0.34	0.35	0.47
h 15.00	0.44	0.46	0.47	0.49	0.37	0.44	0.48	0.54	0.29	0.3	0.31	0.4

Results of DGP show that the presence of the louvres produces a generalised reduction of glare effects. In particular, horizontal louvres spaced 20 cm from each other produce better results.

For observers in positions DGP1 and DGP2, which are the more usual in office buildings, and louvres spacing 0.2 m, only in the morning of the winter solstice, when the sun altitude is very low for the East orientation of the façade, glare problems occur.

During the summer season, the presence of louvres spaced 20 cm from each other reduces the DGP below the value of 0.35 (glare mostly not perceived according to EN 17037) at each of the hours examined; with the only exception of the observer position DGP3 at 9.00 in the morning with South orientation (DGP = 0.41).

4 CONCLUSIONS

In this work, the effect of external louvers on a case study building 28 meters high, unobstructed by other buildings on the opposite side of the road, is evaluated regarding both acoustic and daylighting parameters. The results of previous works by the authors concerning only the acoustic effect are summarised and recalled here. To better understand the hypothesis and the details of these results, it is necessary to refer to the cited papers ((Zuccherini et al., 2016) (Fausti et al., 2019) (Zuccherini et al., 2015) (Zucherini et al., 2019).

In general, the acoustic effect of an external louvre could be negative, as it can cause an increase in the sound pressure level on the façade. However, if properly designed and with the bottom side of the louvres lined with sound-absorbing material, this effect can become positive and contribute to reducing the façade sound pressure level by some decibels. On the other hand, the presence of these façade devices significantly reduces the amount of daylighting in the interior, especially with overcast sky conditions, and modifies the distribution of daylight, especially with clear sky conditions.

In this study, only fixed horizontal louvres 20 cm wide, with different spacing and with different façade orientations, are considered for both acoustic and daylighting simulations since acoustic simulations showed that this is the better configuration to reduce the façade sound pressure level. Regarding the latitude of Central Italy (Florence) and an office building with large windows (34.5 % of the floor surface), unobstructed by other buildings on the opposite side of the road, in this configuration, the reduction of Daylight Factor with overcast skies is acceptable also with louvres spaced 20 cm from each other. Moreover, results show that the uniformity factor (ratio between minimum and average daylighting level) is significantly improved both with clear and overcast sky conditions with white (80% reflection factor) external louvres 20 cm wide and spaced 20 cm from each other. Moreover, the presence of the louvres produces a generalised reduction of glare effects in sunny sky conditions.

The results presented in this paper demonstrate that a proper design of external louvres, specifically referring to the characteristics of the building and the latitude of the location, can improve both acoustic insulation properties of the façade and the distribution of daylight in the indoor space, reducing the probability of daylight glare.

Further development of this work will involve evaluating the daylighting effect at other latitudes and studying the effect of the reduction of thermal loads in summer conditions.

Acknowledgements

This work is the extended version of the paper presented at the international conference on Construction, Energy, Environment & Sustainability (CEES 2021), held in Coimbra, Portugal in October 2021 (Secchi, Fausti, Cellai, Parente, Santoni & Zuccherini, 2021).

References

- EN 13363-1: 2003. Solar protection devices combined with glazing - Calculation of solar and light transmittance - Simplified method. <https://standards.iteh.ai/catalog/standards/cen/25977ecf-12cd-4a04-9038-f9734c657740/en-13363-1-2003a1-2007>
- EN 14501: 2006. Blinds and shutters - Thermal and visual comfort -Performance characteristics and classification. <https://standards.iteh.ai/catalog/standards/sist/f7041878-9426-466c-a3cc-ab9102bf8454/sist-en-14501-2006>
- Directive 2010/31/eu of the European parliament and of the council of May 19, 2010, on the Energy Performance of Buildings (recast). <https://eur-lex.europa.eu/LexUriServ/LexUriServ.do?uri=OJ:L:2010:153:0013:0035:EN:PDF>
- Cellai, G., Carletti, C., Sciarpi, F., Secchi, S., Nannipieri, E., Pierangioli, L. (2014). Transparent Building Envelope: Windows and Shading Devices Typologies for Energy Efficiency Refurbishments, Cap.2 "Building Refurbishment for Energy Performance, Green Energy and Technology", Springer International Publishing, Switzerland. <https://www.springerprofessional.de/en/transparent-building-envelope-windows-and-shading-devices-typolo/2056852>
- ECBCS Annex 29/SHC Task 21, 2010. Project Summary Report Daylight in Buildings. https://www.iea-ebc.org/Data/publications/EBC_Annex_29_PSR.pdf
- EN 12464-1:2021. Light and lighting - Lighting of workplaces - Part 1: Indoor workplaces. <https://standards.iteh.ai/catalog/standards/cen/53fc4ff7-e7df-4ebd-a730-0d5f0ea888e0/en-12464-1-2021>
- EN 14501:2005. Blinds and shutters - Thermal and visual comfort - Performance characteristics and classification. <https://standards.iteh.ai/catalog/standards/cen/08a6e37a-8784-484f-88e9-05794adfb27/en-14501-2005>
- EN 17037:2018, Daylight in buildings. <https://standards.iteh.ai/catalog/standards/cen/836e5b91-1eb0-4643-a2ba-7ca5a5988e64/en-17037-2018>
- Directive 2002/49/ec of the European parliament and of the council of June 25, 2002, relating to the Assessment and Management of Environmental Noise. <https://eur-lex.europa.eu/LexUriServ/LexUriServ.do?uri=OJ:L:2002:189:0012:0025:EN:PDF>
- Busa, L., Secchi, S., & Baldini, S. (2010). Effect of façade shape for the acoustic protection of buildings. *Building Acoustics*, 17(4), 317-338. <https://doi.org/10.1260/2F1351-010X.17.4.317>
- Li, K. M., Lui, W. K., Lau, K. K., & Chan, K. S. (2003). A simple formula for evaluating the acoustic effect of balconies in protecting dwellings against road traffic noise. *Applied Acoustics*, 64(7), 633-653. [https://doi.org/10.1016/S0003-682X\(03\)00020-3](https://doi.org/10.1016/S0003-682X(03)00020-3)
- Van Renterghem, T., Hornikx, M., Forssen, J., & Botteldooren, D. (2013). The potential of building envelope greening to achieve quietness. *Building and Environment*, 61, 34-44. <http://dx.doi.org/10.1016/j.buildenv.2012.12.001>
- Granzotto, N., Bettarello, F., Ferluga, A., Marsich, L., Schmid, C., Fausti, P., & Caniato, M. (2017). Energy and acoustic performances of windows and their correlation. *Energy and Buildings*, 136, 189-198. <https://doi.org/10.1016/j.enbuild.2016.12.024>
- Secchi, S., Cellai, G., Fausti, P., Santoni, A., & Martello, N. Z. (2015). Sound transmission between rooms with curtain wall façades: a case study. *Building Acoustics*, 22(3-4), 193-207. <https://doi.org/10.1260/1351-010X.22.3-4.193>
- Hu, Z., Zayed, T., & Cheng, L. (2022). A critical review of acoustic modelling and research on building façade. *Building Acoustics*, 29(1) <https://doi.org/10.1177%2F1351010X211022736>
- Sakamoto, S., & Aoki, A. (2015). Numerical and experimental study on noise shielding effect of eaves/louvers attached on building façade. *Building and Environment*, 94, 773-784. <http://dx.doi.org/10.1016/j.buildenv.2015.05.015>
- Zuccherini Martello, N., Fausti, P., Secchi, S. (2016). Acoustic measurements on a 1:1 scale model of a shading system for building façade in a semi-anechoic chamber, Proceedings of InterNoise 2016, August 21-24, Hamburg, Germany. https://www.researchgate.net/publication/306505595_Acoustic_Measurements_on_a_1_1_Scale_Model_of_a_Shading_System_for_Building_Facade_in_a_Semi-Anechoic_Chamber
- Fausti, P., Secchi, S., Zuccherini Martello, N. (2019). The use of façade sun shading systems for the reduction of indoor and outdoor sound pressure levels. *Building Acoustics*, 26, 3, 181-206. <https://doi.org/10.1177%2F1351010X19863577>
- Sakamoto, S., Lee, H., Ishii, H., Katayama, T., Iwase, S., & Takahashi, K. (2017). In-situ experiment and numerical analysis on an effect of noise shielding louvers attached on a building façade. In INTER-NOISE and NOISE-CON Congress and Conference Proceedings, Vol. 255, No. 6, pp. 1484-1491. Institute of Noise Control Engineering. <https://www.ingentaconnect.com/contentone/ince/incecp/2017/00000255/00000006/art00057>
- Zuccherini Martello, N., Fausti, P., Santoni, A., Secchi, S. (2015). The use of sound absorbing shading systems for the attenuation of noise on building façades. An experimental investigation, *Buildings* 5(4), 1346-1360, <https://doi.org/10.3390/buildings5041346>
- Zuccherini Martello, N., Aletta, F., Fausti, P., Kang, J., Secchi, S. (2019). A psychoacoustic investigation on the effect of external shading devices on building façades, *Applied Sciences*, 6(12), 429. <https://doi.org/10.3390/app6120429>
- Catalina, T., Ene, A., & Biro, A. (2019). Visual and acoustic performance of shading devices—real scale laboratory measurements. In E3S Web of Conferences. Vol. 111, p. 06072. EDP Sciences. https://www.researchgate.net/publication/335141827_Visual_and_acoustic_performance_of_shading_devices_-_real_scale_laboratory_measurements

- Buratti, C., Belloni, E., Merli, F. & Ricciardi, P. (2018). A new index combining thermal, acoustic, and visual comfort of moderate environments in temperate climates, *Building and Environment*, 139, July 2018, 27-37, <https://doi.org/10.1016/j.buildenv.2018.04.038>
- Huang, L., Zhu, Y., Ouyang, Q. & Cao, B. (2012). A study on the effects of thermal, luminous, and acoustic environments on indoor environmental comfort in offices, *Building and Environment*, 49 (2012) 304-309, <http://dx.doi.org/10.1016/j.buildenv.2011.07.022>
- Hangzi, W., Xiaoying, S. & Yue, W. (2020). Investigation of the relationships between thermal, acoustic, illuminous environments and human perceptions, *Journal of Building Engineering*, 32, November 2020, 101839, <https://doi.org/10.1016/j.jobe.2020.101839>
- Technical Report of IEA SHC Task 50.C2/ Methods and tools for lighting retrofits-State of the art review. April 2016. http://task50.iea-shc.org/data/sites/1/publications/Technical_Report_T50_C2_final.pdf
- Technical Report of IEA SHC Task 61.C1 /Workflows and software for the design of integrated lighting solutions. November 2019. <https://task61.iea-shc.org/Data/Sites/1/publications/IEA-SHC-Task61-Workflows-and-software-for-the-design-of-integrated-lighting-solutions.pdf>
- Ahmad, A., Kumar, A., Prakash, O., Amana, A.; Daylight availability assessment and the application of energy simulation software – A literature review. *Materials Science for Energy Technologies* 3 (2020) 679–689. <https://doi.org/10.1016/j.mset.2020.07.002>
- Carletti, C., Cellai, G., Pierangioli, L., Scirpi, F. & Secchi, S. (2017). The influence of daylighting in buildings with parameters nZEB: application to the case study for an office in Tuscany Mediterranean area, *Energy Procedia*, 140, December 2017, 339-350, <https://doi.org/10.1016/j.egypro.2017.11.147>
- Carlucci, S., Causone, F., De Rosa F., and Pagliano L. (2015) A review of indices for assessing visual comfort with a view to their use in optimisation processes to support building integrated design. *Renewable & Sustainable Energy Reviews*. 2015, 47:1016-1033, <https://doi.org/10.1016/j.rser.2015.03.062>
- EN 12665: 2013. Light and lighting - Basic terms and criteria for specifying lighting requirements. <https://standards.iteh.ai/catalog/standards/cen/d7c62c9a-95ac-4ed8-9a40-862805aa5afc/en-12665-2011>
- Galatioto, A. and Beccali, M. (2016). Aspects and issues of daylighting assessment: A review study. *Renewable and Sustainable Energy Reviews*. 66, 852–860.2016. <https://doi.org/10.1016/j.rser.2016.08.018>
- Nabil, A. & Mardaljevic, J. (2005). Useful daylight illuminance: A new paradigm for assessing daylight in buildings, *Lighting Research and Technology* 37(1), March 2005, 41-59, <http://dx.doi.org/10.1191/1365782805li128oa>
- Mardaljevic, J., Andersen, M., Roy, N., & Christoffersen, J. (2012). Daylighting Metrics: Is There a Relation Between Useful Daylight Illuminance and Daylight Glare Probability? Proceedings of BSO Conference 2012: 1st Conference of IBPSA-England, Loughborough, UK, 10-11 September 2012, 189-196. https://publications.ibpsa.org/conference/paper/?id=bsc2012_3B1
- EN ISO 10534-2:2001. Acoustics – Determination of sound absorption coefficient and impedance in impedances tubes – Part 2: Transfer-function method. <https://standards.iteh.ai/catalog/standards/cen/8f9ca271-960d-4042-8937-ccb8cbcd20/en-iso-10534-2-2001>
- Delany, M. E., & Bazley, E. N. (1970). Acoustical properties of fibrous absorbent materials. *Applied acoustics*, 3(2), 105-116. [https://doi.org/10.1016/0003-682X\(70\)90031-9](https://doi.org/10.1016/0003-682X(70)90031-9)
- Miki, Y. (1990). Acoustical properties of porous materials-Modifications of Delany-Bazley models. *Journal of the Acoustical Society of Japan* (E), 11(1), 19-24. <https://doi.org/10.1250/ast.11.19>
- www.relux.com
- Maamari, F., Fontoynt, M., Adra, N. (2006). Application of the CIE test cases to assess the accuracy of lighting computer programs. *Energy and Buildings*, 38(7), July 2006, 869-877. <https://doi.org/10.1016/j.enbuild.2006.03.016>
- Bhavani, R.G., and Khan, M.A. (2011). Advanced Lighting simulation tools for daylighting purpose: powerful features and related issues. *Trends in Applied Sciences Research* 6(4), 345-363. <https://scialert.net/abstract/?doi=tasr.2011.345.363>
- Kaempf, J., Paule, B., Basurto, C., Bodart, M., Boer, J., Bueno, B., Dubois, M.C., Geisler-Moroder, D., Fusco, M., Hegi, M., Jørgensen, M., Roy, N., Wienold, J. (2016). Methods and tools for lighting Retrofits: State of the art review, A Technical Report of IEA SHC Task 50, online: http://task50.iea-shc.org/Data/Sites/1/publications/Technical_Report_T50_C2_final.pdf
- Bouroussis C.A., Nikolaou D.T., Topalis F.V. (2019). Test report on the validation of Relux Desktop 2019 against CIE 171:2006 – May 2019, https://relux.com/assets/static/global/documents/ReluxDesktop_validation_report_Final.pdf
- CIE 171:2010. Test cases to assess the accuracy of lighting computer programs. CIE, Vienna, 2006. <https://cie.co.at/publications/test-cases-assess-accuracy-lighting-computer-programs>
- Iversen, A., Roy, N., Hvass, M., Jørgensen, M., Christoffersen, J., Osterhaus, W., Johnsen, K. (2013) Daylight calculations in practice: An investigation of the ability of nine daylight simulation programs to calculate the daylight factor in five typical rooms. SBI 2013:26 Danish Building Research Institute, Aalborg University. 2013. <https://vbn.aau.dk/en/publications/daylight-calculations-in-practice-an-investigation-of-the-ability>
- Mardaljevic, J. (2013). Rethinking daylighting and compliance, *Journal of Sustainable Design & Applied Research*. 1. 3, Article 1. Available at: <https://arrow.tudublin.ie/sdar/vol1/iss3/1/>, <https://doi.org/10.21427/D7HJ0C>
- Danny, H.W.Li, Shuyang, Li, Wenqiang, C. and Siwei L. (2018). Analysis of Point Daylight Factor (PDF) Average Daylight Factor (ADF) and Vertical Daylight Factor (VDF) under various unobstructed CIE Standard Skies. *IOP Conf. Ser.: Mater. Sci. Eng.* 556 012044. <https://iopscience.iop.org/article/10.1088/1757-899X/556/1/012044>
- Xu, Y., Yuehong, S., Xin, C. (2014). Application of RELUX simulation to investigate energy saving potential from daylighting in a new educational building in UK, *Energy and Buildings*, Volume 74, 2014. <https://doi.org/10.1016/j.enbuild.2014.01.024>
- Kose, B., & Kazanasmaz, T., (2020). Applicability of a Prismatic Panel to Optimise Window Size and Depth of a South-facing Room for a Better Daylight Performance. *Light & Engineering*. 63-67. <http://dx.doi.org/10.33383/2019-038>
- CIE S 011/E:2003 - Spatial distribution of daylight - CIE standard general sky. <https://cie.co.at/publications/spatial-distribution-daylight-cie-standard-general-sky>

- Darula, S. and Kittler, R. (2002). CIE general sky standard defining luminance distributions. Proc. Conf. eSim 2002. The Canadian conference on building energy simulation. Montreal, Canada. http://www.ustarch.sav.sk/wp-content/uploads/darula_kittler_proc_conf_esim_2002.pdf
- Kensek, K., & Suk, J.Y. (2011). Daylight Factor (overcast sky) versus Daylight Availability (clear sky) in Computer-based Daylighting Simulations. [https://www.semanticscholar.org/paper/Daylight-Factor-\(overcast-sky\)-versus-Daylight-sky\)-Kensek-Suk/155fe1ef6424944a9056249809ae9d941e140539](https://www.semanticscholar.org/paper/Daylight-Factor-(overcast-sky)-versus-Daylight-sky)-Kensek-Suk/155fe1ef6424944a9056249809ae9d941e140539)
- Secchi, S., Fausti, P., Cellai, G., Parente, M., Santoni, A. & Zuccherini, N.M. (2021). The acoustic and daylighting effects of external façade sun shading systems. Proceedings of International Conference on Construction, energy, Environment and Sustainability, Coimbra, Portugal, 12-15 October 2021



JOURNAL OF FAÇADE DESIGN & ENGINEERING

VOLUME 10 / NUMBER 1 / 2022

V Editorial

Ulrich Knaack, Thaleia Konstantinou

001 Selection of Exterior Wall System and MCDM Derived Decision

Andelka Štilić, Igor Štilić

029 Towards a Human Centred Approach for Adaptive Façades

Mine Koyaz, Alejandro Prieto, Aslıhan Ünlü, Ulrich Knaack

055 Exploring the Impact of Geometry and Fibre Arrangements on Daylight Control in Bistable Kinetic Shades

Elena Vazquez, Jose Duarte

075 Circular, biomimicry-based, and energy-efficient façade development for renovating terraced dwellings in the Netherlands

Ana Luíza Binow Bitar, Ivar Bergmans, Michiel Ritzen

105 Process Automation to Improve the Building Engineering Design Analysis of Non-Repetitive Façade Geometries

Jacopo Montali, Thomas Henriksen

119 Empirical validation of co-simulation models for adaptive building envelopes

Esther Borkowski, Alessandra Luna-Navarro, Michalis Michael, Mauro Overend, Dimitrios Rovas, Rokia Raslan

155 The acoustic and daylighting effects of external façade sun shading systems

Simone Secchi, Patrizio Fausti, Gianfranco Cellai, Martina Parente, Andrea Santoni, Nicolò Zuccherini Martello

TU DELFT

ISSN PRINT 2213-302X

ISSN ONLINE 2213-3038

